

**Exploring drivers of leaf bacterial community dynamics across temperature-driven phenology in two temperate tree species**

Jordan Wilson-Morrison

A thesis submitted to the University of Ottawa  
in partial fulfillment of the requirements for the degree of

Master of Science in Biology

Department of Biology, Faculty of Science  
University of Ottawa

In collaboration with:

University of British Columbia (UBC), Department of Forest and Conservation Sciences

Canadian Airborne Biodiversity Observatory (CABO)

Agriculture and Agri-Food Canada (AAFC)

© Jordan Wilson-Morrison, Ottawa, Canada, 2025

## TABLE OF CONTENTS

<b>DEDICATIONS</b> .....	<b>V</b>
<b>ACKNOWLEDGMENTS</b> .....	<b>VI</b>
<b>ABSTRACT</b> .....	<b>VIII</b>
<b>STATEMENT OF CONTRIBUTIONS</b> .....	<b>IX</b>
<b>LIST OF FIGURES</b> .....	<b>X</b>
<b>LIST OF TABLES</b> .....	<b>XVII</b>
<b>LIST OF APPENDICES</b> .....	<b>XIX</b>
<b>DATA AVAILABILITY</b> .....	<b>XIX</b>
<b>LIST OF ABBREVIATIONS</b> .....	<b>XX</b>
<b>Chapter 1: General Introduction</b> .....	<b>1</b>
Relevance .....	1
Background .....	3
Research Aims and Objectives.....	7
Motivation and Approach.....	8
<b>Chapter 2: Growing degree days shape host-specific leaf bacterial community dynamics and thermal niche strategies in two functionally similar temperate tree species*</b> .....	<b>11</b>
1.0 INTRODUCTION.....	12
2.0 MATERIALS AND METHODS .....	15
2.1 Host Leaf Sampling and Estimating Seasonal Phenology (Growing Degree Days).....	15
2.2 DNA Extraction.....	17
2.3 Amplification and Sequencing of 16S rRNA Gene.....	17
2.4 Sequence Quality Control, Filtering, and Taxonomic Assignment of ASVs.....	18
2.5 Statistical Analyses.....	18
2.5.1 Bacterial Alpha Diversity Patterns.....	19
Alpha Diversity Calculations .....	19
Alpha Diversity Modelling and Statistical Analysis .....	19
2.5.2 Bacterial Community Structure (Beta Diversity) .....	20
2.5.3 Relative Abundance and Taxonomic Profiles.....	21
2.5.4 Differential Abundance Analysis.....	21
2.5.5 Niche Width Analysis .....	22

3.0 RESULTS.....	24
3.1 Seasonal GDD accumulation drives bacterial richness more than species identity and shapes community composition in functionally similar hosts.....	25
3.2 Specific taxa were enriched in the leaf microbiomes of birch and aspen as GDDs accumulated across phenology .....	32
3.3 Leaf microbiomes exhibited host-specific thermal niche strategies dominated by specialists across a seasonal GDD gradient .....	36
4.0 DISCUSSION .....	38
4.1 GDD accumulation shapes species-specific patterns of alpha diversity .....	39
4.2 Community composition and turnover reflect host-specific thermal trajectories .....	40
4.3 GDDs reveal distinct taxonomic and thermal enrichment patterns .....	41
4.4 Niche width patterns support ecological filtering and divergent strategies.....	42
4.5 Broader implications and future directions .....	44
5.0 CONCLUSION .....	46
<b>Chapter 3: General Conclusions.....</b>	<b>47</b>
<b>LITERATURE CITED .....</b>	<b>50</b>
<b>APPENDIX.....</b>	<b>67</b>
<b>S2.0 SUPPLEMENTAL MATERIALS AND METHODS .....</b>	<b>71</b>
S2.2 DNA Extraction.....	71
S2.4 Sequence Quality Control, Filtering, and Taxonomic Assignment of ASVs.....	71
S2.5 Statistical Analyses .....	72
S2.5.1 Bacterial Alpha Diversity Patterns.....	72
Interspecific Model Selection (Alpha Diversity) .....	73
Intraspecific Model Selection (Alpha Diversity) .....	74
Marginal and Conditional R <sup>2</sup> Calculation .....	75
Pairwise Comparisons of Host–Phenology Interaction Effects .....	75
Pairwise Comparisons of Host Species Effects Across Phenology.....	76
Pairwise Comparisons of Growing Degree Day Effects Within Host Species .....	76
S2.5.4 Differential Abundance Analysis .....	77
<b>S3.0 SUPPLEMENTAL RESULTS .....</b>	<b>78</b>
S3.1 Alpha Diversity .....	78
S3.2 Community Composition and Structure.....	84
S3.3 Differential Abundance Analysis .....	88

**SUPPLEMENTAL FIGURES AND TABLES ..... 92**

## DEDICATIONS

To my family  
whose unwavering love, support,  
and encouragement made this  
journey possible.

Vikki Wilson  
Chad Wilson-Morrison

And to my cat, Indi,  
for seeing me through the toughest of times.

## ACKNOWLEDGMENTS

I acknowledge that the land I have worked and lived on throughout this research, and beyond, is the traditional, unceded territory of the Anishinaabe–Algonquin territory of the Three Fires Confederacy of Ontario, Anishinaabewaki. I acknowledge that Mont Saint-Bruno near Montreal, Québec from which tree leaves were sampled is located on the traditional, unceded territory of the Kanien'kehá:ka Nation, part of the Haudenosaunee Confederacy, who are the recognized custodians of the land. I also recognize the earlier presence of the St. Lawrence Iroquoians, whose villages once shaped this region.

---

I extend my deepest gratitude towards my thesis supervisors, Dr. Warren Cardinal-McTeague and Dr. Julian Starr, for their guidance, feedback, and continued support. Your encouragement and confidence in me, even when mine wavered, provided the motivation for me to work hard on a project I take great pride in. I would also like to thank my thesis committee advisors, Dr. Cory Harris and Dr. Christina Davy, for their invaluable insights and advice. To Dr. Itumeleng Moroenyane, our collaboration in metagenomics was pivotal; I could not have done this work without you. Many thanks to Rosalie Beauchamp-Rioux, whose work paved the way for this research to be possible, as well as Sabrina Demers-Thibeau, Etienne Laliberté, and the rest of the Canadian Airborne Biodiversity Observatory (CABO) team. I would also thank Dr. Shan Kothari, whose expertise and willingness to always help was very much appreciated.

I thank Dr. Tyler Smith for allowing me to work in the molecular labs at Agriculture and Agri-Food Canada (AAFC) and for giving me a concrete foundation to perform research without hiccups by taking me on as your student and employee. To Tracy James, you had so much on

your plate, but you went above and beyond to help me and supplement my lab training—many thanks to you. To Dr. Julien Martin, your graduate course in advanced biostatistics was not only a fantastic experience, but it became instrumental in guiding my research; thank you for taking the time to meet with me and review some of my statistical modelling and giving me the confidence to proceed with my work.

To my lab colleagues—both at home and abroad—thank you for the comradery, morale support, and mandatory fun. Charlotte Hagelstam-Renshaw, Laurence Bourgeois-Racette, Rati (Ratidzayi) Takawira-Nyenyanya, Saba Nasiri, Miah Godek, and Rykkar Jackson, I am so very grateful to have met you all and for the many discussions; my thesis is better because of it. To Dr. Subbaiah Mechanda, thank you for teaching me everything I needed to know about the wet lab. Your mentorship, not only in research, but about career and life, was formative and I will forever consider you a close friend. To Cassandra Bradshaw, our “home base” may just be us, but you provided the motivation I needed to come into the lab and get the work done. I’ve made a great friend in you and for that I will be forever thankful; although, I think Julia Miles also counts as an unofficial lab member. To my friends and family—graduate school was not easy; your unwavering support and encouragement through my times of stress made all of this possible.

Funding for my research was provided by the Natural Sciences and Engineering Research Council of Canada’s (NSERC) Alexander Graham Bell Canada Graduate Scholarship Master’s (CGS–M), the Dr. Pearl Weinberger Memorial Scholarship, and the Don E. McAllister Memorial Scholarship. Through the Federal Student Work Experience Program (FSWEP), I was also employed with Agriculture and Agri-Food Canada (AAFC); separately, the Department of Forest and Conservation Sciences at the University of British Columbia (UBC) provided financial support.

## ABSTRACT

Leaf microbiomes are vital to host and ecosystem functions, yet their interplay with host phenology remains ill-resolved in temperate forests, where climate change is shifting phenological timing. We investigate how cumulative growing degree days (GDDs)—an index of the active, useable heat energy directing phenology—shape leaf bacterial dynamics and ecological strategies, comparing two functionally similar but phylogenetically distant trees: Grey birch (*Betula populifolia*) and trembling aspen (*Populus tremuloides*). 16S rRNA amplicon sequencing captured variation across seven GDDs from June–October 2018 and relative impacts of host identity and GDDs on bacterial diversity, taxonomic enrichment, and niche breadth were tested. Host differences in amplicon sequence variant (ASV) richness were primarily shaped by GDDs, increasing non-linearly and non-monotonically with GDDs in birch but remaining stable in aspen; Shannon diversity was unaffected by GDDs and remained consistently higher in aspen. Beta diversity diverged seasonally; birch microbiomes underwent marked restructuring at higher GDDs, while aspen exhibited compositional overlap. Overall, birch hosted more GDD-limited ASVs, with disproportionate enrichment of generalists like *Endobacter* and *1174-901-12*, whereas aspen hosted more even communities of specialists like *Nocardioides* and *Pelomonas*. The prominence of unclassified ASVs emphasizes a need to resolve microbial “dark matter”. Niche analysis showed that ~81% of ASVs were thermal specialists, but species-specific patterns emerged: birch leaves supported communities with wider niches, while aspen maintained narrower niches. Though typically used to predict phenology, our results suggest that the cumulative thermal environment—as tracked by GDDs—imposes ecological filtering on leaf microbiomes based on thermal niche compatibility. Together, this study advances our understanding of microbial ecology *in situ* and expands the utility of the GDD metric.

## STATEMENT OF CONTRIBUTIONS

---

I, Jordan Wilson-Morrison, contributed to the majority of the work conducted towards completion of this thesis. This includes the molecular DNA lab work (extractions and PCR amplifications), as well as all bioinformatic and metagenomic analyses. Sequencing was outsourced to Genome Québec. I wrote all three chapters included in this thesis, and I intend to publish Chapter 2 in the *Phytobiomes Journal*.

My M.Sc. supervisors and external collaborators also contributed to this work. Both Dr. Warren Cardinal-McTeague and Dr. Julian Starr contributed to the overall development, direction, and review of each chapter of my thesis. Dr. Subbaiah Mechanda provided invaluable laboratory training in molecular biology and contributed to the project development and data collection related to leaf specimens. Dr. Itumeleng Moroenyane, my research collaborator at Stellenbosch University, provided guidance and direction in metagenomic analyses. Dr. Etienne Laliberté, lead researcher at the Canadian Airborne Biodiversity Observatory (CABO), and Rosalie Beauchamp-Rioux, a former M.Sc. student at the Université de Montreal, provided the project foundation and leaf samples needed to complete this metagenomic work. All contributors will be asked to provide helpful comments on the parts of this thesis that they co-authored, and for approval of the final content prior to submission to *Phytobiomes*.

---

## LIST OF FIGURES

- Figure 1.1.** The plant associated microbiome provides benefits to the plant through various direct and indirect mechanisms that help to shape leaf functional traits. These benefits include growth promotion, stress tolerance, plant defense and immunity, phytohormone stimulation, and dysbiosis prevention. In contrast, functional traits may be altered predictably by non-beneficial, or pathogenic, microorganisms. These traits are heavily impacted by leaf microbial activity. Figure made using: <https://biorender.com>..... 4
- Figure 1.2.** Schematic demonstrating the difference between **(A)** intraspecific variation (variation within a host species) and **(B)** interspecific variation (variation between host species). In this study, “Host Species A” and “Host Species B” represent the two host study systems, grey birch and trembling aspen. .... 8
- Figure 1.3.** Overview of the metagenomics workflow used in this study. Raw sequencing reads were processed using the DADA2 pipeline, including quality filtering, denoising, chimera removal, and amplicon sequence variant (ASV) inference. Taxonomic classification was performed using the SILVA reference database, followed by diversity analyses (ASV richness, Shannon diversity, beta diversity), taxonomic profiling, differential abundance analysis, and assessments of Levin’s niche breadth. Statistical analyses, including linear mixed models (LMMs), PERMANOVA, and differential abundance testing (DESeq2), were applied to assess the impact of host species identity, growing degree days (GDD), and individual plant factors on the leaf microbiome. Figure made using: <https://biorender.com>. .... 10
- Figure 2.1.** Cumulative growing degree days (GDDs;  $T_{\text{base}} = 5^{\circ}\text{C}$ ) across the 2018 growing season at the study site in Québec. Cumulative GDDs were calculated as the daily mean temperature minus the  $5^{\circ}\text{C}$  base threshold, summed across all days with positive values. Vertical dashed lines represent leaf sampling dates. This curve reflects the seasonal progression of thermal energy accumulation—a physiologically relevant metric for predicting plant phenology and a key environmental driver of microbiome dynamics in this study. .... 25
- Figure 2.2.** Leaf bacterial community diversity and composition patterns of two host tree species, grey birch (purple) and trembling aspen (orange), across a season phenological gradient of GDD accumulation (June–October 2018) using 16S rRNA gene amplicon sequencing showing **(A)** comparisons of amplicon sequence variant (ASV) richness (left) and Shannon diversity (right). Bold horizontal bars represent the median and the error bars indicate a measure of variability of the data at each GDD sampling value. Circular data points represent individual samples of birch and aspen leaves taken at each

sampling point along the GDD continuum (total  $n = 71$ ), which are horizontally jittered to avoid overlap. n.s. = non-significant host species differences ( $P$ -value  $* < 0.05$  and  $** < 0.01$ ); and **(B)** Principal Coordinate Analysis (PCoA) of leaf bacterial community beta diversity based on Bray-Curtis dissimilarities. Each data point denotes a host plant individual sampled at GDDs 437 (empty circle), 605 (empty square), 1087 (empty diamond), 1606 (filled diamond), 1992 (filled square), 2140 (filled circle), and 2219 (asterisk). ..... 27

**Figure 2.3.** Taxonomic composition and differential abundance of leaf bacterial communities of grey birch and trembling aspen. **(A)** Genus-level taxonomic profiles of relative abundance for birch (top) and aspen (bottom) as GDDs ( $T_{\text{base}} = 5^{\circ}\text{C}$ ) accumulate over seasonal host phenology. For visual practicality, only the top 20 most abundant genera are shown, but the general pattern remains consistent, regardless. **(B)** Differential abundance analysis (*DESeq2*) showing significant changes ( $p_{\text{adj}} < 0.05$ ) in the relative abundance of leaf bacterial ASVs (colour-coded) within birch (top) and aspen (bottom) in response to GDD accumulation ( $T_{\text{base}} = 5^{\circ}\text{C}$ ). The  $\log_2(\text{fold-change})$  represents the rate of change in abundance for every 1-unit increase in GDD and can be interpreted as a regression slope on a  $\log_2$  scale. A positive  $\log_2(\text{fold-change})$  indicates that the ASV significantly increased in abundance as GDDs increased, while a negative  $\log_2(\text{fold-change})$  demonstrates that there was a significant decline in the ASV's abundance as GDDs increased. Note that colours do not correlate to relatedness of taxa. The  $P$ -value is calculated using the Wald test, and the adjusted  $P$ -value ( $p_{\text{adj}}$ ) is calculated using the Benjamini–Hochberg method. A full list of the significantly differentially abundant ASVs, including unidentified ASVs, and all summary statistics can be found in Supplementary Tables S9–S10. .... 33

**Figure 2.4.** Thermal niche breadth of leaf-associated bacterial ASVs across seasonal heat accumulation and host species. Levins' niche width index was derived from relative abundances and used to quantify the breadth of thermal persistence for each ASV across a seasonal GDD ( $T_{\text{base}} = 5^{\circ}\text{C}$ ) gradient, a physiologically relevant measure of heat accumulation that tracks host phenological progression. ASVs with niche width  $\leq 1.5$  were classified as specialists,  $\geq 2.25$  as generalists, and those in between as intermediate. **(A)** Proportion of ASVs classified as thermal specialists, intermediates, or generalists, faceted by host species. **(B)** Seasonal trends in ASV niche width across GDD accumulation for each host species. Boxplots represent the distribution of ASV-level niche width values per GDD time point (median, IQR, whiskers), with outliers shown as points. Dashed red and blue lines indicate specialist and generalist thresholds, respectively. **(C)** Genus-level distributions of niche width among focal bacterial genera. Narrow boxes (e.g., *Fron dih abitans*, *Nocardio ides*, and *Pseudomonas*) reflect low genus-level diversity or consistent niche breadth. **(D)** Niche width of focal ASVs from key genera, illustrating intra-genus variability in thermal niche strategy and highlighting

the ecological importance of unclassified ASVs. Bars represent individual ASVs; dashed lines mark classification thresholds as in prior panels, where red is the threshold for thermal specialists and blue is the threshold for thermal generalists. ASVs are colour-coded by genus. .... 37

**Supplementary Figure S1.** Leaf bacterial ASV accumulation curve indicating the cumulative number of recovered ASVs (Kindt’s exact method) as a function of sampling effort with 95% confidence interval for **(A)** all samples and **(B)** the positive control. .... 92

**Supplementary Figure S2.** Preston log-normal curve indicating the total number of leaf bacterial ASVs recovered (area under the curve) and the proportion of rare ASVs recovered. Sequencing recovered both abundant and rare ASVs, as indicated by the peak and truncation points at both ends of the curve. .... 93

**Supplementary Figure S3.** Untransformed relationship between accumulated growing degree days at a base temperature of 5°C (GDD\_5C) and the **(A)** ASV richness and **(B)** Shannon diversity index (H') across two host tree species, grey birch (left panels) and trembling aspen (right panels). The scatter plots show individual sample data points, while the blue lines represent linear regression fits. The red lines depict additional smoothing for trend visualization. .... 94

**Supplementary Figure S4.** Principal Coordinate Analysis (PCoA) showing multivariate dispersion of leaf bacterial communities comparing interspecific differences between grey birch and trembling aspen, represented by the host ‘Species’ variable. This figure is based on the Bray-Curtis dissimilarity between the two host tree species’ leaf bacterial communities, denoted by ‘Species’. .... 99

**Supplementary Figure S5.** Homogeneity of multivariate dispersion (distance to centroid) of leaf bacterial communities comparing interspecific differences between grey birch and trembling aspen represented by the host ‘Species’ variable. This figure is based on the Bray-Curtis dissimilarity between the two host tree species’ leaf bacterial communities, denoted by ‘Species’. .... 100

**Supplementary Figure S6.** Principal Coordinate Analysis (PCoA) showing multivariate dispersion of leaf bacterial communities comparing interspecific differences between grey birch and trembling aspen throughout seasonal phenology, considering only the variable of accumulated growing degree days at a base temperature of 5°C (‘GDD\_5C’). This figure is based on the Bray-Curtis dissimilarity between the two host tree species’ leaf bacterial communities regarding ‘GDD\_5C’. .... 101

**Supplementary Figure S7.** Homogeneity of multivariate dispersion (distance to centroid) of leaf bacterial communities comparing interspecific differences between grey birch and

trembling aspen throughout seasonal phenology, considering only the variable of accumulated growing degree days at a base temperature of 5°C ('GDD\_5C'). This figure is based on the Bray-Curtis dissimilarity between the two host tree species' leaf bacterial communities regarding 'GDD\_5C'..... 102

**Supplementary Figure S8.** Homogeneity of multivariate dispersion (distance to centroid) of leaf bacterial communities comparing interspecific differences between the interaction of grey birch with GDDs and the interaction of trembling aspen with GDDs, throughout seasonal phenology, considering the interaction variable ('Species:GDD\_5C'). This figure is based on the Bray-Curtis dissimilarity between the two host tree species' leaf bacterial communities regarding 'GDD\_5C'. Comparisons of interest are those between host species at shared GDD points. .... 103

**Supplementary Figure S9.** Principal Coordinate Analysis (PCoA) showing multivariate dispersion of leaf bacterial communities within grey birch based on the Bray-Curtis dissimilarity across growing degree days at a base temperature of 5°C ('GDD\_5C'). 104

**Supplementary Figure S10.** Homogeneity of multivariate dispersion (distance to centroid) of leaf bacterial communities within grey birch based on the Bray-Curtis dissimilarity across growing degree days at a base temperature of 5°C ('GDD\_5C')..... 105

**Supplementary Figure S11.** Principal Coordinate Analysis (PCoA) showing multivariate dispersion of leaf bacterial communities within grey birch based on the Bray-Curtis dissimilarity across individual plant identifiers, or Plant ID ('Plant\_ID'). .... 106

**Supplementary Figure S12.** Homogeneity of multivariate dispersion (distance to centroid) of leaf bacterial communities within grey birch based on the Bray-Curtis dissimilarity across individual plant identifiers, or Plant ID ('Plant\_ID'). .... 107

**Supplementary Figure S13.** Principal Coordinate Analysis (PCoA) showing multivariate dispersion of leaf bacterial communities within trembling aspen based on the Bray-Curtis dissimilarity across growing degree days at a base temperature of 5°C ('GDD\_5C')..... 108

**Supplementary Figure S14.** Homogeneity of multivariate dispersion (distance to centroid) of leaf bacterial communities within trembling aspen based on the Bray-Curtis dissimilarity across growing degree days at a base temperature of 5°C ('GDD\_5C'). 109

**Supplementary Figure S15.** Principal Coordinate Analysis (PCoA) showing multivariate dispersion of leaf bacterial communities within trembling aspen based on the Bray-Curtis dissimilarity across individual plant identifiers, or Plant ID ('Plant\_ID').....110

**Supplementary Figure S16.** Homogeneity of multivariate dispersion (distance to centroid) of leaf bacterial communities within trembling aspen based on the Bray-Curtis dissimilarity across individual plant identifiers, or Plant ID ('Plant\_ID'). .....111

**Supplementary Figure S17.** Principal Coordinate Analysis (PCoA) comparing leaf bacterial communities of grey birch (pink) and trembling aspen (turquoise) based on Bray-Curtis dissimilarity as host seasonal phenological change progresses, represented by accumulated growing degree days at a base temperature of 5°C (GDDs). Data has been subset by GDD to pinpoint the greatest differences between host species' bacterial community composition. Each data point denotes a plant individual sampled at GDDs (A) 437, (B) 605, (C) 1087, (D) 1606, (E) 1992, (F) 2140, and (G) 2219. The more proximal samples are to one another, the more similar their community composition is. In contrast, samples that are further from one another are more dissimilar and distinct in their foliar bacterial community composition.....112

**Supplementary Figure S18.** Principal Coordinate Analysis (PCoA) of leaf bacterial communities within a population of (A) grey birch and (B) trembling aspen individuals based on Bray-Curtis dissimilarity along host seasonal phenology, represented by accumulated GDDs ( $T_{base} = 5^{\circ}C$ ) and grouped by general phenology. Each data point denotes a plant individual sampled at GDDs 437 (open circle), 605 (open square), 1087 (open diamond), 1606 (filled diamond), 1992 (filled triangle), 2140 (filled square), and 2219 (asterisk). Early-mid phenology (blue) encompasses 437 and 605 GDDs; mid-late phenology (green) denotes 1087 and 1606 GDDs; and late phenology to senescence onset (goldenrod) corresponds to 1992, 2140, and 2219 GDDs. Samples that are more distal from one another are more dissimilar and distinct in their foliar bacterial community composition than those proximal.....113

**Supplementary Figure S19.** Phylum-level comparison of taxonomic profiles showing the interspecific and intraspecific patterns of change in the relative abundances of leaf bacterial communities of (A) grey birch and (B) trembling aspen throughout seasonal host phenological change (measured as GDDs at a base temperature of 5°C). Note that the relatedness of colour shades does not reflect the relatedness of bacterial phylogenetic relationships. ....115

**Supplementary Figure S20.** Differential abundance analysis (*DESeq2*) at the phylum-level showing significant changes ( $p_{adj} < 0.05$ ) in the relative abundance of leaf bacterial ASVs (colour-coded) within (A) birch and (B) aspen in response to GDD accumulation ( $T_{base} = 5^{\circ}C$ ). The  $\log_2(\text{fold-change})$  represents the rate of change in abundance for every 1-unit increase in GDD and can be interpreted as a regression slope on a  $\log_2$  scale. A positive  $\log_2(\text{fold-change})$  indicates that the ASV significantly increased in abundance as GDDs increased, while a negative  $\log_2(\text{fold-change})$  demonstrates that

there was a significant decline in the ASV's abundance as GDDs increased. Note that colours do not correlate to relatedness of taxa. The *P*-value is calculated using the Wald test, and the adjusted *P*-value ( $p_{adj}$ ) is calculated using the Benjamini–Hochberg method. A full list of the significantly differentially abundant ASVs, including unidentified ASVs, and all summary statistics can be found in Supplementary Tables S9–S10.....116

**Supplementary Figure S21.** Differential abundance analysis (*DESeq2*) showing significant changes ( $p_{adj} < 0.05$ ) in the relative abundance of leaf bacterial ASVs within and between grey birch and trembling aspen across the entirety of host phenology at (A) the phylum-level and (B) the genus-level. A positive  $\log_2(\text{fold-change})$  indicates that ASVs were significantly more differentially abundant in birch, while a negative  $\log_2(\text{fold-change})$  demonstrates that ASVs were significantly more differentially abundant in aspen. Note that colours do not correlate to relatedness of taxa. A full list of the significantly differentially abundant ASVs, including unidentified ASVs, and all summary statistics can be found in *Supplementary Table S8* of the Supplementary Information section. ....118

**Supplementary Figure S22.** Differential abundance analysis (*DESeq2*) showing significant changes ( $p_{adj} < 0.05$ ) in the relative abundance of leaf bacterial ASVs (genus-level colour-coded) within and between grey birch and trembling aspen GDDs ( $T_{base} = 5^\circ\text{C}$ ) are accumulated at a base temperature of  $5^\circ\text{C}$  at GDD sampling points (A) 437, (B) 605, (C) 1087, (D) 1606, (E) 1992, (F) 2140, and (G) 2219. GDDs are a thermo-temporal measure of host plant seasonal phenological change. A positive  $\log_2(\text{fold-change})$  indicates that ASVs were significantly more differentially abundant in birch, while a negative  $\log_2(\text{fold-change})$  demonstrates that ASVs were significantly more differentially abundant in aspen. A full list of the significantly differentially abundant ASVs, including unidentified ASVs, and all summary statistics can be found in *Supplementary Table S9* of the Supplementary Information section..... 120

**Supplementary Figure S23.** Thermal niche breadth of leaf-associated bacterial ASVs across seasonal heat accumulation and host species. Levins' niche width index was derived from relative abundances and used to quantify the breadth of thermal persistence for each ASV across a seasonal GDD ( $T_{base} = 5^\circ\text{C}$ ) gradient, a physiologically relevant measure of heat accumulation that tracks host phenological progression. ASVs with niche width  $\leq 1.5$  were classified as specialists,  $\geq 2.25$  as generalists, and those in between as intermediate. This figure shows the proportion of ASVs across all samples, regardless of host species, classified as thermal specialists, intermediates, or generalists. .... 122

**Supplementary Figure S24.** Distribution of ASV-level thermal niche breadths across host species. Violin plots show the distribution and density of Levins' niche width values for

bacterial ASVs associated with grey birch and trembling aspen, calculated using relative abundance across continuous growing degree day (GDD<sub>5°C</sub>) values. Horizontal dashed lines represent fixed classification thresholds for thermal specialists ( $\leq 1.5$ , red) and generalists ( $\geq 2.25$ , blue), with intermediate values falling in between. Distributions are based on ASVs present in at least two GDD timepoints. .... 123

## LIST OF TABLES

<b>Table 2.1.</b> Cumulative growing degree days (GDDs) at a base temperature of 5°C and their corresponding sampling dates classified into generalized phenological periods for temperate trees in the Northern Hemisphere. ....	16
<b>Table 2.2.</b> Summary of the impact of host species identity (S), GDD accumulation at $T_{\text{base}} = 5^{\circ}\text{C}$ (GDD_5C), and their interaction (S x GDD_5C) on the leaf bacterial alpha diversities of grey birch and trembling aspen using linear mixed modeling (LMMs). <sup>a</sup> .....	28
<b>Table 2.3.</b> Summary of pairwise comparisons of host species-specific differences in leaf bacterial alpha diversity at each GDD sampling point ( $T_{\text{base}} = 5^{\circ}\text{C}$ ) using the emmeans package in R to evaluate the effect of host species identity (S) as seasonal phenology progresses. <sup>a</sup> .....	29
<b>Table 2.4.</b> Permutational analysis of variance (PERMANOVA) testing the impact of host species identity ('Species'), GDD accumulation at $T_{\text{base}} = 5^{\circ}\text{C}$ ('GDD_5C') as a proxy for host phenology, and their two-way interaction ('Species x GDD_5C') on differences in leaf beta diversity and bacterial community composition within and between grey birch and trembling aspen.....	31
<b>Supplementary Table S1.</b> Summary of pairwise comparisons using the <i>emmeans</i> package in R to assess the interaction between host species identity and GDDs at a base temperature of 5°C ('Species:GDD_5C') on leaf ASV richness comparing each GDD sampling point in the growing season between grey birch ( <i>Betula</i> ) and trembling aspen ( <i>Populus</i> ). <sup>a</sup> ...	95
<b>Supplementary Table S2.</b> Summary of pairwise comparisons using the <i>emmeans</i> package in R to evaluate the differential effects of GDDs at a base temperature of 5°C ('GDD_5C') on leaf bacterial ASV richness within grey birch. Analyses were conducted between each sampling point combination of 'GDD_5C', accounting for the LMM structure. <sup>a</sup> .	96
<b>Supplementary Table S3.</b> Summary of statistical tests (ANOVA and Kruskal-Wallis) evaluating the impact of overall individual host plant characteristics ('Plant_ID') on leaf ASV richness and Shannon diversity at different points in the growing season for grey birch. <sup>a</sup> .....	97
<b>Supplementary Table S4.</b> Summary of statistical tests (ANOVA and Kruskal-Wallis) evaluating the impact of overall individual host plant characteristics ('Plant_ID') on the inverse of foliar ASV richness and Shannon diversity at different points in the growing season for trembling aspen.....	98

<b>Supplementary Table S5.</b> Permutational analysis of variance (PERMANOVA) for grey birch (top) and trembling aspen (bottom) testing the impact of GDDs at a base temperature of 5°C ('GDD_5C') as a proxy for host phenology, individual plant identification ('Plant_ID'), and their interaction on leaf bacterial beta diversity and community structure. <sup>a</sup> .....	114
<b>Supplementary Table S6.</b> List of differentially abundant ASVs within grey birch leaf samples across a GDD ( $T_{\text{base}} = 5^{\circ}\text{C}$ ) gradient as determined by differential abundance analysis ( <i>DESeq2</i> ). <sup>a</sup> .....	125
<b>Supplementary Table S7.</b> List of differentially abundant ASVs within trembling aspen leaf samples across a GDD ( $T_{\text{base}} = 5^{\circ}\text{C}$ ) gradient as determined by differential abundance analysis ( <i>DESeq2</i> ). <sup>a</sup> .....	127
<b>Supplementary Table S8.</b> List of total differentially abundant taxa between grey birch and trembling aspen across host phenology as determined by differential abundance analysis ( <i>DESeq2</i> ). <sup>a</sup> .....	128
<b>Supplementary Table S9.</b> List of differentially abundant taxa between grey birch and trembling aspen as growing degree days (GDDs) are accumulated at a base temperature of 5°C at GDD sampling points (a) 437, (b) 605, (c) 1087, (d) 1606, (e) 1992, (f) 2140, and (g) 2219 as determined by differential abundance analysis ( <i>DESeq2</i> ). <sup>a</sup> .....	130
<b>Supplementary Table S10.</b> ASV-level thermal niche width, classification, and taxonomic annotation. This table reports Levins' niche width index for each bacterial ASV, calculated from scaled relative abundance across continuous GDD ( $T_{\text{base}} = 5^{\circ}\text{C}$ ) values. <sup>a</sup> .....	136

## LIST OF APPENDICES

<b>Table A1.</b> Summary of the most common bacterial taxa found within the phyllosphere and endosphere of plant leaves. Major phyla are displayed with their most common associated member classes and genera. The Gram status of each is listed, along with a brief description of their most important functions in the phyllosphere and endosphere (Durand et al. 2018; Kembel et al. 2014; Redford et al. 2010). .....	67
---	----

## DATA AVAILABILITY

Sequence data will be submitted to public databases with the publication of Chapter 2.

All other data, code, and analyses will also be submitted to GitHub upon publication at:

<https://github.com/jordan-dwm>.

## **LIST OF ABBREVIATIONS**

AIC: Akaike Information Criterion

ANOVA: Analysis of Variance

ASV: Amplicon Sequence Variant

BIC: Bayesian Information Criterion

C: Carbon

CABO: Canadian Airborne Biodiversity Observatory

DOY: Day of Year

GDD: Growing Degree Days

GDP: Gross Domestic Product

H': Shannon Diversity

H<sub>2</sub>O<sub>2</sub>: Hydrogen Peroxide

LMM: Linear Mixed-Model

Log<sub>2</sub>FC: Logarithm Base 2 of Fold Change

N: Nitrogen

OTU: Operational Taxonomic Unit

PCoA: Principal Coordinates Analysis

PERMANOVA: Permutational Multivariate Analysis of Variance

$R'$ : Richness

$R^2_c$ : Conditional  $R^2$

$R^2_m$ : Marginal  $R^2$

RDP: Ribosomal Database Project

rRNA: Ribosomal Ribonucleic Acid

$T_{base}$ : Base Temperature

$T_{max}$ : Temperature Maxima

$T_{min}$ : Temperature Minima

VOC: Volatile Organic Compound

# Chapter 1

## General Introduction

1        Microbial ecology examines the interactions between microorganisms, their hosts, and the  
2 environment, integrating microbiology, ecology, genetics, and metagenomic bioinformatics to  
3 understand microbial community dynamics. Microbes play essential roles in nutrient cycling,  
4 plant health, and ecosystem function; as rising temperatures accelerate shifts in plant phenology,  
5 investigating how leaf microbiomes respond is critical for conservation, forest management, and  
6 ecological modeling. In this thesis, I explore how bacterial dynamics—both between and within  
7 host species—are shaped in the leaf phyllosphere and endosphere microbiomes of two broadleaf  
8 deciduous trees. Focusing on temperate forests in Parc national du Mont-Saint-Bruno, Quebec,  
9 this study aims to characterize and compare general trends and patterns of variation in bacterial  
10 diversity and community composition along the seasonal progression of host phenology,  
11 measured as growing degree day (GDD;  $T_{\text{base}} = 5^{\circ}\text{C}$ ) accumulation. The overarching goal of my  
12 project is to build a foundational understanding of the processes influencing bacterial community  
13 dynamics in the leaf microbiomes of temperate forests.

### 14 **Relevance**

15        Widespread environmental changes are accelerating biodiversity loss, with over 60% of  
16 ecosystem services degraded since the 1950s and projected global GDP losses of 7% by 2050  
17 (Markandya 2015). Additionally, climate change is altering plant phenology, shifting  
18 developmental events like leaf emergence and senescence (Meier et al. 2021; Piao et al. 2019).  
19 Temperate forests experience distinct dormancy and growth cycles regulated by seasonal

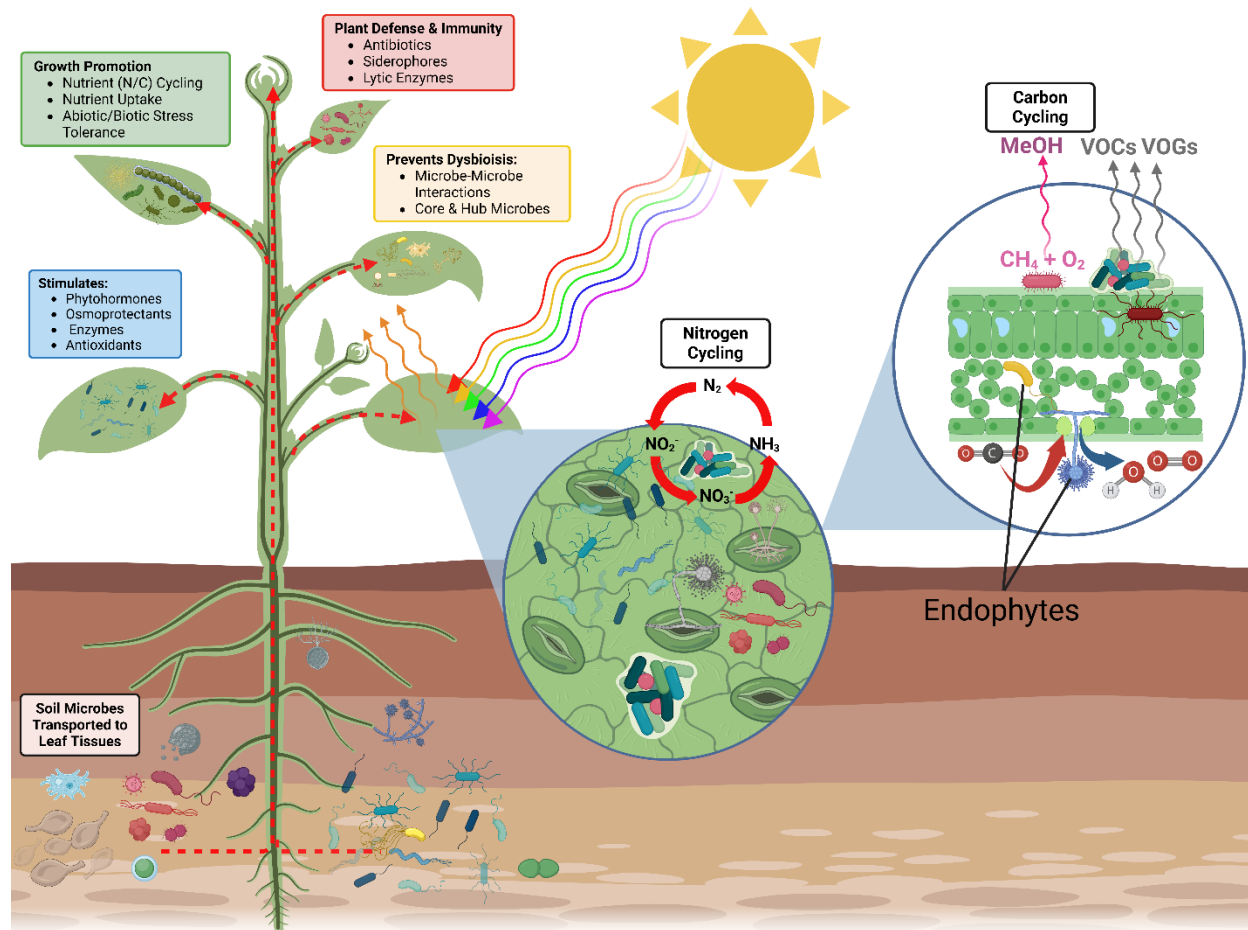
20 accumulation of thermal energy; hence, the GDD index provides a physiologically relevant  
21 metric quantifying tree phenology (McMaster and Wilhelm 1997; Prentice et al. 1992). Leaf  
22 microbiomes contribute to key biogeochemical processes—including C and N cycling, pollutant  
23 degradation, and the synthesis of compounds important for plant productivity—and exhibit  
24 reciprocal interactions with plant functional traits, both shaping and responding to them  
25 (Chaudhry et al. 2021; Lajoie and Kembel 2021; Thapa et al. 2017). Consequently, climate-  
26 driven shifts in phenology may disrupt leaf microbial dynamics, influencing plant health,  
27 ecosystem function, and forest resilience (Trivedi et al. 2020). Climate-driven shifts in  
28 temperature and precipitation are already impacting microbial networks of temperate trees  
29 (Sangiorgio et al. 2024; Wang et al. 2023), expanding pathogen ranges (Lahlali et al. 2024), and  
30 destabilizing plant-microbe interactions (Hacquard et al. 2022), yet the relation between  
31 temperature-driven phenological changes and the leaf microbiome remains virtually unexplored.

32         While research has expanded in tropical and agricultural systems, temperate forest leaf  
33 microbiomes remain understudied. Methodological limitations—including taxonomic biases,  
34 incomplete reference databases, and bioinformatics bottlenecks—further hinder progress in  
35 resolving plant-microbe interactions (Bharti and Grimm 2021; Leite et al. 2022; Zhang et al.  
36 2021). Nonetheless, the economic potential of plant microbiomes in silviculture is increasingly  
37 recognized (Uroz et al. 2016), while also revealing broader implications for public health in  
38 urban and urban-adjacent areas (Hanski et al. 2012). In the face of a rapidly changing climate,  
39 addressing these gaps is essential for advancing ecological research and its practical applications.  
40 Notably, accrued data and associated results from this study will contribute to genetic databases  
41 and the improvement of assessments of biodiversity, plant health and phytopathology, ecosystem  
42 function, and climate change impacts.

## 43 **Background**

44 My research contributes to microbial ecology by investigating how host species identity  
45 and biologically active thermal energy, measured as GDD accumulation, shape bacterial diversity  
46 and community composition in temperate forest leaves, providing insight into how temperature-  
47 driven shifts in tree phenology impact the leaf microbiome, with consequences for plant  
48 functional traits, health, and ecosystem function.

49 Plants are not isolated organisms; they exist in association with complex microbial  
50 communities that colonize their surfaces and internal tissues (Fig. 1.1). As part of the plant  
51 holobiont, the leaf harbors microbiomes that inhabit two primary niches: the phyllosphere,  
52 comprising the leaf surface, and the endosphere, consisting of internal leaf tissues (Redford et al.  
53 2010; Vorholt 2012). Despite the oligotrophic, nutrient-poor, and environmentally harsh  
54 conditions of the leaf, microbes play key roles in biogeochemical processes, nutrient cycling,  
55 plant health, and ecosystem function (Chaudhry et al. 2021; Lajoie and Kembel 2021; Thapa et  
56 al. 2017). For example, leaf-associated microbes influence host immunity, stress tolerance, and  
57 microbial interactions through the production of secondary metabolites, biosurfactants, and plant  
58 hormone analogs (Vorholt 2012). By enhancing their own fitness through these adaptive  
59 mechanisms, bacteria can indirectly or directly improve plant fitness. These microbial  
60 assemblages are diverse; in particular, bacteria dominate the leaf microbiome (Durand et al.  
61 2018; Kembel et al. 2014). A summary of commonly detected bacterial taxa found in and on  
62 leaves and their known ecological functions is provided in Table A1 (Appendix).



63

64 **Figure 1.1.** The plant associated microbiome provides benefits to the plant through various direct and  
 65 indirect mechanisms that help to shape leaf functional traits. These benefits include growth promotion,  
 66 stress tolerance, plant defense and immunity, phytohormone stimulation, and dysbiosis prevention. In  
 67 contrast, functional traits may be altered predictably by non-beneficial, or pathogenic, microorganisms.  
 68 These traits are heavily impacted by leaf microbial activity. Figure made using: <https://biorender.com>.

69 Microbial community assembly is shaped by both deterministic and stochastic processes,

70 influencing the diversity and structure of the leaf microbiome (Moroenyane et al. 2021a,b).

71 Deterministic processes, such as host filtering and competition, impose selective pressures that

72 favor specific microbial taxa based on plant traits, leaf chemistry, and microenvironmental

73 conditions. In contrast, stochastic processes, including dispersal and ecological drift, contribute

74 to variability in microbial composition, leading to chance-based fluctuations in community

75 structure (Chaudhry et al. 2021; Kembel et al. 2014; Moroenyane et al. 2021a,b). The relative

76 influence of these processes remains an open question and is expected to vary drastically across

77 spatial and temporal scales, particularly in temperate forest ecosystems undergoing dramatic  
78 seasonal transitions.

79 Host species identity is a well-established driver of leaf microbiome structure, with  
80 studies showing significant interspecific variation in microbial composition (Emmett et al. 2017;  
81 Laforest-Lapointe et al. 2016a,b; Redford et al. 2010). Variations between plants growing in  
82 proximity suggest that functional traits like leaf morphology and secondary metabolites mediate  
83 leaf microbial dynamics (Kembel et al. 2014). Consequently, tree species may exert differential  
84 selection pressures on leaf microbiota, affecting interspecific differences in microbiome  
85 diversity, composition, and functional roles. Notably, most research has focused on highly  
86 divergent taxa (e.g., angiosperms vs. gymnosperms), leaving gaps in our understanding of  
87 microbial variation among functionally similar, less divergent species, broadly speaking  
88 (Laforest-Lapointe et al. 2016a,b; Lajoie and Kembel 2021; Sangiorgio et al. 2024; Wang et al.  
89 2023). This study investigates the leaf bacterial dynamics of two widespread deciduous broadleaf  
90 tree species, grey birch (*Betula populifolia*) and trembling aspen (*Populus tremuloides*). Grey  
91 birch is a stress-tolerant pioneer species native to northeastern North America. Thriving in  
92 nutrient-poor, disturbed habitats, its high phenotypic plasticity and rapid growth make it an ideal  
93 system for studying microbial dynamics under fluctuating conditions (Lavoie and Pellerin 2015).  
94 Trembling aspen, the most widely distributed tree in North America, can form extensive clonal  
95 stands; it, too, is a pioneer species but prefers drier, well-drained soils (Greer et al. 2016). Their  
96 distinct ecological strategies provide a comparative framework for examining differences in  
97 microbiome structure across functionally similar yet phylogenetically distant host tree species.

98 Furthermore, unlike tropical ecosystems and controlled greenhouse conditions, temperate  
99 forests experience pronounced seasonal temperature fluctuations, driving distinct dormancy and

100 growth cycles (Piao et al. 2019). In temperate deciduous forests and high-latitude regions like  
101 Canada, tree phenology is governed by developmental thresholds that are regulated by  
102 accumulated thermal energy above a species-specific base temperature. Given that climate  
103 change is inducing shifts in plant phenology (Meier et al. 2021; Piao et al. 2019), cumulative  
104 GDDs provide a physiologically relevant metric for tracking phenological shifts by integrating  
105 thermo-temporal dynamics, improving predictions of key stages like budburst and leaf expansion  
106 over models based on static calendar-based methods despite thermo-temporal and interannual  
107 seasonal variations (McMaster and Wilhelm 1997; Prentice et al. 1992).

108         Distinct from broad metrics like mean annual temperature or spatial proxies such as  
109 elevation and latitude/longitude—which conflate climatic, spatial, and ecological factors—GDD  
110 accumulation represents the active, useable heat energy that an organism has received during a  
111 given period, at a finer resolution (McMaster and Wilhelm 1997; Prentice et al. 1992). Emerging  
112 evidence suggests that seasonal changes in temperature and precipitation influence tree  
113 phyllosphere bacterial communities by altering physicochemical conditions of the environment  
114 (Hacquard et al. 2022; Sangiorgio et al. 2024; Wang et al. 2023); thus, as rising temperatures  
115 accelerate GDD accumulation, altered trends in seasonal host phenology may generate  
116 disruptions to microbial colonization patterns, plant-microbe interactions, and broader ecosystem  
117 processes. To the best of our knowledge, and despite increasing recognition that host filtering  
118 and temperature shape leaf microbial communities, no studies have examined how the leaf  
119 microbiome responds to a phenology-regulating thermal metric like GDD accumulation. Yet, as  
120 climate change alters temperature regimes and extends growing seasons, temperature-driven  
121 shifts in plant phenology are increasingly recognized as a key ecological concern (Meier et al.  
122 2021; Piao et al. 2019).

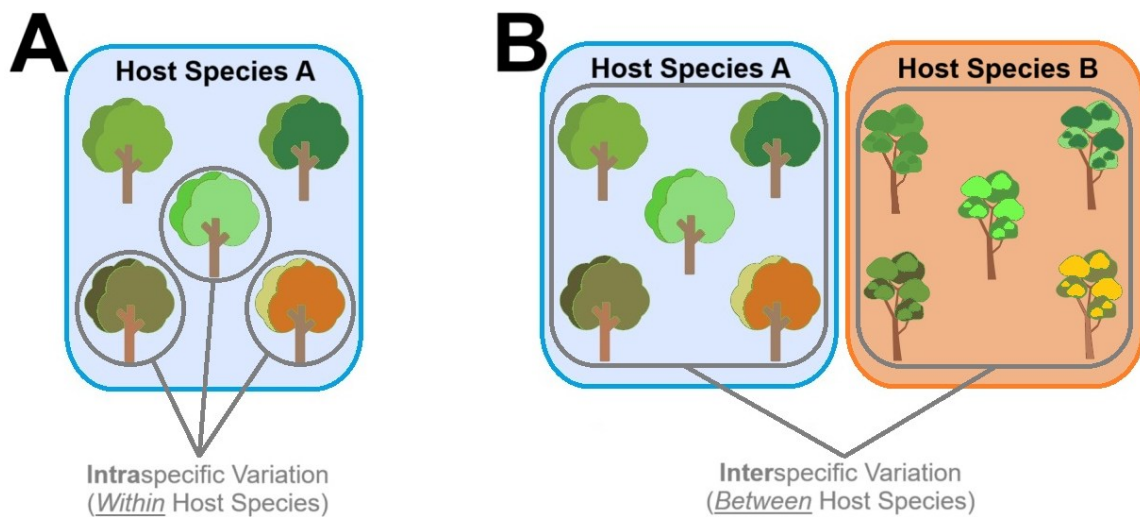
123 Similarly, although time, temperature, and plant developmental compartments have been  
124 shown to influence plant microbial dynamics discretely, attempts to identify a direct link to  
125 seasonal phenological change through the lens of a continuous, temperature-based framework  
126 such as GDD accumulation are lacking (Ginnan et al. 2022; Moroenyane et al. 2021a,b;  
127 Sangiorgio et al. 2024). As such, high-resolution analyses integrating these variables are needed  
128 to clarify how seasonal phenology influences bacterial diversity and community structure in  
129 temperate forest leaves and deduce the ecological mechanisms underlying plant microbial  
130 seasonal assembly and dynamics.

### 131 **Research Aims and Objectives**

132 The primary aim of this M.Sc. project is to assess how host species identity and  
133 temperature-driven phenology influence bacterial diversity and community composition in the  
134 leaf phyllosphere and endosphere of deciduous broadleaf trees in a temperate forest of Quebec.  
135 Using a metacommunity framework, this study examines microbial variations along a gradient of  
136 GDD accumulation, focusing on two co-occurring species—grey birch and trembling aspen—  
137 which share broad functional groupings (deciduousness; broadleaf leaf type) but with divergent  
138 phylogenetic histories. The specific objectives of my study are to: (1) Determine the relative  
139 influence of host species identity and GDD accumulation on seasonal patterns of leaf bacterial  
140 diversity and community composition; (2) investigate whether the microbiomes of two  
141 functionally similar but phylogenetically distinct host tree species respond similarly or  
142 divergently to GDD accumulation; (3) observe how thermal timing (GDD accumulation)  
143 structures leaf bacterial microbiomes across host seasonal phenology; and (4) ascertain whether  
144 or not leaf bacterial communities exhibit thermal niche differentiation over time, and deduce how  
145 patterns of generalist and specialist taxa vary within and between host species along phenology.

146 **Motivation and Approach**

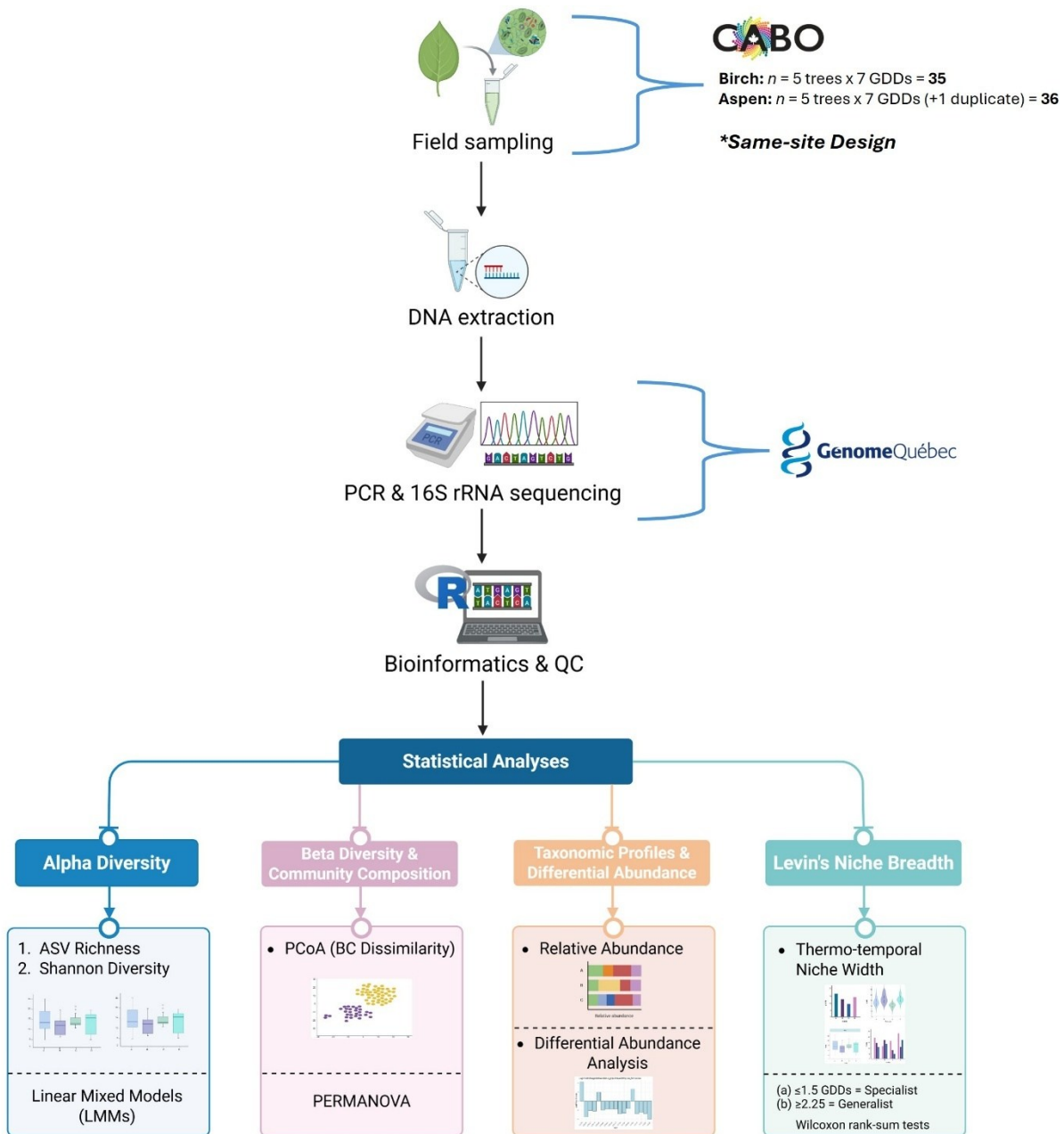
147 My study is motivated by the need to improve our understanding of how climate-driven  
148 phenological shifts influence leaf phyllosphere and endosphere bacterial diversity and  
149 community structure to better predict microbial responses to environmental change and inform  
150 ecological modeling, forest management, and climate adaptation. I examine microbial  
151 persistence and community shifts across host phenology in response to GDD accumulation,  
152 assessing interspecific (between-host species) and intraspecific (within-host species) variation  
153 (Fig. 1.2). Climate change is altering phenological timing, especially in broadleaved species; yet,  
154 its impact on leaf microbiomes remains poorly understood (Meier et al. 2021; Piao et al. 2019).  
155 To address this, I applied a metacommunity framework using cumulative GDDs to quantify  
156 phenological changes in leaf bacterial microbiomes and assess deterministic versus stochastic  
157 bacterial assembly, providing a scalable, physiologically relevant approach for predicting  
158 microbial responses to climate-driven phenological shifts (McMaster and Wilhelm 1997;  
159 Prentice et al. 1992).



160

161 **Figure 1.2.** Schematic demonstrating the difference between **(A)** intraspecific variation (variation within a  
162 host species) and **(B)** interspecific variation (variation between host species). In this study, “Host Species  
163 A” and “Host Species B” represent the two host study systems, grey birch and trembling aspen.

164 My thesis is structured around a single main chapter (Chapter 2), which presents the  
165 primary research investigation. High-throughput 16S rRNA gene sequencing was used to  
166 characterize bacterial diversity and composition in the phyllosphere and endosphere of grey birch  
167 and trembling aspen at the ASV level. Using R, linear mixed models assessed the effects of host  
168 species, plant identity, and GDD accumulation on microbial alpha diversity, while beta diversity  
169 analyses assessed changes in community composition by employing Principal Coordinates  
170 Analysis (PCoA) and PERMANOVAs. Taxonomic profiles were generated using the SILVA  
171 reference database and differential abundance testing identified microbial shifts across  
172 phenological stages. Finally, thermal niche breadth was determined using Levin's niche width  
173 The general workflow is provided in Figure 1.3 (R Core Team, 2024).



174

175 **Figure 1.3.** Overview of the metagenomics workflow used in this study. Raw sequencing reads were  
 176 processed using the DADA2 pipeline, including quality filtering, denoising, chimera removal, and amplicon  
 177 sequence variant (ASV) inference. Taxonomic classification was performed using the SILVA reference  
 178 database, followed by diversity analyses (ASV richness, Shannon diversity, beta diversity), taxonomic  
 179 profiling, differential abundance analysis, and assessments of Levin's niche breadth. Statistical analyses,  
 180 including linear mixed models (LMMs), PERMANOVA, and differential abundance testing (DESeq2), were  
 181 applied to assess the impact of host species identity, growing degree days (GDD), and individual plant  
 182 factors on the leaf microbiome. Figure made using: <https://biorender.com>.

## Chapter 2

# **Growing degree days shape host-specific leaf bacterial community dynamics and thermal niche strategies in two functionally similar temperate tree species\***

Jordan Wilson-Morrison<sup>1,2,3</sup>, Itumeleng Moroenyane<sup>4</sup>, Rosalie Beauchamp-Rioux<sup>5</sup>, Subbaiah Mechanda<sup>2</sup>, Etienne Laliberté<sup>5</sup>, Julian Starr<sup>1</sup>, Warren Cardinal-McTeague<sup>3</sup>

1. Department of Biology, University of Ottawa, Gendron Hall, Room 286, 30 Marie Curie Pvt., Ottawa, Ontario K1N 6N5, Canada.
2. Agriculture and Agri-Food Canada (AAFC), 960 Carling Ave., Ottawa, Ontario K1A 0C6, Canada.
3. Department of Forest and Conservation Sciences, Forest Sciences Centre, University of British Columbia, 2424 Main Mall, Vancouver, British Columbia V6T 1Z4, Canada.
4. Plant Holobiont Lab, Department of Botany and Zoology, Stellenbosch University, Merriman Avenue, Stellenbosch, Western Cape, 7600, South Africa.
5. Canadian Airborne Biodiversity Observatory (CABO), Institut de recherche en biologie végétale (IRBV), 4101 Sherbrooke St. E., Montreal, Quebec H1X 2B2, Canada.

\*Manuscript intended for submission to *Phytobiomes Journal (APS)*

## 183 1.0 INTRODUCTION

184 The phyllosphere—the total aboveground surface of plants—hosts a vast and dynamic  
185 assemblage of microorganisms that influence plant function, fitness, and ecosystem processes  
186 (Chaudhry et al. 2021; Vorholt 2012). Among these, leaf-associated bacteria play a central role in  
187 nutrient cycling, atmospheric interactions, and protection against pathogens, making them  
188 critical ecological actors (Kembel et al. 2014; Compant et al. 2019). Although the diversity and  
189 structure of phyllosphere microbiomes vary within and between host species, they often exhibit  
190 stable core assemblages shaped by their host species, environmental conditions, and  
191 spatiotemporal processes (Grady et al. 2019; Kembel et al. 2014). Yet, the mechanisms  
192 governing the seasonal assembly and turnover of these communities remain incompletely  
193 understood, particularly with respect to temperature-mediated processes and their interplay with  
194 host phenology (i.e., the seasonal timing of plant processes and development).

195 In temperate ecosystems, the timing of plant growth and development (i.e., phenology)  
196 unfolds gradually and sequentially through the growing season, strongly directed by the  
197 accumulation of heat units (McMaster and Wilhelm 1997; Prentice et al. 1992). Since phenology  
198 follows temperature-driven schedules, growing degree days (GDDs) are a well-established,  
199 biologically meaningful metric that captures this progression by quantifying the accumulation of  
200 daily thermal energy above a species- or process-specific baseline temperature, below which  
201 development is assumed negligible (McMaster and Wilhelm 1997; Prentice et al. 1992). Widely  
202 used in agronomy and ecological modeling, GDDs have proven particularly valuable in  
203 predicting the pace of plant maturity, regardless of annual temperature fluctuations. Thus, GDDs  
204 serve as a standardized physiological clock that often tracks phenology more reliably than Julian  
205 date and enable high-resolution comparisons across years, individuals, and ecosystems. Indeed,

206 microbial taxa with distinct thermal preferences or phenological associations may exhibit  
207 seasonal turnover along the GDD continuum, paralleling classical theories of trait-based  
208 environmental filtering and niche partitioning, with thermal accumulation acting as a seasonal  
209 environmental filter that constrains bacterial persistence, recruitment, and turnover in the leaf  
210 phyllosphere and endosphere (Weiher et al. 1998; Chase and Leibold 2003).

211         While recent studies have begun to infer plant microbial responses to temperature from  
212 experimental warming (Faticov et al. 2021), elevational gradients (Huang et al. 2023; Wang et al.  
213 2023), mean annual temperature, and continental-scale climate gradients (Sangiorgio et al. 2024),  
214 these studies mainly focus on the rhizosphere and/or fungi; moreover, these approaches can  
215 obscure fine-scale seasonal ecological dynamics and conflate temperature effects with other  
216 climate variables or long-range microbial dispersal. In contrast, this study examines thermal  
217 accumulation under shared environmental conditions *in situ*, allowing clearer attribution of  
218 microbial responses to thermal-time dynamics in natural forest ecosystems. GDDs offer a  
219 continuous metric that integrates temperature-regulated host phenology with the ecological  
220 context in which leaf microbiomes assemble and shift temporally. Additionally, while host  
221 species identity is widely acknowledged as a dominant—if not the primary—factor shaping the  
222 leaf microbiome (Laforest-Lapointe et al. 2016a,b; Lajoie and Kembel 2021), its role relative to  
223 seasonal thermal accumulation, and how these effects interact, remains underexplored, especially  
224 within functionally similar host groups.

225         To address these gaps, we investigated how temperature accumulation, expressed as  
226 GDDs, influences the diversity, composition, and ecological structure of bacterial communities  
227 inhabiting the leaf phyllosphere and endosphere of two temperate tree species: Grey birch  
228 (*Betula populifolia* Marshall; Betulaceae, Fagales) and trembling aspen (*Populus tremuloides*

229 Michx.; Salicaceae, Malpighiales). Belonging to different orders, these Rosids are functionally  
230 similar (fast-growing, early-successional, deciduous broadleaf species), yet phylogenetically  
231 distant, enabling us to assess microbial responses within a shared environment while providing a  
232 unique opportunity to disentangle host functional similarity from phylogenetic relatedness in  
233 microbiome responses. By sampling host leaves from naturally co-occurring trees growing in the  
234 same forest site in Québec at seven points along the seasonal GDD gradient, we minimized  
235 environmental confounders and isolated the effects of cumulative thermal-time (GDDs), host  
236 species identity, and their two-way interaction. My primary objective is to describe general  
237 patterns of seasonal phenological variation in leaf bacterial phyllosphere and endosphere  
238 microbiomes of grey birch and trembling aspen across a gradient of GDD accumulation.  
239 Specifically, I seek to address the following research questions:

- 240 1. Do the microbiomes of two functionally similar but phylogenetically distinct host tree  
241 species—birch and aspen—respond similarly or divergently to GDD accumulation?
- 242 2. How does thermal timing (GDD accumulation) structure the diversity and composition of  
243 leaf bacterial communities across host seasonal phenology?
- 244 3. Do bacterial communities exhibit thermal niche differentiation over time, and how do  
245 patterns of generalism and specialization vary within and between host species?

246 I hypothesized that (1) host species identity is the primary driver of leaf microbial  
247 community turnover, shaping presence, abundance, and diversity; (2) despite shared functional  
248 type, grey birch and trembling aspen will host distinct microbiomes with divergent temperature-  
249 driven seasonal dynamics, but that there will be a lesser degree of interspecific variation  
250 compared to other studies due to functional similarity; (3) GDD accumulation will have a  
251 significant indirect impact on shaping leaf microbial dynamics through the interaction between

252 host biotic attributes (i.e., host identity) and thermally-regulated phenology, reflecting species-  
253 specific interactions with GDD accumulation; and (4) bacterial taxa and ASVs will exhibit  
254 thermal niche differentiation along the GDD gradient, with each species hosting leaf  
255 microbiomes that exhibit distinct ecological strategies.

256 By focusing on continuous thermal accumulation as both a proxy for phenology and an  
257 ecological gradient in its own right, this study advances understanding of plant-microbe  
258 interactions in temperate forests. This study extends phenological modeling into the microbial  
259 domain, where cumulative temperature not only influences host phenology but also drives  
260 microbiome diversity, structure, and potential ecological consequences. Furthermore, this work  
261 offers novel insights into how microbiomes respond to seasonal thermal dynamics and  
262 underscores the importance of integrating microbial ecology with climate-sensitive phenological  
263 frameworks in a rapidly warming world. In doing so, we explore the potential of leaf  
264 microbiomes to act as biosensors of active heat accumulation related to host phenological  
265 change, revealing possible unrealized applications of the GDD index to microbial ecology.

## 266 **2.0 MATERIALS AND METHODS**

267 All data processing and statistical analyses were performed using R v.2024.09.0 (R Core  
268 Team 2024). An  $\alpha = 0.05$  was used as the significance threshold.

269 **2.1 Host Leaf Sampling and Estimating Seasonal Phenology (Growing Degree Days)**—To  
270 assess the leaf bacteriome over host phenology, 36 leaf disk samples of trembling aspen  
271 (*Populus tremuloides* Michx., Salicaceae, Malpighiales) and 35 leaf samples of grey birch  
272 (*Betula populifolia* Marshall, Betulaceae, Fagales) were provided by my collaborators at the  
273 Canadian Airborne Biodiversity Observatory (CABO), found at <https://www.caboscience.org>

274 and at the Université de Montréal. Alongside the samples, sample data were also provided by my  
 275 CABO colleagues (Kothari et al. 2023). Upon receipt, all leaf disk samples were stored in a -  
 276 80°C freezer. These leaf disks were collected along a six-month chronosequence spanning the  
 277 months of June 2018 to October 2018; roughly, specimens were sampled biweekly (Table 1). For  
 278 each sample, a large group of sunlit leaves (>3 h estimated sun exposure per day) were collected  
 279 at the same vertical position; for each tree, the same branch or neighboring branches from the  
 280 same individual were sampled. Leaves with noticeable damage were avoided.

281 **Table 2.1.** Cumulative growing degree days (GDDs) at a base temperature of 5°C and their  
 282 corresponding sampling dates classified into generalized phenological periods for temperate trees in the  
 283 Northern Hemisphere.

Cumulative Growing Degree Days ( $T_{base} = 5^{\circ}\text{C}$ )	Sampling Date	General Phenological Period
437	June 8, 2018	Early-Mid
605	June 21, 2018	Early-Mid
1087	July 19, 2018	Mid
1606	August 16, 2018	Mid-Late
1992	September 11, 2018	Late
2140	September 24, 2018	Late
2219	October 8, 2018	Late-Early Senescence

284 Since this study seeks to evaluate phenology as a continuous response variable that  
 285 encompasses both thermal and temporal dimensions, sampling dates were converted to  
 286 cumulative growing degree days (GDDs) using 2018 temperature data from the Montréal/Saint-  
 287 Hubert weather station in Québec. To calculate cumulative GDDs at a base temperature of 5°C  
 288 from the first day of the year ( $j = 1$ ) to a given sampling day of the year ( $DOY$ )  $i$ , the following  
 289 equation was employed, as described by McMaster and Wilhelm (1997):

290 
$$\text{Cumulative GDD on } DOY\ i = \sum_{j=1}^i \left[ \frac{(T_{max,j} + T_{min,j})}{2} \right] - T_{base}$$

291           Where  $T_{max,j}$  is the temperature maxima on sampling day  $j$ ,  $T_{min,j}$  is the temperature  
292 minima on sampling day  $j$ , and  $T_{base}$  is the chosen base temperature of 5°C. Thus, GDDs 437,  
293 605, 1087, 1606, 1992, 2140, and 2219 represent the cumulative GDD sampling points along the  
294 continuum of host phenology (Table 1). For each of the two host species, five individual plants  
295 were sampled at each of the seven GDDs ( $N = 10$ ), with the exception of an inadvertently  
296 repeated sample taken from the same aspen individual at GDD = 1087, resulting in  $N = 11$   
297 (Kothari et al. 2023). The additional aspen sample was retained to avoid omitting potentially  
298 valuable microbiome data, resulting in a total sample size of  $n = 71$  samples, with 35 samples for  
299 birch and 36 samples for aspen. Each individual serves as a biological replicate, and the same  
300 individuals are resampled at each GDD point, providing temporal resolution across the seven  
301 GDD points.

302 **2.2 DNA Extraction**—To isolate microbial DNA from leaf disks, the Qiagen DNeasy<sup>®</sup>  
303 PowerLyzer<sup>®</sup> PowerSoil<sup>®</sup> kit was used according to the manufacturer’s instructions, with some  
304 procedural adjustments. Although the extraction protocol calls for up to 0.25 g of sample, only  
305 20 mg of leaf tissue was used due to limited leaf material. To account for microbial “kitome”  
306 effects exerted by the three DNA extraction kits used, a negative control was performed;  
307 additionally, there were two positive controls prepared using the ZymoBIOMICS™ Microbial  
308 Community Standard (Catalog No. D6300, Zymo Research Corp., Irvine, CA, USA).

309 **2.3 Amplification and Sequencing of 16S rRNA Gene**—To conduct microbiome profiling, PCR  
310 amplification and sequencing targeted the V3-V4 hypervariable regions of the bacterial 16S  
311 rRNA gene. All PCRs and sequencing were conducted at the Genome Québec Innovation  
312 Centre. To amplify 16S rRNA regions, the Illumina primer pair 520F

313 (AGCAGCCGCGGTAAT)/799R2 (CAGGGTATCTAATCCTGTT) was used to exclude  
314 chloroplast sequences, targeting an amplicon length of approximately 280 bp (Edwards et al.  
315 2007). All primers were fitted with adapter sequences for multiplex sequencing. Extracted DNA  
316 was organized and submitted on the Genome Québec Innovation Centre’s sequencing  
317 submission portal, Nanuq. Sequencing libraries were constructed with this DNA using paired-  
318 end reads on the Illumina MiSeq platform (Moroenyane et al. 2021a; Moroenyane et al. 2021b;  
319 Zhou et al. 2011).

320 **2.4 Sequence Quality Control, Filtering, and Taxonomic Assignment of ASVs**—Reads were  
321 processed using the *DADA2* pipeline in R (Callahan et al. 2016; Lajoie and Kembel 2021; R  
322 Core Team 2024). Next, an amplicon sequence variant (ASV) table was generated from the  
323 merged sequences. Chimeric sequences were identified and removed using the  
324 ‘removeBimeraDenovo()’ function, which reconstructs chimeras from segments of abundant  
325 parent sequences (Callahan et al. 2017). In this dataset, approximately 97.74% of sequences were  
326 non-chimeric. Reads identified as mitochondria and chloroplasts were removed, and samples  
327 from GDD 323 were excluded due to missing data for *P. tremuloides*. Altogether, these  
328 adjustments reduced the total number of reads to 133015 and resulted in 1731 ASVs.

329 **2.5 Statistical Analyses**—All statistical analyses were conducted using R v.2024.09.0 (R Core  
330 Team, 2024). The bacterial ASV abundance data were normalized such that the summed relative  
331 abundance of all ASVs of each sample was equal to one. All analyses were repeated to assess  
332 both interspecific and intraspecific variation in host tree microbiomes, with specific adjustments  
333 that will be described in the following sections.

334 **2.5.1 Bacterial Alpha Diversity Patterns—Sampling Effort and ASV Diversity:** ASV  
335 accumulation curves were generated for all samples and for the positive control using the  
336 ‘specaccum()’ function from the *vegan* package to determine if the sampling effort was sufficient  
337 to recover the majority of ASV diversity (Oksanen et al. 2022; Moroenyane et al. 2021a;  
338 Moroenyane et al. 2021b). In this study, the curve asymptotes in both cases, indicating that the  
339 sampling effort captured the majority of detectable ASV diversity (Supplementary Fig. S1). To  
340 evaluate the estimated richness and occurrence of both abundant and rare taxa, Preston log-  
341 normal curves were generated using the ‘prestondistr()’ function in *vegan*. The observed data  
342 fitted well to the normal distribution, suggesting a high probability that both abundant and rare  
343 ASVs were captured in this study (Supplementary Fig. S2).

344 **Alpha Diversity Calculations:** From the *vegan* package, ASV richness (the total number  
345 of unique ASVs per sample) was calculated using the ‘specnumber()’ function, and Shannon  
346 diversity was calculated using the ‘diversity()’ function with the index parameter set to  
347 “shannon” (Oksanen et al. 2022; Moroenyane et al. 2021a; Moroenyane et al. 2021b). To  
348 visualize diversity patterns, raw data for both metrics were plotted as a function of GDD  
349 accumulation at  $T_{\text{base}} = 5^{\circ}\text{C}$  and their associated months for both host species.

350 **Alpha Diversity Modelling and Statistical Analysis:** To evaluate the effects of  
351 accumulated thermal energy (GDDs), host identity, and their interaction on bacterial alpha  
352 diversity, ASV richness and Shannon diversity were modeled using linear mixed models (LMMs)  
353 using the ‘lmer()’ function from *lme4* (Bates et al. 2015). Separate models were fit for inter- and  
354 intraspecific comparisons according to model assumptions and diagnostics. For interspecific  
355 models, ASV richness was log-transformed, and Shannon diversity was square-root transformed.  
356 Fixed effects included host species identity, GDDs ( $T_{\text{base}} = 5^{\circ}\text{C}$ ), and their interaction, with

357 ‘Plant\_ID’ included as a random effect to account for repeated measures. Intraspecific models  
358 were constructed separately for each host species, with appropriate transformations applied to  
359 meet model assumptions (Supplemental Methods S2.5.1). To assess post-hoc contrasts, estimated  
360 marginal means were generated using the *emmeans* package, and both marginal ( $R^2_m$ ) and  
361 conditional ( $R^2_c$ )  $R^2$  values were calculated to quantify explanatory power of the models and  
362 fixed effects (Lenth 2024). Final model structures, full model diagnostics, pairwise comparisons,  
363 and methodological details are presented in the *Supplementary Methods*.

364 **2.5.2 Bacterial Community Structure (Beta Diversity)**— To assess beta diversity, a  
365 Bray-Curtis dissimilarity matrix was generated using ‘vegdist()’ in *vegan*, and principal  
366 coordinate analysis (PCoA) was conducted using ‘pcoa()’ from *ape* to visualize inter- and  
367 intraspecific differences in leaf bacterial communities along a GDD accumulation gradient  
368 (Moroenyane et al. 2021a; Oksanen et al. 2022; Paradis and Schliep 2019). Multivariate  
369 dispersion was evaluated using ‘betadisper()’ followed by ‘permutest()’, employing ANOVA  
370 with 999 permutations (Moroenyane et al. 2021a; Oksanen et al. 2022). Next, post-hoc pairwise  
371 comparisons of all variable groupings were assessed via ‘TukeyHSD()’ (R Core Team 2024).  
372 Finally, the 95% confidence intervals for the Tukey HSD results of each variable grouping were  
373 plotted (Moroenyane et al. 2021a). For interspecific comparisons, groupings included host  
374 ‘Species’, ‘GDD\_5C’, and their two-way interaction. For intraspecific comparisons, groupings  
375 included ‘GDD\_5C’ and ‘Plant\_ID’. These steps evaluated whether significant differences in  
376 beta diversity detected in subsequent PERMANOVA analyses could be influenced by unequal  
377 within-group variability.

378 To determine the drivers of variation in community composition and quantify their  
379 explanatory power, PERMANOVA was performed with 999 permutations using the ‘adonis2()’

380 function in *vegan*, to model the effects of host species ('Species'), cumulative growing degree  
381 days at a base temperature of 5°C ('GDD\_5C'), and their two-way interaction on leaf bacterial  
382 community composition and turnover (Faticov et al. 2021; Moroenyane et al. 2021a; Oksanen et  
383 al. 2022). For intraspecific comparisons, the same method was applied, but PERMANOVA was  
384 used to model the effects of 'GDD\_5C', 'Plant\_ID', and their two-way interaction on leaf  
385 bacterial community composition. All models here were run using absolute ASV count data.

386         **2.5.3 Relative Abundance and Taxonomic Profiles**—Using the 'tax\_glom()' and  
387 'transform\_sample\_counts()' functions from the *phyloseq* package in R, the relative abundances  
388 of leaf bacterial taxa were calculated and then plotted at the phylum and genus levels for birch  
389 and aspen across GDDs to evaluate and compare general phenological patterns in taxonomic  
390 shifts within and between host species (McMurdie and Holmes 2013). All recovered bacterial  
391 phyla were presented, but only the top 20 genera by relative abundance were visualized, as the  
392 large number of genera—particularly those with lower abundances—made comprehensive  
393 visualization impractical. Relative abundances were calculated within each sample by dividing  
394 ASV counts by the sample's total read count, yielding proportions that sum to 1. This  
395 transformation standardizes for sequencing depth while preserving sample-specific community  
396 composition. Taxonomic profiles of leaf bacterial relative abundances were generated as a  
397 preliminary analysis to evaluate general phenological patterns in taxonomic shifts and identify  
398 dominant bacterial taxa associated with each host tree species and phenological stage.

399         **2.5.4 Differential Abundance Analysis**—To assess how leaf bacterial ASVs (and their  
400 associated taxonomic assignments) responded to seasonal GDD accumulation, differential  
401 abundance analysis was performed using the *DESeq2* package in conjunction with the *phyloseq*  
402 package (Faticov et al. 2021; Love et al. 2014; McMurdie and Holmes 2013). Analyses were

403 conducted separately for each host species (grey birch and trembling aspen) to identify ASVs  
404 whose relative abundance changed significantly across the seasonal gradient of thermal  
405 accumulation, measured as continuous GDDs. Starting with the filtered *phyloseq* object, the  
406 abundance data was converted into a *DESeq2* object using the ‘*phyloseq\_to\_deseq2()*’ function.  
407 For each species, the model formula “~ GDD\_5C” was used, treating GDD as a continuous  
408 numeric predictor. This allowed testing for log<sub>2</sub> fold changes in ASV abundance per unit  
409 increase in cumulative GDD, effectively modeling temperature-driven phenological progression  
410 without discretizing the thermal gradient. Size factors were estimated internally using *DESeq2*’s  
411 default method, which applies median-of-ratios normalization to account for library size  
412 differences. Dispersion estimates and shrinkage of log<sub>2</sub> fold changes were calculated using the  
413 default *DESeq2* pipeline. *P*-values were adjusted for multiple testing using the Benjamini–  
414 Hochberg false discovery rate (FDR) method (Faticov et al. 2021; Love et al. 2014). ASVs were  
415 considered significantly differentially abundant across GDD when FDR-adjusted  $p < 0.05$ .

416 To facilitate ecological interpretation, we annotated differentially abundant ASVs to the  
417 genus level and visualized patterns of log<sub>2</sub> fold change across the GDD gradient. Positive log<sub>2</sub>  
418 fold changes indicate increased abundance with thermal accumulation, while negative values  
419 denote declines with increased heat accumulation. This approach enabled us to identify thermally  
420 limited taxa within each host species and relate their seasonal enrichment or depletion to broader  
421 patterns of microbial succession and niche differentiation. For species-specific seasonal  
422 differential abundance analyses, please see *S2.5.4 Differential Abundance Analysis* in the  
423 Supplemental Materials and Methods.

424 **2.5.5 Niche Width Analysis**—To assess bacterial thermal niche breadth across GDD  
425 accumulation, Levins’ niche width index was calculated for each ASV using the ‘*niche.width()*’

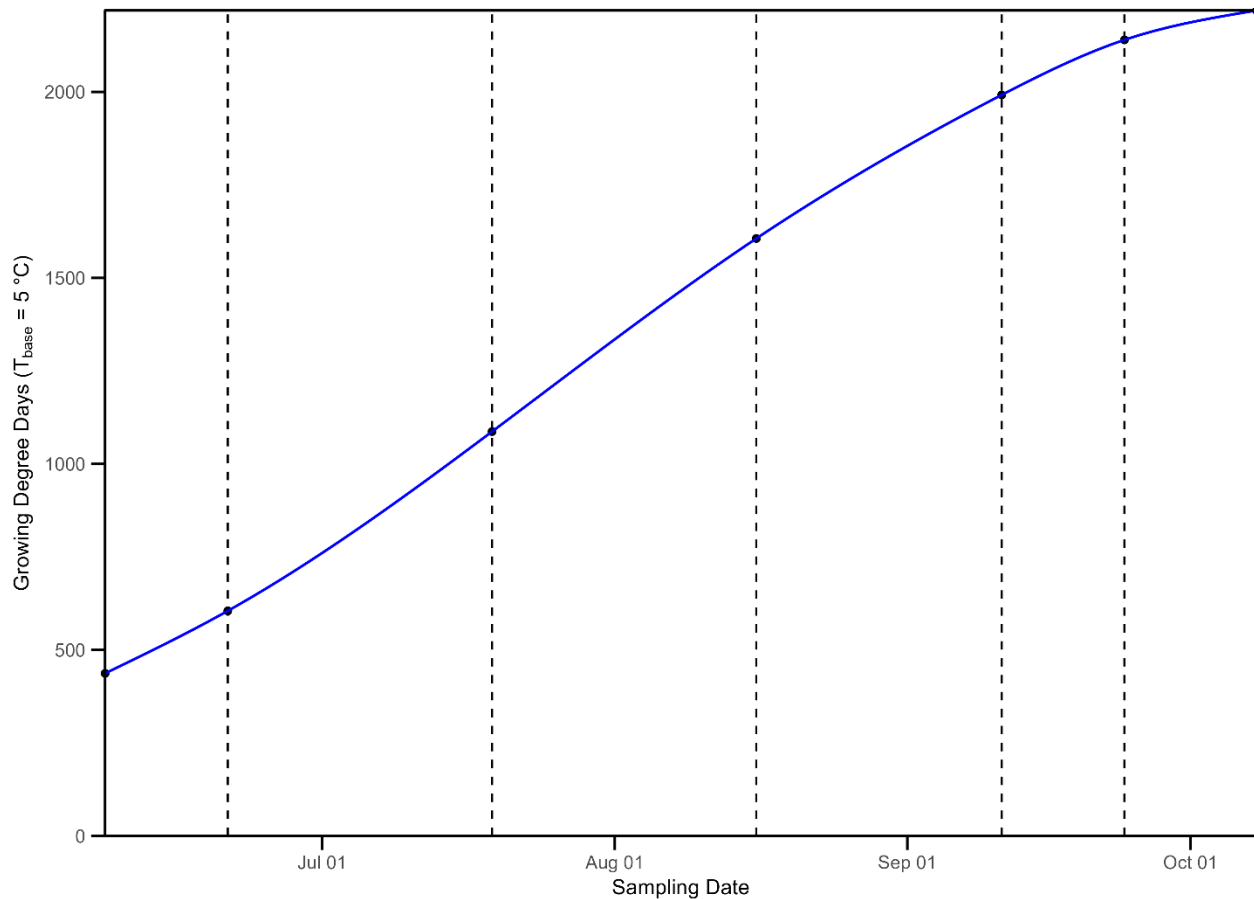
426 function from the *spaa* package in R. Input data consisted of scaled relative abundances of ASVs  
427 across continuous GDD values to standardize across sequencing depth, summed within each  
428 unique GDD value, thus capturing microbial distribution across thermal time. This formulation  
429 incorporates both the presence and evenness of an ASV's abundance across thermal conditions.  
430 Notably, ASVs were retained only if they exhibited non-zero relative abundance across at least  
431 two distinct GDD values, to avoid inflating niche width estimates with single-point occurrences.  
432 To classify ecological strategies, we applied fixed thresholds: ASVs with niche width  $\leq 1.5$  were  
433 designated thermal specialists, those with  $\geq 2.25$  as generalists, and those in between as  
434 intermediate. These thresholds were selected to reflect strongly concentrated distributions ( $\geq 2$   
435 GDDs) versus moderate-to-even distributions across  $\geq 3$  GDDs, while excluding transient or  
436 ambiguously distributed taxa.

437         Distribution of ASV niche breadth were visualized using histograms and proportional bar  
438 plots of specialist, intermediate, and generalist classifications. Classification distributions were  
439 also compared between host species using faceted bar plots. To assess temporal patterns, we  
440 generated boxplots of ASV niche width across cumulative GDD values, subset by host species.  
441 To evaluate taxonomic variation, we plotted niche width by bacterial genus (focal genera only)  
442 and by individual ASV. Total ASV proportion plots (Supplementary Fig. S23) and violin plots of  
443 ASV niche widths by host species (Supplementary Fig. S24) were additionally produced and  
444 included to illustrate distributional spread. Differences in niche width distributions between host  
445 species were tested using Wilcoxon rank-sum tests.

### 446 3.0 RESULTS

447           Across the 2018 growing season, the growing degree day (GDD;  $T_{\text{base}} = 5^{\circ}\text{C}$ )  
448 accumulation curve increased in a sigmoidal fashion, with the highest rates observed during mid-  
449 phenology—occurring between mid-July and the end of August. This pattern of GDD  
450 accumulation offers a cumulative measure of thermal exposure and seasonal progression for both  
451 host species (Fig. 2.1). Sampling dates spanned a cumulative GDD range of 437 to 2219,  
452 capturing early leaf expansion through senescence. This GDD trajectory served as the primary  
453 ecological axis for analyzing temporal shifts in microbial diversity, community composition, and  
454 thermal niche breadth.

455           The amplicon sequence variant (ASV) accumulation curve reveals that sampling  
456 recovered a considerable number of bacterial ASVs, and its asymptote demonstrates saturation or  
457 near-saturation, indicating that sampling effort was comprehensive enough (Supplementary Fig.  
458 S1). Additionally, the Preston log-normal curve is bell-shaped and exhibits practically perfect  
459 overlap with the expected normal distribution; this communicates that sequencing was deep  
460 enough to detect rare and low-abundance bacterial taxa (Supplementary Fig. S2). Taken together,  
461 these figures demonstrate that sampling effort not only recovered the most abundant taxa but also  
462 rare taxa, permitting a more complete insight into the leaf bacterial communities (Moroenyane et  
463 al. 2021a).



464

465 **Figure 2.1.** Cumulative growing degree days (GDDs;  $T_{\text{base}} = 5^{\circ}\text{C}$ ) across the 2018 growing season at the  
 466 study site in Québec. Cumulative GDDs were calculated as the daily mean temperature minus the  $5^{\circ}\text{C}$   
 467 base threshold, summed across all days with positive values. Vertical dashed lines represent leaf  
 468 sampling dates. This curve reflects the seasonal progression of thermal energy accumulation—a  
 469 physiologically relevant metric for predicting plant phenology and a key environmental driver of  
 470 microbiome dynamics in this study.

471 **3.1 Seasonal GDD accumulation drives bacterial richness more than species identity**

472 **and shapes community composition in functionally similar hosts**—Alpha diversity patterns

473 revealed distinct species-specific trajectories over phenology (Fig. 2.2A). Trembling aspen

474 consistently exhibited higher Shannon diversity than grey birch, regardless of GDD ( $P = 0.0413$ ),

475 suggesting stable and more even microbial communities in aspen across the season. In contrast,

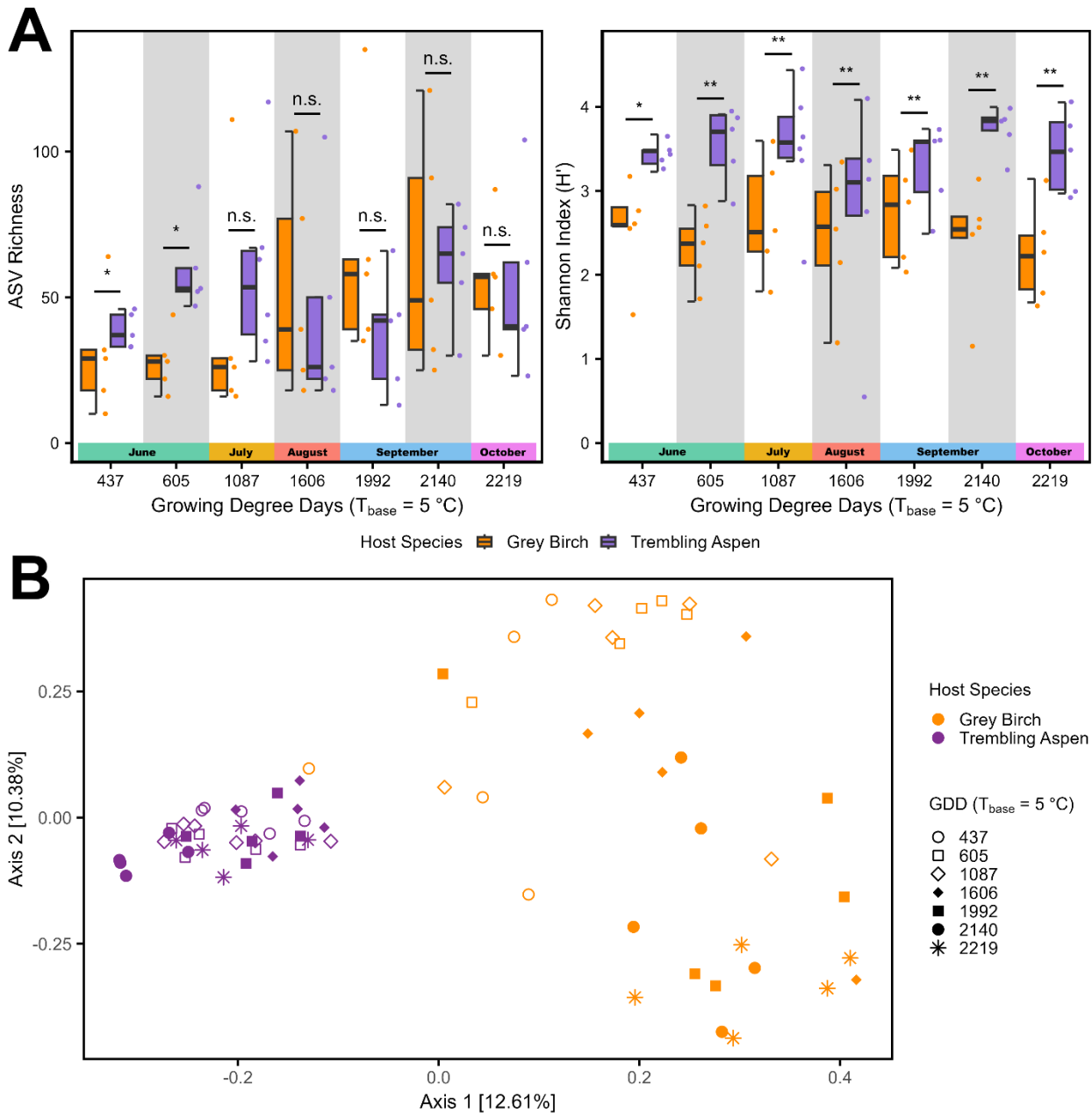
476 ASV richness was more dynamic and sensitive to GDD accumulation, particularly in birch.

477 Linear mixed models showed significant effects of host species ( $P = 0.0086$ ), GDD ( $P = 0.0004$ ),

478 and their interaction ( $P = 0.0053$ ) on ASV richness (Table 2.2). Notably, the interaction (Species

479 x GDD) explained ~32.6% of the variance via fixed effects ( $R^2_c = 0.326$ ) and ~9.94% ( $R^2_m =$   
480 0.0994) when accounting for plant-level random effects. While aspen maintained relative overall  
481 stability across GDDs with modest seasonal variation, birch exhibited a general increase in  
482 richness. However, this pattern was not strictly linear or monotonic: richness rose early, dipped at  
483 mid-season, and rebounded in late phenology, suggesting a multi-phase or non-linear response  
484 (Fig. 2.2A; Supplementary Fig. S3A). Post-hoc pairwise comparisons at specific GDDs  
485 (Supplementary Table S1) found no significant interspecific differences, suggesting the  
486 interaction reflects cumulative patterns rather than sharp divergence at individual time points.

487 While host species explained the most variance in Shannon diversity ( $R^2_c = 34.1\%$ ;  $R^2_m =$   
488 26.1%), highlighting its role in shaping microbial evenness, it contributed minimally to ASV  
489 richness ( $R^2_c = 14.4\%$ ;  $R^2_m = 1.33\%$ ), where cumulative GDDs played a larger role ( $R^2_c = 19.2\%$ ;  
490  $R^2_m = 6.17\%$ ). This suggests host species differences influence evenness and relative abundance  
491 more strongly, while environmental factors like cumulative GDDs shape the total number of  
492 unique ASVs present; in fact, its influence on ASV richness diminishes beyond early-mid  
493 phenology (GDD 605), shifting to host-specific interactions with environmental variables (Table  
494 2.3).



495

496 **Figure 2.2.** Leaf bacterial community diversity and composition patterns of two host tree species, grey  
 497 birch (purple) and trembling aspen (orange), across a season phenological gradient of GDD accumulation  
 498 (June–October 2018) using 16S rRNA gene amplicon sequencing showing **(A)** comparisons of amplicon  
 499 sequence variant (ASV) richness (left) and Shannon diversity (right). Bold horizontal bars represent the  
 500 median and the error bars indicate a measure of variability of the data at each GDD sampling value.  
 501 Circular data points represent individual samples of birch and aspen leaves taken at each sampling point  
 502 along the GDD continuum (total  $n = 71$ ), which are horizontally jittered to avoid overlap. n.s. = non-  
 503 significant host species differences ( $P$ -value  $<0.05$  and  $<<0.01$ ); and **(B)** Principal Coordinate Analysis  
 504 (PCoA) of leaf bacterial community beta diversity based on Bray-Curtis dissimilarities. Each data point  
 505 denotes a host plant individual sampled at GDDs 437 (empty circle), 605 (empty square), 1087 (empty  
 506 diamond), 1606 (filled diamond), 1992 (filled square), 2140 (filled circle), and 2219 (asterisk).

507 **Table 2.2.** Summary of the impact of host species identity (S), GDD accumulation at  $T_{base} = 5^{\circ}C$   
 508 (GDD\_5C), and their interaction (S x GDD\_5C) on the leaf bacterial alpha diversities of grey birch and  
 509 trembling aspen using linear mixed modeling (LMMs).<sup>a</sup>

	Host Species (S)			Growing Degree Days 5°C (GDD_5C)			Interaction (S x GDD_5C)		
	<i>P</i>	$R^2_c$	$R^2_m$	<i>P</i>	$R^2_c$	$R^2_m$	<i>P</i>	$R^2_c$	$R^2_m$
<b>Interspecific<sup>b</sup></b>									
ASV R'	0.00855**	0.144	0.0133	0.000364***	0.192	0.0617	0.00531**	0.326	0.0994
H'	0.0413*	0.341	0.261	0.881	0.34	0.000551	0.978	0.262	0.159
<b>Birch<sup>c</sup></b>									
ASV R'	—	—	—	0.000247***	0.513	0.25	—	—	—
H'	—	—	—	0.731	0.163	0.00297	—	—	—
<b>Aspen<sup>d</sup></b>									
ASV R'	—	—	—	0.427	0.113	0.0164	—	—	—
H'	—	—	—	0.857	0.0374	0.000908	—	—	—

510 <sup>a</sup> Three separate LMMs were run for interspecific comparisons, intraspecific comparisons within each host  
 511 species. Conditional- $R^2$  ( $R^2_c$ ) and marginal- $R^2$  ( $R^2_m$ ) values were calculated using `r.squaredGLMM()` in the  
 512 *MuMIn* package (Bartoń 2023) by running separate models with the same random effect structure but only  
 513 a single fixed effect included ( $P$ -value  $* < 0.05$ ,  $** < 0.01$  and  $*** < 0.001$ ).

514 <sup>b</sup> Interspecific (between-species) results from LMMs for log-transformed ASV richness (ASV R') and square-  
 515 root transformed Shannon diversity (H') comparing leaf microbiomes of grey birch and trembling aspen.

516 <sup>c</sup> Intraspecific (within-species) results from LMMs for ASV richness (ASV R') and Shannon diversity (H') in  
 517 grey birch leaf microbiomes, which have both undergone reciprocal transformations.

518 <sup>d</sup> Intraspecific (within-species) results from LMMs for reciprocally-transformed ASV richness (ASV R') and  
 519 square-root transformed Shannon diversity (H') in trembling aspen leaf microbiomes.

520 Intraspecific analyses further reinforced that the ASV richness of birch microbiomes  
 521 significantly increased with GDD ( $P = 0.00025$ ), explaining over 50% of variance when plant-  
 522 level random effects were included ( $R^2_c = 0.513$ ) and 25% of the variance through fixed effects  
 523 ( $R^2_m = 0.25$ ). However, richness did not differ significantly across individual GDD time points  
 524 (Supplementary Table S2), suggesting a continuous overall trend rather than discrete shifts.  
 525 Within aspen, neither richness nor Shannon diversity varied significantly with GDD. Moreover,  
 526 no significant plant-level effects were observed within species across any GDD (Supplementary  
 527 Tables S6–S7), indicating that environmental gradients, particularly temperature accumulation,  
 528 exert more influence over alpha diversity patterns than individual plant identity. Collectively,

529 these results highlight that functionally similar hosts exhibit divergent alpha diversity responses  
 530 over phenology.

531 **Table 2.3.** Summary of pairwise comparisons of host species-specific differences in leaf bacterial alpha  
 532 diversity at each GDD sampling point (Tbase = 5°C) using the emmeans package in R to evaluate the  
 533 effect of host species identity (S) as seasonal phenology progresses.<sup>a</sup>

GDD_5C	ASV Richness <sup>b</sup>				Shannon Diversity <sup>c</sup>			
	Host Species (S)				Host Species (S)			
	emmean	SE	t-ratio	P	emmean	SE	t-ratio	P
437	-0.6399	0.257	-2.489	0.0198*	-0.263	0.101	-2.602	0.0139*
605	-0.5553	0.238	-2.333	0.0305*	-0.263	0.0924	-2.851	0.0088**
1087	-0.3126	0.198	-1.578	0.146	-0.263	0.0732	-3.596	0.0046**
1606	-0.0513	0.191	-0.269	0.795	-0.263	0.0696	-3.782	0.0048**
1992	0.1431	0.212	0.675	0.512	-0.263	0.08	-3.288	0.0051**
2140	0.2176	0.225	0.967	0.348	-0.263	0.0863	-3.05	0.0065**
2219	0.2574	0.233	1.105	0.284	-0.263	0.09	-2.924	0.0078**

534 <sup>a</sup> Pairwise comparisons only show host species effects, independent of any interaction with GDD, since  
 535 comparisons were isolated to each GDD sampling point, taking the original LMM structures into account.  
 536 The table shows the estimated marginal means (emmean), standard error (SE), *t-ratio*, and *P-values* for  
 537 each GDD sampling point (*P*-value \* $<0.05$ , \*\* $<0.01$ , and \*\*\* $<0.001$ ).

538 <sup>b</sup> ASV richness (R') was log-transformed to align with interspecific LMM assumptions. While host species  
 539 identity may significantly affect ASV R' at earlier GDDs, other seasonal factors may play a larger role in  
 540 shaping interspecific variation in ASV richness beyond earlier-season, lower GDDs.

541 <sup>c</sup> Shannon diversity (H') was square-root transformed to align with interspecific LMM assumptions. H' is  
 542 heavily impacted by host species identity at all points in the growing season, implying it is a strong  
 543 predictor of interspecific variation in H'.

544 To compare seasonal phenological patterns of leaf bacterial beta diversity and community  
 545 structure between birch and aspen across the GDD gradient, a Bray-Curtis dissimilarity matrix  
 546 was generated. Initial analyses of homogeneity and multivariate dispersion helped determine the  
 547 relative influence of between-community composition (variance among samples) and within-  
 548 community composition (variance within replicates) on the overall structure of leaf bacterial  
 549 communities (Moroenyane et al. 2021a). There was significant multivariate dispersion between  
 550 host species (Supplementary Figs. S4–S5). Between birch and aspen, heterogeneous dispersion  
 551 was significant ( $F = 22.812$ ,  $P = 0.001$ ) for host species identity, but little multivariate dispersion

552 was observed across GDDs (Supplementary Figs. S6–S7). Neither species exhibited significant  
553 heterogeneous dispersion across GDDs ( $F = 0.242$ ,  $P = 0.948$ ), and pairwise comparisons using  
554 Tukey HSD tests confirmed non-significant differences in community structure between GDDs.  
555 Thus, despite variations in data spread, central tendencies (means) remained similar.

556 Finally, the interaction between host species and GDDs was assessed, revealing increased  
557 multivariate dispersion compared to any individual variable alone (Supplementary Fig. S8). This  
558 interaction showed significant heterogeneity in dispersion ( $F = 4.724$ ,  $P = 0.001$ ). However, as  
559 this interaction compares all possible combinations of ‘Species’ and ‘GDD\_5C’, including across  
560 dissimilar levels of GDDs, caution is warranted in interpreting these results. This interaction may  
561 not exclusively reflect variations within the same GDD levels, which was the primary focus of  
562 this analysis. Thus, for biological relevance, pairwise comparisons of dispersion using a Tukey  
563 HSD test were only assessed for species-GDD interactions occurring within shared GDDs, but  
564 not across differing GDDs. The Tukey HSD revealed relevant significant differences between  
565 birch leaf interactions with 605 GDDs and aspen leaf interactions with 605 GDDs (early  
566 phenology;  $P = 0.023$ ), as well as between birch’s interaction with 2219 GDDs and aspen’s  
567 interaction with 2219 GDDs (senescence onset;  $P = 0.0021$ ).

568 Principal Coordinate Analysis (PCoA) was performed using Bray-Curtis dissimilarity to  
569 visualize changes in leaf bacterial community structure between grey birch and trembling aspen  
570 across phenology (Fig. 2.2B). PERMANOVA found significant effects from host species identity  
571 ( $F = 9.061$ ,  $P = 0.001$ ), accumulated GDDs ( $F = 3.384$ ,  $P = 0.001$ ), and their interaction ( $F =$   
572  $3.022$ ,  $P = 0.001$ ) on bacterial community variation (Table 2.4). Host species identity explained  
573 ~11% of the variation ( $R^2 = 0.11$ ), GDDs ~4.1% ( $R^2 = 0.041$ ), and the interaction ~3.67% ( $R^2 =$

574 0.0367). The PCoA presents clear separation of bacterial communities based on host species  
575 identity, mostly along Axis 2, though there was no clear separation based on GDDs between  
576 species (Fig. 2.2B). A weak positive correlation was observed between Axis 1 and GDDs  
577 (Spearman's  $\rho = 0.108$ ,  $P = 0.368$ ), indicating no significant association between Axis 1 and  
578 GDDs. In contrast, Axis 2 showed a moderate negative correlation with GDDs ( $\rho = -0.53$ ,  $P =$   
579  $2.25 \times 10^{-6}$ ), suggesting that increasing GDD values are significantly associated with lower Axis 2  
580 scores. Therefore, the directionality in the PCoA from early-phenology (low GDDs) to late-  
581 phenology (high GDDs) is likely associated with Axis 2, which shows a statistically significant  
582 seasonal thermal gradient.

583 **Table 2.4.** Permutational analysis of variance (PERMANOVA) testing the impact of host species identity  
584 ('Species'), GDD accumulation at  $T_{base} = 5^{\circ}\text{C}$  ('GDD\_5C') as a proxy for host phenology, and their two-  
585 way interaction ('Species x GDD\_5C') on differences in leaf beta diversity and bacterial community  
586 composition within and between grey birch and trembling aspen.

Source of Variation	SS	$R^2$	F	P
Species	3.3513	0.11	9.061	0.001***
GDD_5C	1.2516	0.041	3.384	0.001***
Species x GDD_5C	1.1178	0.0367	3.022	0.001***
Residuals	24.7794	0.812	—	—

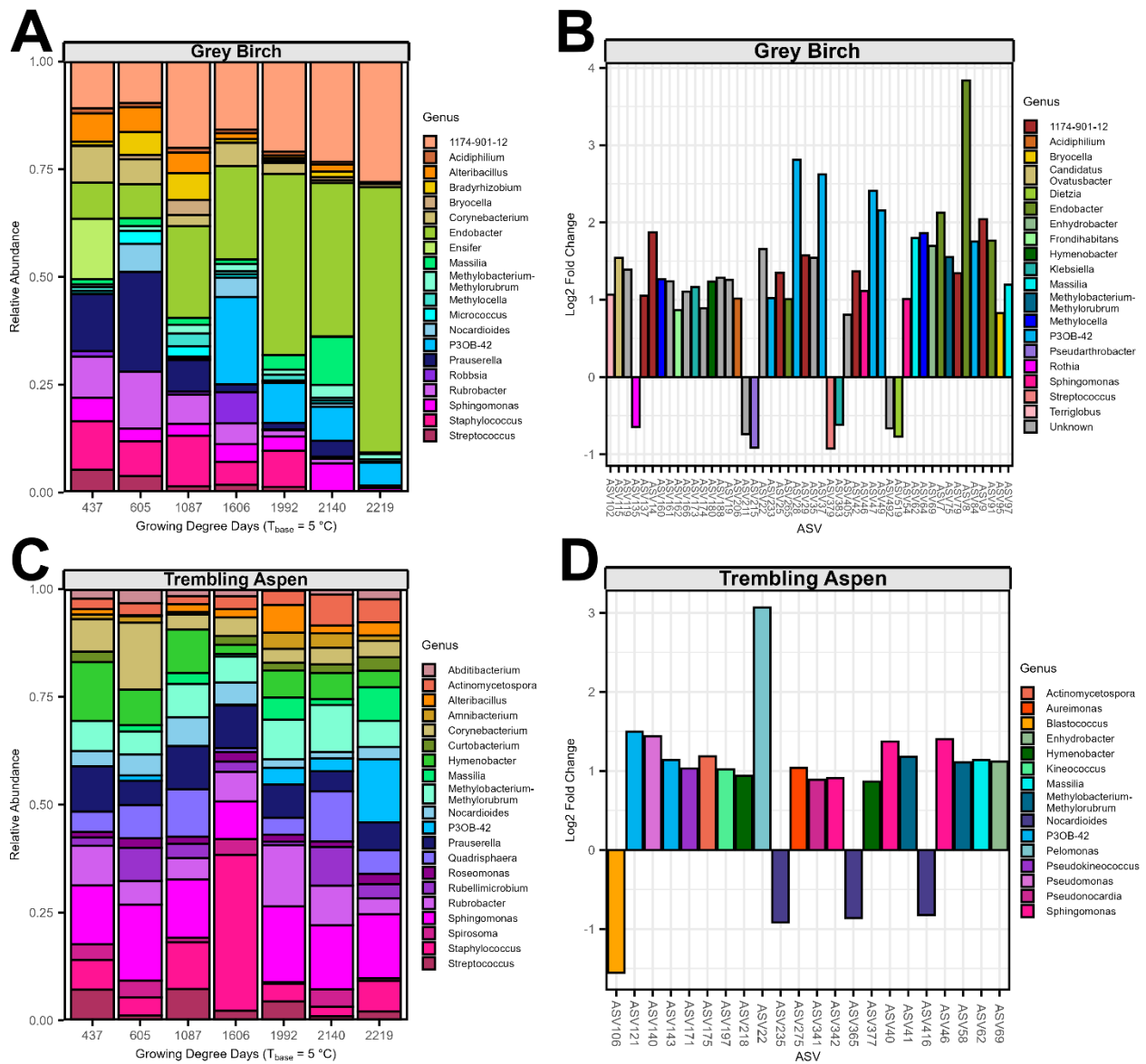
587 <sup>a</sup> Asterisks indicate  $P$ -values \* $<0.05$ , \*\* $<0.01$  and \*\*\* $<0.001$ .

588 Within each species, we tested whether bacterial community composition changed across  
589 GDDs. In grey birch, PERMANOVA showed that GDDs significantly shaped community  
590 composition ( $F = 6.024$ ,  $P = 0.01$ ,  $R^2 = 0.149$ ), while trembling aspen showed a weaker but  
591 significant GDD effect ( $F = 1.288$ ,  $P = 0.023$ ,  $R^2 = 0.037$ ). However, within-species PCoAs  
592 revealed limited visual separation across phenology, except for weak directional shifts along  
593 Axis 1 in both species (Spearman's  $\rho = -0.715$  in birch;  $\rho = -0.337$  in aspen). Analyses of  
594 multivariate dispersion (betadisper) indicated subtle shifts in variability, with late-season

595 dispersion changes in aspen ( $F = 4.005$ ,  $P = 0.004$ ) and marginal variation in birch ( $F = 2.512$ ,  $P$   
596  $= 0.048$ ), but no consistent or strongly significant dispersion patterns across most GDDs or  
597 Plant\_IDs. Full dispersion and plant-level PERMANOVA results are presented in  
598 Supplementary Results (S3.1) and Supplementary Table S5.

599 In this study, both grey birch and trembling aspen exhibit significant associations  
600 between GDDs and Axis 1 when examined intraspecifically, indicating a clear relationship  
601 between community composition and GDDs within each species. However, when compared  
602 interspecifically, the relationship shifts, with GDDs associating significantly with Axis 2 instead.  
603 This phenomenon can be attributed to the interaction between species and GDDs, as highlighted  
604 by the significant ‘Species:GDD\_5C’ term in the PERMANOVA analysis (Table 2.4).

605 ***3.2 Specific taxa were enriched in the leaf microbiomes of birch and aspen as GDDs***  
606 ***accumulated across phenology***—Across the seasonal GDD gradient, leaf bacterial communities  
607 of grey birch and trembling aspen were dominated by Proteobacteria but exhibited distinct  
608 taxonomic and temporal patterns (Fig. 2.3A; Supplementary Fig. S19). In birch, Proteobacteria  
609 steadily increased from ~52% relative abundance at 437 GDDs to a peak of ~87.5% at 2140  
610 GDDs, coinciding with a marked decline in Actinobacteria from ~30% to ~3.5%. In contrast,  
611 aspen exhibited fluctuating Proteobacteria levels, peaking early and late in the season (~50%  
612 relative abundance) but dipping mid-season (~30% at 1606 GDDs), while Actinobacteria  
613 remained relatively stable (~25–35%).



614

615 **Figure 2.3.** Taxonomic composition and differential abundance of leaf bacterial communities of grey birch  
 616 and trembling aspen. **(A)** Genus-level taxonomic profiles of relative abundance for birch (top) and aspen  
 617 (bottom) as GDDs ( $T_{base} = 5^{\circ}C$ ) accumulate over seasonal host phenology. For visual practicality, only the  
 618 top 20 most abundant genera are shown, but the general pattern remains consistent, regardless. **(B)**  
 619 Differential abundance analysis (*DESeq2*) showing significant changes ( $p_{adj} < 0.05$ ) in the relative  
 620 abundance of leaf bacterial ASVs (colour-coded) within birch (top) and aspen (bottom) in response to  
 621 GDD accumulation ( $T_{base} = 5^{\circ}C$ ). The  $\log_2(\text{fold-change})$  within birch represents the rate of change in abundance  
 622 for every 1-unit increase in GDD and can be interpreted as a regression slope on a  $\log_2$  scale. A positive  
 623  $\log_2(\text{fold-change})$  indicates that the ASV significantly increased in abundance as GDDs increased, while  
 624 a negative  $\log_2(\text{fold-change})$  demonstrates that there was a significant decline in the ASV's abundance  
 625 as GDDs increased. Note that colours do not correlate to relatedness of taxa. The *P*-value is calculated  
 626 using the Wald test, and the adjusted *P*-value ( $p_{adj}$ ) is calculated using the Benjamini–Hochberg method.  
 627 A full list of the significantly differentially abundant ASVs, including unidentified ASVs, and all summary  
 628 statistics can be found in Supplementary Tables S9–S10.

629 Firmicutes followed host-specific trajectories: in birch, it declined from early peaks  
630 (~15%) to ~3.5% late-season, whereas in aspen, it peaked at ~35% mid-season (1606 GDDs)  
631 before tapering off. Additional phyla such as Myxococcota and Bacteroidota displayed distinct  
632 host and seasonal signatures. Myxococcota surged mid-season in birch (~15% at 1606 GDDs)  
633 but peaked later in aspen (~8.5% at 2219 GDDs). Bacteroidota, though minor overall, declined  
634 steadily in birch but remained higher and more variable in aspen (~5–27%).

635 At the genus level, birch microbiomes showed a clear directional shift toward dominance  
636 by *Endobacter* and *1174-901-12*, which rose from <10% to ~62.5% and ~28.5%, respectively, by  
637 senescence onset (2219 GDDs; Fig. 2.3A). This pattern was accompanied by successive  
638 replacements: early-season dominance by *Ensifer* (~13.5%) gave way to *Prauserella* (~22% at  
639 605 GDDs), then *P3OB-42* (~20.5% at 1606 GDDs), and eventually *Massilia* (~11.5% at 2140  
640 GDDs). These transitions suggest a seasonal succession of dominant taxa in birch. In contrast,  
641 aspen maintained a more stable community structure with moderate fluctuations across genera  
642 and fewer dominant shifts. Notable exceptions include a sharp mid-season spike in  
643 *Staphylococcus* (~37% at 1606 GDDs, primarily driven by a single plant) and a late-season  
644 increase in *Pelomonas* (~24% at 2219 GDDs).

645 Distinct genera were preferentially associated with each host. Birch harbored genera such  
646 as *1174-901-12*, *Bradyrhizobium*, *Endobacter*, *Methylocella*, and *Robbsia*—often absent or rare  
647 in aspen—while aspen was enriched in taxa like *Hymenobacter*, *Quadrisphaera*, and *Pelomonas*.  
648 Shared genera, including *Prauserella*, *Staphylococcus*, and *Rubrobacter*, displayed divergent  
649 trajectories across hosts. For example, *Prauserella* declined sharply in birch mid-season but  
650 persisted longer in aspen. *Methylobacterium-Methylorubrum* is a transient, low-abundance taxa  
651 in birch, but remains a persistent key genus in aspen. By the end of the season, birch

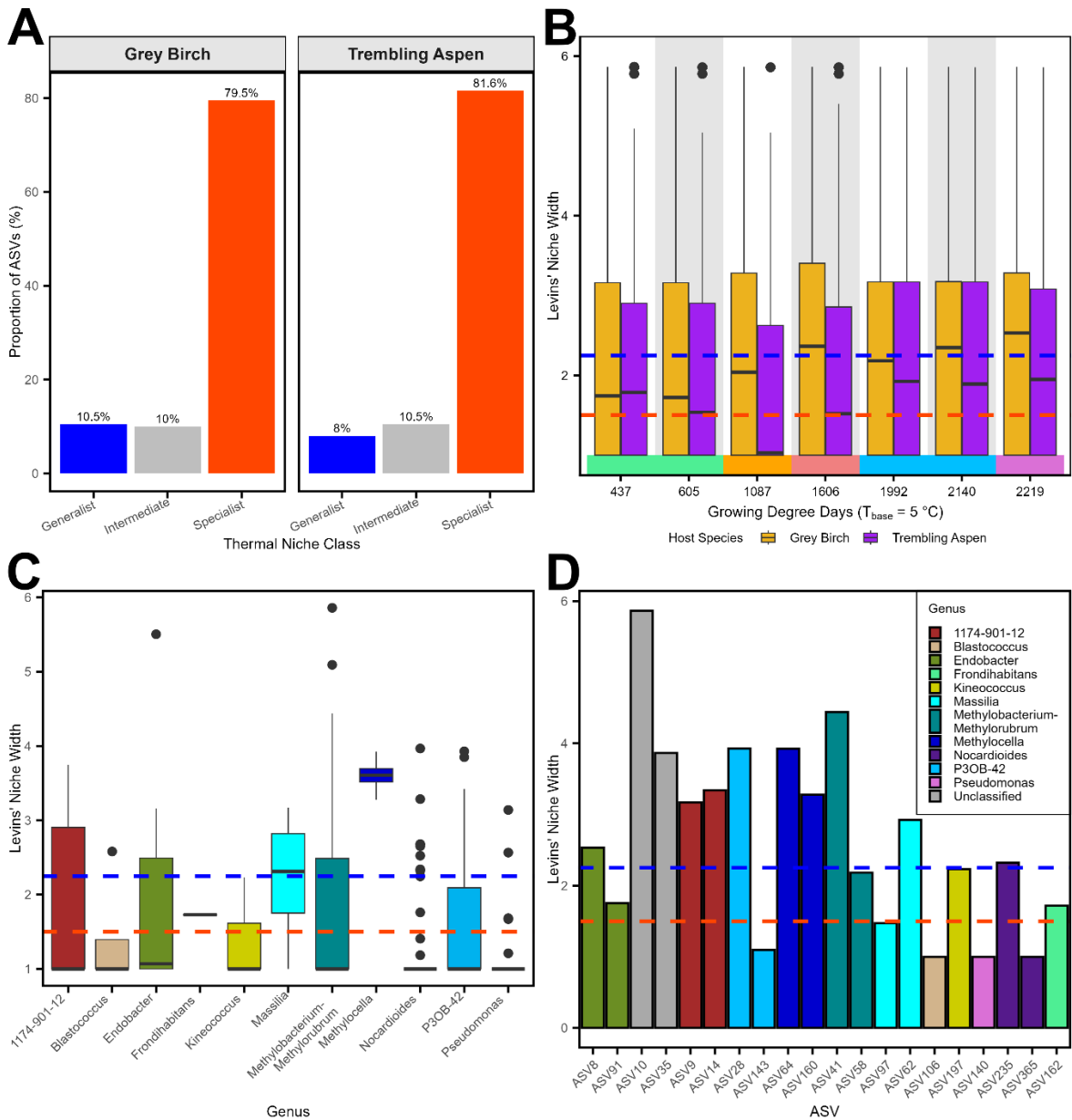
652 communities were strongly dominated by three genera—*Endobacter*, *1174-901-12*, and *P3OB-*  
653 *42*—suggesting a pronounced community simplification. Conversely, aspen retained a more even  
654 distribution of taxa, with no single genus maintaining long-term dominance. These contrasts  
655 underscore divergent community assembly trajectories: birch microbiomes trended toward  
656 reduced evenness, while aspen maintained higher taxonomic heterogeneity despite GDD  
657 accumulation.

658 Differential abundance analysis identified bacterial ASVs that significantly varied in  
659 abundance with increasing cumulative GDDs, indicating temperature-driven shifts in leaf  
660 microbiome composition (Fig. 2.3B; Supplementary Tables S6–S7). Analyses were conducted  
661 separately for birch and aspen using continuous GDD as a predictor. In birch, 47 ASVs were  
662 significantly differentially abundant across the thermal gradient (FDR < 0.05), showing both  
663 enrichment and depletion patterns indicative of dynamic microbial turnover; however, most  
664 ASVs were enriched at higher GDDs. Notably, ASVs within *Endobacter*, *1174-901-12*, *Massilia*,  
665 *P3OB-42*, and *Methylocella* exhibited strong positive log<sub>2</sub> fold changes with GDD, particularly  
666 during late-season accumulation. Conversely, ASVs associated with genera such as  
667 *Pseudarthrobacter*, *Streptococcus*, *Rothia*, and *Dietzia* exhibited depletion patterns in their  
668 abundance with increasing GDD accumulation (Supplementary Fig. S6).

669 In contrast, aspen hosted fewer differentially abundant ASVs (22 total), where most  
670 ASVs were also enriched at increasing GDD values (Fig. 2.3B; Supplementary Table S7). ASVs  
671 of the *Pelomonas* genus displayed strong enrichment at higher cumulative GDDs; other genera,  
672 such as *Hymenobacter*, *Sphingomonas*, *Pseudomonas*, *P3OB-42*, and *Methylobacterium-*  
673 *Methylorubrum* also demonstrated positive enrichment in abundance as GDDs accumulated  
674 seasonally. Moreover, two major genera exhibited depletion trends with increasing GDD

675 accumulation: *Nocardioides* and *Blastococcus*. Some genera—like *P3OB-42*, *Enhydrobacter*,  
676 *Sphingomonas*, and *Massilia*—were shared between hosts but showed divergent responses.  
677 These patterns underscore differences in thermal microbiome trajectories between the two  
678 functionally similar hosts, with birch supporting more dynamic microbial succession along the  
679 GDD continuum. Nevertheless, ASVs of the leaf bacterial communities exhibited host-specific  
680 patterns of thermal enrichment. Notably, unclassified ASVs comprised a significant portion of  
681 differentially abundant microbes both when comparing host species, and when comparing across  
682 higher and lower GDDs, emphasizing potential deeper ecological significance. For results of  
683 temporal patterns in differential abundance between host species, see Supplementary Figures  
684 S21–S22 and Supplementary Tables S8–S9.

685 ***3.3 Leaf microbiomes exhibited host-specific thermal niche strategies dominated by***  
686 ***specialists across a seasonal GDD gradient***—To assess how bacterial thermal niche breadth  
687 varied across the growing season and between hosts, we calculated Levins' niche width index for  
688 each ASV using relative abundances scaled within each species × GDD sample. Most ASVs  
689 displayed narrow thermal persistence ranges, with 81.1% classified as thermal specialists (niche  
690 width  $\leq 1.5$ ) and only 8.5% as generalists ( $\geq 2.25$ ), across all samples (Supplementary Fig. S23;  
691 Supplementary Table S10). When faceted by host species, results show that grey birch hosts  
692 slightly more thermal generalist ASVs (~10.3%) than aspen (~8%;  $W = 376056$ ,  $P = 0.3144$ ),  
693 whereas aspen hosts slightly more thermal specialists than birch (Fig. 2.4A;  $W = 293830$ ,  $P =$   
694  $0.3455$ ); regardless, Wilcoxon rank sum tests determined that these differences were non-  
695 significant.



696

697 **Figure 2.4.** Thermal niche breadth of leaf-associated bacterial ASVs across seasonal heat accumulation  
 698 and host species. Levins' niche width index was derived from relative abundances and used to quantify  
 699 the breadth of thermal persistence for each ASV across a seasonal GDD ( $T_{\text{base}} = 5^{\circ}\text{C}$ ) gradient, a  
 700 physiologically relevant measure of heat accumulation that tracks host phenological progression. ASVs  
 701 with niche width  $\leq 1.5$  were classified as specialists,  $\geq 2.25$  as generalists, and those in between as  
 702 intermediate. **(A)** Proportion of ASVs classified as thermal specialists, intermediates, or generalists,  
 703 faceted by host species. **(B)** Seasonal trends in ASV niche width across GDD accumulation for each host  
 704 species. Boxplots represent the distribution of ASV-level niche width values per GDD time point (median,  
 705 IQR, whiskers), with outliers shown as points. Dashed red and blue lines indicate specialist and generalist  
 706 thresholds, respectively. **(C)** Genus-level distributions of niche width among focal bacterial genera.  
 707 Narrow boxes (e.g., *Fronthabitans*, *Nocardioideis*, and *Pseudomonas*) reflect low genus-level diversity or  
 708 consistent niche breadth. **(D)** Niche width of focal ASVs from key genera, illustrating intra-genus variability  
 709 in thermal niche strategy and highlighting the ecological importance of unclassified ASVs. Bars represent  
 710 individual ASVs; dashed lines mark classification thresholds as in prior panels, where red is the threshold  
 711 for thermal specialists and blue is the threshold for thermal generalists. ASVs are colour-coded by genus.

712           When visualized over seasonal GDD accumulation, the distribution of niche widths per  
713 host revealed diverging dynamics: birch leaf communities trended toward broader generalist  
714 niche distributions mid- to late-phenology, whereas aspen communities remained more stable but  
715 maintained a higher proportion of thermal specialists (Fig. 2.4B). Several focal genera exhibited  
716 distinct GDD-directed ecological strategies, though within-genus variability in ASV-level niche  
717 breadths highlighted the limitations of genus-level generalizations (Fig. 2.4C–D). For example,  
718 ASVs of the *Methylocella* genus demonstrated strict thermal generalist strategies, both at the  
719 genus- and ASV-level. In contrast, at the genus-level, *Massilia* wavers above the threshold of a  
720 generalist and *Nocardioides* appears to be a strict thermal specialist (Fig. 2.4C) but both contain  
721 ASVs that can be either specialists or generalists (Fig. 2.4D). Again, these results warrant caution  
722 when generalizing genus-level observations to the ASV-level. As in differential abundance  
723 analysis, unclassified ASVs comprised a significant portion of both extremes, underscoring the  
724 ecological relevance of poorly characterized taxa. In summary, these findings implicate GDD  
725 accumulation gradients as more than a phenological index—they represent thermal and temporal  
726 microbial niche spaces in and on the leaf microhabitats of grey birch and trembling aspen. For  
727 detailed niche width results, see Supplementary Table S10.

## 728 **4.0 DISCUSSION**

729           This study demonstrates that growing degree days (GDDs;  $T_{\text{base}} = 5^{\circ}\text{C}$ )—a  
730 physiologically grounded measure of cumulative temperature—serve not only as a proxy for  
731 plant phenology but also as a direct ecological axis that structures leaf-associated bacterial  
732 diversity, composition, and thermal niche strategies. Across a continuous seasonal gradient, leaf  
733 microbiomes of two functionally similar temperate tree species, grey birch (*B. populifolia*) and  
734 trembling aspen (*P. tremuloides*), exhibited divergent trajectories in alpha diversity, beta

735 diversity, taxonomic composition, and inferred ecological strategies. These findings support the  
736 emerging view that microbial community dynamics in the phyllosphere are shaped by both host  
737 traits and environmental conditions, particularly temperature accumulation as it relates to GDDs  
738 and phenology, and that these factors interact in species-specific ways to shape microbiome  
739 assembly dynamics over seasonal time.

740 ***4.1 GDD accumulation shapes species-specific patterns of alpha diversity***—Alpha  
741 diversity patterns revealed decoupled responses between richness and Shannon diversity over  
742 phenology (Fig. 2.2A; Table 2.2). In birch, ASV richness increased significantly with GDD  
743 accumulation ( $P = 0.0004$ ), while richness in aspen remained largely stable ( $P = 0.427$ ). Notably,  
744 the host species  $\times$  GDD interaction was significant ( $P = 0.0053$ ), accounting for  $\sim 32.6\%$  of fixed-  
745 effect variance in ASV richness, but post-hoc tests showed no significant interspecific  
746 differences at individual GDDs (Supplementary Table S1), suggesting this pattern reflects  
747 gradual divergence rather than sharp shifts. In contrast, Shannon diversity was consistently  
748 higher in aspen ( $P = 0.0413$ ) and remained unaffected by GDDs in either species ( $P = 0.857$ ),  
749 indicating host species as the primary driver of evenness.

750 These results imply that while GDD accumulation shapes bacterial ASV recruitment and  
751 presence, observed differences in evenness distributions were more strongly associated with host  
752 species identity. This supports prior work suggesting that host traits, rather than environmental  
753 factors like GDDs and temperature per se, regulate community evenness (Laforest-Lapointe et al.  
754 2016a; Lajoie & Kembel 2021). Yet, the elevated responsiveness of ASV richness to GDDs  
755 suggests that thermal-time plays a foundational role in determining microbial presence,  
756 especially during mid-to-late phenology (1087–1992 GDDs)—a period of accelerated thermal  
757 accumulation and ecological change. Nonetheless, while GDD and host identity explained

758 significant variation in ASV richness and Shannon diversity, respectively, the high residual  
759 variance (>70%) suggests that stochastic processes—such as ecological drift or unmeasured  
760 microenvironmental factors—may contribute substantially to alpha diversity, even in a shared  
761 environment. Regardless, these findings demonstrate that even functionally similar host species  
762 can exhibit species-specific seasonal patterns in alpha diversity and responses to GDD  
763 accumulation, despite their phylogenetic distance.

764 ***4.2 Community composition and turnover reflect host-specific thermal trajectories—***  
765 Beta diversity patterns further underscore the distinct seasonal responses of birch and aspen to  
766 thermal accumulation, despite similar leaf types (Fig. 2.2B). In birch, communities exhibited  
767 significant turnover and multivariate dispersion mid-to-late season, with clear separation  
768 between early and late GDD samples, suggesting microbiome restructuring events along the  
769 GDD gradient (Supplementary Fig. S18A). In aspen, communities remained more  
770 compositionally stable, though subtle directional changes were observed (Supplementary Fig.  
771 S18B). These host-specific differences in microbial trajectories reflect the influence of both  
772 deterministic filtering and potential functional redundancy among microbial taxa. Although host  
773 species identity explained more variance in community composition than GDDs, the inclusion of  
774 only two host species limits our ability to attribute this pattern to host-regulated control.

775 Together with the modest explanatory power of host identity in richness models ( $R^2 =$   
776 1.33%), and the greater contribution of GDDs and its interaction with host ( $R^2 = 6.17%$  and  
777 9.94%, respectively), these results support the environmental filtering hypothesis (Weiher et al.  
778 1998), where abiotic conditions—in this case, temperature accumulation—select for bacterial  
779 taxa suited to prevailing thermal regimes. However, beta diversity models showed limited  
780 explanatory power from fixed effects, with residuals exceeding 70% of total variance. This

781 underscores the potential role of stochastic processes—such as priority effects, drift, or fine-scale  
782 spatial heterogeneity—in shaping foliar community composition beyond host and thermal  
783 filtering alone. Regardless, that such turnover occurs between functionally similar hosts grown in  
784 a shared environment challenges prior findings that functional type predicts microbiome  
785 similarity (Grady et al. 2019) and instead aligns with work highlighting the primacy of  
786 phylogenetic distance and species-specific traits over broad ecological strategies and growth  
787 forms (Sangiorgio et al. 2024; Laforest-Lapointe et al. 2016b). Thus, these findings warrant  
788 caution when generalizing findings at the host functional type level to the species-level.

789 **4.3 GDDs reveal distinct taxonomic and thermal enrichment patterns**—Differential  
790 abundance analysis revealed taxa exhibiting strong enrichment or depletion across the thermal  
791 gradient, with pronounced species-specificity. Birch hosted a greater number of GDD-limited  
792 ASVs, many enriched during discrete thermal transitions (e.g., 1087–1606 GDDs), including  
793 genera such as *Methylocella*, *Endobacter*, *1174-901-12*, and *P3OB-42* (Fig. 2.3). In contrast,  
794 aspen microbiomes featured fewer differentially abundant ASVs but displayed consistent  
795 enrichment in specialist genera such as *Methylobacterium-Methylorubrum*, *Pelomonas*,  
796 *Quadrisphaera* and *Hymenobacter*. This taxon-level differentiation highlights the utility of  
797 GDDs in identifying thermal-time windows of microbiome reorganization and succession.  
798 Unclassified ASVs comprised a significant proportion of differentially enriched taxa and showed  
799 strong, consistent thermal-time signatures—especially in birch—underscoring their potential role  
800 in phenological microbiome restructuring and the ecological relevance of microbial “dark  
801 matter” (Bodor et al. 2020; Hedlund et al. 2014; Nobu et al. 2015; Zhang et al. 2023).

802 Among the most strongly enriched and thermally limited genus in grey birch was the  
803 newly assigned *Endobacter*, a genus of strictly aerobic, catalase-positive acetic acid bacteria

804 within Acetobacteraceae (Ramírez-Bahena et al. 2013). Interestingly, this family forms part of  
805 the early-branching acetous clade characterized by vestigial photosynthetic traits and incomplete  
806 oxidation metabolism (Raspor and Goranovič 2008). These traits suggest an epiphytic lifestyle  
807 well-adapted to oxidative phyllosphere environments. The catalase activity of *Endobacter* may  
808 be especially advantageous in birch, which is known to produce hydrogen peroxide (H<sub>2</sub>O<sub>2</sub>) as  
809 part of its leaf surface defenses; catalase-mediated detoxification would enable *Endobacter* to  
810 persist or even thrive under oxidative stress (Niu and Liao 2016; Oksanen et al. 2005; Pellinen et  
811 al. 2002).

812         Moreover, *Endobacter* species metabolize ethanol—a compound often emitted as a  
813 volatile organic compound (VOC) in birch foliage—into acetic acid (Hellén et al. 2021; Maja et  
814 al. 2014; Ramírez-Bahena et al. 2013; Rastogi et al. 2015). This metabolic niche likely confers a  
815 competitive advantage in birch canopies during periods of active VOC production, particularly in  
816 mid-to-late phenology. *Endobacter*'s detection on the leaves of grey birch, particularly during  
817 late-season phenology and increased GDDs, may reflect adaptation to microaerobic, nutrient-  
818 fluctuating niches typical of maturing or senescing foliage. The strong, late-season enrichment of  
819 *Endobacter* observed in birch, but much less in aspen, aligns with these host-specific ecological  
820 traits and further highlights the role of temperature-driven phenological shifts in selecting for  
821 metabolically compatible microbiota. This positions *Endobacter* as a potential redox modulator  
822 or sugar-oxidizing commensal in the leaf phyllosphere-endosphere continuum, consistent with  
823 broader metacommunity responses to cumulative GDDs. This study encourages future work in  
824 elucidating the ecological roles of this potentially key bacterial genus.

825         **4.4 Niche width patterns support ecological filtering and divergent strategies**—Thermal  
826 niche breadths, calculated via Levins' index, revealed strong ecological filtering across the GDD

827 continuum: 81.1% of ASVs were classified as thermal specialists (niche width  $\leq 1.5$ ), with only  
828 8.5% identified as generalists ( $\geq 2.25$ ; Supplementary Fig. S23). Host-specific patterns were  
829 evident—birch hosted a slightly higher proportion of generalists (10.3%) than aspen (8.0%),  
830 while aspen maintained a higher proportion of specialists throughout the season (Fig. 2.4A–B).  
831 These patterns suggest that birch supports broader microbial turnover, potentially due to dynamic  
832 phenological shifts or weaker host-associated differences, whereas aspen maintains more  
833 compositionally stable and specialized communities. Notably, several genera contained both  
834 specialist and generalist ASVs (e.g., *Nocardioides*, *Massilia*), illustrating the limitations of  
835 genus-level inferences and reinforcing the need for ASV-level resolution in ecological studies  
836 (Fig. 2.4C–D). This is especially true since functional assessments of microbiomes can be  
837 confounded by strain-level variability and functional redundancy across bacterial taxa (Barnes et  
838 al. 2020).

839         When plotted across GDDs, birch showed a mid-to-late season increase in generalist  
840 ASVs, aligning with observed community restructuring and increased taxonomic dynamism. In  
841 contrast, aspen displayed narrower niche widths. These results align with classical niche theory  
842 (Chase and Leibold 2003), where community structure emerges from trait distributions along  
843 environmental gradients—in this case, thermally regulated phenological space. This study  
844 presents evidence for niche theory’s extension into the microbial realm (Baquero et al. 2021)

845         Genera such as *Methylocella* exemplified consistent generalist strategies across hosts and  
846 GDDs, likely reflecting their facultative methanotrophic metabolism and broad thermal tolerance  
847 (Crombie and Murrell 2014; Dedysh et al. 2005; Dunfield and Dedysh 2014). In contrast, genera  
848 like *Nocardioides*, *Blastococcus*, and *Pseudarthrobacter* appeared as strict specialists at the  
849 genus level. Differential abundance of *Nocardioides* shows a preference for relatively lower

850 cumulative GDD conditions; as a mesophilic genus that includes psychrotolerant strains, its  
851 affinity for the earlier GDDs of June 2018—when temperatures were neither extreme—is  
852 ecologically consistent (Schiraldi and De Rose 2014). Nonetheless, genera such as *Massilia*,  
853 *Nocardioides*, and *P3OB-42* exemplify the intra-genus variation in thermal strategies revealed by  
854 ASV-level comparisons, underscoring the value of high-resolution ecological analysis.

855         Although we cannot make definitive claims about adaptive evolution, certain taxa such as  
856 *Methylocella*, *Nocardioides*, and *Pelomonas* showed GDD-specific enrichment patterns  
857 consistent with known thermal tolerances, suggesting potential physiological adaptation to  
858 seasonal temperature regimes. However, these interpretations remain cautious without functional  
859 or genomic validation. Instead, we emphasize that the observed patterns—bacterial turnover,  
860 niche partitioning, and host-specific responses to GDD accumulation—reflect ecological  
861 selection across a dynamic thermal-time gradient rather than adaptive shifts per se. This finding  
862 underscores that even closely related strains may exhibit divergent ecological strategies, and that  
863 niche theory applies at a microevolutionary scale in leaf bacterial communities.

864         **4.5 Broader implications and future directions**—Taken together, this study positions  
865 GDD accumulation not only as a model for plant phenological progression but as a predictive  
866 ecological filter shaping microbial assembly in the phyllosphere. By integrating alpha and beta  
867 diversity, DESeq2-derived enrichment, and thermal niche breadths, this study provides a  
868 multifaceted view of how seasonal temperature accumulation structures leaf bacterial  
869 communities across two functionally similar but phylogenetically distinct tree species. GDDs  
870 offer a biologically relevant and scalable index for understanding microbial phenology and may  
871 prove critical in forecasting microbial responses to ongoing climatic shifts. Future studies should  
872 extend this work by incorporating more diverse host species, interannual datasets, and trait-based

873 plant-microbe metrics (e.g., exudate profiles, cuticle chemistry). Metatranscriptomic or  
874 functional profiling approaches would also provide insight into the metabolic roles of  
875 differentially abundant and unclassified taxa. Additionally, experimental manipulation of GDD  
876 accumulation—via warming chambers or phenological decoupling—could disentangle the causal  
877 roles of temperature, host development, and microbial succession in shaping these complex and  
878 dynamic communities. Finally, the large proportion of residual variance observed in our models  
879 highlights the need to account for stochasticity and context-dependent variability when  
880 interpreting microbiome assembly, especially in natural forest systems.

881         Although our findings cannot directly test the extended phenotype concept—which  
882 requires demonstrating that externally expressed traits are shaped by host genotypes—they raise  
883 questions relevant to it. The extended phenotype framework describes traits influenced by an  
884 organism’s genes but expressed outside its body, such as microbial communities modulated by  
885 host genetic or physiological factors (Dawkins 1982; Hawkes et al. 2021). In this study, we  
886 observed clear species-specific patterns in leaf microbiome structure and diversity that unfolded  
887 across phenological time, alongside consistent responses to GDD accumulation. These findings  
888 suggest that thermal filtering alone may not fully explain community dynamics; instead, host  
889 identity and phenology appear to also shape microbial trajectories through indirect mechanisms  
890 such as microhabitat structuring or developmental cues (Ginnan et al. 2022; Kembel and Mueller  
891 2014; Laforest-Lapointe et al. 2016a,b).

892         If microbial communities track thermally regulated phenology and contribute to host  
893 function, they may act as ecologically relevant traits—and potential targets of selection—  
894 particularly as climate change disrupts plant–microbe synchrony (Ginnan et al. 2022; Meier et al.  
895 2021; Piao et al. 2019; Xu et al. 2023). To evaluate whether leaf microbiomes truly constitute

896 extended host phenotypes, future work will require the integration of host plant genotype data,  
897 functional trait profiles, transcriptomics, and broader cross-species comparisons to disentangle  
898 the relative contributions of host regulation, environmentally contingent filtering, and  
899 stochasticity.

## 900 **5.0 CONCLUSION**

901 In summary, this study demonstrates that cumulative growing degree days (GDDs;  $T_{\text{base}} =$   
902  $5\text{ }^{\circ}\text{C}$ ) act not only as a physiologically relevant proxy for plant phenology, but as a direct metric  
903 of the thermal ecological filtering that shapes leaf bacterial diversity and composition. Across a  
904 continuous seasonal gradient, GDDs more strongly explained ASV richness than host identity,  
905 while Shannon diversity reflected species-specific differences, being unimpacted by GDD  
906 accumulation. Host species identity explained a greater proportion of variance in community  
907 composition than GDDs, though both had significant effects. Given that this study included two  
908 host species, its findings should be interpreted cautiously and do not confirm host-regulated  
909 control. Birch (*B. populifolia*) leaf microbiomes underwent directional mid-to-late phenology  
910 restructuring, enriched in generalists and GDD-limited taxa like *Endobacter*, while aspen (*P.*  
911 *tremuloides*) communities remained compositionally stable and even with narrower thermal  
912 niches. Niche width analysis revealed ~81% of ASVs were thermal specialists, and unclassified  
913 taxa showed strong GDD-linked enrichment, underscoring the ecological role of microbial “dark  
914 matter”. Collectively, the results position the leaf microbiome as a dynamic, environmentally  
915 responsive feature of the plant holobiont in functionally similar but phylogenetically distant  
916 hosts, jointly shaped by host identity and the cumulative thermal energy directing host  
917 phenology. Thus, GDDs offer a scalable tool for predicting leaf microbiome responses to  
918 phenological and climatic change—an increasingly urgent task in the face of global warming.

## Chapter 3

### General Conclusions

919           This study establishes growing degree days (GDDs;  $T_{\text{base}} = 5^{\circ}\text{C}$ ) as a biologically  
920 meaningful and mechanistically informative axis for interpreting microbiome dynamics in the  
921 leaf phyllosphere and endosphere. By sampling two functionally similar but phylogenetically  
922 distinct temperate tree species—grey birch (*B. populifolia*) and trembling aspen (*P.*  
923 *tremuloides*)—along a continuous seasonal gradient of cumulative heat energy, we show that  
924 GDDs structure leaf bacterial communities in a host-specific, ecologically directional manner.  
925 Specifically, GDDs more strongly predicted ASV richness than host identity alone, whereas  
926 Shannon diversity remained unimpacted and better explained by differences in host species  
927 identity, indicating a decoupling of microbial presence from evenness and revealing layered  
928 influences of environment and host. Across all comparisons, GDD accumulation significantly  
929 modulated community composition and beta diversity.

930           Thermal accumulation was also linked to microbial turnover events, GDD-limited  
931 taxonomic enrichments, and phenology-driven niche partitioning, particularly in birch, which  
932 exhibited directional restructuring of its microbiome in mid-to-late season. By senescence onset  
933 (2219 GDDs), however, interspecific differences diminished, potentially due to microhabitat  
934 homogenization, relaxed host filtering, or colonization by generalist, stress-tolerant taxa. Such  
935 findings emphasize the seasonal fluidity of host-microbe interactions and support the  
936 environmental filtering hypothesis under dynamic phenological conditions. These patterns were  
937 underpinned by a dominant prevalence of thermal specialists (~81%), but with host-specific  
938 variation: birch supported greater mid-season influxes of generalists, while aspen maintained

939 narrower niche widths and compositional stability. Such findings extend niche theory into the  
940 microbial domain and reinforce the importance of GDDs as both an indirect (via phenological  
941 interaction) and direct (via cumulative thermal filtering) force in microbial assembly.

942 Differential abundance analysis revealed that certain taxa—including *Endobacter*, *1174-*  
943 *901-12*, and *P3OB-42* in birch, and *Pelomonas*, *Nocardioides*, and *Hymenobacter* in aspen—  
944 were strongly limited by GDD accumulation. The late-season surge of *Endobacter*, an aerobic,  
945 catalase-positive acetic acid bacterium possibly adapted to hydrogen peroxide-rich birch  
946 phyllospheres, highlights how microbial metabolic traits may align with host-specific chemical  
947 environments and seasonally timed resource niches. The ecological responsiveness of  
948 unclassified ASVs, particularly in birch, underscores the relevance of microbial “dark matter” in  
949 phyllosphere ecology and emphasizes the limitations of genus-level resolution alone. They  
950 consistent appearance of understudied genera like *Endobacter* and unidentified ASVs in this  
951 study emphasize a need to improve culture-independent methods.

952 While this study offers novel insights, it is not without limitations. The focus on only two  
953 tree species—moderately related and ecologically similar—limits generalizability to more  
954 phylogenetically or functionally diverse systems; it also limits the ability to assess host species  
955 control. The absence of interannual data prevents robust conclusions about temporal stability or  
956 climate-linked interannual shifts. Additionally, constraints on sample size limited the ability to  
957 fully explore hierarchical variance structures, such as inter- versus intra-individual variation.  
958 High residual variance across models (>70%) further suggests that stochastic processes, such as  
959 ecological drift, likely interact with deterministic thermal filtering to shape community assembly.

Together, these findings support a view of the leaf bacterial microbiome as a dynamic,  
thermally responsive community shaped by both thermal environmental filtering and differences

in host species identity. While we cannot confirm that foliar microbiomes represent extended host phenotypes, the observed species-specific patterns across phenological time and thermal accumulation raise compelling questions for future study. As global temperatures rise and plant phenology shifts, understanding how thermal-time indices like GDDs shape microbiome dynamics will be critical for predicting microbiome resilience, turnover, and potential feedback to host function. By integrating high-resolution community analysis with a cumulative thermal framework, this study provides a scalable, ecologically grounded foundation for future research into the thermal ecology of plant–microbe interactions.

960 **LITERATURE CITED**

- 961 Aarts, E., Verhage, M., Veenliet, J.V., Dolan, C.V., Van Der Sluis, S. 2014. A solution to  
962 dependency: using multilevel analysis to accommodate nested data. *Nat Neurosci.*  
963 17(4):491–496. <https://doi.org/10.1038/nn.3648>
- 964 Ajmal, A.W., Yasmin, H., Hassan, M.N., Khan, N., Jan, B.L., Mumtaz, S. 2022. Heavy Metal–  
965 Resistant Plant Growth–Promoting *Citrobacter werkmanii* Strain WWN1 and  
966 *Enterobacter cloacae* Strain JWM6 Enhance Wheat (*Triticum aestivum* L.) Growth By  
967 Modulating Physiological Attributes and Some Key Antioxidants Under Multi-Metal  
968 Stress. *Front Microbiol.* 13. <https://doi.org/10.3389/fmicb.2022.815704>
- 969 Almario, J., Mahmoudi, M., Kroll, S., Agler, M., Placzek, A., Mari, A., Kemen. E. 2022. The  
970 Leaf Microbiome of *Arabidopsis* Displays Reproducible Dynamics and Patterns  
971 throughout the Growing Season. *mBio.* 13:e02825-21.  
972 <https://doi.org/10.1128/mbio.02825-21>
- 973 Andrés-Barrao, C., Alzubaidy, H., Jalal, R., Mariappan, K. G., De Zélicourt, A., Bokhari, A.,  
974 Artyukh, O., Alwutayd, K., Rawat, A., Shekhawat, K., Almeida-Trapp, M., Saad, M. M.,  
975 Hirt, H. 2021. Coordinated bacterial and plant sulfur metabolism in *Enterobacter* sp.  
976 SA187–induced plant salt stress tolerance. *P Natl Acad Sci USA.* 118(46).  
977 <https://doi.org/10.1073/pnas.2107417118>
- 978 Asaf, S., Numan, M., Khan, A.L., Al-Harrasi, A. 2020. *Sphingomonas*: from diversity and  
979 genomics to functional role in environmental remediation and plant growth. *Crit Rev*  
980 *Biotechnol.* 40(2):138–152. <https://doi.org/10.1080/07388551.2019.1709793>

981 Baquero, F., Coque, T.M., Galán, J.C., Martínez, J.L. 2021. The origin of niches and species in  
982 the bacterial world. *Front Microbiol.* 12:657986.  
983 <https://doi.org/10.3389/fmicb.2021.657986>

984 Barnes, E.M., Carter, E.L., Lewis, J.D. 2020. Predicting Microbiome Function Across Space is  
985 Confounded by Strain-Level Differences and Functional Redundancy Across Taxa. *Front*  
986 *Microbiol.* 11:101. <https://doi.org/10.3389/fmicb.2020.00101>

987 Bartoń, K. 2023. MuMIn: multi-model inference. R Package v1.47.5.  
988 <https://cran.r-project.org/web/packages/MuMIn/index.html>.

989 Bates, D., Mächler, M., Bolker, B., Walker, S. 2015. Fitting Linear Mixed-Effects Models Using  
990 lme4. *J Stat Softw.* 67(1):1–48. <https://doi.org/10.18637/jss.v067.i01>.  
991 <https://cran.r-project.org/web/packages/lme4/citation.html>

992 Bharti, R., Grimm, D. G. 2021. Current challenges and best-practice protocols for microbiome  
993 analysis. *Brief Bioinform.* 22(1):178–193. <https://doi.org/10.1093/bib/bbz155>

994 Bodor, A., Boundedjoum, N., Vincze, G.E., Erdeiné Kis, Á., Laczi, K., Bende, G., Szilágyi, Á.,  
995 Kovács, T., Perei, K., Rákhely, G. 2020. Challenges of unculturable bacteria:  
996 environmental perspectives. *Rev Environ Sci Bio.* 19(1):1–22.  
997 <https://doi.org/10.1007/s11157-020-09522-4>

998 Callahan, B.J., Mcmurdie, P.J., Rosen, M.J., Han, A.W., Johnson, A.J.A., Holmes, S.P. 2016.  
999 DADA2: High-resolution sample inference from Illumina amplicon data. *Nat Methods.*  
1000 13:581–583. doi: 10.1038/nmeth.3869

1001 Callahan, B.J., Mcmurdie, P.J., Holmes, S.P. 2017. Exact sequence variants should replace  
1002 operational taxonomic units in marker-gene data analysis. ISME J. 11(12):2639–2643.  
1003 doi: 10.1038/ismej.2017.119

1004 Callahan, B.J., Wong, J., Heiner, C., Oh, S., Theriot, C.M., Gulati, A.S., McGill, S.K.,  
1005 Dougherty. 2019. High-throughput amplicon sequencing of the full-length 16S rRNA  
1006 gene with single-nucleotide resolution. Nucleic Acids Res. 47(18):e103. doi:  
1007 10.1093/nar/gkz569

1008 Chase, J.M., and Leibold, M.A. 2003. Ecological Niches: Linking Classical and Contemporary  
1009 Approaches. University of Chicago Press, Chicago. [http://dx.doi.org/10.7208/chicago/](http://dx.doi.org/10.7208/chicago/9780226101811.001.0001)  
1010 [9780226101811.001.0001](http://dx.doi.org/10.7208/chicago/9780226101811.001.0001)

1011 Chaudhry, V., Runge, P., Sengupta, P., Doehlemann, G., Parker, J.E., Kemen, E. 2021. Shaping  
1012 the leaf microbiota: plant–microbe–microbe interactions. J Exp Bot. 72(1):36–56. doi:  
1013 10.1093/jxb/eraa417

1014 Chen, A., Contreras, L.M., Keitz, B.K. 2017 Imposed Environmental Stresses Facilitate Cell-  
1015 Free Nanoparticle Formation by *Deinococcus radiodurans*. Appl Environ Microb. 83(18).  
1016 <https://doi.org/10.1128/aem.00798-17>

1017 Chiarello, M., McCauley, M., Villéger, S., Jackson, C.R. 2022. Ranking the biases: The choice  
1018 of OTUs vs. ASVs in 16S rRNA amplicon data analysis has stronger effects on diversity  
1019 measures than rarefaction and OTU identity threshold. PLOS ONE. 17(2): e0264443.  
1020 <https://doi.org/10.1371/journal.pone.0264443>

- 1021 Compant, S., Samad, A., Faist, H., Sessitsch, A. 2019. A review on the plant microbiome:  
1022 Ecology, functions, and emerging trends in microbial application. 19:29–37. J Adv Res.  
1023 doi: 10.1016/j.jare.2019.03.004
- 1024 Copeland, J.K., Yuan, L., Layeghifard, M., Wang, P.W., Guttman, D.S. 2015. Seasonal  
1025 community succession of the phyllosphere microbiome. Mol Plant Microbe In. 28:274–  
1026 285. doi: 10.1094/MPMI-10-14-0331-FI
- 1027 Crombie, A.T., and Murrell, J.C. 2014. Trace-gas metabolic versatility of the facultative  
1028 methanotroph *Methylocella silvestris*. Nature. 510(7503):148–151.  
1029 <https://doi.org/10.1038/nature13192>
- 1030 Dawkins, R. 1982. The extended phenotype (Vol. 8). Oxford: Oxford university press.
- 1031 Delgado-Baquerizo, M., Giaramida, L., Reich, P.B., Khachane, A.N., Hamonts, K., Edwards, C.,  
1032 Lawton, L.A., Singh, B.K. 2016. Lack of functional redundancy in the relationship  
1033 between microbial diversity and ecosystem functioning. J Ecol. 104(4):936–946.  
1034 <https://doi.org/10.1111/1365-2745.12585>
- 1035 Dedysh, S.N., Knief, C., Dunfield, P.F. 2005. *Methylocella* species are facultatively  
1036 methanotrophic. J Bacteriol. 187(13):4665–4670.  
1037 <https://doi.org/10.1128/JB.187.13.4665-4670.2005>
- 1038 Dunfield, P.F., and Dedysh, S.N. 2014. *Methylocella*: A gourmand among methanotrophs. Trends  
1039 Microbiol. 22(7):368–369. <https://doi.org/10.1016/j.tim.2014.05.004>

1040 Durand, A., Maillard, F., Alvarez-Lopez, V., Guinchard, S., Bertheau, C., Valot, B., Blaudez, D.,  
1041 Chalot, M. 2018. Bacterial diversity associated with poplar trees grown on a Hg-  
1042 contaminated site: community characterization and isolation of Hg-resistant plant growth  
1043 promoting bacteria. *Sci Total Environ.* 622:1165–1177. doi:  
1044 10.1016/j.scitotenv.2017.12.069

1045 Edgar, R.C. 2018. Updating the 97% identity threshold for 16S ribosomal RNA OTUs.  
1046 *Bioinformatics.* 34(14):2371–2375. doi:10.1093/bioinformatics/bty113

1047 Edwards, J.E., Huws, S.A., Kim, E.J., Kingston-Smith, A.H. 2007. Characterization of the  
1048 dynamics of initial bacterial colonization of nonconserved forage in the bovine rumen.  
1049 *FEMS Microbiol Ecol.* 62(3):323–335. <https://doi.org/10.1111/j.1574-6941.2007.00392.x>

1050 Emmett, B.D., Youngblut, N.D., Buckley, D.H., Drinkwater, L.E. 2017. Plant Phylogeny and  
1051 Life History Shape Rhizosphere Bacterial Microbiome of Summer Annuals in an  
1052 Agricultural Field. *Front Microbiol.* 8:2414. <https://doi.org/10.3389/fmicb.2017.02414>

1053 Franza, T., Sauvage, C., Expert, D. 1999. Iron regulation and pathogenicity in *Erwinia*  
1054 *chrysanthemi* 3937: role of the fur repressor protein. *Mol Plant Microbe In.* 12(2):119–  
1055 128. <https://doi.org/10.1094/mpmi.1999.12.2.119>

1056 Faticov, M., Abdelfattah, A., Roslin, T., Vacher, C., Hambäck, P., Blanchet, F. G., Lindahl, B. D.,  
1057 Tack, A. J. M. 2021. Climate warming dominates over plant genotype in shaping the  
1058 seasonal trajectory of foliar fungal communities on oak. *New Phytol.* 231:1770–1783.  
1059 doi: 10.1111/nph.17434

- 1060 Ginnan, N.A., De Anda, N.I., Campos Freitas Vieira, F., Rolshausen, P.E., Roper, M.C. 2022.  
1061 Microbial turnover and dispersal events occur in synchrony with plant phenology in the  
1062 perennial evergreen tree crop *citrus sinensis*. mBio. 13(3):e00343-22.  
1063 <https://doi.org/10.1128/mbio.00343-22>
- 1064 Grady, K.L., Sorenson, J.W., Stopnisek, N., Guittar, J., Shade, A. 2019. Assembly and  
1065 seasonality of core phyllosphere microbiota on perennial biofuel crops. Nat Commun.  
1066 10:4135. <https://doi.org/10.1038/s41467-019-11974-4>
- 1067 Hacquard, S., Wang, E., Slater, H., Martin, F. 2022. Impact of global change on the plant  
1068 microbiome. New Phytol. 234(6):1907–1909. <https://doi.org/10.1111/nph.18187>
- 1069 Hanski, I., Von Hertzen, L., Fyhrquist, N., Koskinen, K., Torppa, K., Laatikainen, T., Karisola, P.,  
1070 Auvinen, P., Paulin, L., Mäkelä, M. J., Vartiainen, E., Kosunen, T. U., Alenius, H.,  
1071 Haahtela, T. 2012. Environmental biodiversity, human microbiota, and allergy are  
1072 interrelated. P Natl Acad Sci USA. 109(21):8334–8339.  
1073 <https://doi.org/10.1073/pnas.1205624109>
- 1074 Hawkes, C.V., Kjølner, R., Raaijmakers, J.M., Riber, L., Christensen, S., Rasmussen, S.,  
1075 Christensen, J.H., Dahl, A.B., Westergaard, J.C., Nielsen, M., Brown-Guedira, G.,  
1076 Hansen, L.H. 2021. Extension of plant phenotypes by the foliar microbiome. Annu Rev  
1077 Plant Biol. 72:823–46. doi: 10.1146/annurev-arplant-080620-114342
- 1078 Hedlund, B.P., Dodsworth, J.A., Murugapiran, S.K., Rinke, C., Woyke, T. 2014. Impact of  
1079 single-cell genomics and metagenomics on the emerging view of extremophile

1080 “microbial dark matter.” *Extremophiles*. 18(5):865–875. <https://doi.org/10.1007/s00792->  
1081 [014-0664-7](https://doi.org/10.1007/s00792-014-0664-7)

1082 Hellén, H., Praplan, A.P., Tykkä, T., Helin, A., Schallhart, S., Schiestl-Aalto, P.P., Bäck, J.,  
1083 Hakola, H. 2021. Sesquiterpenes and oxygenated sesquiterpenes dominate the voc (C<sub>5</sub>–  
1084 CO<sub>2</sub>) emissions of downy birches. *Atmos Chem Phys*. 21(10):8045–8066.  
1085 <https://doi.org/10.5194/acp-21-8045-2021>

1086 Hinsu, A., Dumadiya, A., Joshi, A., Kotadiya, R., Andharia, K., Koringa, P., and Kothari, R.  
1087 2021. To culture or not to culture: a snapshot of culture-dependent and culture-  
1088 independent bacterial diversity from peanut rhizosphere. *PeerJ*. 9:e12035. doi:  
1089 10.7717/peerj.12035

1090 Huang, Z., Su, Y., Lin, S., Wu, G., Cheng, H., Huang, G. 2023. Elevational patterns of microbial  
1091 species richness and evenness across climatic zones and taxonomic scales. *Ecol Evol*.  
1092 13:e10594. <https://doi.org/10.1002/ece3.10594>

1093 Hugerth, L.W. and Andersson, A.F. 2017. Analysing Microbial Community Composition  
1094 Through Amplicon Sequencing: From Sampling to Hypothesis Testing. *Front Microbiol*.  
1095 8:1561. <https://doi.org/10.3389/fmicb.2017.01561>

1096 Kang, S.M., Joo, G.J., Hamayun, M., Na, C.I., Shin, D.H., Kim, H.Y., Hong, J.K., Lee, I.J. 2009.  
1097 Gibberellin production and phosphate solubilization by newly isolated strain of  
1098 *Acinetobacter calcoaceticus* and its effect on plant growth. *Biotechnol Lett*. 31(2):277–  
1099 281. <https://doi.org/10.1007/s10529-008-9867-2>

- 1100 Kembel, S.W., O'Connor, T.K., Arnold, H.K., Green, J.I. 2014. Relationships between  
1101 phyllosphere bacterial communities and plant functional traits in a neotropical forest.  
1102 PNAS. 11(38):13715–13720. doi: 10.1073/pnas.1216057111
- 1103 Kembel, S.W., and Mueller, R.C. 2014. Plant traits and taxonomy drive host associations in  
1104 tropical phyllosphere fungal communities. *Botany*. 92(4): 303-311.  
1105 <https://doi.org/10.1139/cjb-2013-0194>
- 1106 Khalifa, A.Y.Z., Alsyeeh, A.M., Almalki, M.A., Saleh, F.A. 2016. Characterization of the plant  
1107 growth promoting bacterium, *Enterobacter cloacae* MSR1, isolated from roots of non-  
1108 nodulating *Medicago sativa*. *Saudi J Biol Sci*. 23(1):79–86.  
1109 <https://doi.org/10.1016/j.sjbs.2015.06.008>
- 1110 Kothari, S., Beauchamp-Rioux, R., Blanchard, F., Crofts, A.L., Girard, A., Guilbeault-Mayers,  
1111 X., Hacker, P.W., Pardo, J., Schweiger, A.K., Demers-Thibeault, S., Bruneau, A., Coops,  
1112 N.C., Kalacska, M., Vellend, M., and Laliberté, E. 2023. Predicting leaf traits across  
1113 functional groups using reflectance spectroscopy. *New Phytol*. 238:549–566.  
1114 <https://doi.org/10.1111/nph.18713>
- 1115 Laforest-Lapointe, I., Messier, C., Kembel, S.W. 2016a. Host species identity, site and time drive  
1116 temperate tree phyllosphere bacterial community structure. *Microbiome*. 4:27. doi:  
1117 10.1186/s40168-016-0174-1
- 1118 Laforest-Lapointe, I., Messier, C., Kembel, S.W. 2016b. Tree phyllosphere bacterial  
1119 communities: exploring the magnitude of intra- and inter-individual variation among host  
1120 species. *PeerJ*. 4:e2367. doi: 10.7717/peerj.2367

1121 Laforest-Lapointe, I., Paquette, A., Messier, C., Kembel, S.W. 2017. Leaf bacterial diversity  
1122 mediates plant diversity and ecosystem function relationships. *Nature*. 546:145–147.  
1123 <https://doi.org/10.1038/nature22399>

1124 Lahlali, R., Taoussi, M., Laasli, S.E., Gachara, G., Ezzouggari, R., Belabess, Z., Aberkani, K.,  
1125 Assouguem, A., Meddich, A., El Jarroudi, M., Barka, E.A. 2024. Effects of climate  
1126 change on plant pathogens and host-pathogen interactions. *Crop Environ*. 3(3):159–170.  
1127 <https://doi.org/10.1016/j.crope.2024.05.003>

1128 Lajoie, G., and Kembel, S.W. 2021. Host neighborhood shapes bacterial community assembly  
1129 and specialization on tree species across a latitudinal gradient. *Ecol Mongr*.  
1130 91(2):e01443. doi: 10.1002/ecm.1443

1131 Leite, M.F.A., Van Den Broek, S.W.E.B., Kuramae, E.E. 2022. Current challenges and pitfalls in  
1132 soil metagenomics. *Microorganisms*. 10(10):1900.  
1133 <https://doi.org/10.3390/microorganisms10101900>

1134 Lenth, R. 2024. *emmeans*: Estimated Marginal Means, aka Least-Squares Means. R package  
1135 version 1.10.5, <https://rvlenth.github.io/emmeans/>

1136 Love, M.I., Huber, W., and Anders, S. 2014. Moderated estimation of fold change and dispersion  
1137 for RNA-seq data with DESeq2. *Genome Biol*. 15:550. doi: 10.18129/B9.bioc.DESeq2

1138 Lüdtke, D., Ben-Shachar, M., Patil, I., Waggoner, P., Makowski, D. 2021. performance: An R  
1139 Package for Assessment, Comparison and Testing of Statistical Models. *J Open Source*  
1140 *Softw*. 6(60):3139. doi: 10.21105/joss.03139.  
1141 <https://cran.r-project.org/web/packages/performance/citation.html>

1142 Macedo-Raygoza, G.M., Valdez-Salas, B., Prado, F.M., Prieto, K.R., Yamaguchi, L.F., Kato,  
1143 M.J., Canto-Canché, B.B., Carrillo-Beltrán, M., Di Mascio, P., White, J.F., Beltrán-  
1144 García, M.J. 2019. *Enterobacter cloacae*, an Endophyte That Establishes a Nutrient-  
1145 Transfer Symbiosis With Banana Plants and Protects Against the Black Sigatoka  
1146 Pathogen. Front Microbiol. 10. <https://doi.org/10.3389/fmicb.2019.00804>

1147 Maja, M. M., Kasurinen, A., Yli-Pirila, P., Joutsensaari, J., Klemola, T., Holopainen, T.,  
1148 Holopainen, J.K. 2014. Contrasting responses of silver birch VOC emissions to short-  
1149 and long-term herbivory. Tree Physiol. 34(3):241–252.  
1150 <https://doi.org/10.1093/treephys/tpt127>

1151 Markandya, A. (2015), “The Economic Feedbacks of Loss of Biodiversity and Ecosystems  
1152 Services”, OECD Environment Working Papers, No. 93, OECD Publishing, Paris,  
1153 <https://doi.org/10.1787/5jrqqv610fg6-en>

1154 McMaster, G. S., and Wilhelm, W. W. 1997. Growing degree-days: one equation, two  
1155 interpretations. Agr Forest Meteorol. 87(4):291–300.  
1156 [https://doi.org/10.1016/S0168-1923\(97\)00027-0](https://doi.org/10.1016/S0168-1923(97)00027-0)

1157 McMurdie, P.J., and Holmes, S. 2013. phyloseq: An R Package for Reproducible Interactive  
1158 Analysis and Graphics of Microbiome Census Data. PLoS ONE. 8(4):e61217.  
1159 <https://doi.org/10.1371/journal.pone.0061217>

1160 Meier, M., Vitasse, Y., Bugmann, H., Bigler, C. 2021. Phenological shifts induced by climate  
1161 change amplify drought for broad-leaved trees at low elevations in switzerland. Agr  
1162 Forest Meteorol. 307:108485. <https://doi.org/10.1016/j.agrformet.2021.108485>

1163 Mhatre, S., Singh, N.K., Wood, J.M., Parker, C.W., Pukall, R., Verburg, S., Tindall, B.J.,  
1164 Neumann-Schaal, M., Venkateswaran, K. 2020. Description of Chloramphenicol  
1165 Resistant *Kineococcus rubinsiae* sp. nov. Isolated From a Spacecraft Assembly Facility.  
1166 Front Microbiol. 11. <https://doi.org/10.3389/fmicb.2020.01957>

1167 Moroenyane, I., Tremblay, J., Yergeau, É. 2021a. Temporal and spatial interactions modulate the  
1168 soybean microbiome. FEMS Microbiol Ecol. 97:fiaa206. doi: 10.1093/femsec/fiaa206

1169 Moroenyane, I., Mendes, L., Tremblay, J., Tripathi, B., and Yergeau, É. 2021b. Plant  
1170 compartments and developmental stages modulate the balance between niche-based and  
1171 neutral processes in soybean microbiome. Microb Ecol. 82:416–428.  
1172 <https://doi.org/10.1007/s00248-021-01688-w>

1173 Niu, L., and Liao, W. 2016. Hydrogen peroxide signaling in plant development and abiotic  
1174 responses: crosstalk with nitric oxide and calcium. Front Plant Sci. 7.  
1175 <https://doi.org/10.3389/fpls.2016.00230>

1176 Nobu, M.K., Narihiro, T., Rinke, C., Kamagata, Y., Tringe, S.G., Woyke, T., Liu, W.T. 2015.  
1177 Microbial dark matter ecogenomics reveals complex synergistic networks in a  
1178 methanogenic bioreactor. ISME J. 9(8):1710–1722.  
1179 <https://doi.org/10.1038/ismej.2014.256>

1180 Osdaghi, E., Young, A.J., Harveson, R.M. 2020. Bacterial wilt of dry beans caused by  
1181 *Curtobacterium flaccumfaciens* pv. *flaccumfaciens*: A new threat from an old enemy.  
1182 Mol Plant Pathol. 21(5):605–621. <https://doi.org/10.1111/mpp.12926>

1183 Oksanen, J., Blanchet, F. G., Friendly, M., Kindt, R., Legendre, P., McGlinn, D., Minchin, P. R.,  
1184 O'Hara, R. B., Simpson, G. L., Solymos, P., Stevens, M. H.H., Szoecs, E., and Wagner,  
1185 H. 2022. vegan: Community ecology package.  
1186 <https://cran.r-project.org/web/packages/vegan/index.html>

1187 Oksanen, E., Riikonen, J., Kaakinen, S., Holopainen, T., Vapaavuori, E. 2005. Structural  
1188 characteristics and chemical composition of birch (*Betula pendula*) leaves are modified  
1189 by increasing CO<sub>2</sub> and ozone. Glob Change Biol. 11(5):732–748.  
1190 <https://doi.org/10.1111/j.1365-2486.2005.00938.x>

1191 Pellinen, R. I., Korhonen, M.-S., Tauriainen, A. A., Palva, E. T., Kangasjärvi, J. 2002. Hydrogen  
1192 peroxide activates cell death and defense gene expression in birch. Plant Physiol.  
1193 130(2):549–560. <https://doi.org/10.1104/pp.003954>

1194 Piao, S., Liu, Q., Chen, A., Janssens, I. A., Fu, Y., Dai, J., Liu, L., Lian, X., Shen, M., Zhu, X.  
1195 2019. Plant phenology and global climate change: current progresses and challenges.  
1196 Global Change Biol. 25(6):1922–1940. <https://doi.org/10.1111/gcb.14619>

1197 Paradis, E., Schliep, K. 2019. ape 5.0: an environment for modern phylogenetics and  
1198 evolutionary analyses in R. Bioinformatics. 35:526-528. doi:  
1199 10.1093/bioinformatics/bty633. <https://cran.r-project.org/web/packages/ape/index.html>

1200 Passera, A., Compant, S., Casati, P., Maturo, M.G., Battelli, G., Quaglino, F., Antonielli, L.,  
1201 Salerno, D., Brasca, M., Toffolatti, S.L., Mantegazza, F., Delledonne, M., Mitter, B. 2019.  
1202 Not Just a Pathogen? Description of a Plant-Beneficial *Pseudomonas syringae* Strain.  
1203 Front Microbiol. 10. <https://doi.org/10.3389/fmicb.2019.01409>

- 1204 Pfaff, B. 2008. Analysis of Integrated and Cointegrated Time Series with R, Second edition.  
1205 Springer, New York. ISBN 0-387-27960-1, <https://www.pfaffikus.de>.  
1206 <https://doi.org/10.1007/978-0-387-75967-8>
- 1207 Phillips, R.W., Wiegel, J., Berry, C.J., Fliermans, C., Peacock, A.D., White, D.C., Shimkets, L.J.  
1208 2002. *Kineococcus radiotolerans* sp. nov., a radiation-resistant, gram-positive bacterium.  
1209 Int J Syst Evol Micr. 52(3):933–938. <https://doi.org/10.1099/00207713-52-3-933>
- 1210 Prentice, I.C., Cramer, W., Harrison, S.P., Leemans, R., Monserud, R.A., Solomon, A.M. 1992.  
1211 Special Paper: A Global Biome Model Based on Plant Physiology and Dominance, Soil  
1212 Properties and Climate. J Biogeogr. 19(2):117–134. <https://doi.org/10.2307/2845499>
- 1213 Preston, G. M. 2004. Plant perceptions of plant growth-promoting *Pseudomonas*. Philos T Roy  
1214 Soc B. 359(1446):907–918. <https://doi.org/10.1098/rstb.2003.1384>
- 1215 R Core Team. 2024. R: A language and environment for statistical computing. R Foundation for  
1216 Statistical Computing, Vienna, Austria. <https://www.R-project.org/>
- 1217 Radhakrishnan, R., Hashem, A., Abd\_Allah, E.F. 2017. *Bacillus*: A Biological Tool for Crop  
1218 Improvement through Bio-Molecular Changes in Adverse Environments. Front Physiol.  
1219 8. <https://doi.org/10.3389/fphys.2017.00667>
- 1220 Ramírez-Bahena, M.H., Tejedor, C., Martín, I., Velázquez, E., Peix, A. 2013. *Endobacter*  
1221 *medicaginis* gen. nov., sp. nov., isolated from alfalfa nodules in an acidic soil. Int J Syst  
1222 Evol Micr. 63(Pt\_5):1760–1765. <https://doi.org/10.1099/ijs.0.041368-0>

- 1223 Raspor, P., Goranovič, D. 2008. Biotechnological applications of acetic acid bacteria. *Crit Rev*  
1224 *Biotechnol.* 28(2):101–124. <https://doi.org/10.1080/07388550802046749>
- 1225 Rastogi, S., Pandey, M.M., Kumar Singh Rawat, A. 2015. Medicinal plants of the genus *betula*--  
1226 traditional uses and a phytochemical-pharmacological review. *J Ethnopharmacol.*  
1227 159:62–83. <https://doi.org/10.1016/j.jep.2014.11.010>
- 1228 Redford, A.J., Bowers, R.M., Knight, R., Linhart, Y., Fierer, N. 2010. The ecology of the  
1229 phyllosphere: geographic and phylogenetic variability in the distribution of bacteria on  
1230 tree leaves. *Environ Microbiol.* 12:2885–2893. doi: 10.1111/j.1462-2920.2010.02258.x
- 1231 Sangiorgio, D., Cáliz, J., Mattana, S., Barceló, A., De Cinti, B., Elustondo, D., Hellsten, S.,  
1232 Magnani, F., Matteucci, G., Merilä, P., Nicolas, M., Ravaioli, D., Thimonier, A.,  
1233 Vanguelova, E., Verstraeten, A., Waldner, P., Casamayor, E. O., Peñuelas, J., Mencuccini,  
1234 M., Guerrieri, R. 2024. Host species and temperature drive beech and Scots pine  
1235 phyllosphere microbiota across European forests. *Commun Earth Environ.* 5(1):747.  
1236 <https://doi.org/10.1038/s43247-024-01895-6>
- 1237 Schiraldi, C., De Rosa, M. 2014. Mesophilic Organisms. In: Drioli, E., Giorno, L. (eds)  
1238 *Encyclopedia of Membranes.* Springer, Berlin, Heidelberg. [https://doi.org/10.1007/978-3-](https://doi.org/10.1007/978-3-642-40872-4_1610-2)  
1239 [642-40872-4\\_1610-2](https://doi.org/10.1007/978-3-642-40872-4_1610-2)
- 1240 Stone, B.W.G., Jackson, C.R. 2021. Seasonal Patterns Contribute More Towards Phyllosphere  
1241 Bacterial Community Structure than Short-Term Perturbations. *Microb Ecol.* 81(1):146–  
1242 156. <https://doi.org/10.1007/s00248-020-01564-z>

- 1243 Sweeny, A.R, Lemon, H., Ibrahim, A., Watt, K.A., Wilson, K., Childs, D.Z., Nussey, D.H., Free,  
1244 A., McNally, L. 2023. A mixed-model approach for estimating drivers of microbiota  
1245 community composition and differential taxonomic abundance. *mSystems*. 8:e00040-23.  
1246 <https://doi.org/10.1128/msystems.00040-23>
- 1247 Thapa, S., Prasanna, R., Ranjan, K., Velmourougane, K., Ramakrishnan, B. 2017. Nutrients and  
1248 host attributes modulate the abundance and functional traits of phyllosphere microbiome  
1249 in rice. *Microbiol Res*. 204:55–64. doi: 10.1016/j.micres.2017.07.007
- 1250 Trivedi, P., Leach, J.E., Tringe, S.G., Sa, T., Singh, B.K. 2020. Plant–microbiome interactions:  
1251 from community assembly to plant health. *Nat Rev Microbiol*. 18(11):607–621.  
1252 <https://doi.org/10.1038/s41579-020-0412-1>
- 1253 Uroz, S., Buée, M., Deveau, A., Mieszkin, S., Martin, F. 2016. Ecology of the forest microbiome:  
1254 highlights of temperate and boreal ecosystems. *Soil Biol Biochem*. 103:471–488.  
1255 <https://doi.org/10.1016/j.soilbio.2016.09.006>
- 1256 Vacher, C., Hampe, A., Porté, A.J., Sauer, U., Compant, S., Morris, C.E. 2016. The Phyllosphere:  
1257 Microbial Jungle at the Plant–Climate Interface. *Annu Rev Ecol Evol S*. 47(1):1–24.  
1258 <https://doi.org/10.1146/annurev-ecolsys-121415-032238>
- 1259 Vorholt, J.A. 2012. Microbial life in the phyllosphere. *Nat Rev Microbiol*. 10:828–840.  
1260 <https://doi.org/10.1038/nrmicro2910>
- 1261 Wang, X., Yuan, Z., Ali, A., Yang, T., Lin, F., Mao, Z., Ye, J., Fang, S., Hao, Z., XugaoWang,  
1262 Le Bagousse-Pinguet, Y. 2023. Leaf traits and temperature shape the elevational patterns

1263 of phyllosphere microbiome. *Journal of Biogeography*. 50(12):2135–2147.  
1264 <https://doi.org/10.1111/jbi.14719>

1265 Weiher, E., Clarke, G.D.P., Keddy, P.A. 1998. Community assembly rules, morphological  
1266 dispersion, and the coexistence of plant species. *Oikos*. 81(2):309.  
1267 <https://doi.org/10.2307/3547051>

1268 Xu, S., Yuan, Y., Song, P., Cui, M., Zhao, R., Song, X., Cao, M., Zhang, Y., Yang, J. 2023. The  
1269 spatial patterns of diversity and their relationships with environments in rhizosphere  
1270 microorganisms and host plants differ along elevational gradients. *Front Microbiol*.  
1271 14:1079113. doi: 10.3389/fmicb.2023.1079113

1272 Zhang, L., Chen, F., Zeng, Z., Xu, M., Sun, F., Yang, L., Bi, X., Lin, Y., Gao, Y., Hao, H., Yi, W.,  
1273 Li, M., Xie, Y. 2021. Advances in metagenomics and its application in environmental  
1274 microorganisms. *Front Microbiol*. 12:766364. <https://doi.org/10.3389/fmicb.2021.766364>

1275 Zhang, Y., Wang, Y., Tang, M., Zhou, J., Zhang, T. 2023. The microbial dark matter and “wanted  
1276 list” in worldwide wastewater treatment plants. *Microbiome*. 11(1):59.  
1277 <https://doi.org/10.1186/s40168-023-01503-3>

1278 Zeng, H.Y., Yao, N. 2022. Sphingolipids in plant immunity. *Phytopathol Res*. 4(1).  
1279 <https://doi.org/10.1186/s42483-022-00125-1>

1280 Zheng, K., Hong, Y., Guo, Z., Debnath, S.C., Yan, C., Li, K., Chen, G., Xu, J., Wu, F., Zheng, D.,  
1281 Wang, P. 2022. *Acinetobacter sedimenti* sp. nov., isolated from beach sediment. *Int J Syst*  
1282 *Evol Micr*. 72(11). <https://doi.org/10.1099/ijsem.0.005609>

1283 Zhou, H.W., Li, D.F., Tam, N.F., Jiang, X.T., Zhang, H., Sheng, H.F., Qin, J., Liu, X., Zou, F.  
1284 2011. BIPES, a cost-effective high-throughput method for assessing microbial diversity.  
1285 ISME J. 5(4):741–749. <https://doi.org/10.1038/ismej.2010.160>

1286 **APPENDIX**

1287 **Table A1.** Summary of the most common bacterial taxa found within the phyllosphere and  
 1288 endosphere of plant leaves. Major phyla are displayed with their most common associated  
 1289 member classes and genera. The Gram status of each is listed, along with a brief description of  
 1290 their most important functions in the phyllosphere and endosphere (Durand et al. 2018; Kembel  
 1291 et al. 2014; Redford et al. 2010).

Major Phyla	Common Member Classes	Common Member Genera	Examples of Function(s)	Gram Stain (+/-)
Pseudomonadota	Alphaproteobacteria	<i>Sphingomonas</i>	Highly associated with Poplar trees ( <i>Populus</i> sp.). Produce growth hormones (e.g. sphinganol) to promote plant growth (Asaf et al. 2020).	-
		<i>Hyphomicrobium</i>	Methanotrophic (i.e., carbon cycling); Methylobacterium is highly associated with Poplar ( <i>Populus</i> sp.) trees (Chaudhry et al. 2021).	
		<i>Methylibium</i>		
		<i>Methylobacterium</i>		
		<i>Methylocapsa</i>		
		<i>Methylocella</i>		
		<i>Methylocystis</i>		
	Betaproteobacteria	<i>Azospirillum</i>	Diazotrophic (i.e., N <sub>2</sub> fixation).	
		<i>Acetobacter</i>		
		<i>Burkholderia</i>		
		<i>Methylibium</i>	Methanotrophic (i.e., carbon cycling)	
Gammaproteobacteria	<i>Pantoea</i>		Phytopathogens and necrotrophs, but many species promote plant growth, fix N <sub>2</sub> , degrade toxins, and produce antibiotics (Chaudhry et al. 2021).	
	<i>Erwinia</i>	Common phytopathogens (cause bacterial fire blight and soft rot; can co-opt plant immune signals); pectolytic; leach and compete for iron from plant host tissues (Expert 1999).		

		<i>Enterobacter</i>	Many promote plant growth; bolster plant immunity via acetoin production in some hosts; role in sulfur metabolism and cycling (Andrés-Barrao et al. 2021; Khalifa et al. 2016). Some species are diazotrophic/N <sub>2</sub> fixing (Macedo-Raygoza et al. 2019). Some are phytopathogens.
		<i>Citrobacter</i>	Plant-growth promoting bacteria; high heavy metal (HM) resistance helps host avoid HM toxicity (increasing concentrations of HMs reduces chlorophyll content). Has been shown reduce proline in leaves; Role in PO <sub>4</sub> <sup>-3</sup> sequestration (Ajmal et al. 2022).
		<i>Acinetobacter</i>	Promotes plant growth (increase in biomass and chlorophyll content); solubilizes PO <sub>4</sub> <sup>-3</sup> (in solid or liquid media, e.g. leaf tissue). Some strains produce gibberellins (Kang et al. 2009); significant VOC production. Presence can completely alter leaf microbiome: e.g., presence is positively correlated with <i>Bacillus</i> sp. (Zheng et al. 2022).
		<i>Pseudomonas</i>	Phytopathogens ( <i>Pseudomonas syringae</i> is a common, economically destructive one); can produce lipopeptides that are lytic and inhibit growth (Preston 2004). Many strains promote plant growth by synthesizing phytohormones and suppressing many other pathogens. Distinct VOC profile (Passera et al. 2019). Syringafactin production adsorbs to

			waxy leaf cuticle and increases rate of water diffusion across isolated cuticles and attracts water to hydrophobic surfaces exposed to high relative humidity; stomatal aperture regulation (Chaudhry et al. 2021).	
Actinomycetota	Actinomycetes	<i>Kineococcus</i>	Highly associated with Poplar trees ( <i>Populus</i> sp.). Some strains contain carotenoid pigments that absorb light at wavelengths of 444, 471, and 501 nm (Phillips et al. 2002). Exhibits antibiotic resistance and produces many types of antibiotics: e.g., some strains produce chloramphenicol, which inhibits the uptake of salt ions by plant tissues, inhibiting growth (Mhatre et al. 2020).	+
		<i>Curtobacterium</i>	Economically significant phytopathogen. An agent of bacterial wilt and leaf spot (Osdaghi et al. 2020).	
Bacillota	Bacilli	<i>Bacillus</i>	Many functions in plant hosts; crucial role in plant immunity, nutrient uptake, and N <sub>2</sub> fixation. Modulates gene expression profile of some plant leaves to promote plant growth; siderophores and exopolysaccharide production to adjust ionic balance and water content, and transport of toxic ions away. Regulates intracellular phytohormone metabolism. Promotes stress tolerance by modifying host stress-response genes, proteins, phytohormones, and metabolites	+

			(Rhadhakrishnan et al. 2017).	
Bacteroidota	Cytophagia	<i>Hymenobacter</i>	Plant growth-promoting bacteria that is highly associated with Poplar trees ( <i>Populus</i> sp.). Can degrade fungal chitin. Phototrophic and isolated from high-UV environments, which is beneficial to phyllosphere (Stone and Jackson 2020).	-
	Sphingobacterii	<i>Sphingobacterium</i>	Sphingophospholipid production, which helps in plant immunity to regulate pathogens and mediate the delicate microbe-host balance (Zheng and Yao 2022). Order Sphingobacteriales represents approximately 21-22% of tree phyllosphere sequences (Redford et al. 2010).	
Deinococcota	Deinococcii	<i>Deinococcus</i>	Contains a pink-coloured carotenoid pigment called deinoxanthin (reflectance is a mixture of red and purple ends of the VIS spectrum). Extremophiles tolerant to high doses of UV and gamma radiation. Biosynthesis of cell-free metal nanoparticles to tolerate heavy metal stress (Chen et al. 2017).	+

1292 **S2.0 SUPPLEMENTAL MATERIALS AND METHODS**

1293 ***S2.2 DNA Extraction***—This study uses a culture-independent sampling method, which is more  
1294 representative of the true microbial community than culture-dependent methods (Bodor et al.  
1295 202; Hinsu et al. 2021; Hugerth and Andersson 2017; Redford et al. 2010).

1296 To achieve complete lysis of plant cell walls and all microbial cells for representative  
1297 sampling, two sterile 4.7 mm stainless steel beads were added to each PowerBead tube, and a  
1298 vertical mixer mill was used to pulverize frozen samples at 25 Hz for five 1 min cycles. Once  
1299 grinding was complete, each sample tube was incubated with lysis buffer in a heated shaker at  
1300 65°C for 30 min at 800 rpm; additionally, samples were vortexed every 10 min. Rather than  
1301 incubating the tubes at 2–8°C for 5 min, the samples were incubated on ice for 7 min to yield  
1302 optimal DNA purity. Isolated DNA was run on a 1% agarose gel and a Qubit 2.0 fluorometer  
1303 assay was performed to quantify the DNA product for each sample.

1304 ***S2.4 Sequence Quality Control, Filtering, and Taxonomic Assignment of ASVs***— Quality of  
1305 both forward and reverse reads was assessed with the ‘plotQualityProfile()’ function to ensure  
1306 quality scores exceeded 30 and to determine the optimal truncation length for filtering. Using the  
1307 ‘filterAndTrim()’ function, sequences were filtered and trimmed: forward reads were truncated to  
1308 240 bases, reverse reads to 230 bases, with a maximum of 0 ambiguous bases allowed, a  
1309 maximum expected error (maxEE) of 2, a truncation quality threshold (truncQ) of 2, and PhiX  
1310 sequences removed (rm.phix = TRUE). Paired reads were then merged with the ‘mergePairs()’  
1311 function, which only combines reads if they overlap by at least 12 bases and match exactly in the  
1312 overlap region (Callahan et al. 2016). Notably, ASVs are exact sequences derived from high-  
1313 throughput sequencing, providing a high resolution of microbial diversity without relying on

1314 clustering thresholds like operational taxonomic units (OTUs). This approach improves accuracy  
1315 and reproducibility by capturing fine genetic variations (Callahan et al. 2017; Callahan et al.  
1316 2019; Chiarello et al. 2022).

1317         A total of 3046486 reads passed the quality filtering step, resulting in 1790 ASVs.  
1318 Taxonomy was then assigned to these ASVs using the ‘assignTaxonomy()’ function, which  
1319 employs the naive Bayesian classifier method (Callahan et al. 2016). This function requires a  
1320 reference training set with known taxonomy and generates taxonomic assignments based on  
1321 training FASTA files from the RDP, GreenGenes, and SILVA databases. Additionally, species-  
1322 level classifications were obtained through exact matching of ASVs with reference strains, as this  
1323 method is considered most accurate for 16S gene fragments with 100% identity (Callahan et al.  
1324 2016; Edgar 2018). The ‘addSpecies()’ function used species-assignment training FASTA files  
1325 from the SILVA and RDP 16S databases for this purpose.

1326 ***S2.5 Statistical Analyses***—All statistical analyses were conducted using R v.2024.09.0 (R Core  
1327 Team, 2024).

1328         ***S2.5.1 Bacterial Alpha Diversity Patterns— Statistical Model Construction and***  
1329 **Diagnosics:** Preliminary analysis of the data included assessing homogeneity of slopes faceted  
1330 by fixed effects and generating scatterplot matrices using the ‘scatterplotMatrix()’ function from  
1331 the *car* package. Applying the ‘lmer()’ function from the *lme4* package, multiple linear mixed  
1332 models (LMMs) were constructed to model ASV richness (ASV R’) and Shannon diversity (H’)  
1333 within (intraspecific) and between (interspecific) host species to explore the impacts of host  
1334 species identity, host phenology (GDDs), and their two-way interaction, with varying  
1335 transformations on the response variable data and plant identity (‘Plant\_ID’) set as the random  
1336 effect (Bates et al. 2015; Faticov et al. 2021; Sweeny et al. 2023).

1337           Subsequently, formal normality tests were conducted using the ‘shapiro.test()’ function in  
1338 base R. Diagnostic statistics were generated using the ‘check\_model()’ function from the  
1339 *performance* package to assess homogeneity of variance, linearity, collinearity, influential  
1340 observations, and normality of residuals for each LMM (Lüdecke et al. 2021). Model fits were  
1341 compared using the ‘anova()’ function, and the best models were identified based on the lowest  
1342 Akaike Information Criterion (AIC), the lowest Bayesian Information Criterion (BIC), the lowest  
1343 deviance, and the highest log-likelihood.

1344           **Interspecific Model Selection (Alpha Diversity):** For interspecific host comparisons of  
1345 leaf bacterial alpha diversity, the best-fitting LMMs—which satisfied statistical diagnostic  
1346 checks and normalized residuals—log-transformed ASV richness ( $\log(\text{ASV } R')$ ) and square-root  
1347 transformed Shannon diversity ( $\sqrt{H'}$ ). Both metrics were independently modeled as functions of  
1348 the fixed effects of host tree species (‘Species’), GDD accumulation (‘GDD\_5C’), and their two-  
1349 way interaction (‘Species:GDD\_5C’), with ‘Plant\_ID’ included as a random effect. A more  
1350 complex model incorporating a nested random effect structure [(1 | Species / Plant\_ID)] was  
1351 considered but found to be unstable, producing convergence warnings and unreliable parameter  
1352 estimates. This instability is likely due to the small sample size at the higher species-level, with  
1353 only two species being compared, which limits the ability of the model to partition variability  
1354 reliably. Often, studies suggest more than two grouping levels for reliable nesting—ideally, at  
1355 least five (Aarts et al. 2014). Therefore, a simpler random effect structure [(1 | Plant\_ID)] was  
1356 used to ensure model stability and reliable inference, recognizing that this approach pools  
1357 intraspecific data and does not explicitly account for potential differences between species in  
1358 ‘Plant\_ID’-specific effects. While the simpler model provided reliable estimates, it does not  
1359 explicitly partition intraspecific and interspecific variability. To address this for downstream

1360 analyses of intraspecific variation, I fit separate models for each species to analyze intraspecific  
1361 variation. However, comparisons of interspecific and intraspecific variation should be interpreted  
1362 cautiously due to the absence of an explicit nested random effect structure and the limited  
1363 sampling design. For ASV richness (ASV R'), the best fit interspecific LMM was as follows:

1364 
$$\log(\text{ASV } R') \sim \text{Species} + \text{GDD\_5C} + \text{Species: GDD\_5C} + (1 | \text{Plant\_ID})$$

1365 For Shannon diversity (H'), the best fit interspecific LMM was as follows:

1366 
$$\sqrt{H'} \sim \text{Species} + \text{GDD\_5C} + \text{Species: GDD\_5C} + (1 | \text{Plant\_ID})$$

1367 **Intraspecific Model Selection (Alpha Diversity):** To address this limitation, I also  
1368 analyzed intraspecific (within-species) variation by fitting separate LMMs for each species,  
1369 where 'Plant\_ID' was modeled as a random effect. To satisfy diagnostic criteria and normalize  
1370 residuals for sample data within-species, models selected for birch leaves involved reciprocal  
1371 transformations of both bacterial ASV richness ( $\frac{1}{\text{ASV } R'}$ ) and Shannon diversity ( $\frac{1}{H'}$ ), both  
1372 modeled as functions of the fixed effect 'GDD\_5C' and the random effect 'Plant\_ID'. For birch,  
1373 the best fit intraspecific LMM for ASV richness (ASV R') was as follows:

1374 
$$\frac{1}{\text{ASV } R'} \sim \text{GDD\_5C} + (1 | \text{Plant\_ID})$$

1375 For birch, the best fit intraspecific LMM for Shannon diversity (H') was as follows:

1376 
$$\frac{1}{H'} \sim \text{GDD\_5C} + (1 | \text{Plant\_ID})$$

1377 Within aspen, ASV richness was reciprocally transformed ( $\frac{1}{\text{ASV } R'}$ ), while Shannon  
1378 diversity was square-root transformed ( $\sqrt{H'}$ ), both also modeled as a function of the fixed effect

1379 ‘GDD\_5C’ and the random effect ‘Plant\_ID’. Additionally, ‘GDD\_5C’ was treated as a  
1380 continuous numeric variable in the LMMs. For all intraspecific models within both tree species,  
1381 ‘Plant\_ID’ was modeled as a random effect to account for variability among individual plants  
1382 while avoiding the overparameterization and instability that arose from including ‘Plant\_ID’ as a  
1383 fixed effect. This approach provided a more reliable model fit while still capturing individual-  
1384 level variability. For aspen, the best fit intraspecific LMM for ASV richness (ASV R') was as  
1385 follows:

$$1386 \quad \frac{1}{ASV R'} \sim GDD\_5C + (1 | Plant\_ID)$$

1387 For aspen, the best fit intraspecific LMM for Shannon diversity (H') was as follows:

$$1388 \quad \sqrt{H'} \sim GDD\_5C + (1 | Plant\_ID)$$

1389 **Marginal and Conditional R<sup>2</sup> Calculation:** For each statistically significant fixed  
1390 effect, both marginal R<sup>2</sup> (R<sup>2</sup><sub>m</sub>) and conditional R<sup>2</sup> (R<sup>2</sup><sub>c</sub>) values were calculated separately using  
1391 the ‘r.squaredGLMM()’ function from the *MuMIn* package, whilst retaining the same random  
1392 effects (Faticov et al. 2021; Bartoń 2023). The R<sup>2</sup><sub>m</sub> value quantifies the proportion of variance  
1393 explained by the fixed effects alone, highlighting their contribution to the model. In contrast, the  
1394 R<sup>2</sup><sub>c</sub> value represents the total variance explained by both fixed and random effects, providing  
1395 insight into the overall fit of the model (Nakagawa et al. 2017; Lüdecke et al. 2021).

1396 **Pairwise Comparisons of Host–Phenology Interaction Effects:** To evaluate how leaf  
1397 bacterial ASV richness and Shannon diversity vary in response to the interaction between their  
1398 host species and accumulated GDDs (‘Species:GDD\_5C’), pairwise comparisons were  
1399 conducted using the ‘emmeans()’ function from the *emmeans* package in R (Lenth 2024). The

1400 ‘emmeans()’ function calculates the estimated marginal means for each level of comparison  
1401 using the fitted LMM, and then conducts t-tests on the differences (contrasts) between these  
1402 means to assess the significance of pairwise comparisons. Its t-tests incorporated the regression  
1403 slope for the continuous variable ‘GDD\_5C’ and accounted for random effects (‘Plant\_ID’),  
1404 residual variance, and model-specific degrees of freedom, ensuring accurate p-values and  
1405 confidence intervals (Lenth 2024). Note that only pairwise comparisons of interactions made  
1406 within the same GDD were considered (e.g., comparing birch’s interaction with GDD 437 to  
1407 aspen’ interaction with GDD 437) for the sake of biological relevance. Overall, this permits  
1408 investigation of how host species’ phenological change interacts with its physiology to impact  
1409 leaf bacterial differences, and whether these species-specific differences are detectable.

1410       **Pairwise Comparisons of Host Species Effects Across Phenology:** To isolate the  
1411 ‘Species’ differences at each ‘GDD\_5C’ value, independent of GDD but still taking the LMM  
1412 structure into consideration, *emmeans* was used with the specification: “specs = pairwise ~  
1413 Species | GDD\_5C” (Lenth 2024). The ‘emmeans()’ function calculates the estimated marginal  
1414 means for each level of ‘Species’ at specified values of ‘GDD\_5C’ using the fitted LMM, and it  
1415 then conducts t-tests on the differences (contrasts) between these means to assess the significance  
1416 of pairwise comparisons. This method permits accurate pairwise comparisons by avoiding the  
1417 loss of nuance associated with subsetting the data by GDD, then comparing each species at each  
1418 GDD, without the additional consideration of the random effect. This technique explores how the  
1419 differential influence of host species identity on bacterial alpha diversity varies across  
1420 temperature-driven phenological stages (GDDs).

1421       **Pairwise Comparisons of Growing Degree Day Effects Within Host Species:** If the  
1422 LMMs identified ‘GDD\_5C’ as significantly impacting either alpha diversity metric within birch

1423 or aspen (i.e., intraspecific comparisons), the *emmeans* package in R was used for pairwise  
1424 comparisons of ‘GDD\_5C’ to identify specific GDDs driving this variation and to pinpoint  
1425 where bacterial alpha diversity differed most over host phenology (Lenth 2024). Since  
1426 ‘Plant\_ID’ was modeled as a random effect, direct pairwise comparisons of individual plants  
1427 were not possible. Instead, I subset the data by GDD within each host species and compared  
1428 differences in ‘Plant\_ID’ effects within each subset.

1429 To validate subsetting by GDD, I first assessed temporal autocorrelation using  
1430 Kwiatkowski–Phillips–Schmidt–Shin (KPSS) tests for ASV richness and Shannon diversity  
1431 using the ‘ur.kpss()’ function from the *urca* package (Moroenyane et al. 2021a; Pfaff 2008).  
1432 Normality of alpha diversity data within each GDD subset was tested using ‘shapiro.test()’. For  
1433 normal data, ANOVAs assessed the effects of ‘Plant\_ID’ on alpha diversity at each GDD with the  
1434 ‘aov()’ function from the *stats* package, followed by residual normality checks. For non-normal  
1435 data, non-parametric Kruskal-Wallis tests were conducted using the ‘kruskal.test()’ function from  
1436 the *stats* package (Moroenyane et al. 2021a; R Core Team 2024). This approach identified GDDs  
1437 and individual plants with significant impacts on bacterial alpha diversity, providing insights into  
1438 thermo-temporal and individual variation within each host species.

1439 ***S2.5.4 Differential Abundance Analysis***—To assess which ASVs (and their associated  
1440 taxonomic assignments) were most differentially abundant between birch and trembling aspen as  
1441 GDDs accumulate, and overall, differential abundance analysis was performed using the *DESeq2*  
1442 package in conjunction with the *phyloseq* package (Faticov et al. 2021; Love et al. 2014;  
1443 McMurdie and Holmes 2013). *DESeq2* takes count data and normalizes them. To account for  
1444 multiple comparisons, *P*-values were adjusted using the Benjamini-Hochberg procedure (Faticov  
1445 et al. 2021; Love et al. 2014). Differential abundance analysis was performed comparing the two

1446 host tree species overall and then subsequently, the data were subset by GDD and differential  
1447 abundance analysis at each GDD was assessed. *DESeq2* takes count data and normalizes them.  
1448 To account for multiple comparisons, *P*-values were adjusted using the Benjamini-Hochberg  
1449 procedure (Faticov et al. 2021; Love et al. 2014). Differential abundance analysis was performed  
1450 comparing the two host tree species overall and then subsequently, the data were subset by GDD  
1451 and differential abundance analysis at each GDD was assessed.

1452         The purpose of conducting differential abundance analysis, in conjunction with  
1453 visualizing relative abundance profiles over GDDs, is to statistically identify bacterial taxa that  
1454 show significant changes in enrichment between birch and aspen across phenological  
1455 progression overall, and at the specific GDDs sampled. This method allows for precise relative  
1456 quantification of how specific taxa respond to the effects of host identity across cumulative  
1457 GDDs, accounting for variability and noise in the data. Differential abundance analysis identifies  
1458 taxa with significant patterns of variation, offering actionable insights into host-specific  
1459 microbiome dynamics, phenological shifts, and the ecological or functional roles of bacterial  
1460 ASVs. This approach complements taxonomic visualizations of relative abundance by  
1461 highlighting rare, low-abundance, or unidentified ASVs that may disproportionately influence  
1462 microbial dynamics but remain underrepresented in standard taxonomic profiles (Faticov et al.  
1463 2021; Love et al. 2014; McMurdie and Holmes 2013).

### 1464 **S3.0 SUPPLEMENTAL RESULTS**

1465 ***S3.1 Alpha Diversity***—In early-mid season comparisons, aspen had higher ASV richness than  
1466 birch. However, this trend inverted mid-late season, with birch surpassing aspen, except near the  
1467 end of the season (2140 GDDs). Shannon diversity differed significantly between the two tree

1468 species ( $P = 0.0413$ ), with consistently higher values observed in aspen compared to birch across  
1469 phenology (Fig. 2.2). Despite the observed patterns, overlapping bar plots and large error bars  
1470 suggest caution in visual interpretations. Therefore, the results of the LMMs were used to further  
1471 assess the impact of host species identity and GDDs on alpha diversity more reliably (Table 2.2).

1472         For ASV richness, which underwent logarithmic transformation when modelling, host  
1473 species identity ( $P = 0.00855$ ), GDDs ( $P = 0.000364$ ), and their interaction ( $P = 0.00531$ )  
1474 significantly influenced variation between host species' leaf bacterial microbiomes (Table 2.2).  
1475 Host species identity explained  $\sim 1.33\%$  of variance when considering only fixed effects ( $R^2_m =$   
1476  $0.0133$ ) and  $\sim 14.4\%$  when including random effects ( $R^2_c = 0.144$ ). Specifically, the model  
1477 revealed significant differences in ASV richness between the two species: aspen exhibited higher  
1478 ASV richness compared to birch (estimate = 0.859), with back-transformed ASV richness  
1479 estimates of approximately 48.7 for aspen and about 20.1 for birch at 'GDD\_5C' = 0. GDDs  
1480 alone explained  $\sim 6.17\%$  of ASV richness variance ( $R^2_m = 0.0617$ ); however, if random effects are  
1481 included, GDDs describes  $\sim 19.2\%$  of the variance in ASV richness ( $R^2_c = 0.192$ ). Additionally,  
1482 there was a positive association between GDDs and ASV richness for birch (estimate =  
1483  $0.000463$ ), indicating that each unit increase in GDD resulted in a multiplicative increase in ASV  
1484 richness, though this increase was multi-phase and non-linear.

1485         The interaction between species identity and GDDs explained  $\sim 9.94\%$  ( $R^2_m = 0.0994$ ) of  
1486 the variation observed in ASV richness when considering only fixed effects (Table 2.2). When  
1487 taking both fixed and random effects into account, the interaction between host tree species  
1488 identity and accumulated GDDs explains  $\sim 32.6\%$  of the variance in ASV richness ( $R^2_c = 0.326$ ).  
1489 Further, the interaction term (estimate =  $-0.000502$ ) suggested that for aspen, the relationship  
1490 was less positive, with a slight decrease in ASV richness as GDD increased (combined effect

1491 estimate = -0.0000387). The interaction between host species-specific traits and temperature-  
1492 dependent phenological shifts (i.e., accumulated GDDs) explains the most variation in leaf ASV  
1493 richness and is more significant than either factor alone. This interaction drives differences in  
1494 ASV richness among host species, with species identity moderating the effect of GDDs on  
1495 microbial richness. However, caution is warranted in interpreting this result, as the interaction  
1496 term includes all possible combinations of ‘Species’ and ‘GDD\_5C’, spanning differing levels of  
1497 GDDs. This broad comparison may not exclusively capture variations within the same GDD  
1498 sampling points, which were the primary focus for biological relevance. Nonetheless, the  
1499 findings emphasize significant species-specific responses to temperature accumulation  
1500 (‘GDD\_5C’) and its influence on microbial ASV richness within forest ecosystems.

1501       As stated, while the LMM identifies significant ‘Species:GDD\_5C’ interactions for ASV  
1502 richness, it does not differentiate between biologically meaningful comparisons (e.g., interactions  
1503 between host species at the same GDD) and less relevant ones (e.g., interactions across different  
1504 GDDs). LMMs detect overall patterns but do not explicitly test interactions at specific GDD  
1505 levels. Instead, they identify whether the relationship between the two variables, GDDs and ASV  
1506 richness, differs between groups of host species overall. While this broad approach provides  
1507 statistical evidence for an interaction, the interpretation requires careful contextualization, like  
1508 narrowing comparisons to specific GDDs that reflect similar phenological stages. To refine  
1509 interpretation, post-hoc pairwise comparisons were conducted using the *emmeans* package in R,  
1510 comparing interactions within the same GDD values (e.g., the interaction of birch vs. aspen with  
1511 GDD 437); comparisons across different GDD groupings were discarded for biological relevance  
1512 (Supplementary Table S1). The significant interaction in the overall LMM indicates that ASV  
1513 richness responds to phenological progression (GDDs) in a host-specific manner. However,

1514 pairwise comparisons at individual GDDs revealed no significant differences between the two  
1515 species, suggesting the interaction reflects cumulative trends across the phenological gradient  
1516 rather than discrete shifts at specific GDDs.

1517         Regarding Shannon diversity, which was square-root transformed during LMM analysis,  
1518 only host species identity ( $P = 0.0413$ ) significantly impacted bacterial diversity (Table 2.2).  
1519 Host species identity alone explained ~26.1% of the variance in Shannon diversity when  
1520 considering only fixed effects ( $R^2_m = 0.261$ ), increasing to ~34.1% when random effects were  
1521 included ( $R^2_c = 0.341$ ). Specifically, aspen exhibited a higher Shannon diversity compared to the  
1522 reference species birch (estimate = 0.264), with back-transformed estimates indicating an alpha  
1523 diversity of approximately 2.56 for aspen relative to 2.49 for birch when ‘GDD\_5C’ = 0. GDDs  
1524 and their interaction with species identity had no significant effect on Shannon diversity,  
1525 suggesting that the relationship between species identity and Shannon diversity remains  
1526 independent of GDD accumulation (Table 2.2). Thus, species identity plays a crucial role in  
1527 determining Shannon diversity, while the effects of accumulated GDDs may be minimal in this  
1528 context. The model accounted for variability among different plants, with random effects  
1529 associated with ‘Plant\_ID’ contributing to the overall model fit. Overall, these findings  
1530 underscore the importance of host species identity in shaping the leaf bacterial microbiome’s  
1531 Shannon diversity, independent of the effects of GDD.

1532         Subsequently, the *emmeans* package was used to assess the points during host phenology  
1533 where interspecific differences in ASV richness and Shannon diversity were most pronounced  
1534 (Lenth 2024). By using “specs = pairwise ~ Species | GDD\_5C”, *emmeans*—whilst respecting  
1535 the structure of the LMM—calculated pairwise comparisons between ‘Species’ alone at each  
1536 level of ‘GDD\_5C’ to investigate species-specific differences in alpha diversity independent of

1537 their interaction with GDDs to see where ‘Species’ exert their greatest influence on alpha  
1538 diversity during the growing season (Table 2.3). Regarding ASV richness, significant  
1539 interspecific differences were observed at GDD 437 ( $t = -2.489$ ,  $P = 0.0198$ ) and GDD 605 ( $t = -$   
1540  $2.333$ ,  $P = 0.0305$ ). Similarly, Shannon diversity was analyzed across GDD intervals, revealing  
1541 significant species-specific impacts at all GDD values (all  $P < 0.05$ ; Table 2.3). This pattern  
1542 highlights strong species-specific differences in evenness throughout the growing season.  
1543 Notably, Shannon diversity, which accounts for both richness and evenness, showed a more  
1544 persistent impact of host species across the entire season compared to ASV richness.

1545         Within birch, there was no overall change in Shannon diversity over the GDD gradient,  
1546 though bacterial ASV richness increased with GDD accumulation (Fig. 2.2; Supplementary Fig.  
1547 S3). Conversely, aspen exhibited no change in both ASV richness and Shannon diversity as  
1548 GDDs accumulated (Fig. 2.2; Supplementary Fig. S3). When examining variation from one  
1549 GDD to the next, birch demonstrated non-linear relationships in both ASV richness and Shannon  
1550 diversity, though the trajectory of these cycles differed between the two metrics (Fig. 2.2). In  
1551 aspen, oscillating non-linear relationships were observed, with increases in diversity during  
1552 early-mid season, followed by mid-late season declines, and a final increase near the season’s  
1553 end, with reductions in diversity at maximal GDDs (Fig. 2.2).

1554         Intraspecific (within-species) statistical analyses of GDD influence on bacterial diversity  
1555 in birch revealed that GDDs had a significant impact on the inverse of ASV richness ( $P =$   
1556  $0.000247$ ), explaining ~25% of variance in the fixed model ( $R^2_m = 0.25$ ) and ~51.3% ( $R^2_c =$   
1557  $0.513$ ) when random effects were included (Table 2.2). The negative coefficient for GDD  
1558 (estimate =  $-1.47 \times 10^{-5}$ ) indicates that as GDD increases, the value of  $\frac{1}{\text{ASV R}}$  decreases. Thus, a

1559 decrease in  $\frac{1}{ASV\ R}$  means that ASV richness itself is increasing with increasing GDD, indicating  
1560 that higher temperatures positively affect biodiversity by enhancing ASV richness. The estimated  
1561 intercept indicates a baseline species richness of approximately 19.1 individuals at zero GDD  
1562 within birch. The model accounted for variability among different plants, with random effects  
1563 associated with 'Plant\_ID' contributing to the overall model fit. These findings underscore the  
1564 importance of temperature in shaping the species richness of leaf bacterial communities in birch,  
1565 while also demonstrating that host plant identity has a minimal effect on variability in species  
1566 richness among individuals. However, GDDs did not significantly affect Shannon diversity ( $P =$   
1567  $0.731$ ) in birch. In contrast, GDD accumulation exhibited no significant effect in aspen on either  
1568 ASV richness ( $P = 0.427$ ) or Shannon diversity ( $P = 0.857$ ), suggesting that other variables not  
1569 considered in this study and stochastic processes likely drive diversity within aspen (Table 2.2).

1570         Within birch, only ASV richness was significantly impacted by GDDs; therefore,  
1571 pairwise comparisons of GDDs were conducted using the *emmeans* package in R to investigate  
1572 whether specific GDDs were driving variation in ASV richness with birch, or if the impact of  
1573 GDDs is more global or consistent across the season (Supplementary Table S2). Results of this  
1574 test indicate that no combination of pairwise comparisons between GDDs were significantly  
1575 different. In other words, within birch, ASV richness is not significantly different between any  
1576 given set of GDDs. This suggests that while GDDs have a significant overarching, consistent  
1577 effect on ASV richness within birch across the season, the differences in richness between  
1578 individual time points are not substantial enough to be statistically significant. Pairwise  
1579 comparisons between GDDs within aspen were not conducted since neither alpha diversity  
1580 metric was significantly impacted by GDDs.

1581           Finally, further testing with ANOVA and Kruskal-Wallis methods on GDD-subset data  
1582 assessed intraspecific variation of individuals in both species ('Plant\_ID') at each GDD  
1583 (Supplementary Tables S6–S7). However, since 'GDD\_5C' is treated as a continuous variable,  
1584 KPSS tests were performed to assess the appropriateness of GDDs being subset and categorized  
1585 in this manner. All KPSS tests for temporal autocorrelation indicate that—both interspecifically  
1586 and intraspecifically—ASV richness and Shannon diversity were not temporally autocorrelated.  
1587 The tests were unable to reject the null hypothesis that the datasets were stationary ( $P > 0.05$ ).  
1588 Therefore, this data is not temporally linked, and it is appropriate to subset the data by GDD  
1589 value to determine 'Plant\_ID' differences within each host species.

1590           For birch, individual plant attributes ('Plant\_ID') did not significantly affect either ASV  
1591 richness or Shannon diversity at any GDD sampling point (i.e., plant individuals did not differ  
1592 significantly in their alpha diversity at any given GDD), indicating that GDDs are a more critical  
1593 driver of bacterial diversity (Supplementary Table S3). Similarly, aspen showed no significant  
1594 effect of 'Plant\_ID' on bacterial diversity at any given GDD sampling point (Supplementary  
1595 Table S4). However, since GDDs have no significant impact on alpha diversity within aspen, it  
1596 reinforces the notion that environmental and host factors not investigated here may be driving  
1597 alpha diversity dynamics within aspen.

1598           ***S3.2 Community Composition and Structure***—When subset by GDD, the greatest  
1599 differences between the host tree species in bacterial community structure occurred at 605 (early-  
1600 mid phenology), 1606 (mid-late phenology), 2140, and 2219 GDDs, representing key stages of  
1601 seasonal phenology—the latter two of which represent late phenology and near senescence  
1602 (Supplementary Fig. S17). Thus, variation in leaf bacterial community structure between birch

1603 and aspen is driven primarily by host species, with the most pronounced differences occurring  
1604 early-mid, mid-late, and late phenology. To assess beta-diversity patterns and the structure of  
1605 bacterial communities within birch, a Bray-Curtis dissimilarity matrix was applied. Similarly, the  
1606 Bray-Curtis dissimilarity matrix was used to assess community structure within aspen, starting  
1607 with homogeneity and multivariate dispersion analyses to gauge the impact of these variances on  
1608 the structure of leaf bacterial communities. Analyses of homogeneity and multivariate dispersion  
1609 assessed the relative impact of between- and within-community compositions (Moroenyane et al.  
1610 2021).

1611         In birch, increased multivariate dispersion occurred at GDDs that aligned with early-mid  
1612 and late phenological stages (Supplementary Figs. S9–S10). Leaf bacterial communities of birch  
1613 leaves exhibited marginally significant heterogeneous dispersion across GDDs ( $F = 2.512$ ,  $P =$   
1614  $0.048$ ). However, Tukey's HSD post-hoc tests revealed that while some specific comparisons,  
1615 such as between 437 and 2219 GDDs, approached significance ( $P = 0.0549$ ), most comparisons  
1616 showed no statistically significant differences in dispersion (all  $P > 0.05$ ). This suggests that  
1617 while certain GDD thresholds may influence community variability, the differences are not  
1618 consistently strong across all groups. Despite variations in data spread, central tendencies  
1619 (means) remained similar. Analysis revealed only one plant (Plant\_ID: 8553879) with a  
1620 deviation in multivariate dispersion, suggesting it is potentially driving most within-species  
1621 differences. However, across all birch trees, there was no significant multivariate dispersion  
1622 (Supplementary Figs. S11–S12). The leaf bacterial communities did not show significant  
1623 heterogeneous dispersion ( $F = 0.848$ ,  $P = 0.51$ ), with a Tukey HSD test confirming non-  
1624 significant differences in means between groups.

1625 In trembling aspen, multivariate dispersion was limited across GDDs, except during late  
1626 phenological stages (Supplementary Figs. S13–S14). Here, leaf bacterial communities  
1627 demonstrated significant heterogeneous dispersion ( $F = 4.005$ ,  $P = 0.004$ ). Post-hoc Tukey HSD  
1628 tests identified the point at which the season reaches 2140 GDDs as a potential driver of these  
1629 differences, demonstrating significant dispersion compared to other GDD sampling points: 437  
1630 ( $P = 0.0367$ ), 605 ( $P = 0.0173$ ), 1087 ( $P = 0.00768$ ), 1606 ( $P = 0.00342$ ), 1992 ( $P = 0.0278$ ), and  
1631 2219 ( $P = 0.0231$ ). This indicates that the conditions at 2140 GDDs promote greater  
1632 homogeneity in bacterial community structure, particularly distinguishing late-season stages  
1633 from mid-late and early-season stages, while no significant differences were found between early  
1634 and mid-season stages (Supplementary Fig. S11). Regarding individual plants, only one tree  
1635 (Plant\_ID: 8987955) showed slight deviation in multivariate dispersion (Supplementary Figs.  
1636 S15–S16), but overall, there was no significant multivariate dispersion across all aspen plants ( $F$   
1637  $= 0.582$ ;  $P = 0.678$ ), with a Tukey HSD test further confirming non-significant differences  
1638 between groups.

1639 To visualize and investigate bacterial community structure changes across GDDs within  
1640 each species, Principal Coordinate Analysis (PCoA) using Bray-Curtis dissimilarity was  
1641 performed for each host, exclusively (Supplementary Fig. S18). Within birch, PERMANOVA  
1642 (Supplementary Table S5) revealed that GDDs significantly impacted leaf bacterial community  
1643 shifts throughout host phenology ( $F = 6.024$ ,  $P = 0.01$ ), explaining  $\sim 14.9\%$  of the variation ( $R^2 =$   
1644  $0.149$ ). ‘Plant\_ID’ did not significantly influence community variation ( $F = 1.159$ ,  $P = 0.231$ ),  
1645 nor did the interaction between ‘Plant\_ID’ and GDDs ( $F = 1.159$ ,  $P = 0.231$ ; Supplementary Fig.  
1646 S18A; Supplementary Table S5). In aspen, PERMANOVA showed GDDs significantly impacted  
1647 community variation across host phenology ( $F = 1.288$ ,  $P = 0.023$ ), though the effect was modest

1648 ( $R^2 = 0.037$ ). In contrast, 'Plant\_ID' ( $F = 0.91$ ;  $P = 0.952$ ) and its interaction with GDDs ( $F =$   
1649  $0.963$ ;  $P = 0.735$ ) did not significantly affect leaf bacterial community structure (Supplementary  
1650 Fig. S18B; Supplementary Table S5).

1651 Despite the significant impact of GDDs, the PCoA did not clearly separate bacterial  
1652 communities across GDDs within either species (Supplementary Fig. S18). When grouped by  
1653 generalized phenological periods (early-mid, mid-late, late-senescence), there is no clear  
1654 separation, except for in birch where early-mid phenology and late phenology-senescence  
1655 demonstrate clear separation (Supplementary Fig. S18A). Both groupings share overlap with  
1656 mid-phenology, supporting the idea of mid-season restructuring. However, it is important to note  
1657 that generalized phenological periods are unbalanced in their groupings. Within birch, a  
1658 significant negative correlation was observed between Axis 1 and GDDs (Spearman's  $\rho = -$   
1659  $0.715$ ,  $P = 1.344 \times 10^{-6}$ ), indicating that increasing GDD values correspond to lower Axis 1 scores  
1660 and demonstrating directionality within birch leaf microbiomes. Axis 2 showed a weak, non-  
1661 significant correlation with GDDs ( $\rho = 0.272$ ,  $P = 0.115$ ), suggesting this axis is not strongly  
1662 associated with the seasonal variation captured in the ordination. Therefore, the directionality in  
1663 the PCoA, from early-mid phenology (low GDDs) to late phenology and early senescence (high  
1664 GDDs), is likely driven by Axis 1, reflecting a significant seasonal phenological gradient along  
1665 this axis.

1666 Despite no clear separation in the PCoA for aspen, a significant negative correlation was  
1667 observed between Axis 1 and GDDs (Spearman's  $\rho = -0.337$ ,  $P = 0.044$ ; Supplementary Fig.  
1668 S18B). In contrast, Axis 2 showed no significant correlation with GDDs (Spearman's  $\rho = -0.17$ ,  
1669  $P = 0.32$ ). This indicates that increasing GDD values are associated with lower Axis 1 values,

1670 suggesting a potential seasonal directional relationship. Therefore, the observed negative  
1671 correlation along Axis 1 indicates a significant seasonal phenological trend in response to GDDs  
1672 within the aspen dataset. The low  $R^2$  and high residual  $R^2$  further implies that a combination of  
1673 unexamined environmental variables and stochasticity likely shape leaf microbiome structure.

1674 **S3.3 Differential Abundance Analysis**—Across the entire growing season, differential  
1675 abundance analysis revealed a notable contrast in the number of differentially abundant ASVs  
1676 between birch and aspen, measured as  $\log_2$  fold change ( $\log_2$ FC). Overall, birch had only three  
1677 ASVs that were significantly more abundant compared to aspen, whereas aspen exhibited a total  
1678 of 14 ASVs that were significantly more abundant relative to birch (Supplementary Fig. S20;  
1679 Supplementary Table S8). In birch, the ASVs with the highest positive  $\log_2$ FC (indicating greater  
1680 relative abundance compared to aspen) were ASV10 (unidentified Proteobacteria), ASV39  
1681 (*Endobacter* sp.), and ASV186 (*PMMRI* sp.), in descending order. Conversely, aspen exhibited  
1682 over four times as many ASVs with a negative  $\log_2$ FC (indicating greater relative abundance  
1683 compared to birch), including ASV86 (*Erwiniaceae*), ASV106 (*Blastococcus* sp.), ASV44  
1684 (*Methylobacterium-Methylorubrum* sp.), ASV33 (*Quadrisphaera* sp.), ASV81 (*Hymenobacter*  
1685 sp.), and ASV36 (*Rubellimicrobium* sp.).

1686 When the data were subset by GDD sampling points, differential abundance analysis  
1687 identified one ASV (ASV10) with a positive  $\log_2$ FC, indicating significantly greater relative  
1688 abundance in birch compared to aspen at GDD 437 (Supplementary Fig. S22; Supplementary  
1689 Table S9). At 605 GDDs, 15 ASVs were identified as differentially abundant, with 4 showing  
1690 positive  $\log_2$ FC (birch enriched) and 11 showing negative  $\log_2$ FC (aspen enriched). At 1087  
1691 GDDs (mid-phenology), the number of differentially abundant ASVs increased to 18, with 10

1692 enriched in birch and 8 in aspen. By 1606 accumulated GDDs, the total decreased to 10  
1693 differentially abundant ASVs, with 1 enriched in aspen and 9 in birch. As phenology progressed  
1694 to late-season (1992 GDDs), the number rose to 29, with 25 ASVs enriched in birch and 4 in  
1695 aspen. The number of differentially abundant ASVs peaked at 2140 GDDs, with 45 identified—  
1696 25 enriched in birch and 20 in aspen. At 2219 accumulated GDDs (senescence onset), the total  
1697 decreased to 32, with 20 ASVs enriched in birch and 12 in aspen.

1698           At each GDD along host phenology, birch consistently exhibited a higher number of  
1699 ASVs with significant differential abundance compared to aspen. From the beginning of  
1700 phenological sampling (437 GDDs), the number of differentially abundant ASVs increased  
1701 steadily until 1087 GDDs. This was followed by a decrease at 1606 GDDs, before rising again  
1702 into late-season (1992 and 2140 GDDs) and tapering slightly by 2219 GDDs. Both hosts share  
1703 this similar trend, with peaks in  $\log_2FC$  occurring earlier and late in the growing season  
1704 (Supplementary Fig. S22; Supplementary Table S9). Notably, ASV10, identified only to the  
1705 phylum Proteobacteria in the SILVA database, was consistently more abundant in birch than  
1706 aspen across all GDDs, highlighting its potential ecological and functional relevance to birch.

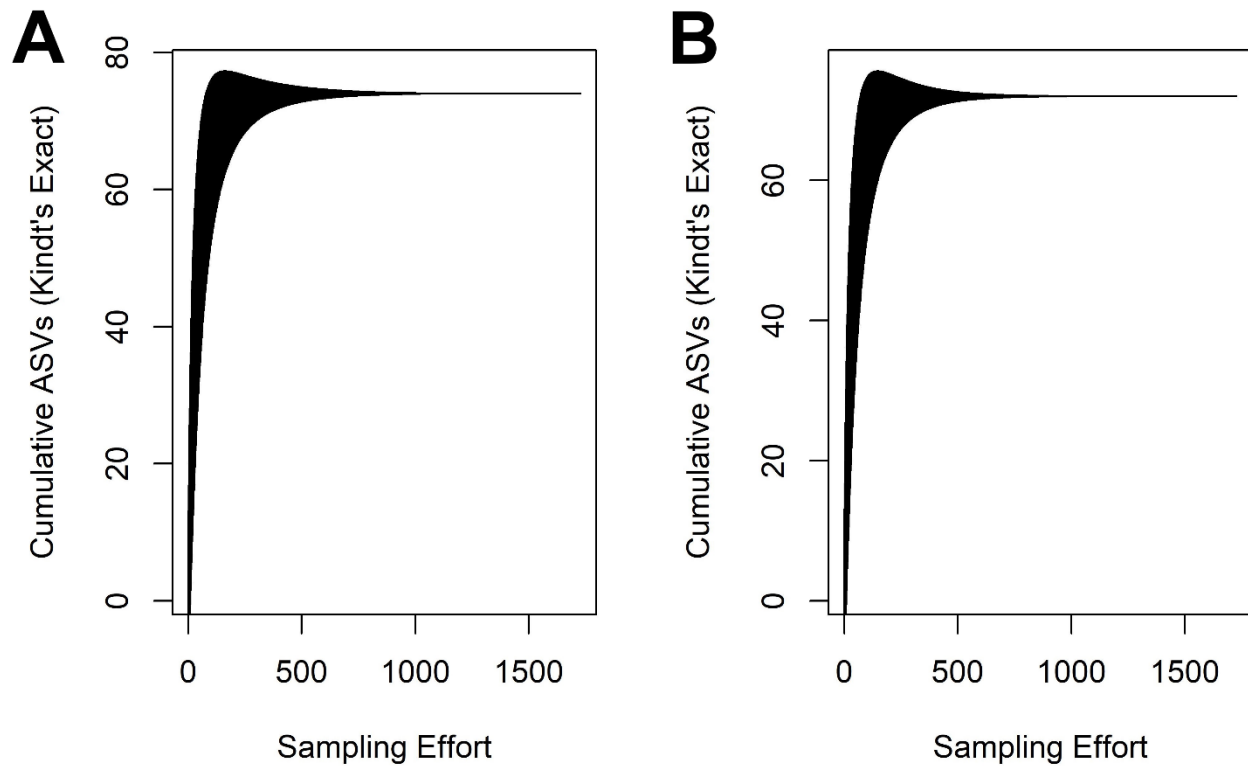
1707           Across the phenological gradient, several ASVs were consistently enriched in birch  
1708 compared to aspen, with notable shifts in the composition of these ASVs across GDDs  
1709 (Supplementary Figs. S21-S22; Supplementary Tables S11-S12). At 437 GDDs, only ASV10  
1710 (unidentified Proteobacteria) was enriched in birch. By 605 GDDs, ASV19 (unidentified  
1711 Proteobacteria) emerged as the second most enriched ASV in birch. By 1087 GDDs, ASV10 and  
1712 ASV19 were joined by ASV35 (unidentified beyond Bacteria), ASV8 (*Endobacter* sp.), ASV42  
1713 (*1174-901-12* sp.), and ASV95 (*Bryocella* sp.). At GDD 1606, ASV9 (*1174-901-12* sp.) and

1714 ASV49 (*P3OB-42* sp.) became prominent. By 1992 GDDs, 16 additional ASVs exhibited  
1715 significant enrichment in birch, with ASV10 remaining the most enriched. New ASVs, such as  
1716 ASV7 (*Endobacter* sp.), ASV14 (*1174-901-12* sp.), and ASV97 (*Massilia* sp.), appeared at this  
1717 stage. At GDD 2140, ASV7 (*Endobacter* sp.) overtook ASV10 as the most enriched ASV,  
1718 followed by ASV9, ASV19, ASV29, ASV25, ASV14, ASV8, and ASV35. By GDD 2219,  
1719 ASV7 and ASV8 (both *Endobacter* sp.) surpassed ASV10, while ASV109 (*Massilia* sp.) and  
1720 ASV37 (*Myxococcota*) also emerged among the most enriched ASVs.

1721 In contrast, aspen had fewer differentially abundant ASVs across phenology, overall  
1722 (Supplementary Fig. S22; Supplementary Table S9). At the start (437 GDDs), no ASVs were  
1723 differentially abundant relative to birch, but by 605 GDDs, 11 ASVs were differentially  
1724 abundant, including ASV33 (*Quadrisphaera* sp.), ASV59 (unidentified Bacteria), ASV54  
1725 (*Sphingomonas* sp.), and ASV32 (*Sphingomonas* sp.), in descending order of abundance. By  
1726 1087 GDDs, the number of differentially abundant ASVs decreased slightly, with ASV33  
1727 remaining the most prominent. Other significant ASVs at this time included ASV106  
1728 (*Blastococcus* sp.), ASV81 (*Hymenobacter* sp.), ASV60 (*Sphingomonas* sp.), and ASV93  
1729 (*Corynebacterium* sp.). At 1606 GDDs, the number decreased further, with only ASV44  
1730 (*Methylobacterium-Methylorubrum* sp.) being significantly enriched—a pattern also observed at  
1731 605, 1087, and 2140 GDDs. By 1992 GDDs, the number of differentially abundant ASVs  
1732 slightly increased, with ASV172 (*Massilia timonae*) showing the most significant enrichment,  
1733 followed by ASV59, ASV33, and ASV414 (*Amnibacterium* sp.). At 2140 GDDs, there was a  
1734 more substantial increase in differentially abundant ASVs. ASV36 (*Rubellimicrobium* sp.)  
1735 exhibited the greatest change, followed by ASV45 (*Actinomycetospora iriomotensis*), ASV33,  
1736 and ASV44. Other notable ASVs at this stage included ASV41 (*Methylobacterium-*

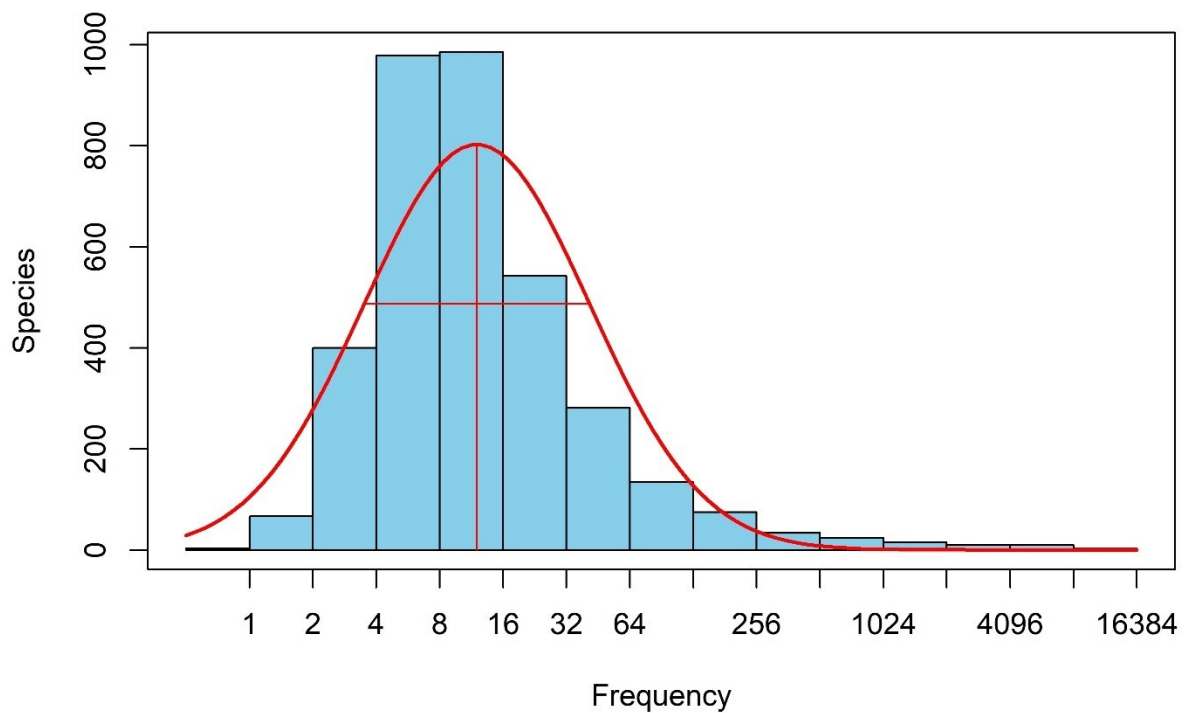
1737 *Methylobacterium* sp.), ASV80 (*Amnibacterium* sp.), and ASV59 (unidentified Bacteria). By 2219  
1738 GDDs, ASV45 remained the most abundant, followed by ASV59 and ASV33, among others.

1739 Overall, differentially abundant ASVs in birch were primarily dominated by  
1740 Proteobacteria, Acidobacteriota, and Myxococcota (Supplementary Figs. S21–S22;  
1741 Supplementary Tables S11–S12). Key genera in birch included *Endobacter* sp., *1174-901-12* sp.,  
1742 *Bryocella* sp., *P3OB-42* sp., and *Massilia* sp. Notably, ASV10, which was the most consistently  
1743 differentially abundant ASV across birch’s seasonal phenology, could only be identified to the  
1744 phylum level. In contrast, aspen exhibited differential enrichment of ASVs from  
1745 Actinobacteriota and Bacteroidota, though it shared some Proteobacteria ASVs with birch. Key  
1746 genera in aspen included *Quadrisphaera*, *Sphingomonas*, *Blastococcus*, *Hymenobacter*,  
1747 *Methylobacterium-Methylobacterium*, *Corynebacterium*, and *Rubellimicrobium*, with *Massilia*  
1748 *timonae* and *Actinomycespora iriomotensis* identified as significant at the species level.



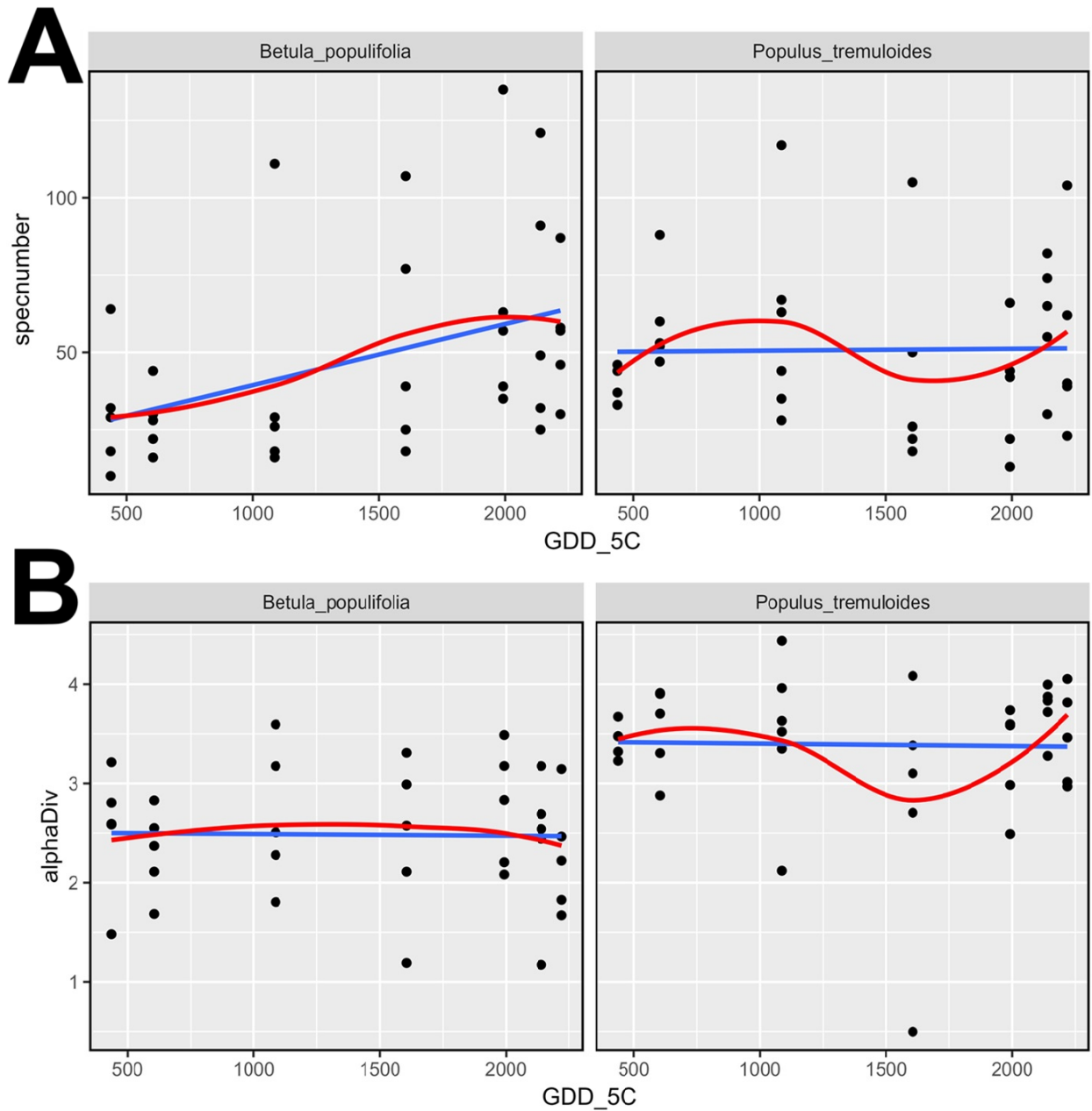
1750

1751 **Supplementary Figure S1.** Leaf bacterial ASV accumulation curve indicating the cumulative  
1752 number of recovered ASVs (Kindt's exact method) as a function of sampling effort with 95%  
1753 confidence interval for **(A)** all samples and **(B)** the positive control.



1754

1755 **Supplementary Figure S2.** Preston log-normal curve indicating the total number of leaf  
 1756 bacterial ASVs recovered (area under the curve) and the proportion of rare ASVs recovered.  
 1757 Sequencing recovered both abundant and rare ASVs, as indicated by the peak and truncation  
 1758 points at both ends of the curve.



1759

1760 **Supplementary Figure S3.** Untransformed relationship between accumulated growing degree  
 1761 days at a base temperature of 5°C (GDD\_5C) and the **(A)** ASV richness and **(B)** Shannon  
 1762 diversity index ( $H'$ ) across two host tree species, grey birch (left panels) and trembling aspen  
 1763 (right panels). The scatter plots show individual sample data points, while the blue lines  
 1764 represent linear regression fits. The red lines depict additional smoothing for trend visualization.

1765 **Supplementary Table S1.** Summary of pairwise comparisons using the *emmeans* package in R  
 1766 to assess the interaction between host species identity and GDDs at a base temperature of 5°C  
 1767 ('Species:GDD\_5C') on leaf ASV richness comparing each GDD sampling point in the growing  
 1768 season between grey birch (*Betula*) and trembling aspen (*Populus*).<sup>a</sup>

<b>ASV Richness<sup>b</sup></b>				
<b>Species x GDD_5C</b>	<b>emmean</b>	<b>SE</b>	<b>t-ratio</b>	<b>P</b>
<i>Betula.437-Populus.437</i>	-0.63991	0.257	-2.489	0.451
<i>Betula.605-Populus.605</i>	-0.55532	0.238	-2.333	0.552
<i>Betula.1087-Populus.1087</i>	-0.31261	0.198	-1.578	0.917
<i>Betula.1606-Populus.1606</i>	-0.05127	0.191	-0.269	1
<i>Betula.1992-Populus.1992</i>	0.1431	0.212	0.675	1
<i>Betula.2140-Populus.2140</i>	0.21763	0.225	0.967	0.999
<i>Betula.2219-Populus.2219</i>	0.25741	0.233	1.105	0.996

1769 <sup>a</sup> Table shows the test statistics and associated estimated marginal means (emmean), standard  
 1770 error (*SE*), the *t-ratio*, and *P*-values for each comparison. Results indicate that while the  
 1771 interaction between host species identity and GDDs is significant in the overall model, pairwise  
 1772 comparisons of the species interaction at individual GDD points show no significant  
 1773 differences (*P*-value \*<0.05, \*\*<0.01 and \*\*\*<0.001).

1774 <sup>b</sup> ASV richness was log-transformed to meet model assumptions.

1775 **Supplementary Table S2.** Summary of pairwise comparisons using the *emmeans* package in R  
 1776 to evaluate the differential effects of GDDs at a base temperature of 5°C ('GDD\_5C') on leaf  
 1777 bacterial ASV richness within grey birch. Analyses were conducted between each sampling point  
 1778 combination of 'GDD\_5C', accounting for the LMM structure.<sup>a</sup>

<b>Grey Birch</b>				
<b>ASV Richness<sup>b</sup></b>				
<b>GDD_5C</b>	<b>emmean</b>	<b>SE</b>	<b>t-ratio</b>	<b>P</b>
437-605	6.85E-03	0.00972	0.705	0.991
437-1087	6.78E-03	0.00972	0.697	0.992
437-1606	1.84E-02	0.00972	1.89	0.505
437-1992	2.79E-02	0.00972	2.869	0.102
437-2140	2.43E-02	0.00972	2.5	0.203
437-2219	2.66E-02	0.00972	2.735	0.132
605-1087	-7.23E-05	0.00972	-0.007	1
605-1606	1.15E-02	0.00972	1.186	0.893
605-1992	2.10E-02	0.00972	2.164	0.35
605-2140	1.75E-02	0.00972	1.796	0.563
605-2219	1.97E-02	0.00972	2.03	0.423
1087-1606	1.16E-02	0.00972	1.193	0.89
1087-1992	2.11E-02	0.00972	2.172	0.346
1087-2140	1.75E-02	0.00972	1.803	0.559
1087-2219	1.98E-02	0.00972	2.037	0.419
1606-1992	9.52E-03	0.00972	0.979	0.954
1606-2140	5.93E-03	0.00972	0.61	0.996
1606-2219	8.21E-03	0.00972	0.844	0.977
1992-2140	-3.58E-03	0.00972	-0.368	0.999
1992-2219	-1.31E-03	0.00972	-0.134	1
2140-2219	2.28E-03	0.00972	0.234	1

1779 <sup>a</sup> The table shows the estimated marginal means (emmean), standard error (SE), *t-ratio*, and *P*-  
 1780 *values* for each GDD sampling point. Results highlight that while 'GDD\_5C' exerts a  
 1781 significant overall impact on (1/ASV R') within *B. populifolia*, the changes in richness  
 1782 between specific 'GDD\_5C' values are not large enough to reach statistical significance. (*P*-  
 1783 value \*<0.05, \*\*<0.01, and \*\*\*<0.001).

1784 <sup>b</sup> ASV richness underwent a reciprocal transformations to meet model assumptions.

1785 **Supplementary Table S3.** Summary of statistical tests (ANOVA and Kruskal-Wallis)  
 1786 evaluating the impact of overall individual host plant characteristics ('Plant\_ID') on leaf ASV  
 1787 richness and Shannon diversity at different points in the growing season for grey birch.<sup>a</sup>

GDD_5C	ASV Richness <sup>b</sup>			Shannon Diversity <sup>c</sup>		
	$\chi^2$	<i>F-value</i>	<i>P</i>	$\chi^2$	<i>F-value</i>	<i>P</i>
437	—	0.034	0.866	4	—	0.406
605	—	0.32	0.611	—	6.09	0.0902
1087	4	—	0.406	—	2.274	0.229
1606	—	1.848	0.267	—	0.511	0.526
1992	—	0.198	0.686	—	3.369	0.164
2140	—	0.063	0.819	—	0.047	0.842
2219	—	0.001	0.979	—	0.001	0.981

1788 <sup>a</sup> The analyses were performed on data subset by accumulated GDDs at a base temperature of  
 1789 5°C ('GDD\_5C'). The table shows the test statistics and associated  $\chi^2$ -, *F*-, and *P*-values for  
 1790 each phenological stage. Results indicate that 'Plant\_ID' did not significantly affect ASV  
 1791 richness nor Shannon diversity at any point in the season in both host species (*P*-value \*<0.05,  
 1792 \*\*<0.01 and \*\*\*<0.001).

1793 <sup>b</sup> ASV richness underwent a reciprocal transformation to meet model assumptions.

1794 <sup>c</sup> Shannon diversity underwent a reciprocal transformation to meet model assumptions.

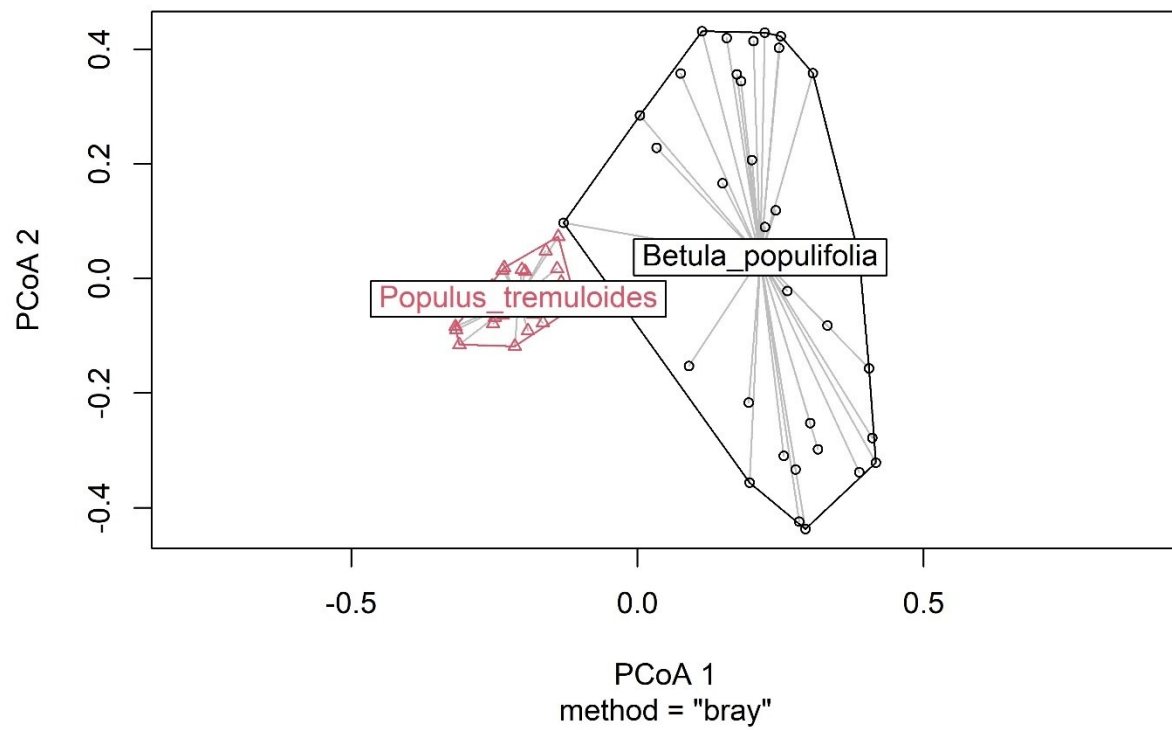
1795 **Supplementary Table S4.** Summary of statistical tests (ANOVA and Kruskal-Wallis)  
 1796 evaluating the impact of overall individual host plant characteristics ('Plant\_ID') on the inverse  
 1797 of foliar ASV richness and Shannon diversity at different points in the growing season for  
 1798 trembling aspen.

GDD_5C	ASV Richness <sup>b</sup>			Shannon Diversity <sup>c</sup>		
	Plant_ID			Plant_ID		
	$\chi^2$	<i>F-value</i>	<i>P</i>	$\chi^2$	<i>F-value</i>	<i>P</i>
437	—	0.963	0.399	—	0.058	0.825
605	—	0.241	0.657	—	0.134	0.739
1087	—	0.049	0.836	—	1.402	0.302
1606	4	—	0.406	—	0.213	0.676
1992	—	0.045	0.846	—	0.345	0.598
2140	—	1.492	0.309	—	1.083	0.374
2219	—	0.07	0.809	—	0.617	0.489

1799 <sup>a</sup> The analyses were performed on data subset by accumulated growing degree days at a base  
 1800 temperature of 5°C ('GDD\_5C'). The table shows the test statistics and associated  $\chi^2$ -, *F*-, and  
 1801 *P*-values for each phenological stage. Results indicate that 'Plant\_ID' did not significantly  
 1802 affect ASV richness nor Shannon diversity at any point in the season in both host species (*P*-  
 1803 value \*<0.05, \*\*<0.01 and \*\*\*<0.001).

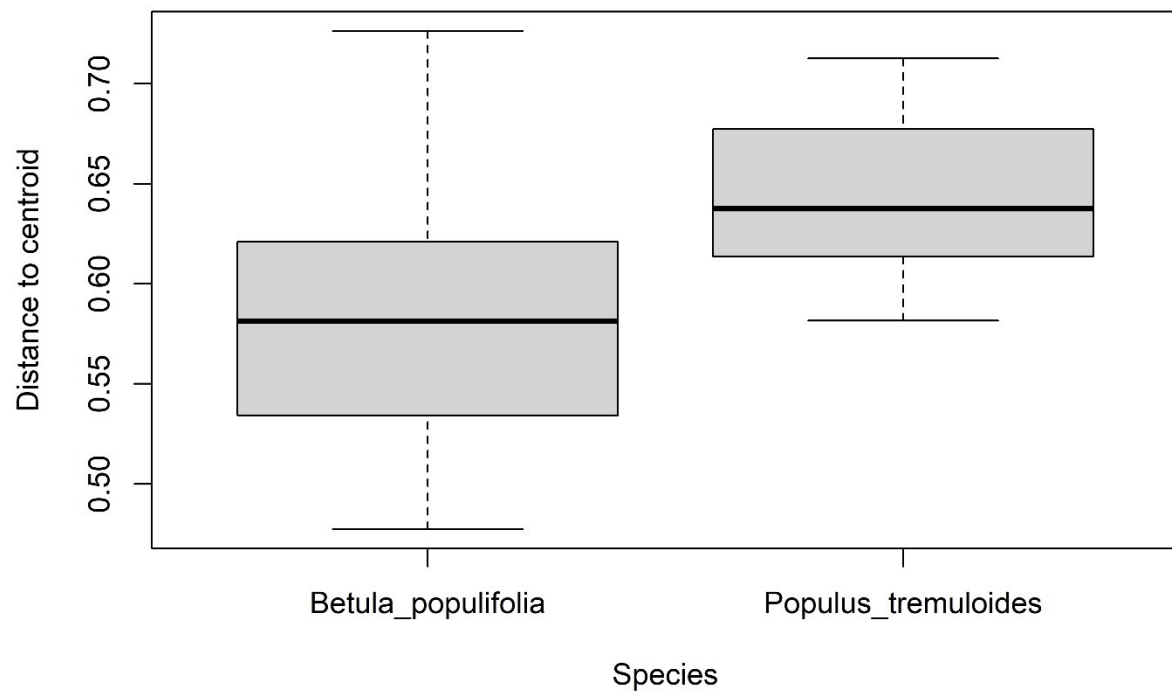
1804 <sup>b</sup> ASV richness underwent a reciprocal transformation to meet model assumptions.

1805 <sup>c</sup> Shannon diversity was square-root transformed to meet model assumptions.



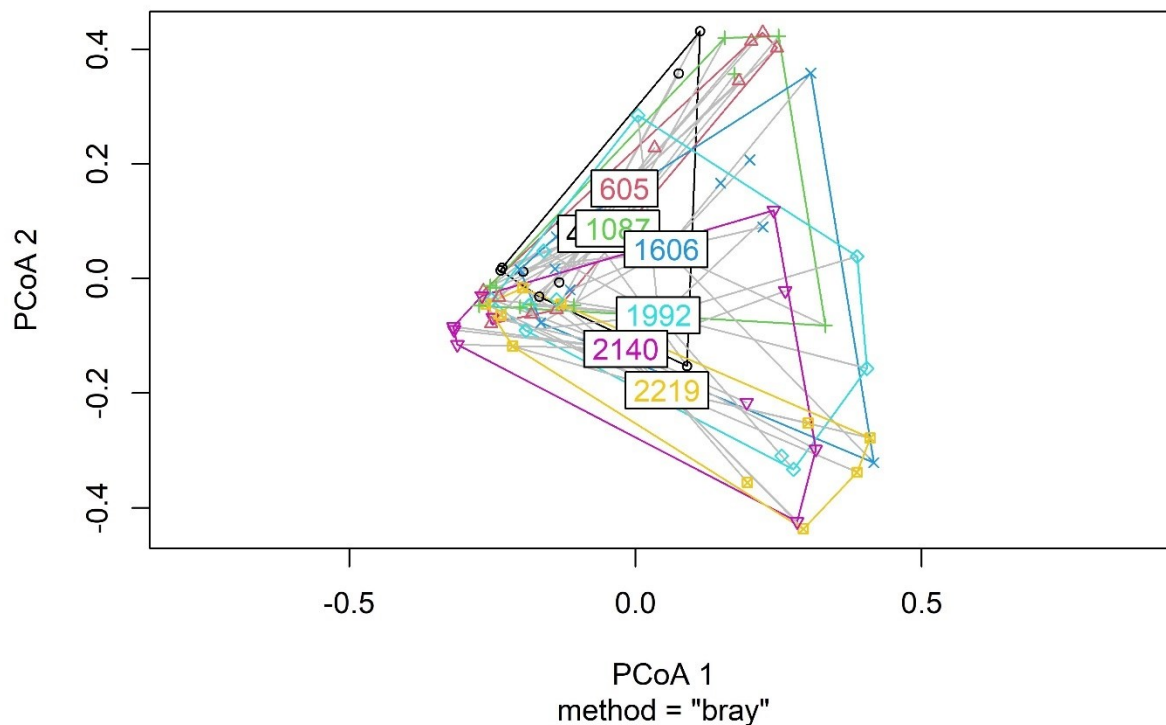
1806

1807 **Supplementary Figure S4.** Principal Coordinate Analysis (PCoA) showing multivariate  
1808 dispersion of leaf bacterial communities comparing interspecific differences between grey birch  
1809 and trembling aspen, represented by the host ‘Species’ variable. This figure is based on the Bray-  
1810 Curtis dissimilarity between the two host tree species’ leaf bacterial communities, denoted by  
1811 ‘Species’.



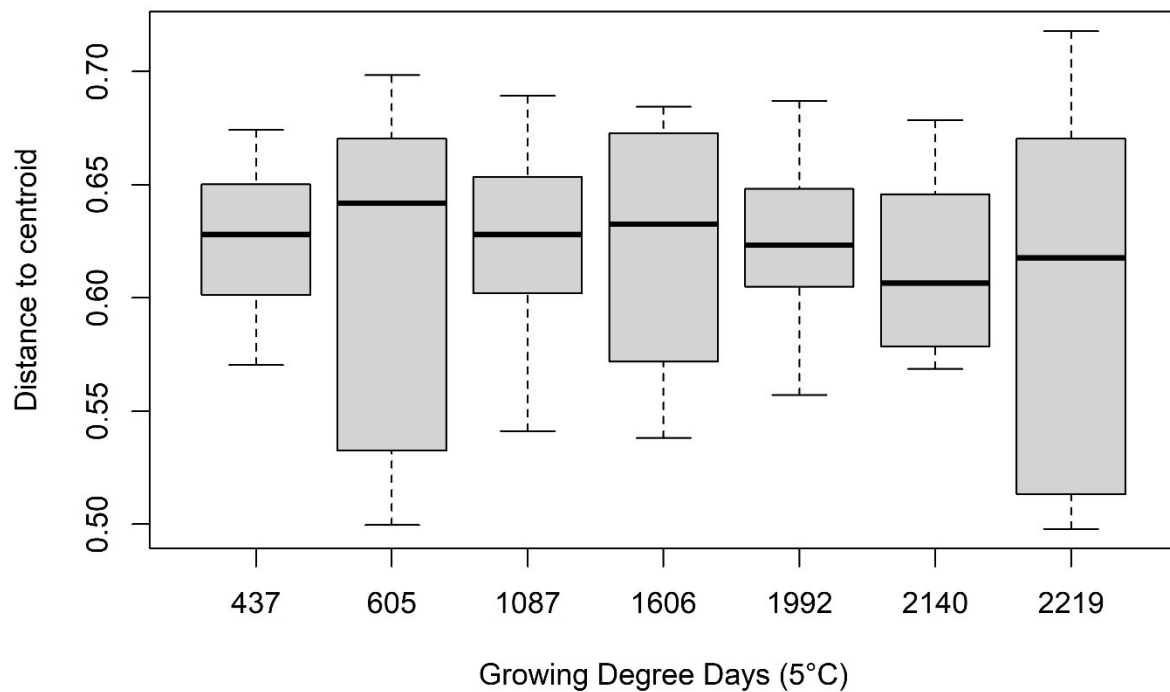
1812

1813 **Supplementary Figure S5.** Homogeneity of multivariate dispersion (distance to centroid) of  
1814 leaf bacterial communities comparing interspecific differences between grey birch and trembling  
1815 aspen represented by the host 'Species' variable. This figure is based on the Bray-Curtis  
1816 dissimilarity between the two host tree species' leaf bacterial communities, denoted by 'Species'.



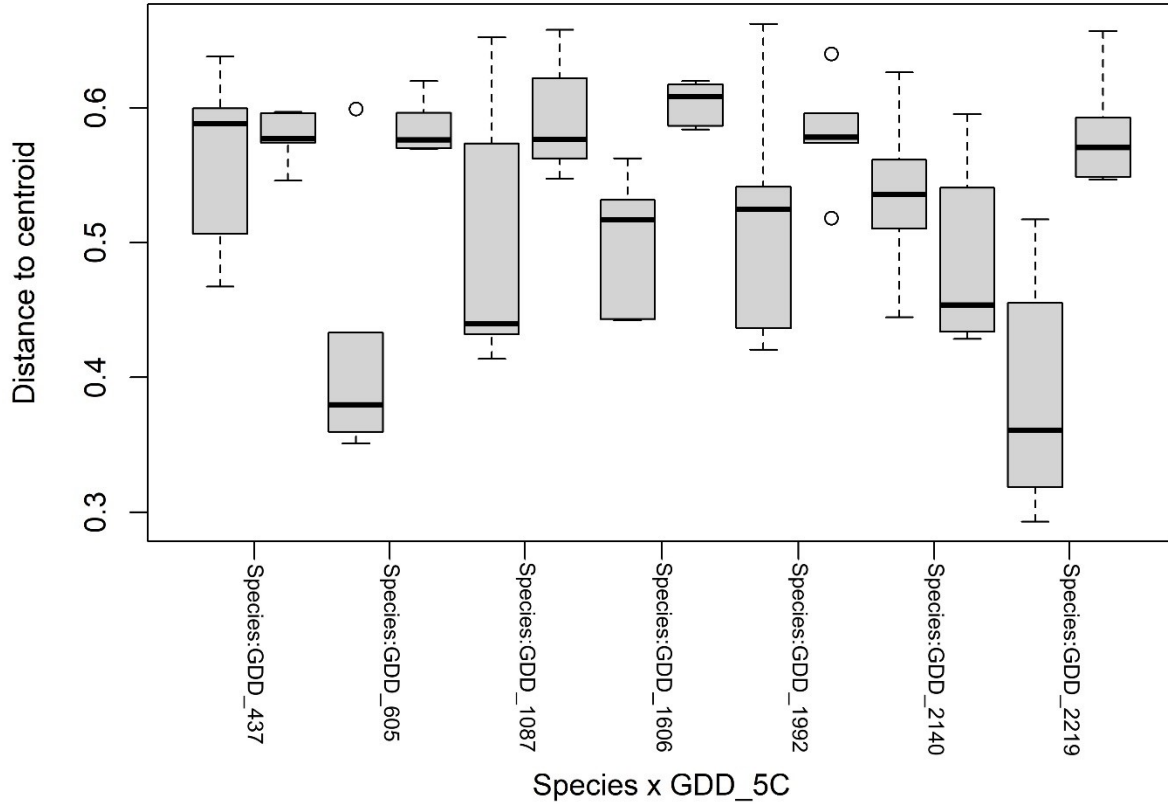
1817

1818 **Supplementary Figure S6.** Principal Coordinate Analysis (PCoA) showing multivariate  
 1819 dispersion of leaf bacterial communities comparing interspecific differences between grey birch  
 1820 and trembling aspen throughout seasonal phenology, considering only the variable of  
 1821 accumulated growing degree days at a base temperature of 5°C ('GDD\_5C'). This figure is  
 1822 based on the Bray-Curtis dissimilarity between the two host tree species' leaf bacterial  
 1823 communities regarding 'GDD\_5C'.



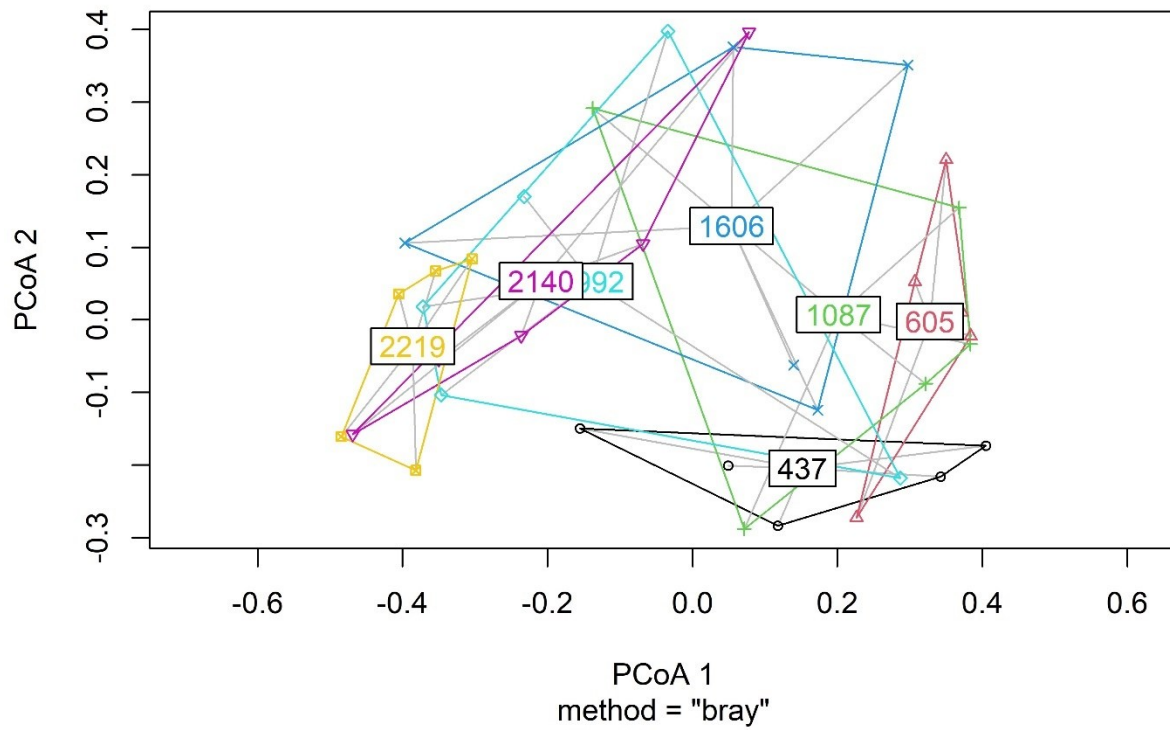
1824

1825 **Supplementary Figure S7.** Homogeneity of multivariate dispersion (distance to centroid) of  
 1826 leaf bacterial communities comparing interspecific differences between grey birch and trembling  
 1827 aspen throughout seasonal phenology, considering only the variable of accumulated growing  
 1828 degree days at a base temperature of 5°C ('GDD\_5C'). This figure is based on the Bray-Curtis  
 1829 dissimilarity between the two host tree species' leaf bacterial communities regarding 'GDD\_5C'.



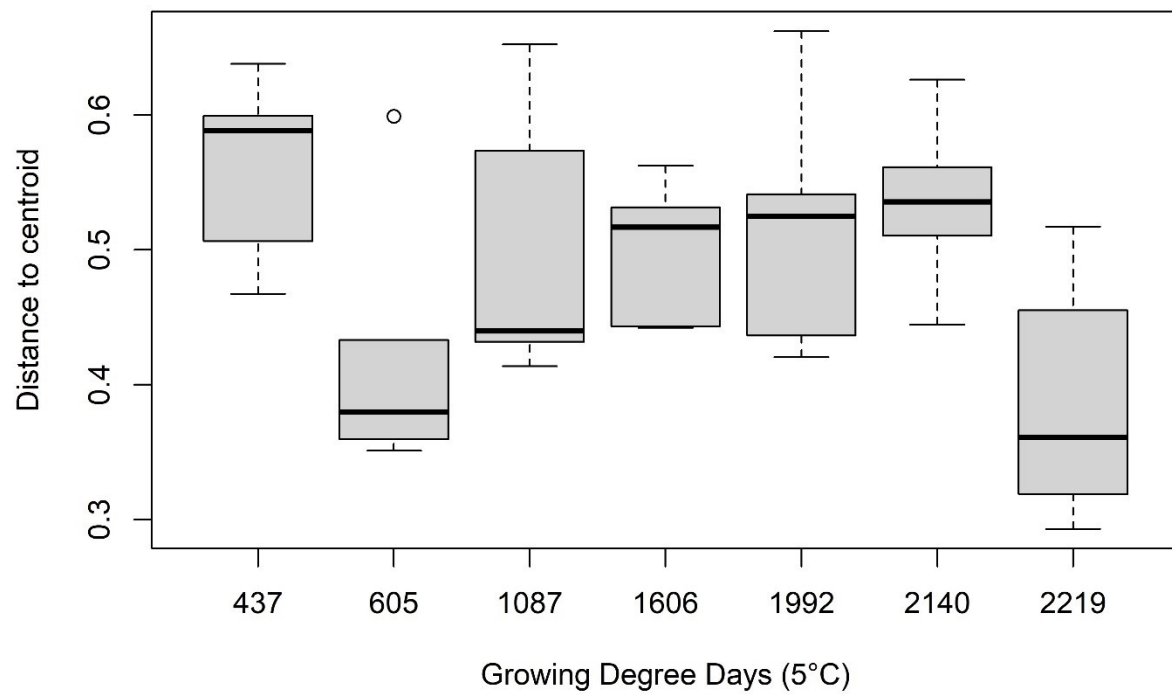
1830

1831 **Supplementary Figure S8.** Homogeneity of multivariate dispersion (distance to centroid) of  
 1832 leaf bacterial communities comparing interspecific differences between the interaction of grey  
 1833 birch with GDDs and the interaction of trembling aspen with GDDs, throughout seasonal  
 1834 phenology, considering the interaction variable ('Species:GDD\_5C'). This figure is based on the  
 1835 Bray-Curtis dissimilarity between the two host tree species' leaf bacterial communities regarding  
 1836 'GDD\_5C'. Comparisons of interest are those between host species at shared GDD points.



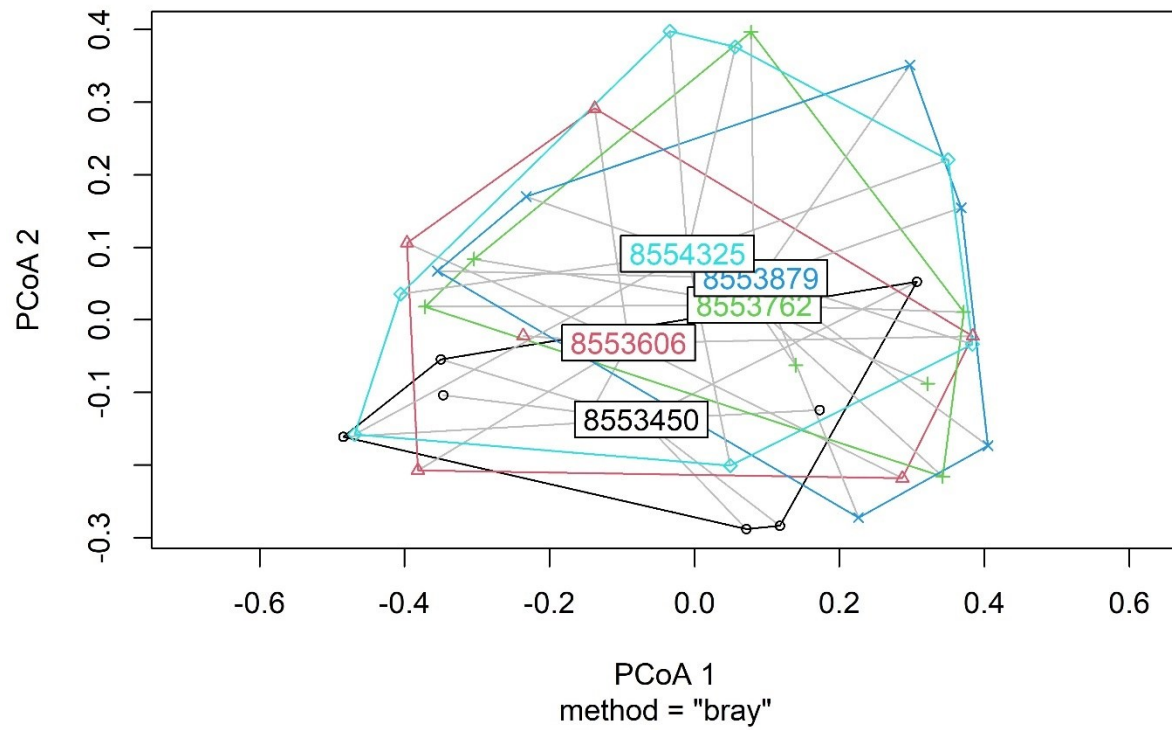
1837

1838 **Supplementary Figure S9.** Principal Coordinate Analysis (PCoA) showing multivariate  
 1839 dispersion of leaf bacterial communities within grey birch based on the Bray-Curtis dissimilarity  
 1840 across growing degree days at a base temperature of 5°C ('GDD\_5C').



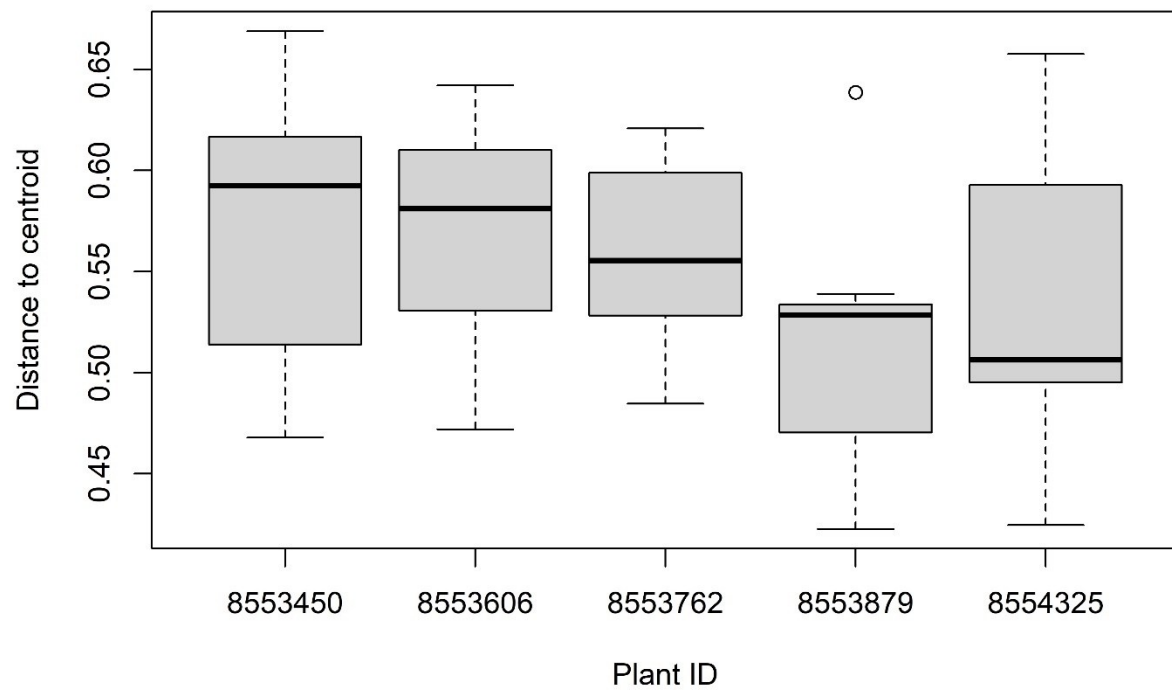
1841

1842 **Supplementary Figure S10.** Homogeneity of multivariate dispersion (distance to centroid) of  
1843 leaf bacterial communities within grey birch based on the Bray-Curtis dissimilarity across  
1844 growing degree days at a base temperature of 5°C ('GDD\_5C').



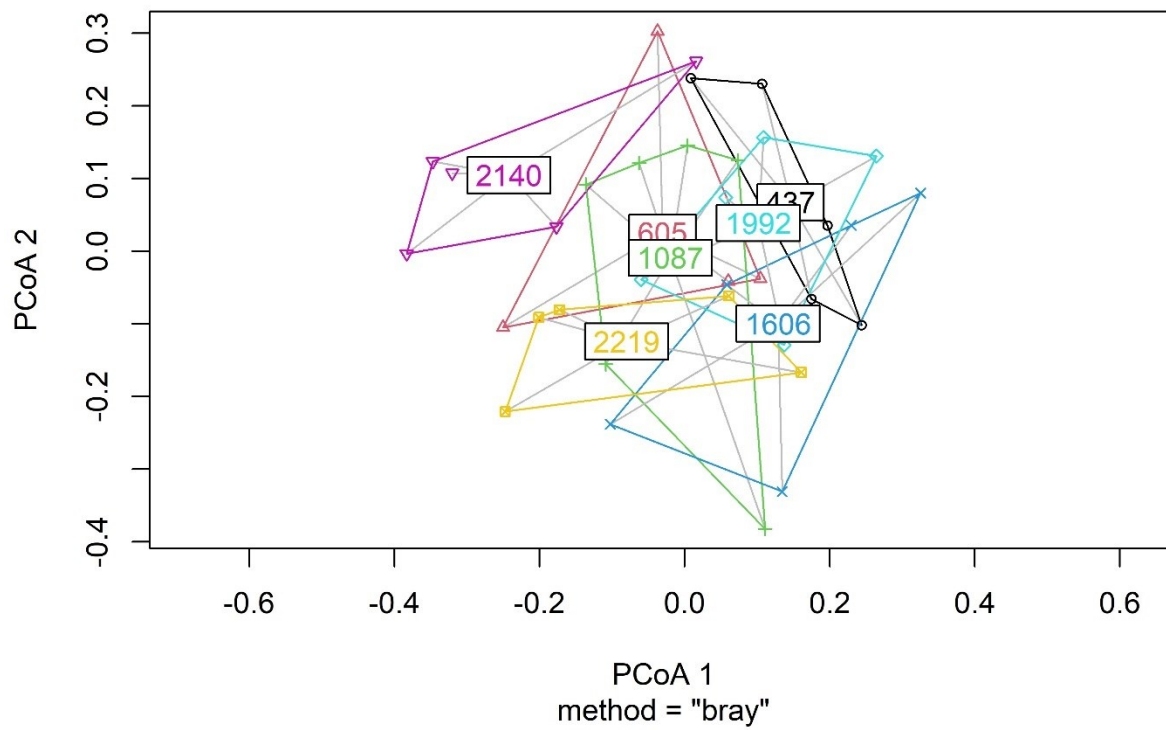
1845

1846 **Supplementary Figure S11.** Principal Coordinate Analysis (PCoA) showing multivariate  
 1847 dispersion of leaf bacterial communities within grey birch based on the Bray-Curtis dissimilarity  
 1848 across individual plant identifiers, or Plant ID ('Plant\_ID').



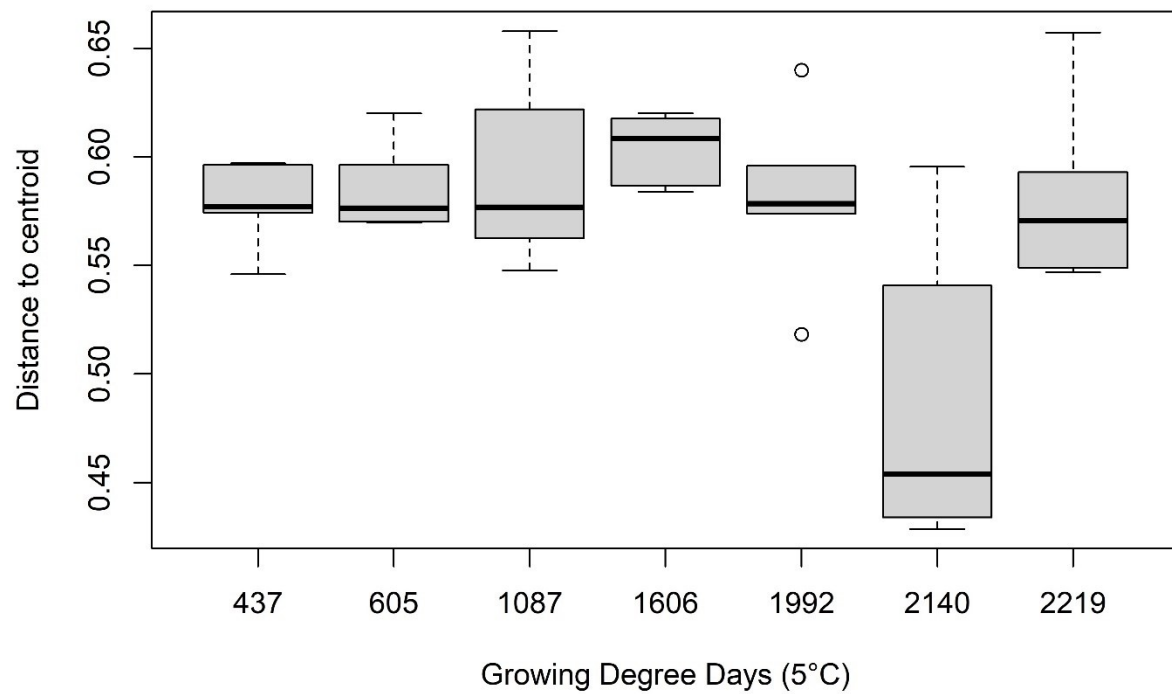
1849

1850 **Supplementary Figure S12.** Homogeneity of multivariate dispersion (distance to centroid) of  
1851 leaf bacterial communities within grey birch based on the Bray-Curtis dissimilarity across  
1852 individual plant identifiers, or Plant ID ('Plant\_ID').



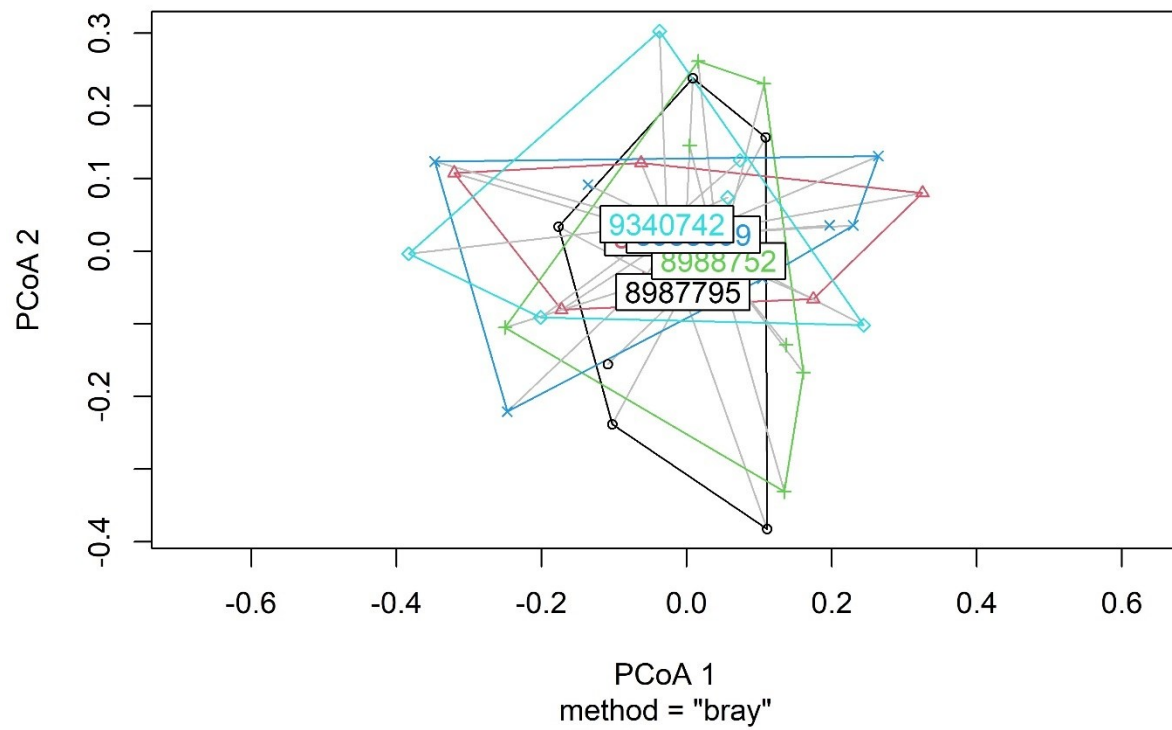
1853

1854 **Supplementary Figure S13.** Principal Coordinate Analysis (PCoA) showing multivariate  
 1855 dispersion of leaf bacterial communities within trembling aspen based on the Bray-Curtis  
 1856 dissimilarity across growing degree days at a base temperature of 5°C ('GDD\_5C').



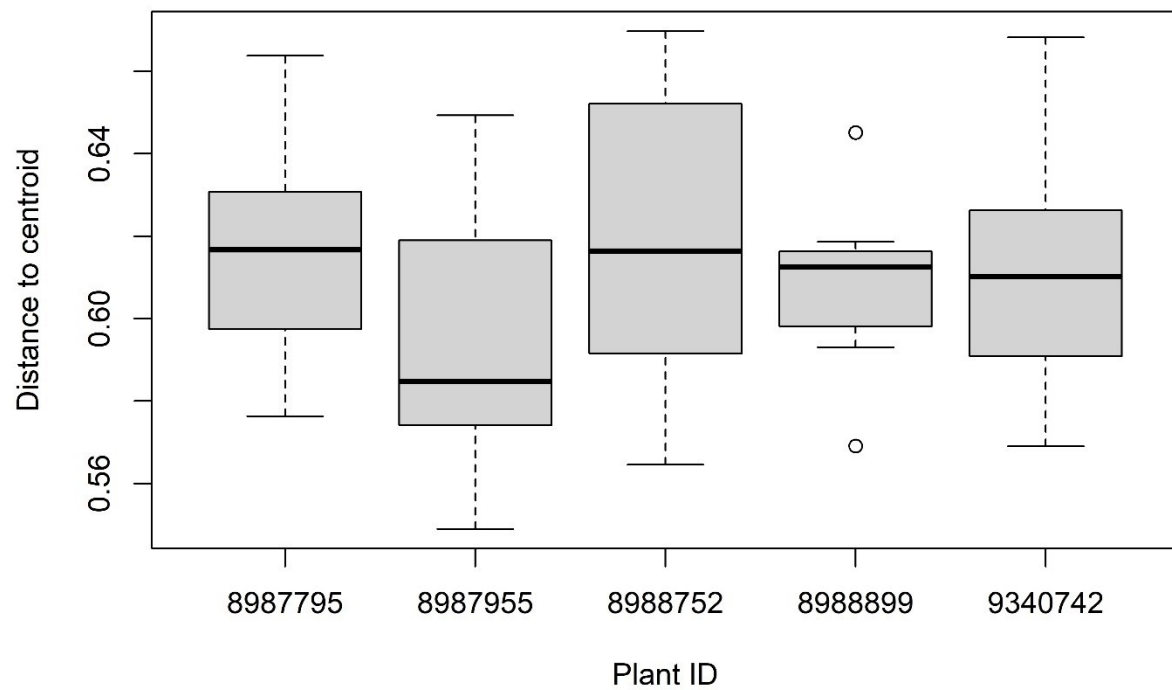
1857

1858 **Supplementary Figure S14.** Homogeneity of multivariate dispersion (distance to centroid) of  
 1859 leaf bacterial communities within trembling aspen based on the Bray-Curtis dissimilarity across  
 1860 growing degree days at a base temperature of 5°C ('GDD\_5C').



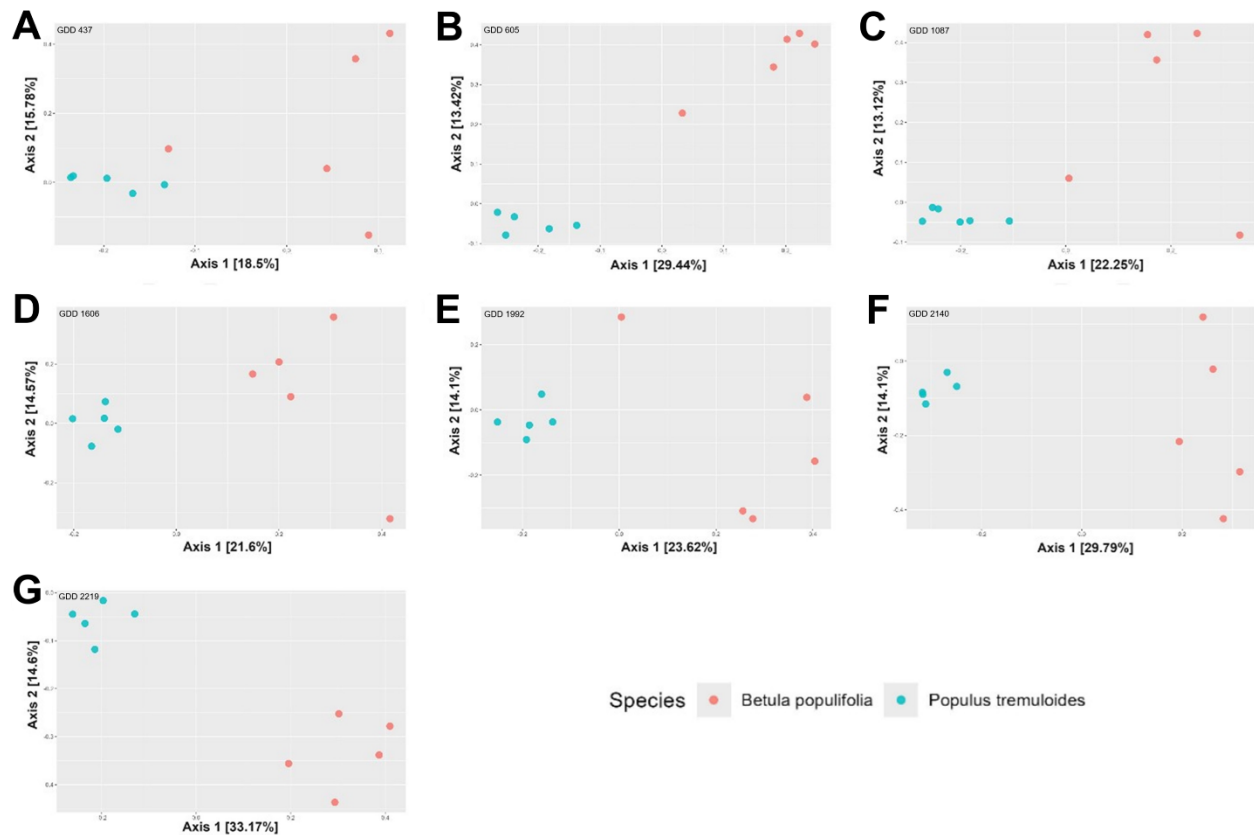
1861

1862 **Supplementary Figure S15.** Principal Coordinate Analysis (PCoA) showing multivariate  
1863 dispersion of leaf bacterial communities within trembling aspen based on the Bray-Curtis  
1864 dissimilarity across individual plant identifiers, or Plant ID ('Plant\_ID').



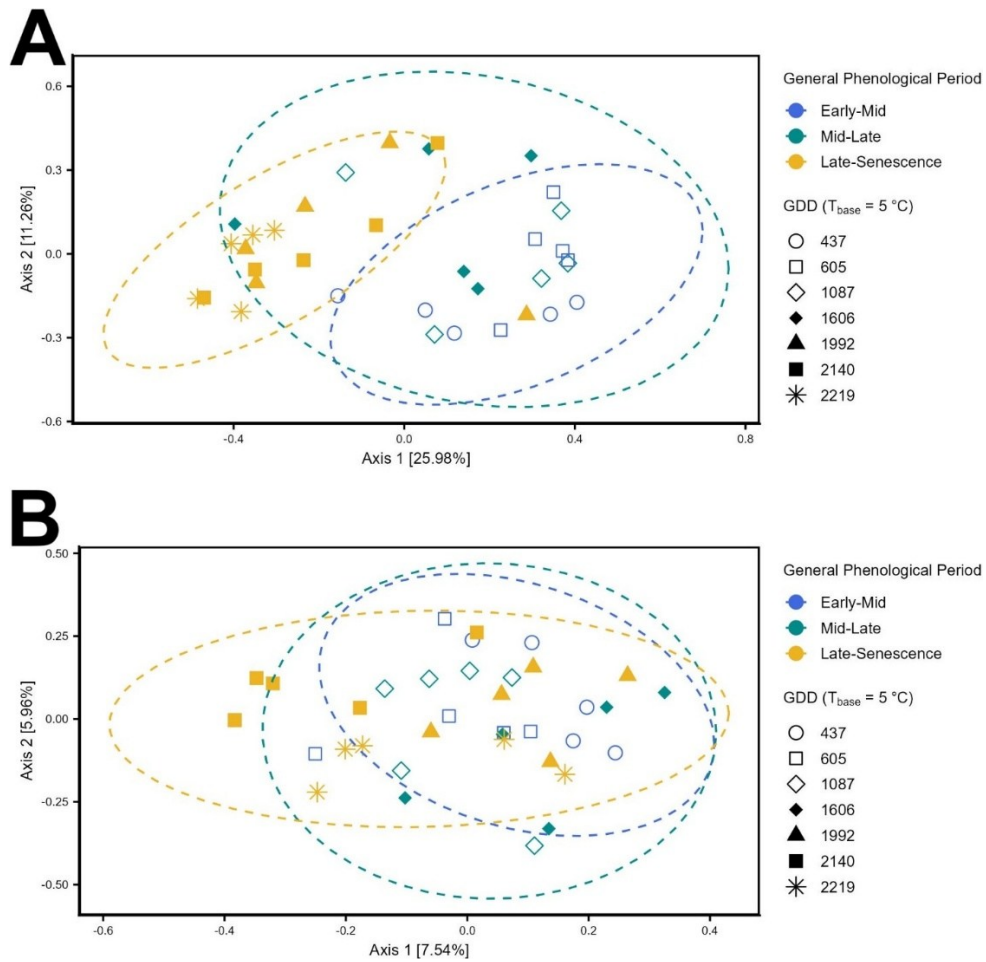
1865

1866 **Supplementary Figure S16.** Homogeneity of multivariate dispersion (distance to centroid) of  
1867 leaf bacterial communities within trembling aspen based on the Bray-Curtis dissimilarity across  
1868 individual plant identifiers, or Plant ID ('Plant\_ID').



1869

1870 **Supplementary Figure S17.** Principal Coordinate Analysis (PCoA) comparing leaf bacterial  
 1871 communities of grey birch (pink) and trembling aspen (turquoise) based on Bray-Curtis  
 1872 dissimilarity as host seasonal phenological change progresses, represented by accumulated  
 1873 growing degree days at a base temperature of 5°C (GDDs). Data has been subset by GDD to  
 1874 pinpoint the greatest differences between host species' bacterial community composition. Each  
 1875 data point denotes a plant individual sampled at GDDs (A) 437, (B) 605, (C) 1087, (D) 1606, (E)  
 1876 1992, (F) 2140, and (G) 2219. The more proximal samples are to one another, the more similar  
 1877 their community composition is. In contrast, samples that are further from one another are more  
 1878 dissimilar and distinct in their foliar bacterial community composition.



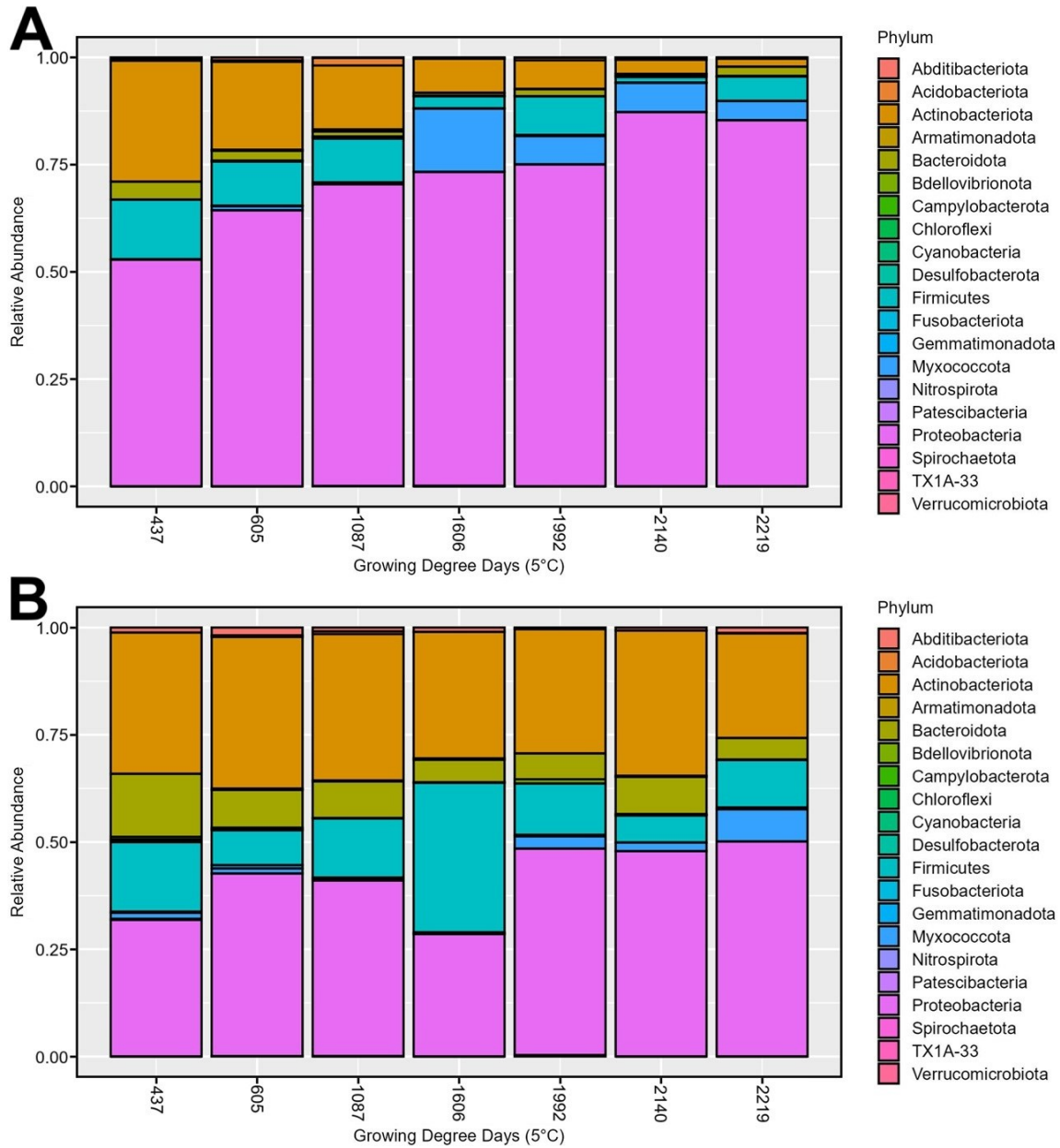
1879

1880 **Supplementary Figure S18.** Principal Coordinate Analysis (PCoA) of leaf bacterial  
 1881 communities within a population of **(A)** grey birch and **(B)** trembling aspen individuals based on  
 1882 Bray-Curtis dissimilarity along host seasonal phenology, represented by accumulated GDDs  
 1883 ( $T_{base} = 5^{\circ}C$ ) and grouped by general phenology. Each data point denotes a plant individual  
 1884 sampled at GDDs 437 (open circle), 605 (open square), 1087 (open diamond), 1606 (filled  
 1885 diamond), 1992 (filled triangle), 2140 (filled square), and 2219 (asterisk). Early-mid phenology  
 1886 (blue) encompasses 437 and 605 GDDs; mid-late phenology (green) denotes 1087 and 1606  
 1887 GDDs; and late phenology to senescence onset (goldenrod) corresponds to 1992, 2140, and 2219  
 1888 GDDs. Samples that are more distal from one another are more dissimilar and distinct in their  
 1889 foliar bacterial community composition than those proximal.

1890 **Supplementary Table S5.** Permutational analysis of variance (PERMANOVA) for grey birch  
 1891 (top) and trembling aspen (bottom) testing the impact of GDDs at a base temperature of 5°C  
 1892 ('GDD\_5C') as a proxy for host phenology, individual plant identification ('Plant\_ID'), and their  
 1893 interaction on leaf bacterial beta diversity and community structure.<sup>a</sup>

	<b>Source of Variation</b>	<b>SS</b>	<b>R<sup>2</sup></b>	<b>F</b>	<b>P</b>
<b>Grey Birch</b>	GDD_5C	1.8135	0.149	6.024	0.001***
	Plant_ID	1.3958	0.115	1.159	0.231
	GDD_5C x Plant_ID	1.3958	0.115	1.159	0.231
	Residuals	7.526	0.62	—	—
<b>Trembling Aspen</b>	GDD_5C	0.5559	0.037	1.288	0.023*
	Plant_ID	1.5715	0.105	0.91	0.952
	GDD_5C x Plant_ID	1.664	0.111	0.963	0.735
	Residuals	11.2264	0.748	—	—

1894 <sup>a</sup> P-value \*<0.05, \*\*<0.01 and \*\*\*<0.001



1895

1896

**Supplementary Figure S19.** Phylum-level comparison of taxonomic profiles showing the

1897

interspecific and intraspecific patterns of change in the relative abundances of leaf bacterial

1898

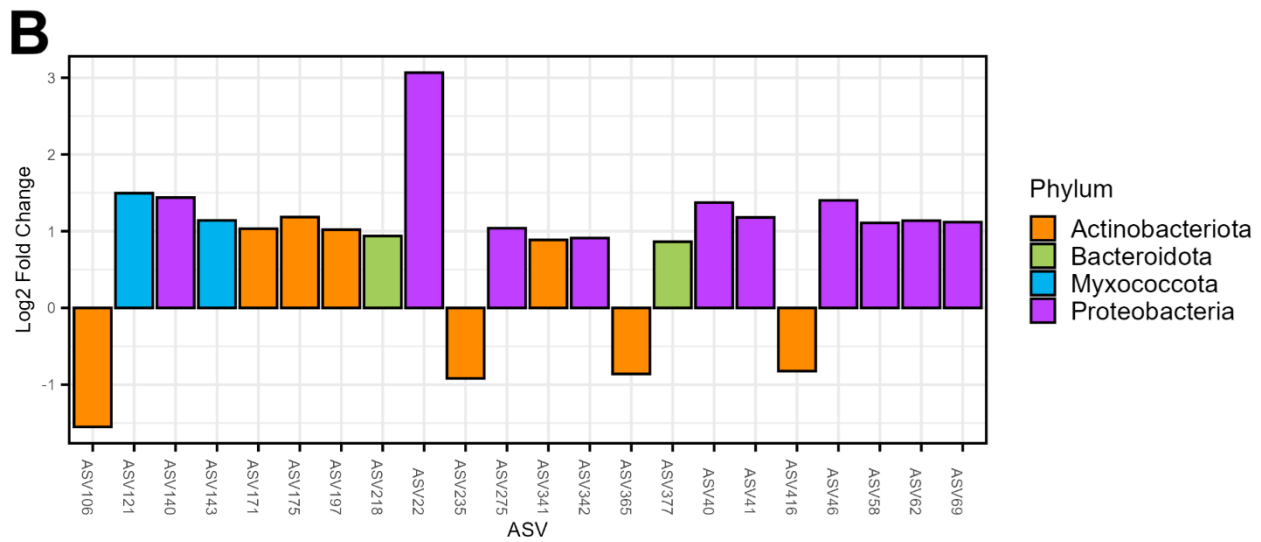
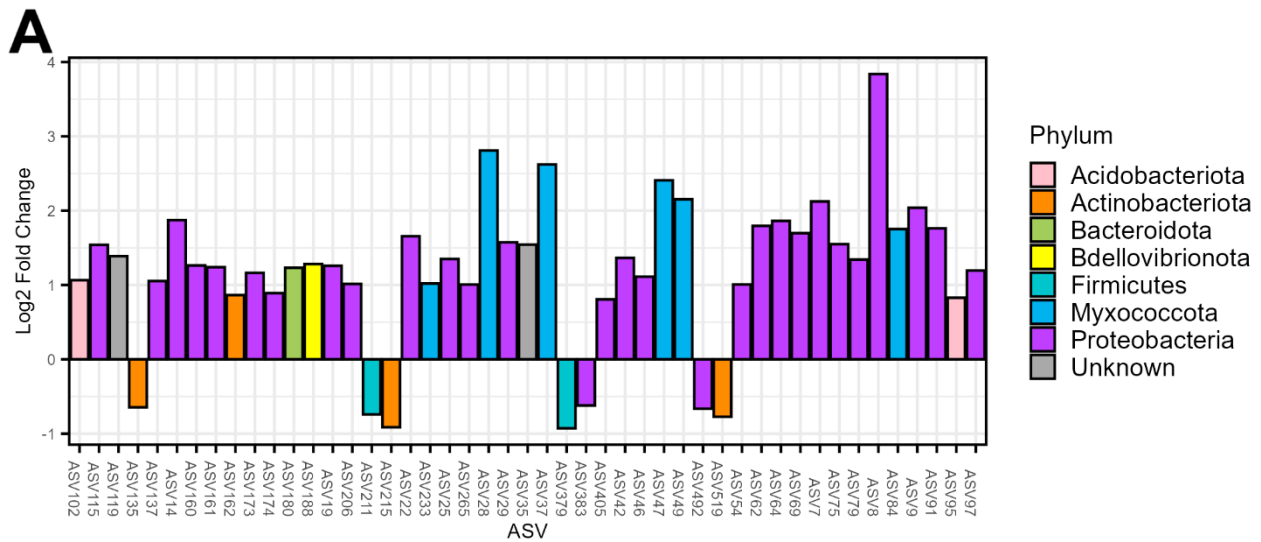
communities of **(A)** grey birch and **(B)** trembling aspen throughout seasonal host phenological

1899

change (measured as GDDs at a base temperature of 5°C). Note that the relatedness of colour

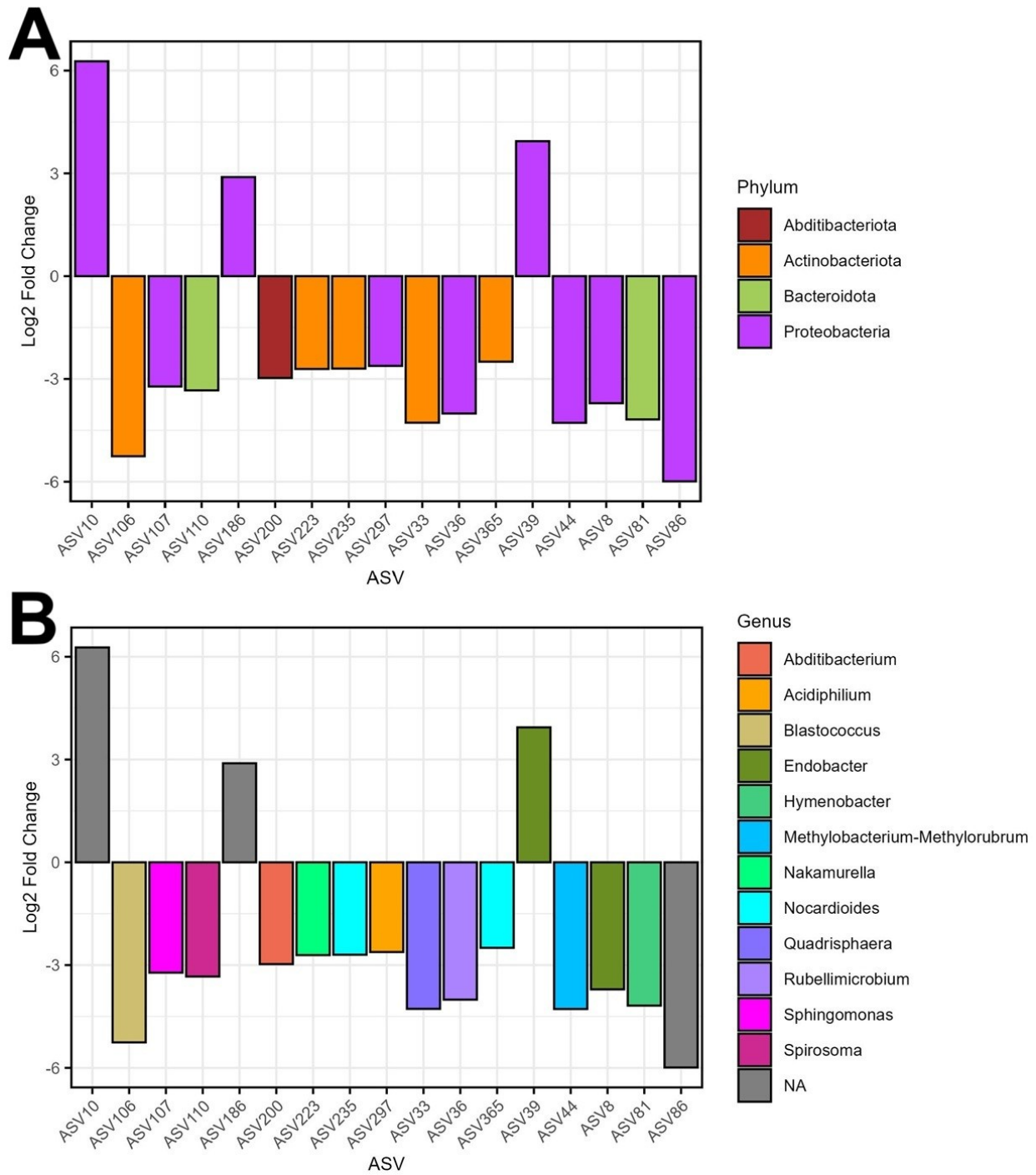
1900

shades does not reflect the relatedness of bacterial phylogenetic relationships.



1901  
 1902 **Supplementary Figure S20.** Differential abundance analysis (*DESeq2*) at the phylum-level  
 1903 showing significant changes ( $p_{adj} < 0.05$ ) in the relative abundance of leaf bacterial ASVs  
 1904 (colour-coded) within **(A)** birch and **(B)** aspen in response to GDD accumulation ( $T_{base} = 5^{\circ}C$ ).  
 1905 The  $\log_2(\text{fold-change})$  represents the rate of change in abundance for every 1-unit increase in  
 1906 GDD and can be interpreted as a regression slope on a  $\log_2$  scale. A positive  $\log_2(\text{fold-change})$   
 1907 indicates that the ASV significantly increased in abundance as GDDs increased, while a negative  
 1908  $\log_2(\text{fold-change})$  demonstrates that there was a significant decline in the ASV's abundance as  
 1909 GDDs increased. Note that colours do not correlate to relatedness of taxa. The *P*-value is

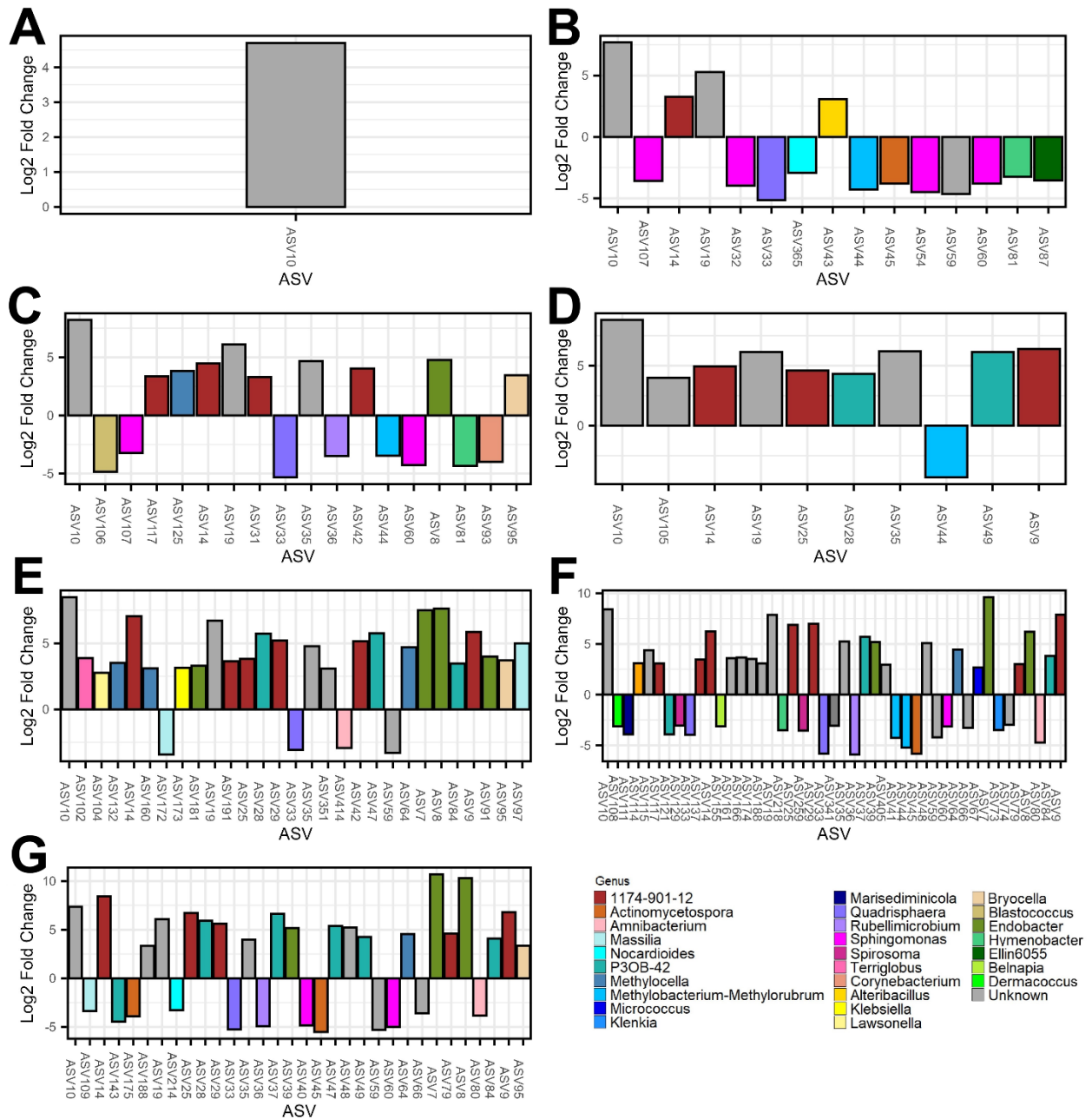
1910 calculated using the Wald test, and the adjusted  $P$ -value ( $p_{\text{adj}}$ ) is calculated using the Benjamini–  
1911 Hochberg method. A full list of the significantly differentially abundant ASVs, including  
1912 unidentified ASVs, and all summary statistics can be found in Supplementary Tables S9–S10.



1913

1914 **Supplementary Figure S21.** Differential abundance analysis (*DESeq2*) showing significant  
 1915 changes ( $\text{padj} < 0.05$ ) in the relative abundance of leaf bacterial ASVs within and between grey  
 1916 birch and trembling aspen across the entirety of host phenology at **(A)** the phylum-level and **(B)**  
 1917 the genus-level. A positive  $\log_2(\text{fold-change})$  indicates that ASVs were significantly more

1918 differentially abundant in birch, while a negative  $\log_2(\text{fold-change})$  demonstrates that ASVs  
1919 were significantly more differentially abundant in aspen. Note that colours do not correlate to  
1920 relatedness of taxa. A full list of the significantly differentially abundant ASVs, including  
1921 unidentified ASVs, and all summary statistics can be found in *Supplementary Table S8* of the  
1922 Supplementary Information section.



1923

1924

**Supplementary Figure S22.** Differential abundance analysis (*DESeq2*) showing significant

1925

changes ( $\text{padj} < 0.05$ ) in the relative abundance of leaf bacterial ASVs (genus-level colour-

1926

coded) within and between grey birch and trembling aspen GDDs ( $T_{\text{base}} = 5^\circ\text{C}$ ) are accumulated

1927

at a base temperature of  $5^\circ\text{C}$  at GDD sampling points **(A)** 437, **(B)** 605, **(C)** 1087, **(D)** 1606, **(E)**

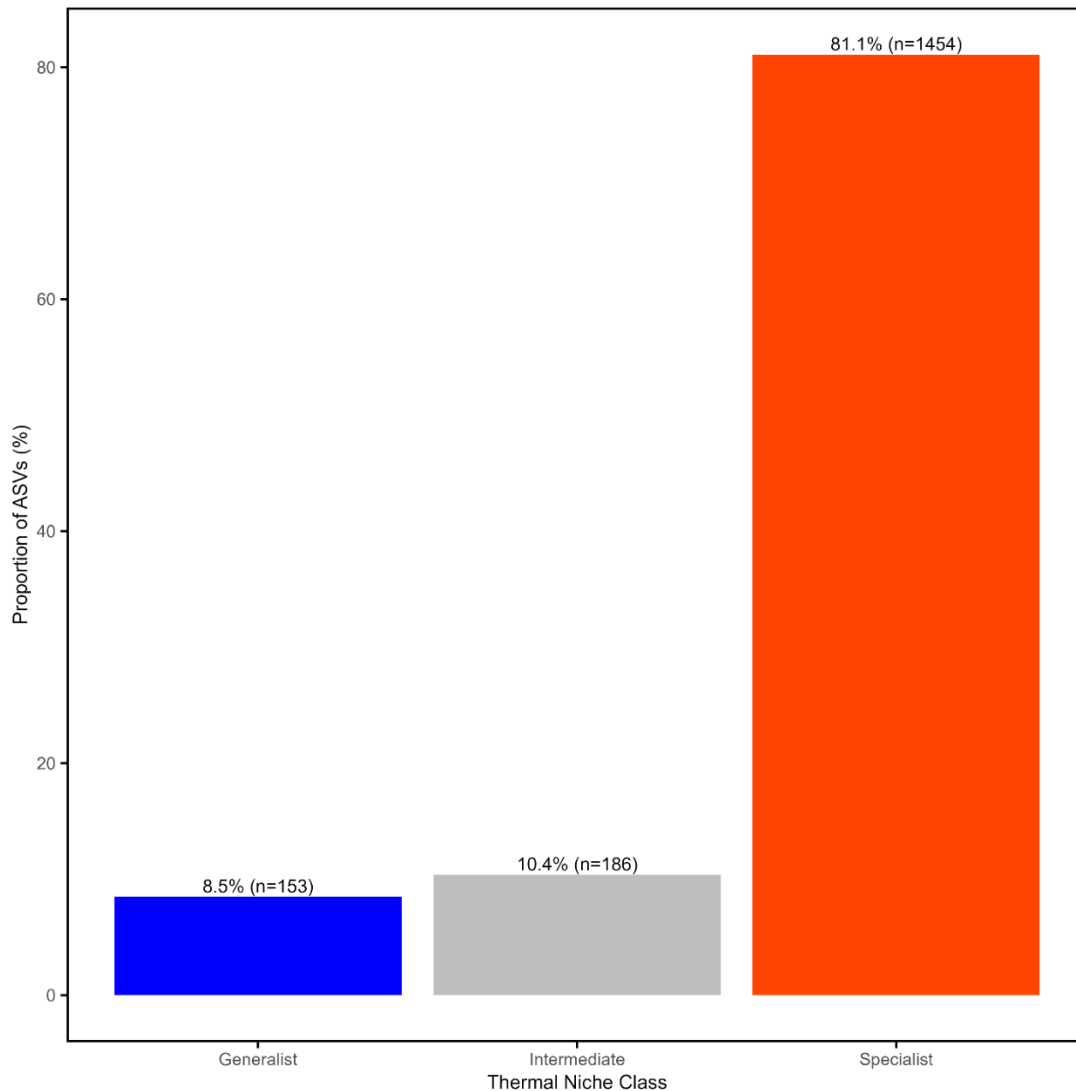
1928

1992, **(F)** 2140, and **(G)** 2219. GDDs are a thermo-temporal measure of host plant seasonal

1929

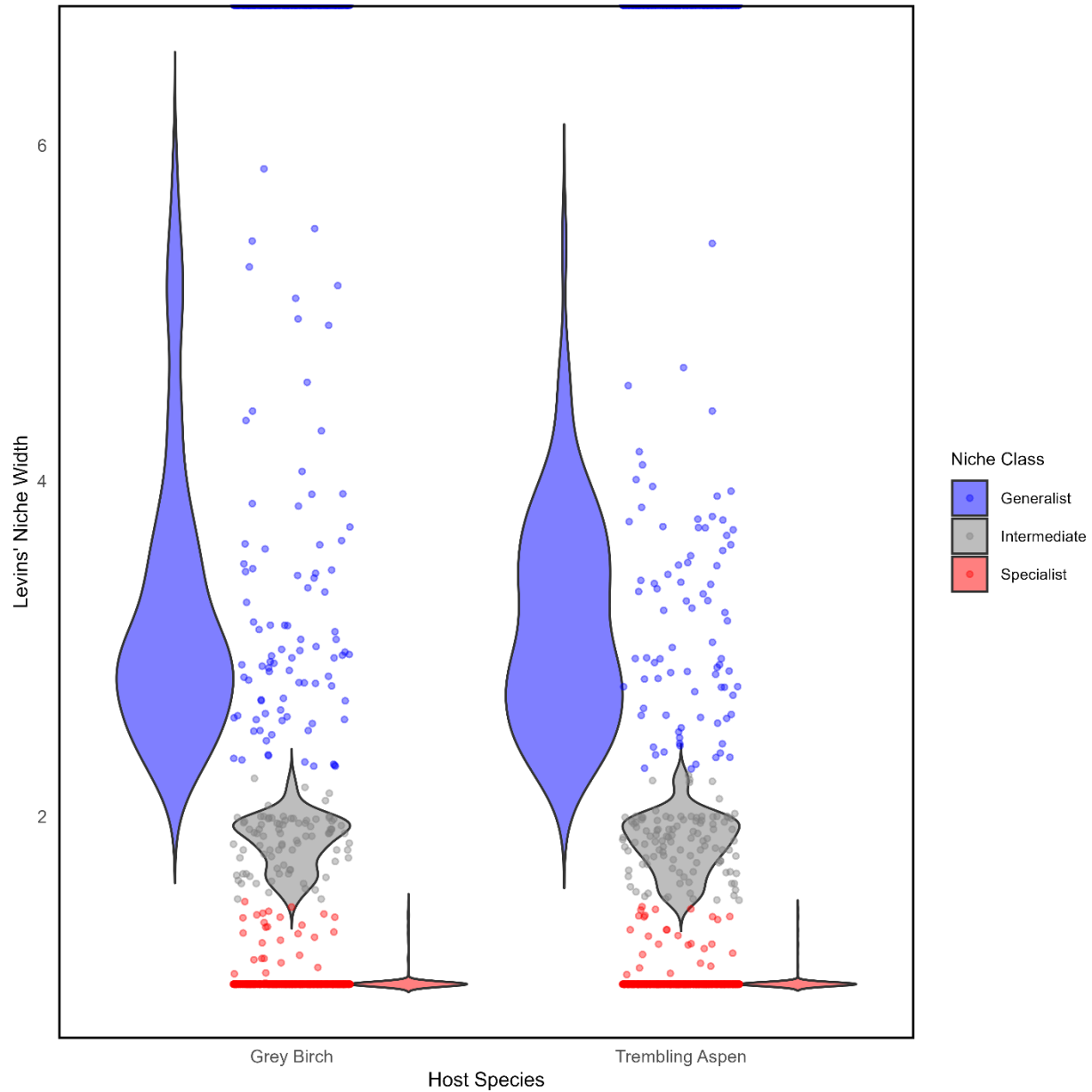
phenological change. A positive  $\log_2(\text{fold-change})$  indicates that ASVs were significantly more

1930 differentially abundant in birch, while a negative  $\log_2(\text{fold-change})$  demonstrates that ASVs  
1931 were significantly more differentially abundant in aspen. A full list of the significantly  
1932 differentially abundant ASVs, including unidentified ASVs, and all summary statistics can be  
1933 found in *Supplementary Table S9* of the Supplementary Information section.



1934

1935 **Supplementary Figure S23.** Thermal niche breadth of leaf-associated bacterial ASVs across  
 1936 seasonal heat accumulation and host species. Levins' niche width index was derived from  
 1937 relative abundances and used to quantify the breadth of thermal persistence for each ASV across  
 1938 a seasonal GDD ( $T_{\text{base}} = 5^{\circ}\text{C}$ ) gradient, a physiologically relevant measure of heat accumulation  
 1939 that tracks host phenological progression. ASVs with niche width  $\leq 1.5$  were classified as  
 1940 specialists,  $\geq 2.25$  as generalists, and those in between as intermediate. This figure shows the  
 1941 proportion of ASVs across all samples, regardless of host species, classified as thermal  
 1942 specialists, intermediates, or generalists.



1943

1944 **Supplementary Figure S24.** Distribution of ASV-level thermal niche breadths across host  
 1945 species. Violin plots show the distribution and density of Levins' niche width values for bacterial  
 1946 ASVs associated with grey birch and trembling aspen, calculated using relative abundance across  
 1947 continuous growing degree day (GDD<sub>s</sub>°C) values. Horizontal dashed lines represent fixed  
 1948 classification thresholds for thermal specialists ( $\leq 1.5$ , red) and generalists ( $\geq 2.25$ , blue), with

- 1949 intermediate values falling in between. Distributions are based on ASVs present in at least two
- 1950 GDD timepoints.

**Supplementary Table S6.** List of differentially abundant ASVs within grey birch leaf samples across a GDD ( $T_{\text{base}} = 5^{\circ}\text{C}$ ) gradient as determined by differential abundance analysis (*DESeq2*).<sup>a</sup>

ASV	Phylum	Class	Order	Family	Genus	Species	Base Mean	Log2 Fold Change	lfcSE	P-value	Adjusted P-value
ASV7	Proteobacteria	Alphaproteobacteria	Acetobacterales	Acetobacteraceae	Endobacter	NA	502.7	2.1242	0.415	3.06E-07	9.13E-06
ASV8	Proteobacteria	Alphaproteobacteria	Acetobacterales	Acetobacteraceae	Endobacter	NA	333.2	3.8387	0.355	2.63E-27	7.08E-25
ASV9	Proteobacteria	Alphaproteobacteria	Rhizobiales	Beijerinckiaceae	1174-901-12	NA	272	2.0397	0.413	7.96E-07	1.95E-05
ASV14	Proteobacteria	Alphaproteobacteria	Rhizobiales	Beijerinckiaceae	1174-901-12	NA	267.8	1.8734	0.312	9.13E-08	3.51E-06
ASV19	Proteobacteria	NA	NA	NA	NA	NA	22.11	1.2589	0.3	2.52E-03	1.94E-02
ASV22	Proteobacteria	Gammaproteobacteria	Burkholderiales	Comamonadaceae	NA	NA	1	1.6566	0.258	2.88E-05	4.56E-04
ASV25	Proteobacteria	Alphaproteobacteria	Rhizobiales	Beijerinckiaceae	1174-901-12	NA	153.2	1.3497	0.351	9.69E-04	9.31E-03
ASV28	Myxococcota	Myxococcia	Myxococcales	Myxococcaceae	P3OB-42	NA	1	2.8095	0.258	1.48E-12	1.99E-10
ASV29	Proteobacteria	Alphaproteobacteria	Rhizobiales	Beijerinckiaceae	1174-901-12	NA	1.086	1.5749	0.25	6.15E-05	8.84E-04
ASV35	NA	NA	NA	NA	NA	NA	92.89	1.5433	0.513	2.26E-05	3.80E-04
ASV37	Myxococcota	Myxococcia	Myxococcales	Myxococcaceae	P3OB-42	NA	1	2.6218	0.258	1.14E-10	1.02E-08
ASV42	Proteobacteria	Alphaproteobacteria	Rhizobiales	Beijerinckiaceae	1174-901-12	NA	93	1.3655	0.417	2.05E-04	2.30E-03
ASV46	Proteobacteria	Alphaproteobacteria	Sphingomonadales	Sphingomonadaceae	Sphingomonas	NA	1	1.1118	0.258	4.31E-03	3.05E-02
ASV47	Myxococcota	Myxococcia	Myxococcales	Myxococcaceae	P3OB-42	NA	22	2.4086	0.239	8.14E-09	5.47E-07
ASV49	Myxococcota	Myxococcia	Myxococcales	Myxococcaceae	P3OB-42	NA	9.171	2.1533	0.396	4.91E-07	1.32E-05
ASV54	Proteobacteria	Alphaproteobacteria	Sphingomonadales	Sphingomonadaceae	Sphingomonas	NA	16.83	1.0076	0.224	6.47E-03	4.14E-02
ASV62	Proteobacteria	Gammaproteobacteria	Burkholderiales	Oxalobacteraceae	Massilia	NA	44.14	1.796	0.493	1.24E-07	4.16E-06
ASV64	Proteobacteria	Alphaproteobacteria	Rhizobiales	Beijerinckiaceae	Methylocella	NA	48.74	1.8622	0.409	5.11E-08	2.60E-06
ASV69	Proteobacteria	Gammaproteobacteria	Pseudomonadales	Moraxellaceae	Enhydrobacter	aerosaccus	1.057	1.6977	0.253	7.80E-06	1.75E-04
ASV75	Proteobacteria	Alphaproteobacteria	Rhizobiales	Beijerinckiaceae	Methylobacterium-	NA	39.17	1.5502	0.397	1.04E-05	1.92E-04
ASV79	Proteobacteria	Alphaproteobacteria	Rhizobiales	Beijerinckiaceae	1174-901-12	NA	38.06	1.3426	0.393	9.66E-05	1.30E-03
ASV84	Myxococcota	Myxococcia	Myxococcales	Myxococcaceae	P3OB-42	NA	37.57	1.7524	0.448	5.80E-08	2.60E-06
ASV91	Proteobacteria	Alphaproteobacteria	Acetobacterales	Acetobacteraceae	Endobacter	NA	31.37	1.7629	0.467	8.77E-06	1.81E-04
ASV95	Acidobacteriota	Acidobacteriae	Acidobacteriales	Acidobacteriaceae (Subgroup 1)	Bryocella	NA	24.26	0.8287	0.468	7.96E-03	4.64E-02
ASV97	Proteobacteria	Gammaproteobacteria	Burkholderiales	Oxalobacteraceae	Massilia	NA	1	1.1951	0.258	1.52E-03	1.28E-02
ASV102	Acidobacteriota	Acidobacteriae	Acidobacteriales	Acidobacteriaceae (Subgroup 1)	Terriglobus	NA	1	1.0656	0.258	2.88E-03	2.15E-02
ASV115	Proteobacteria	Gammaproteobacteria	Gammaproteobacteria	Gammaproteobacteria	Candidatus	NA	26.06	1.5397	0.364	1.07E-05	1.92E-04
ASV119	NA	NA	Incertae Sedis	Unknown Family	Ovatusbacter	NA	1.343	1.389	0.229	1.64E-04	1.94E-03
ASV135	Actinobacteriota	Actinobacteria	Micrococcales	Micrococcaceae	Rothia	mucilaginos	25	-0.646	0.407	5.10E-03	3.52E-02
ASV137	Proteobacteria	Alphaproteobacteria	Rhizobiales	Beijerinckiaceae	1174-901-12	NA	24.83	1.0531	0.481	1.06E-03	9.85E-03
ASV160	Proteobacteria	Alphaproteobacteria	Rhizobiales	Beijerinckiaceae	Methylocella	NA	23.69	1.2631	0.397	1.66E-04	1.94E-03
ASV161	Proteobacteria	Gammaproteobacteria	NA	NA	NA	NA	4.714	1.2397	0.351	6.25E-05	8.84E-04

ASV162	Actinobacteriota	Actinobacteria	Micrococcales	Microbacteriaceae	Frondihabitans	NA	4.971	0.864	0.356	7.24E-03	4.43E-02
ASV173	Proteobacteria	Gammaproteobacteria	Enterobacteriales	Enterobacteriaceae	NA	NA	20.69	1.1626	0.368	1.18E-03	1.02E-02
ASV174	Proteobacteria	Alphaproteobacteria	Rickettsiales	ABI	NA	NA	7.971	0.8904	0.306	6.39E-03	4.14E-02
ASV180	Bacteroidota	Bacteroidia	Cytophagales	Hymenobacteraceae	Hymenobacter	NA	2.857	1.2322	0.343	2.54E-04	2.73E-03
ASV188	Bdellovibrionota	Oligoflexia	0319-6G20	NA	NA	NA	1.514	1.2828	0.245	1.27E-04	1.63E-03
ASV206	Proteobacteria	Alphaproteobacteria	Acetobacterales	Acetobacteraceae	Acidiphilium	NA	11.71	1.0149	0.389	2.08E-03	1.65E-02
ASV211	Firmicutes	Bacilli	Bacillales	Marinococcaceae	NA	NA	19	-0.74	0.418	6.06E-03	4.07E-02
ASV215	Actinobacteriota	Actinobacteria	Micrococcales	Micrococcaceae	Pseudarthrobacter	NA	18.17	-0.914	0.393	1.65E-03	1.34E-02
ASV233	Myxococcota	Myxococcia	Myxococcales	Myxococcaceae	P3OB-42	NA	17.91	1.02	0.428	7.76E-04	8.02E-03
ASV265	Proteobacteria	Alphaproteobacteria	Acetobacterales	Acetobacteraceae	Endobacter	NA	16.43	1.0065	0.459	1.12E-03	1.00E-02
ASV379	Firmicutes	Bacilli	Lactobacillales	Streptococcaceae	Streptococcus	NA	1	-0.927	0.258	9.63E-04	9.31E-03
ASV383	Proteobacteria	Gammaproteobacteria	Enterobacteriales	Enterobacteriaceae	Klebsiella	NA	11.37	-0.621	0.421	7.47E-03	4.47E-02
ASV405	Proteobacteria	Alphaproteobacteria	Acetobacterales	Acetobacteraceae	NA	NA	15.86	0.8065	0.46	7.09E-03	4.43E-02
ASV492	Proteobacteria	Gammaproteobacteria	CCD24	NA	NA	NA	5.857	-0.664	0.37	8.10E-03	4.64E-02
ASV519	Actinobacteriota	Actinobacteria	Corynebacteriales	Dietziaceae	Dietzia	NA	12.77	-0.772	0.433	3.34E-03	2.43E-02

<sup>a</sup> Base mean is the mean of normalized counts of all samples, log<sub>2</sub> fold change refers to the effect size estimate (where positive values mean the ASV significantly increase with GDD accumulation and negative values mean the ASV significantly declines in abundance as GDDs accumulate), lfcSE is the standard error of the log<sub>2</sub> fold change, the *P*-value is calculated using the Wald test, and the adjusted *P*-value (padj) is calculated using the Benjamini–Hochberg method. Shown are ASVs that changed significantly (padj < 0.05) in relative abundance among accumulated GDD sampling points.

**Supplementary Table S7.** List of differentially abundant ASVs within trembling aspen leaf samples across a GDD ( $T_{\text{base}} = 5^{\circ}\text{C}$ ) gradient as determined by differential abundance analysis (*DESeq2*).<sup>a</sup>

ASV	Phylum	Class	Order	Family	Genus	Species	Base Mean	Log2 Fold Change	lfcSE	P-value	Adjusted P-value
ASV22	Proteobacteria	Gammaproteobacteria	Burkholderiales	Comamonadaceae	NA	NA	3.023	3.0657	0.324	3.65E-15	1.19E-12
ASV40	Proteobacteria	Alphaproteobacteria	Sphingomonadales	Sphingomonadaceae	Sphingomonas	NA	2.762	1.3723	0.292	7.93E-04	2.36E-02
ASV41	Proteobacteria	Alphaproteobacteria	Rhizobiales	Beijerinckiaceae	Methylobacterium-	NA	4.302	1.1795	0.334	1.59E-03	3.24E-02
ASV46	Proteobacteria	Alphaproteobacteria	Sphingomonadales	Sphingomonadaceae	Sphingomonas	NA	1.193	1.4018	0.237	1.17E-04	7.65E-03
ASV58	Proteobacteria	Alphaproteobacteria	Rhizobiales	Beijerinckiaceae	Methylobacterium-	NA	114.7	1.1076	0.408	5.53E-04	1.85E-02
ASV62	Proteobacteria	Gammaproteobacteria	Burkholderiales	Oxalobacteraceae	Massilia	NA	1.047	1.1368	0.258	3.85E-04	1.85E-02
ASV69	Proteobacteria	Gammaproteobacteria	Pseudomonadales	Moraxellaceae	Enhydrobacter	aerosaccus	1.717	1.1185	0.257	5.65E-04	1.85E-02
ASV106	Actinobacteriota	Actinobacteria	Frankiales	Geodermatophilaceae	Blastococcus	NA	1.047	-1.551	0.258	7.00E-05	7.63E-03
ASV121	Myxococcota	Myxococcia	Myxococcales	Myxococcaceae	P3OB-42	NA	1.047	1.4946	0.258	1.33E-05	2.18E-03
ASV140	Proteobacteria	Gammaproteobacteria	Pseudomonadales	Pseudomonadaceae	Pseudomonas	NA	22.59	1.438	0.435	1.03E-04	7.65E-03
ASV143	Myxococcota	Myxococcia	Myxococcales	Myxococcaceae	P3OB-42	NA	1.047	1.1399	0.258	1.24E-03	3.19E-02
ASV171	Actinobacteriota	Actinobacteria	Kineosporiales	Kineosporiaceae	Pseudokineococcus	lusitanus	1.193	1.0319	0.24	1.31E-03	3.19E-02
ASV175	Actinobacteriota	Actinobacteria	Pseudonocardiales	Pseudonocardiaceae	Actinomycetospora	NA	1.047	1.1833	0.258	5.37E-04	1.85E-02
ASV197	Actinobacteriota	Actinobacteria	Kineosporiales	Kineosporiaceae	Kineococcus	NA	37.65	1.02	0.225	5.17E-04	1.85E-02
ASV218	Bacteroidota	Bacteroidia	Cytophagales	Hymenobacteraceae	Hymenobacter	NA	48.22	0.9378	0.39	2.41E-03	4.31E-02
ASV235	Actinobacteriota	Actinobacteria	Propionibacteriales	Nocardiodaceae	Nocardioides	NA	29.14	-0.918	0.221	2.07E-03	3.99E-02
ASV275	Proteobacteria	Alphaproteobacteria	Rhizobiales	Rhizobiaceae	Aureimonas	NA	8.472	1.0389	0.405	1.38E-03	3.19E-02
ASV341	Actinobacteriota	Actinobacteria	Pseudonocardiales	Pseudonocardiaceae	Pseudonocardia	NA	1.425	0.8867	0.26	2.52E-03	4.31E-02
ASV342	Proteobacteria	Alphaproteobacteria	Sphingomonadales	Sphingomonadaceae	Sphingomonas	NA	1.309	0.9108	0.228	2.83E-03	4.31E-02
ASV365	Actinobacteriota	Actinobacteria	Propionibacteriales	Nocardiodaceae	Nocardioides	alpinus	1.396	-0.86	0.231	1.46E-03	3.19E-02
ASV377	Bacteroidota	Bacteroidia	Cytophagales	Hymenobacteraceae	Hymenobacter	NA	2.173	0.8629	0.307	2.90E-03	4.31E-02
ASV416	Actinobacteriota	Actinobacteria	Propionibacteriales	Nocardiodaceae	Nocardioides	NA	1.047	-0.824	0.258	2.66E-03	4.31E-02

<sup>a</sup> Base mean is the mean of normalized counts of all samples, log2 fold change refers to the effect size estimate (where positive values mean the ASV significantly increase with GDD accumulation and negative values mean the ASV significantly declines in abundance as GDDs accumulate), lfcSE is the standard error of the log2 fold change, the P-value is calculated using the Wald test, and the adjusted P-value (padj) is calculated using the Benjamini–Hochberg method. Shown are ASVs that changed significantly (padj < 0.05) in relative abundance among accumulated GDD sampling points.

**Supplementary Table S8.** List of total differentially abundant taxa between grey birch and trembling aspen across host phenology as determined by differential abundance analysis (*DESeq2*).<sup>a</sup>

ASV	Phylum	Class	Order	Family	Genus	Species	Base Mean	Log2 Fold Change	lfcSE	P-value	Adjusted P-value
ASV8	Proteobacteria	Alphaproteobacteria	Acetobacterales	Acetobacteraceae	Endobacter	NA	171.2687	-3.70784	1.085316	0.000635	0.025385
ASV10	Proteobacteria	NA	NA	NA	NA	NA	137.118	6.270755	0.974832	1.25398866067e-10	4.0127637e-08
ASV33	Actinobacteriota	Actinobacteria	Kineosporiales	Kineosporiaceae	Quadrisphaera	NA	14.84484	-4.2775	1.040408	3.93327896473e-05	0.003147
ASV36	Proteobacteria	Alphaproteobacteria	Rhodobacterales	Rhodobacteraceae	Rubellimicrobium	NA	13.34271	-4.00882	1.1506	0.000494	0.022573
ASV39	Proteobacteria	Alphaproteobacteria	Acetobacterales	Acetobacteraceae	Endobacter	NA	12.90497	3.938015	1.197973	0.001012	0.029434
ASV44	Proteobacteria	Alphaproteobacteria	Rhizobiales	Beijerinckiaceae	Methylobacterium-Methylorubrum	NA	10.89408	-4.28117	1.138312	0.000169	0.009027
ASV81	Bacteroidota	Bacteroidia	Cytophagales	Hymenobacteraceae	Hymenobacter	NA	4.399651	-4.18257	1.048903	6.67545952102e-05	0.004272
ASV86	Proteobacteria	Gammaproteobacteria	Enterobacterales	Erwiniaceae	NA	NA	4.155869	-5.98926	1.152333	2.01979954147e-07	3.2316793e-05
ASV106	Actinobacteriota	Actinobacteria	Frankiales	Geodermatophilaceae	Blastococcus	NA	3.435446	-5.25636	1.110372	2.20278631775e-06	0.000235
ASV107	Proteobacteria	Alphaproteobacteria	Sphingomonadales	Sphingomonadaceae	Sphingomonas	NA	3.394058	-3.22048	1.008219	0.001402	0.034512
ASV110	Bacteroidota	Bacteroidia	Cytophagales	Spirosomaceae	Spirosoma	NA	3.350635	-3.33335	0.992034	0.000779	0.027701
ASV186	Proteobacteria	Alphaproteobacteria	Caulobacterales	Caulobacteraceae	PMMR1	NA	2.258111	2.891122	0.928947	0.001857	0.035712
ASV200	Abditibacteriota	Abditibacteria	Abditibacteriales	Abditibacteriaceae	Abditibacterium	NA	2.112661	-2.97113	0.898428	0.000943	0.029434
ASV223	Actinobacteriota	Actinobacteria	Frankiales	Nakamurellaceae	Nakamurella	NA	2.01064	-2.70895	0.868453	0.001813	0.035712
ASV235	Actinobacteriota	Actinobacteria	Propionibacteriales	Nocardioideaceae	Nocardioides	NA	1.980932	-2.6976	0.868549	0.001897	0.035712
ASV297	Proteobacteria	Alphaproteobacteria	Acetobacterales	Acetobacteraceae	Acidiphilium	NA	1.734082	-2.61921	0.81449	0.001301	0.034512
ASV365	Actinobacteriota	Actinobacteria	Propionibacteriales	Nocardioideaceae	Nocardioides	alpinus	1.51536	-2.49622	0.795004	0.00169	0.035712

<sup>a</sup> Base mean is the mean of normalized counts of all samples, log2fold change refers to the effect size estimate (where positive values mean the ASV is differentially abundant in birch and negative values mean the ASV is differentially abundant in aspen), lfcSE is the standard error of the log2 fold change, the *P*-value is calculated using the Wald test, and the adjusted *P*-value (padj) is calculated

using the Benjamini–Hochberg method. Shown are ASVs that changed significantly ( $p_{adj} < 0.05$ ) in relative abundance among accumulated GDD sampling points.

**Supplementary Table S9.** List of differentially abundant taxa between grey birch and trembling aspen as growing degree days (GDDs) are accumulated at a base temperature of 5°C at GDD sampling points (a) 437, (b) 605, (c) 1087, (d) 1606, (e) 1992, (f) 2140, and (g) 2219 as determined by differential abundance analysis (*DESeq2*).<sup>a</sup>

ASV	Phylum	Class	Order	Family	Genus	Species	Base Mean	Log2 Fold Change	lfcSE	P-value	Adjusted P-value
<b>(a) GDD_437</b>											
ASV10	Proteobacteria	NA	NA	NA	NA	NA	27	4.700431039	1.106807847	2.17E-05	0.037183063
<b>(b) GDD_605</b>											
ASV10	Proteobacteria	NA	NA	NA	NA	NA	102.7	7.675246219	7.675246219	1.26E-23	9.35E-22
ASV14	Proteobacteria	Alphaproteobacteria	Rhizobiales	Beijerinckiaceae	1174-901-12	NA	5.3	3.263029044	1.104431163	0.003131879	0.023946342
ASV19	Proteobacteria	NA	NA	NA	NA	NA	19.7	5.263024351	1.186902855	9.24E-06	0.000227903
ASV32	Proteobacteria	Alphaproteobacteria	Sphingomonadales	Sphingomonadaceae	Sphingomonas	NA	8.3	-3.96346694	1.346111181	0.003235992	0.023946342
ASV33	Actinobacteriota	Actinobacteria	Kineosporiales	Kineosporiaceae	Quadrisphaera	NA	18.2	-5.14567163	1.063969378	1.32E-06	4.89E-05
ASV43	Firmicutes	Bacilli	Bacillales	Marinococcaceae	Alteribacillus	NA	4.7	3.07038395	1.136781764	0.006914297	0.039358304
ASV44	Proteobacteria	Alphaproteobacteria	Rhizobiales	Beijerinckiaceae	Methylobacterium-Methylorubrum	NA	10.2	-4.27797855	1.203968212	0.000380529	0.005631822
ASV45	Actinobacteriota	Actinobacteria	Pseudonocardiales	Pseudonocardiaceae	Actinomycetospira	iriotensis	7.5	-3.80734999	1.138078739	0.000821584	0.010132871
ASV54	Proteobacteria	Alphaproteobacteria	Sphingomonadales	Sphingomonadaceae	Sphingomonas	NA	11.8	-4.49824413	1.227719895	0.000248403	0.004595453
ASV59	NA	NA	NA	NA	NA	NA	13	-4.64384693	1.412023807	0.001006198	0.010636949
ASV60	Proteobacteria	Alphaproteobacteria	Sphingomonadales	Sphingomonadaceae	Sphingomonas	NA	7.5	-3.80734864	1.284544646	0.003037003	0.023946342
ASV81	Bacteroidota	Bacteroidia	Cytophagales	Hymenobacteraceae	Hymenobacter	NA	5.3	-3.26302946	1.231972655	0.008082075	0.042719541
ASV87	Proteobacteria	Alphaproteobacteria	Sphingomonadales	Sphingomonadaceae	Ellin6055	NA	6.3	-3.53604727	1.261383621	0.005058128	0.031191789
ASV107	Proteobacteria	Alphaproteobacteria	Sphingomonadales	Sphingomonadaceae	Sphingomonas	NA	6.5	-3.58495676	1.265923995	0.004627385	0.031129681
ASV365	Actinobacteriota	Actinobacteria	Propionibacteriales	Nocardiodaceae	Nocardioides	alpinus	4.3	-2.92599574	1.122054859	0.009114965	0.044967161
<b>(c) GDD_1087</b>											
ASV8	Proteobacteria	Alphaproteobacteria	Acetobacterales	Acetobacteraceae	Endobacter	NA	12.90909	4.765525036	1.198503968	7.00E-05	0.001347827
ASV10	Proteobacteria	NA	NA	NA	NA	NA	135.8182	8.217218848	1.028010923	1.31E-15	1.01E-13
ASV14	Proteobacteria	Alphaproteobacteria	Rhizobiales	Beijerinckiaceae	1174-901-12	NA	10.63636	4.472476352	1.330505224	0.000775239	0.007461679
ASV19	Proteobacteria	NA	NA	NA	NA	NA	31.63636	6.095910617	1.259258845	1.29E-06	4.98E-05
ASV31	Proteobacteria	Alphaproteobacteria	Rhizobiales	Beijerinckiaceae	1174-901-12	NA	5	3.29277514	1.187771856	0.005567392	0.026053463

ASV33	Actinobacteriota	Actinobacteria	Kineosporiales	Kineosporiaceae	Quadrisphaera	NA	22.27273	-5.32192086	1.170177557	5.42E-06	0.000139032
ASV35	NA	NA	NA	NA	NA	NA	12.09091	4.666746506	1.23589863	0.00015937	0.002454305
ASV36	Proteobacteria	Alphaproteobacteria	Rhodobacterales	Rhodobacteraceae	Rubellimicrobium	NA	6.545455	-3.48112117	1.260549526	0.005752063	0.026053463
ASV42	Proteobacteria	Alphaproteobacteria	Rhizobiales	Beijerinckiaceae	1174-901-12	NA	8	4.035614497	1.274540534	0.001543761	0.011886963
ASV44	Proteobacteria	Alphaproteobacteria	Rhizobiales	Beijerinckiaceae	Methylobacterium-Methylorubrum	NA	6.454545	-3.45942687	1.176886439	0.003287701	0.021096079
ASV60	Proteobacteria	Alphaproteobacteria	Sphingomonadales	Sphingomonadaceae	Sphingomonas	NA	10.90909	-4.26052111	1.229747474	0.00053112	0.005931704
ASV81	Bacteroidota	Bacteroidia	Cytophagales	Hymenobacteraceae	Hymenobacter	NA	11.45455	-4.33389394	1.252402634	0.000539246	0.005931704
ASV93	Actinobacteriota	Actinobacteria	Corynebacteriales	Corynebacteriaceae	Corynebacterium	NA	9.090909	-3.98488540	1.390983543	0.004172767	0.023195384
ASV95	Acidobacteriota	Acidobacteriae	Acidobacteriales	Acidobacteriaceae (Subgroup 1)	Bryocella	NA	5.545455	3.459424488	1.208984374	0.004217343	0.023195384
ASV106	Actinobacteriota	Actinobacteria	Frankiales	Geodermatophilaceae	Blastococcus	NA	16	-4.8328795	1.47591305	0.001058486	0.009055934
ASV107	Proteobacteria	Alphaproteobacteria	Sphingomonadales	Sphingomonadaceae	Sphingomonas	NA	5.545455	-3.22238775	1.204010701	0.007442266	0.031836358
ASV117	Proteobacteria	Alphaproteobacteria	Rhizobiales	Beijerinckiaceae	1174-901-12	NA	5.181818	3.350490231	1.210520022	0.005643423	0.026053463
ASV125	Proteobacteria	Alphaproteobacteria	Rhizobiales	Beijerinckiaceae	Methylocella	NA	6.909091	3.807346243	1.260468549	0.002522909	0.017660366

**(d) GDD\_1606**

ASV9	Proteobacteria	Alphaproteobacteria	Rhizobiales	Beijerinckiaceae	1174-901-12	NA	42.4	6.388859844	1.437691527	8.84E-06	0.000159067
ASV10	Proteobacteria	NA	NA	NA	NA	NA	227	8.823348757	1.238943648	1.07E-12	7.68E-11
ASV14	Proteobacteria	Alphaproteobacteria	Rhizobiales	Beijerinckiaceae	1174-901-12	NA	22.2	4.940828596	1.149434266	1.72E-05	0.000247634
ASV19	Proteobacteria	NA	NA	NA	NA	NA	71.3	6.135438503	1.243866514	8.12E-07	1.95E-05
ASV25	Proteobacteria	Alphaproteobacteria	Rhizobiales	Beijerinckiaceae	1174-901-12	NA	12.6	4.59692239	1.407998407	0.001095169	0.009856521
ASV28	Myxococcota	Myxococcia	Myxococcales	Myxococcaceae	P3OB-42	NA	35.9	4.330377253	1.315845823	0.000998512	0.009856521
ASV35	NA	NA	NA	NA	NA	NA	37.1	6.193760229	1.173125099	1.29E-07	4.66E-06
ASV44	Proteobacteria	Alphaproteobacteria	Rhizobiales	Beijerinckiaceae	Methylobacterium-Methylorubrum	NA	10.4	-4.30742016	1.393673691	0.001996887	0.014377587
ASV49	Myxococcota	Myxococcia	Myxococcales	Myxococcaceae	P3OB-42	NA	35.6	6.133378832	1.532770245	6.29E-05	0.000755309
ASV105	NA	NA	NA	NA	NA	NA	8.5	3.999991059	1.272888713	0.001675395	0.013403157

**(e) GDD\_1992**

ASV7	Proteobacteria	Alphaproteobacteria	Acetobacterales	Acetobacteraceae	Endobacter	NA	306.4	7.485688943	1.364915204	4.15E-08	1.05E-06
ASV8	Proteobacteria	Alphaproteobacteria	Acetobacterales	Acetobacteraceae	Endobacter	NA	196.8	7.613216633	1.334032315	1.15E-08	4.37E-07
ASV9	Proteobacteria	Alphaproteobacteria	Rhizobiales	Beijerinckiaceae	1174-901-12	NA	206.3	5.856533266	1.598912719	0.000249452	0.00157986
ASV10	Proteobacteria	NA	NA	NA	NA	NA	180.4	8.491029067	1.374771545	6.56E-10	4.99E-08
ASV14	Proteobacteria	Alphaproteobacteria	Rhizobiales	Beijerinckiaceae	1174-901-12	NA	199.3	7.042912351	1.465173923	1.53E-06	2.91E-05

ASV19	Proteobacteria	NA	NA	NA	NA	NA	53.2	6.719711315	1.448000869	3.47E-06	5.28E-05
ASV25	Proteobacteria	Alphaproteobacteria	Rhizobiales	Beijerinckiaceae	1174-901-12	NA	27.1	3.813055748	1.406620245	0.00671226	0.025077988
ASV28	Myxococcota	Myxococcia	Myxococcales	Myxococcaceae	P3OB-42	NA	26.9	5.722447965	1.496693406	0.000131627	0.001278823
ASV29	Proteobacteria	Alphaproteobacteria	Rhizobiales	Beijerinckiaceae	1174-901-12	NA	18.8	5.193758277	1.365634567	0.000142849	0.001278823
ASV33	Actinobacteriota	Actinobacteria	Kineosporiales	Kineosporiaceae	Quadrisphaera	NA	4.7	-3.07038527	1.150674496	0.007622816	0.026333365
ASV35	NA	NA	NA	NA	NA	NA	14.2	4.776093018	1.294399719	0.000224419	0.00155053
ASV42	Proteobacteria	Alphaproteobacteria	Rhizobiales	Beijerinckiaceae	1174-901-12	NA	18.3	5.153792508	1.339477395	0.000119274	0.001278823
ASV47	Myxococcota	Myxococcia	Myxococcales	Myxococcaceae	P3OB-42	NA	27.5	5.754868761	1.518957284	0.00015144	0.001278823
ASV59	NA	NA	NA	NA	NA	NA	5.4	-3.29277659	1.253256665	0.008604617	0.027563185
ASV64	Proteobacteria	Alphaproteobacteria	Rhizobiales	Beijerinckiaceae	Methylocella	NA	13.6	4.711484115	1.294652219	0.000273498	0.001598911
ASV84	Myxococcota	Myxococcia	Myxococcales	Myxococcaceae	P3OB-42	NA	6	3.459423976	1.271075008	0.006495648	0.025077988
ASV91	Proteobacteria	Alphaproteobacteria	Acetobacterales	Acetobacteraceae	Endobacter	NA	8.4	3.981842919	1.326590713	0.002685992	0.013609028
ASV95	Acidobacteriota	Acidobacteriae	Acidobacteriales	Acidobacteriaceae (Subgroup 1)	Bryocella	NA	7	3.70043271	1.179739468	0.001708886	0.009276808
ASV97	Proteobacteria	Gammaproteobacteria	Burkholderiales	Oxalobacteraceae	Massilia	NA	16.5	4.999987671	1.333498118	0.000177168	0.001346478
ASV102	Acidobacteriota	Acidobacteriae	Acidobacteriales	Acidobacteriaceae (Subgroup 1)	Terriglobus	NA	7.8	3.867886743	1.346518959	0.004072275	0.019343307
ASV104	Actinobacteriota	Actinobacteria	Corynebacteriales	Corynebacteriaceae	Lawsonella	clevelandensis	3.9	2.765530219	1.099921682	0.011926981	0.033572243
ASV132	Proteobacteria	Alphaproteobacteria	Rhizobiales	Beijerinckiaceae	Methylocella	NA	6.2	3.510954606	1.230914695	0.004340227	0.019403369
ASV160	Proteobacteria	Alphaproteobacteria	Rhizobiales	Beijerinckiaceae	Methylocella	NA	4.8	3.104330183	1.230352143	0.01163176	0.033572243
ASV172	Proteobacteria	Gammaproteobacteria	Burkholderiales	Oxalobacteraceae	Massilia	timonae	5.9	-3.43295386	1.271362617	0.006929444	0.025077988
ASV173	Proteobacteria	Gammaproteobacteria	Enterobacteriales	Enterobacteriaceae	Klebsiella	NA	9.8	3.137495199	1.294244617	0.015342565	0.041644105
ASV181	Proteobacteria	Alphaproteobacteria	Acetobacterales	Acetobacteraceae	Endobacter	NA	5.4	3.29277441	1.269055679	0.009468314	0.028783675
ASV191	Proteobacteria	Alphaproteobacteria	Rhizobiales	Beijerinckiaceae	1174-901-12	NA	6.7	3.632259709	1.299569003	0.005190412	0.021915073
ASV351	Proteobacteria	Gammaproteobacteria	Enterobacteriales	NA	NA	NA	4.7	3.070383582	1.170356494	0.008704164	0.027563185
ASV414	Actinobacteriota	Actinobacteria	Micrococcales	Microbacteriaceae	Amnibacterium	NA	4.3	-2.9259951	1.215686473	0.016090049	0.042167024

**(f) GDD\_2140**

ASV7	Proteobacteria	Alphaproteobacteria	Acetobacterales	Acetobacteraceae	Endobacter	NA	392.2	9.61358684	1.19163255	7.17E-16	1.03E-13
ASV8	Proteobacteria	Alphaproteobacteria	Acetobacterales	Acetobacteraceae	Endobacter	NA	186.1	6.198475795	1.337456851	3.58E-06	4.68E-05
ASV9	Proteobacteria	Alphaproteobacteria	Rhizobiales	Beijerinckiaceae	1174-901-12	NA	281.5	7.867772108	1.336519153	3.94E-09	1.89E-07
ASV10	Proteobacteria	NA	NA	NA	NA	NA	172.1	8.422885001	1.334184738	2.73E-10	1.97E-08
ASV14	Proteobacteria	Alphaproteobacteria	Rhizobiales	Beijerinckiaceae	1174-901-12	NA	121	6.221572596	1.215688867	3.09E-07	8.91E-06
ASV19	Proteobacteria	NA	NA	NA	NA	NA	115.9	7.850466656	1.708787758	4.34E-06	5.21E-05

ASV25	Proteobacteria	Alphaproteobacteria	Rhizobiales	Beijerinckiaceae	1174-901-12	NA	59.1	6.872807919	1.46937483	2.91E-06	4.18E-05
ASV29	Proteobacteria	Alphaproteobacteria	Rhizobiales	Beijerinckiaceae	1174-901-12	NA	64.3	6.995464698	1.423600457	8.93E-07	2.14E-05
ASV33	Actinobacteriota	Actinobacteria	Kineosporiales	Kineosporiaceae	Quadrisphaera	NA	28.6	-5.81249145	1.079338229	7.23E-08	2.60E-06
ASV35	NA	NA	NA	NA	NA	NA	19.3	5.232648199	1.317193279	7.11E-05	0.00068256
ASV36	Proteobacteria	Alphaproteobacteria	Rhodobacterales	Rhodobacteraceae	Rubellimicrobium	NA	30.6	-5.91168241	1.245337087	2.06E-06	3.30E-05
ASV37	Myxococcota	NA	NA	NA	NA	NA	26.3	5.689284715	1.353167653	2.62E-05	0.000289942
ASV39	Proteobacteria	Alphaproteobacteria	Acetobacterales	Acetobacteraceae	Endobacter	NA	18.5	5.169909179	1.474876983	0.000456066	0.003648532
ASV41	Proteobacteria	Alphaproteobacteria	Rhizobiales	Beijerinckiaceae	Methylobacterium-Methylorubrum	NA	10.1	-4.26302772	1.252897414	0.000667637	0.004578084
ASV44	Proteobacteria	Alphaproteobacteria	Rhizobiales	Beijerinckiaceae	Methylobacterium-Methylorubrum	NA	19.2	-5.22496009	1.097740057	1.94E-06	3.30E-05
ASV45	Actinobacteriota	Actinobacteria	Pseudonocardiales	Pseudonocardiaceae	Actinomycetospira	iriomotensis	29	-5.83288152	1.207676508	1.37E-06	2.81E-05
ASV48	Proteobacteria	Alphaproteobacteria	Acetobacterales	Acetobacteraceae	NA	NA	17.4	5.078939496	1.299795183	9.33E-05	0.000839332
ASV59	NA	NA	NA	NA	NA	NA	9.7	-4.2016282	1.161064339	0.000296003	0.002507321
ASV60	Proteobacteria	Alphaproteobacteria	Sphingomonadales	Sphingomonadaceae	Sphingomonas	NA	4.9	-3.13749871	1.238482705	0.011298106	0.040673182
ASV64	Proteobacteria	Alphaproteobacteria	Rhizobiales	Beijerinckiaceae	Methylocella	NA	11.4	4.446246261	1.275558642	0.000490806	0.003719792
ASV66	Firmicutes	Bacilli	Bacillales	Bacillaceae	NA	NA	8.5	-3.26678314	1.090616689	0.002741264	0.014097931
ASV67	Actinobacteriota	Actinobacteria	Micrococcales	Micrococcaceae	Micrococcus	NA	3.7	2.678067935	1.051318496	0.010854694	0.040078871
ASV73	Actinobacteriota	Actinobacteria	Frankiales	Geodermatophilaceae	Klenkia	NA	12.1	-3.47248431	1.094502392	0.001510491	0.008736434
ASV74	Firmicutes	Bacilli	Bacillales	Marinococcaceae	NA	NA	4.4	-2.96346973	1.217738161	0.014950111	0.047840355
ASV79	Proteobacteria	Alphaproteobacteria	Rhizobiales	Beijerinckiaceae	1174-901-12	NA	4.5	2.999993777	1.226653401	0.014458185	0.047317695
ASV80	Actinobacteriota	Actinobacteria	Micrococcales	Microbacteriaceae	Amnibacterium	NA	13.7	-4.72245948	1.180120064	6.29E-05	0.000646921
ASV84	Myxococcota	Myxococcia	Myxococcales	Myxococcaceae	P3OB-42	NA	7.5	3.807347119	1.222794897	0.001847928	0.010234676
ASV108	Actinobacteriota	Actinobacteria	Micrococcales	Dermacoccaceae	Dermacoccus	nishinomiyaensis	4.8	-3.10433196	1.230742874	0.011658236	0.040946
ASV111	Actinobacteriota	Actinobacteria	Micrococcales	Microbacteriaceae	Marisediminicola	NA	8	-3.90688479	1.218639943	0.001346227	0.008428553
ASV114	Proteobacteria	Alphaproteobacteria	Acetobacterales	Acetobacteraceae	Acidiphilium	NA	4.8	3.104330952	1.165072866	0.007710399	0.031722784
ASV115	Proteobacteria	Gammaproteobacteria	Gammaproteobacteria Incertae Sedis	Unknown Family	Candidatus Ovatusbacter	NA	11	4.392306971	1.310930741	0.000806584	0.005279456
ASV117	Proteobacteria	Alphaproteobacteria	Rhizobiales	Beijerinckiaceae	1174-901-12	NA	4.7	3.070383695	1.164118458	0.008351513	0.0325813
ASV121	Myxococcota	Myxococcia	Myxococcales	Myxococcaceae	P3OB-42	NA	8	-3.90688375	1.324513962	0.003181099	0.015269275
ASV129	Bacteroidota	Bacteroidia	Cytophagales	Spirosomaceae	Spirosoma	NA	4.6	-3.0356199	1.151293383	0.008371584	0.0325813
ASV133	Actinobacteriota	Actinobacteria	Kineosporiales	Kineosporiaceae	Quadrisphaera	NA	8.3	-3.96346886	1.152838354	0.000586008	0.004219256
ASV137	Proteobacteria	Alphaproteobacteria	Rhizobiales	Beijerinckiaceae	1174-901-12	NA	6	3.45942492	1.190417232	0.003660103	0.017001767

ASV155	Proteobacteria	Alphaproteobacteria	Acetobacterales	Acetobacteraceae	Belnapia	NA	4.8	-3.10433192	1.235441261	0.011980054	0.041074472
ASV161	Proteobacteria	Gammaproteobacteria	NA	NA	NA	NA	6.5	3.584956314	1.130380056	0.001516742	0.008736434
ASV166	Proteobacteria	Alphaproteobacteria	Rickettsiales	NA	NA	NA	6.8	3.655344643	1.199286702	0.002304219	0.012289166
ASV174	Proteobacteria	Alphaproteobacteria	Rickettsiales	AB1	NA	NA	6.2	3.510953603	1.306063822	0.007183953	0.031348161
ASV188	Bdellovibrionota	Oligoflexia	0319-6G20	NA	NA	NA	4.7	3.070382897	1.232411923	0.012725478	0.042615554
ASV218	Bacteroidota	Bacteroidia	Cytophagales	Hymenobacteraceae	Hymenobacter	NA	6.2	-3.51095696	1.188099463	0.003125641	0.015269275
ASV259	Bacteroidota	Bacteroidia	Cytophagales	Spirosomaceae	Spirosoma	NA	6.3	-3.53604707	1.283696124	0.005876704	0.02644517
ASV341	Actinobacteriota	Actinobacteria	Pseudonocardiales	Pseudonocardiaceae	Pseudonocardia	NA	4.7	-3.07038527	1.151063378	0.007643296	0.031722784
ASV405	Proteobacteria	Alphaproteobacteria	Acetobacterales	Acetobacteraceae	NA	NA	4.4	2.963468761	1.155276511	0.010312832	0.039080207

**(g) GDD\_2219**

ASV7	Proteobacteria	Alphaproteobacteria	Acetobacterales	Acetobacteraceae	Endobacter	NA	817.3	10.67382273	1.076134031	3.45E-23	2.76E-21
ASV8	Proteobacteria	Alphaproteobacteria	Acetobacterales	Acetobacteraceae	Endobacter	NA	631.2	10.30079566	1.037466248	3.12E-23	2.76E-21
ASV9	Proteobacteria	Alphaproteobacteria	Rhizobiales	Beijerinckiaceae	1174-901-12	NA	394.6	6.804021674	1.224673669	2.76E-08	1.11E-06
ASV10	Proteobacteria	NA	NA	NA	NA	NA	82.7	7.361047507	1.362841915	6.62E-08	2.12E-06
ASV14	Proteobacteria	Alphaproteobacteria	Rhizobiales	Beijerinckiaceae	1174-901-12	NA	171.8	8.420366945	1.130535769	9.47E-14	5.05E-12
ASV19	Proteobacteria	NA	NA	NA	NA	NA	33.7	6.053094702	1.409277236	1.75E-05	0.000310319
ASV25	Proteobacteria	Alphaproteobacteria	Rhizobiales	Beijerinckiaceae	1174-901-12	NA	53.3	6.722443974	1.524634699	1.04E-05	0.000207491
ASV28	Myxococcota	Myxococcia	Myxococcales	Myxococcaceae	P3OB-42	NA	30.4	5.902059023	1.33618928	1.00E-05	0.000207491
ASV29	Proteobacteria	Alphaproteobacteria	Rhizobiales	Beijerinckiaceae	1174-901-12	NA	24.8	5.602869697	1.373506963	4.52E-05	0.000602433
ASV33	Actinobacteriota	Actinobacteria	Kineosporiales	Kineosporiaceae	Quadrisphaera	NA	19.6	-5.25549118	1.348390443	9.71E-05	0.001110278
ASV35	NA	NA	NA	NA	NA	NA	8.4	3.981843273	1.304004022	0.0022615	0.014449167
ASV36	Proteobacteria	Alphaproteobacteria	Rhodobacterales	Rhodobacteraceae	Rubellimicrobium	NA	15.7	-4.9259907	1.330493628	0.000213588	0.002010239
ASV37	Myxococcota	NA	NA	NA	NA	NA	49.7	6.620566552	1.46195289	5.94E-06	0.000158352
ASV39	Proteobacteria	Alphaproteobacteria	Acetobacterales	Acetobacteraceae	Endobacter	NA	18.5	5.169914032	1.244752065	3.28E-05	0.000476533
ASV40	Proteobacteria	Alphaproteobacteria	Sphingomonadales	Sphingomonadaceae	Sphingomonas	NA	23.4	-4.82016914	1.487134994	0.001190088	0.008655184
ASV45	Actinobacteriota	Actinobacteria	Pseudonocardiales	Pseudonocardiaceae	Actinomycetospora iriomotensis	NA	23.3	-5.51095140	1.382965343	6.75E-05	0.000830943
ASV47	Myxococcota	Myxococcia	Myxococcales	Myxococcaceae	P3OB-42	NA	21.4	5.385414411	1.4811417	0.000276917	0.00246148
ASV48	Proteobacteria	Alphaproteobacteria	Acetobacterales	Acetobacteraceae	NA	NA	19.3	5.232646645	1.390337541	0.000167498	0.001674981
ASV49	Myxococcota	Myxococcia	Myxococcales	Myxococcaceae	P3OB-42	NA	10	4.247917493	1.308894643	0.001172761	0.008655184
ASV59	NA	NA	NA	NA	NA	NA	20	-5.28539395	1.250603332	2.38E-05	0.000380146
ASV60	Proteobacteria	Alphaproteobacteria	Sphingomonadales	Sphingomonadaceae	Sphingomonas	NA	16.3	-4.98184238	1.436331294	0.000523471	0.004187769
ASV64	Proteobacteria	Alphaproteobacteria	Rhizobiales	Beijerinckiaceae	Methylocella	NA	12.2	4.548425964	1.302283918	0.000478247	0.004027346

ASV66	Firmicutes	Bacilli	Bacillales	Bacillaceae	NA	NA	6.5	-3.58495648	1.296009912	0.005672262	0.031295237
ASV79	Proteobacteria	Alphaproteobacteria	Rhizobiales	Beijerinckiaceae	1174-901-12	NA	12.6	4.596925937	1.211831919	0.000148617	0.001585247
ASV80	Actinobacteriota	Actinobacteria	Micrococcales	Microbacteriaceae	Amnibacterium	NA	7.7	-3.84799075	1.264840776	0.00234799	0.014449167
ASV84	Myxococcota	Myxococcia	Myxococcales	Myxococcaceae	P3OB-42	NA	9	4.087453754	1.269943956	0.001288138	0.008960957
ASV95	Acidobacteriota	Acidobacteriae	Acidobacteriales	Acidobacteriaceae (Subgroup 1)	Bryocella	NA	5.6	3.35049058	1.204869023	0.005422641	0.030986519
ASV109	Proteobacteria	Gammaproteobacteria	Burkholderiales	Oxalobacteraceae	Massilia	NA	5.7	-3.37850603	1.286852406	0.008654649	0.044669157
ASV143	Myxococcota	Myxococcia	Myxococcales	Myxococcaceae	P3OB-42	NA	11.4	-4.44624759	1.394413165	0.001429558	0.009530389
ASV175	Actinobacteriota	Actinobacteria	Pseudonocardiales	Pseudonocardiaceae	Actinomycetospora	NA	7.9	-3.88751837	1.332840581	0.003537369	0.020962188
ASV188	Bdellovibrionota	Oligoflexia	0319-6G20	NA	NA	NA	5.5	3.321920815	1.260606763	0.008409364	0.044669157
ASV214	Actinobacteriota	Actinobacteria	Propionibacteriales	Nocardioidaceae	Nocardioides	NA	5.3	-3.26302928	1.254956009	0.009319267	0.046596334

<sup>a</sup> Base mean is the mean of normalized counts of all samples, log2fold change refers to the effect size estimate (where positive values mean the ASV is differentially abundant in birch and negative values mean the ASV is differentially abundant in aspen), lfcSE is the standard error of the log2 fold change, the *P*-value is calculated using the Wald test, and the adjusted *P*-value (padj) is calculated using the Benjamini–Hochberg method. Shown are ASVs that changed significantly (padj < 0.05) in relative abundance among accumulated GDD sampling points.

**Supplementary Table S10.** ASV-level thermal niche width, classification, and taxonomic annotation. This table reports Levins' niche width index for each bacterial ASV, calculated from scaled relative abundance across continuous GDD (Tbase = 5°C) values.<sup>a</sup>

ASV	Niche Width	GDD Peak	Relative Abundance	Levin's Niche Class	Genus
ASV7	3.159	2219	2.488E-02	Generalist	Endobacter
ASV8	2.532	2219	2.155E-02	Generalist	Endobacter
ASV9	3.171	2219	1.816E-02	Generalist	1174-901-12
ASV10	5.866	2140	9.561E-03	Generalist	NA
ASV12	2.545	1606	1.646E-02	Generalist	Staphylococcus
ASV14	3.341	1992	1.377E-02	Generalist	1174-901-12
ASV16	1.000	1992	2.257E-05	Specialist	Escherichia-Shigella
ASV17	2.192	2140	1.538E-02	Intermediate	Massilia
ASV19	4.418	2140	7.409E-03	Generalist	NA
ASV22	1.660	2219	7.823E-04	Intermediate	NA
ASV24	2.794	2140	5.642E-03	Generalist	Sphingomonas
ASV25	3.748	2219	4.009E-03	Generalist	1174-901-12
ASV27	1.424	1087	6.770E-05	Specialist	Enterococcus
ASV28	3.929	2140	2.543E-03	Generalist	P3OB-42
ASV29	3.283	2140	4.258E-03	Generalist	1174-901-12
ASV30	1.000	437	8.004E-03	Specialist	Ensifer
ASV31	1.410	2219	7.387E-03	Specialist	1174-901-12
ASV32	3.404	2140	2.731E-03	Generalist	Sphingomonas
ASV33	4.494	605	9.553E-04	Generalist	Quadrisphaera
ASV34	1.000	1992	4.513E-05	Specialist	Pseudomonas
ASV35	3.865	1606	1.625E-03	Generalist	NA
ASV36	3.802	605	2.076E-03	Generalist	Rubellimicrobium
ASV37	2.138	2219	1.963E-03	Intermediate	P3OB-42
ASV38	1.000	2219	6.747E-03	Specialist	Enterococcus
ASV39	5.504	2140	1.309E-03	Generalist	Endobacter
ASV40	3.974	1606	1.557E-03	Generalist	Sphingomonas
ASV41	4.442	1606	1.647E-03	Generalist	Methylobacterium-Methylorubrum

ASV42	3.435	2219	1.249E-03	Generalist	1174-901-12
ASV43	1.000	1087	1.279E-04	Specialist	Alteribacillus
ASV44	5.860	2140	5.943E-04	Generalist	Methylobacterium-Methylorubrum
ASV45	3.611	2219	8.500E-04	Generalist	Actinomycetospora
ASV46	3.520	1992	1.414E-03	Generalist	Sphingomonas
ASV47	2.957	1992	1.805E-03	Generalist	P3OB-42
ASV48	4.337	2219	1.294E-03	Generalist	NA
ASV49	2.554	1606	1.685E-03	Generalist	P3OB-42
ASV50	1.007	2219	4.348E-03	Specialist	Tepidimonas
ASV52	3.171	1992	1.301E-03	Generalist	Massilia
ASV53	1.000	2219	4.205E-03	Specialist	Cloacibacterium
ASV54	4.741	1606	8.425E-04	Generalist	Sphingomonas
ASV55	2.135	2140	1.896E-03	Intermediate	Methylobacterium-Methylorubrum
ASV58	2.182	2140	1.700E-03	Intermediate	Methylobacterium-Methylorubrum
ASV59	3.389	605	6.695E-04	Generalist	NA
ASV60	4.681	2219	6.018E-04	Generalist	Sphingomonas
ASV61	5.038	1606	3.611E-04	Generalist	Bradyrhizobium
ASV62	2.926	1992	1.091E-03	Generalist	Massilia
ASV63	1.000	2219	3.295E-03	Specialist	Anoxybacillus
ASV64	3.923	1992	5.491E-04	Generalist	Methylocella
ASV65	2.963	1606	1.339E-03	Generalist	Curtobacterium
ASV66	1.998	2219	1.204E-04	Intermediate	NA
ASV67	4.345	1992	3.235E-04	Generalist	Micrococcus
ASV68	3.281	1606	1.181E-03	Generalist	Robbsia
ASV69	1.643	1992	1.324E-03	Intermediate	Enhydrobacter
ASV70	3.266	1606	8.876E-04	Generalist	Sphingomonas
ASV71	1.068	2219	2.919E-03	Specialist	P3OB-42
ASV72	1.145	2140	2.625E-03	Specialist	Sphingomonas
ASV73	3.814	605	7.597E-04	Generalist	Klenkia
ASV75	3.488	2219	5.190E-04	Generalist	Methylobacterium-Methylorubrum
ASV76	1.177	2219	2.106E-03	Specialist	P3OB-42
ASV77	1.000	1992	1.956E-03	Specialist	Hymenobacter
ASV78	1.107	1606	1.820E-03	Specialist	Rhizobacter

ASV79	2.905	1992	6.845E-04	Generalist	1174-901-12
ASV80	2.876	2140	4.212E-04	Generalist	Amnibacterium
ASV81	2.862	1087	4.889E-04	Generalist	Hymenobacter
ASV83	2.835	2219	8.199E-04	Generalist	1174-901-12
ASV84	3.421	2219	3.686E-04	Generalist	P3OB-42
ASV85	1.101	605	1.339E-03	Specialist	Erwinia
ASV86	1.000	1087	1.512E-03	Specialist	NA
ASV87	3.620	2219	6.544E-04	Generalist	Ellin6055
ASV88	2.978	1992	8.124E-04	Generalist	Neorhizobium
ASV89	1.000	1087	1.414E-03	Specialist	Pseudomonas
ASV90	1.000	1992	1.647E-03	Specialist	Spirosoma
ASV91	1.753	2219	1.076E-03	Intermediate	Endobacter
ASV92	4.297	437	3.912E-04	Generalist	Streptococcus
ASV93	2.954	1087	5.341E-04	Generalist	Corynebacterium
ASV94	1.803	1087	9.403E-04	Intermediate	Paracoccus
ASV95	4.057	1992	2.783E-04	Generalist	Bryocella
ASV96	1.000	1606	1.331E-03	Specialist	Spirosoma
ASV97	1.471	1992	6.620E-04	Specialist	Massilia
ASV98	3.758	1992	4.513E-04	Generalist	NA
ASV99	1.509	1606	1.038E-03	Intermediate	Roseomonas
ASV100	4.135	2219	3.310E-04	Generalist	Corynebacterium
ASV101	1.062	2219	1.459E-03	Specialist	Methylobacterium-Methylorubrum
ASV102	3.055	2140	5.040E-04	Generalist	Terriglobus
ASV103	3.747	1087	4.438E-04	Generalist	Streptococcus
ASV104	2.836	1606	4.288E-04	Generalist	Lawsonella
ASV105	3.055	1606	3.535E-04	Generalist	NA
ASV106	1.000	1087	1.000E-03	Specialist	Blastococcus
ASV107	3.715	2219	2.633E-04	Generalist	Sphingomonas
ASV108	5.403	1087	3.460E-04	Generalist	Dermacoccus
ASV109	2.033	1087	8.801E-04	Intermediate	Massilia
ASV110	2.785	605	6.695E-04	Generalist	Spirosoma
ASV111	3.581	2219	2.257E-04	Generalist	Marisediminicola
ASV112	1.271	1087	1.053E-03	Specialist	Streptococcus

ASV113	1.000	2219	1.256E-03	Specialist	NA
ASV114	3.174	2219	2.181E-04	Generalist	Acidiphilium
ASV115	2.346	2140	4.739E-04	Generalist	Candidatus Ovatusbacter
ASV116	1.999	1087	4.664E-04	Intermediate	Oxalicibacterium
ASV117	3.044	1087	2.633E-04	Generalist	1174-901-12
ASV118	3.407	605	5.566E-04	Generalist	Roseomonas
ASV119	2.184	2219	6.168E-04	Intermediate	NA
ASV120	2.633	2140	4.212E-04	Generalist	Aureimonas
ASV121	2.774	2140	4.664E-04	Generalist	P3OB-42
ASV122	2.018	2140	7.447E-04	Intermediate	Sphingomonas
ASV123	1.000	2219	1.106E-03	Specialist	Paramesorhizobium
ASV124	1.028	2219	1.083E-03	Specialist	Corynebacterium
ASV125	3.595	1087	3.535E-04	Generalist	Methylocella
ASV126	1.000	605	1.128E-03	Specialist	Corynebacterium
ASV128	3.633	1087	3.235E-04	Generalist	Skermanella
ASV129	3.284	605	4.664E-04	Generalist	Spirosoma
ASV130	1.068	1087	8.801E-04	Specialist	Endobacter
ASV131	1.000	2219	1.031E-03	Specialist	NA
ASV132	3.619	2140	2.332E-04	Generalist	Methylocella
ASV133	2.603	2140	2.031E-04	Generalist	Quadrisphaera
ASV134	5.778	1087	1.204E-04	Generalist	Corynebacterium
ASV135	1.732	1087	6.695E-04	Intermediate	Rothia
ASV137	2.885	2219	2.482E-04	Generalist	1174-901-12
ASV138	1.413	2140	5.566E-04	Specialist	Roseomonas
ASV139	1.972	1992	4.212E-04	Intermediate	Aureimonas
ASV140	1.000	2219	6.695E-04	Specialist	Pseudomonas
ASV141	1.870	1606	9.027E-05	Intermediate	Dermacoccus
ASV142	1.000	1087	7.372E-04	Specialist	Shewanella
ASV143	1.097	2219	5.491E-04	Specialist	P3OB-42
ASV144	2.644	1606	4.363E-04	Generalist	Methylobacterium-Methylorubrum
ASV145	1.000	2219	8.726E-04	Specialist	Thermoanaerobacterium
ASV147	2.759	2140	2.858E-04	Generalist	Brevundimonas
ASV149	1.856	1992	4.664E-04	Intermediate	NA

ASV150	1.305	437	5.566E-04	Specialist	Endobacter
ASV151	1.000	1087	6.695E-04	Specialist	Algoriella
ASV152	3.048	605	2.031E-04	Generalist	Marmoricola
ASV153	1.402	2219	6.093E-04	Specialist	NA
ASV154	4.388	2219	1.881E-04	Generalist	Sphingomonas
ASV155	3.554	2140	1.956E-04	Generalist	Belnapia
ASV156	2.239	2219	4.062E-04	Intermediate	Staphylococcus
ASV157	1.000	1992	7.823E-04	Specialist	Aureimonas
ASV158	1.000	2219	8.726E-04	Specialist	1174-901-12
ASV159	1.290	1606	6.093E-04	Specialist	Neorhizobium
ASV160	3.276	2219	2.031E-04	Generalist	Methylocella
ASV161	2.577	2219	1.279E-04	Generalist	NA
ASV162	1.716	1992	2.633E-04	Intermediate	Fronidhabitans
ASV163	1.185	1087	5.642E-04	Specialist	Nocardioides
ASV164	2.571	1087	3.385E-04	Generalist	Endobacter
ASV165	2.832	1087	2.633E-04	Generalist	Rathayibacter
ASV167	1.174	1606	6.018E-04	Specialist	Roseomonas
ASV168	1.000	1087	6.920E-04	Specialist	NA
ASV169	1.076	1606	2.934E-04	Specialist	Brachybacterium
ASV170	3.757	2219	1.730E-04	Generalist	Quadrisphaera
ASV171	2.387	2219	2.257E-04	Generalist	Pseudokineococcus
ASV172	2.347	1992	2.257E-04	Generalist	Massilia
ASV173	1.000	1992	4.363E-04	Specialist	NA
ASV174	2.600	2140	2.633E-04	Generalist	NA
ASV175	1.608	2219	3.009E-04	Intermediate	Actinomycetospora
ASV176	2.142	605	9.779E-05	Intermediate	Lipingzhangella
ASV178	3.709	605	2.106E-04	Generalist	NA
ASV179	3.068	1087	2.783E-04	Generalist	Methylobacterium-Methylorubrum
ASV180	3.227	2140	2.482E-04	Generalist	Hymenobacter
ASV181	2.451	1087	2.106E-04	Generalist	Endobacter
ASV182	1.000	1606	5.717E-04	Specialist	Tumebacillus
ASV183	1.134	1087	7.823E-04	Specialist	Cellulomonas
ASV184	2.487	1992	3.686E-04	Generalist	Methylobacterium-Methylorubrum

ASV185	1.000	605	7.297E-04	Specialist	Corynebacterium
ASV186	4.167	437	2.031E-04	Generalist	PMMR1
ASV187	3.484	2140	1.580E-04	Generalist	Sphingomonas
ASV188	1.962	2140	2.332E-04	Intermediate	NA
ASV189	2.675	2140	2.708E-04	Generalist	Polaromonas
ASV190	2.529	2219	3.084E-04	Generalist	Sphingomonas
ASV191	1.681	1992	3.159E-04	Intermediate	1174-901-12
ASV192	1.093	2219	5.867E-04	Specialist	NA
ASV193	1.520	1606	4.288E-04	Intermediate	NA
ASV194	2.268	1087	2.106E-04	Generalist	Amnibacterium
ASV195	1.000	2219	6.243E-04	Specialist	NA
ASV197	2.229	2140	1.279E-04	Intermediate	Kineococcus
ASV198	5.092	1087	1.504E-04	Generalist	Methylobacterium-Methylorubrum
ASV199	1.000	1606	5.115E-04	Specialist	NA
ASV200	2.556	605	3.235E-04	Generalist	Abditibacterium
ASV201	1.000	1606	5.190E-04	Specialist	Rubellimicrobium
ASV202	1.795	1606	3.611E-04	Intermediate	Rubellimicrobium
ASV203	2.584	1606	2.858E-04	Generalist	Sphingomonas
ASV204	3.003	1606	2.558E-04	Generalist	NA
ASV205	2.680	1087	2.482E-04	Generalist	Nocardioides
ASV206	2.613	1992	2.858E-04	Generalist	Acidiphilium
ASV207	1.064	1087	4.664E-04	Specialist	Flavisolibacter
ASV208	1.877	2219	3.611E-04	Intermediate	P3OB-42
ASV209	1.840	1087	3.460E-04	Intermediate	NA
ASV210	1.140	2219	5.341E-04	Specialist	Chungangia
ASV211	3.124	1087	1.881E-04	Generalist	NA
ASV212	1.524	2219	4.137E-04	Intermediate	Kineosporia
ASV213	1.253	605	5.266E-04	Specialist	NA
ASV214	2.245	2219	1.956E-04	Intermediate	Nocardioides
ASV215	2.346	1087	1.354E-04	Generalist	Pseudarthrobacter
ASV216	1.000	1087	6.695E-04	Specialist	Acinetobacter
ASV217	1.000	2219	4.513E-04	Specialist	Sphingobium
ASV218	1.679	2140	1.279E-04	Intermediate	Hymenobacter

ASV219	2.857	1606	1.655E-04	Generalist	NA
ASV220	1.000	1606	4.814E-04	Specialist	Kineococcus
ASV221	1.000	1087	4.438E-04	Specialist	NA
ASV222	3.720	1992	1.354E-04	Generalist	Modestobacter
ASV223	3.498	437	1.053E-04	Generalist	Nakamurella
ASV224	1.000	1606	4.739E-04	Specialist	NA
ASV225	2.433	1087	2.558E-04	Generalist	Sphingomonas
ASV226	3.127	437	1.354E-04	Generalist	Massilia
ASV227	2.311	1992	3.084E-04	Generalist	Massilia
ASV228	1.658	2140	3.009E-04	Intermediate	Noviherbaspirillum
ASV229	1.000	2219	5.416E-04	Specialist	Pseudoxanthomonas
ASV230	1.000	1087	4.438E-04	Specialist	Myroides
ASV231	1.888	1087	2.332E-04	Intermediate	Marmoricola
ASV232	2.384	1992	2.558E-04	Generalist	Allorhizobium-Neorhizobium-Pararhizobium- Rhizobium
ASV233	3.850	1992	1.053E-04	Generalist	P3OB-42
ASV234	1.000	1992	5.266E-04	Specialist	NA
ASV235	2.323	1087	2.407E-04	Generalist	Nocardioides
ASV236	1.000	1087	4.363E-04	Specialist	Myroides
ASV237	2.619	2140	1.204E-04	Generalist	Novosphingobium
ASV238	2.896	1087	2.407E-04	Generalist	Terriglobus
ASV239	2.904	1606	2.257E-04	Generalist	Nakamurella
ASV241	1.407	1087	3.535E-04	Specialist	Nocardioides
ASV242	2.017	2219	3.084E-04	Intermediate	Sphingomonas
ASV243	1.683	1992	3.009E-04	Intermediate	Pseudomonas
ASV244	4.676	1087	1.128E-04	Generalist	Aurantimonas
ASV245	3.357	2219	1.655E-04	Generalist	Hymenobacter
ASV246	1.000	1992	4.814E-04	Specialist	Sphingomonas
ASV247	1.000	1992	4.814E-04	Specialist	1174-901-12
ASV248	1.856	1087	3.611E-04	Intermediate	Acidiphilium
ASV249	3.161	605	2.332E-04	Generalist	Abditibacterium
ASV250	3.675	1992	1.354E-04	Generalist	NA
ASV251	1.234	605	4.438E-04	Specialist	Corynebacterium

ASV252	1.000	2140	3.310E-04	Specialist	Methylobacterium-Methylorubrum
ASV253	1.000	1087	3.836E-04	Specialist	Planomicrobium
ASV254	1.787	2219	1.805E-04	Intermediate	Haemophilus
ASV255	1.614	2140	2.633E-04	Intermediate	Roseomonas
ASV256	1.140	2219	4.288E-04	Specialist	Chungangia
ASV258	1.000	1087	3.987E-04	Specialist	Endobacter
ASV259	1.125	2140	2.858E-04	Specialist	Spirosoma
ASV260	2.818	1992	1.354E-04	Generalist	Actinomyces
ASV261	1.000	437	3.460E-04	Specialist	NA
ASV262	1.000	1087	3.686E-04	Specialist	Frateuria
ASV263	1.085	1087	3.535E-04	Specialist	Amaricoccus
ASV264	2.678	1606	1.730E-04	Generalist	Nocardioides
ASV265	2.551	2219	1.580E-04	Generalist	Endobacter
ASV266	3.228	2140	2.106E-04	Generalist	Ellin6055
ASV267	1.000	1606	3.310E-04	Specialist	NA
ASV268	1.825	2219	1.655E-04	Intermediate	Hymenobacter
ASV269	1.933	2219	2.708E-04	Intermediate	Curtobacterium
ASV270	1.000	2140	3.084E-04	Specialist	Methylobacterium-Methylorubrum
ASV271	1.401	1087	2.031E-04	Specialist	Streptococcus
ASV272	3.644	1992	1.429E-04	Generalist	Granulicella
ASV273	1.735	2219	2.934E-04	Intermediate	Kineosporia
ASV274	1.000	1606	3.836E-04	Specialist	Spirosoma
ASV275	1.000	2219	2.708E-04	Specialist	Aureimonas
ASV276	1.000	2140	4.589E-04	Specialist	Subgroup 10
ASV277	2.196	1087	1.881E-04	Intermediate	Kocuria
ASV278	1.910	2219	2.106E-04	Intermediate	Methylobacterium-Methylorubrum
ASV279	1.000	2140	1.956E-04	Specialist	Sphingomonas
ASV280	1.000	1087	3.460E-04	Specialist	Mycobacterium
ASV281	1.000	1087	3.460E-04	Specialist	Sphingomonas
ASV282	1.981	1087	1.204E-04	Intermediate	Kocuria
ASV283	1.000	1087	3.385E-04	Specialist	Amaricoccus
ASV284	1.000	1087	3.385E-04	Specialist	Ornithinicoccus
ASV285	1.000	1087	3.385E-04	Specialist	NA

ASV286	3.215	2219	1.429E-04	Generalist	Corynebacterium
ASV287	1.000	1606	3.611E-04	Specialist	NA
ASV288	1.843	1606	1.956E-04	Intermediate	Paracoccus
ASV289	1.000	2140	2.858E-04	Specialist	Novosphingobium
ASV290	1.000	1087	3.310E-04	Specialist	Agromyces
ASV291	2.599	2140	1.204E-04	Generalist	Ramlibacter
ASV292	2.436	2140	1.580E-04	Generalist	Roseomonas
ASV293	1.000	1087	3.235E-04	Specialist	Bosea
ASV294	1.000	1087	3.235E-04	Specialist	Rothia
ASV295	3.139	1992	1.580E-04	Generalist	Pseudomonas
ASV296	1.000	1087	3.235E-04	Specialist	Pseudomonas
ASV297	2.413	437	1.053E-04	Generalist	Acidiphilium
ASV298	1.000	1606	3.235E-04	Specialist	NA
ASV299	2.840	1606	1.580E-04	Generalist	Actinomycetospora
ASV301	1.210	605	3.535E-04	Specialist	Pseudomonas
ASV302	1.000	1087	3.159E-04	Specialist	NA
ASV303	1.333	1087	2.633E-04	Specialist	Mycobacterium
ASV304	4.299	2219	1.053E-04	Generalist	Finegoldia
ASV305	1.434	1606	2.633E-04	Specialist	NA
ASV306	1.000	2140	2.934E-04	Specialist	Sphingomonas
ASV307	1.241	605	3.686E-04	Specialist	Rubrivirga
ASV308	1.000	1087	3.084E-04	Specialist	Hirschia
ASV309	1.446	1087	2.558E-04	Specialist	Gaiella
ASV310	2.566	1992	9.779E-05	Generalist	Pseudomonas
ASV311	2.367	2219	1.580E-04	Generalist	NA
ASV312	3.007	2219	1.128E-04	Generalist	Fibrella
ASV313	1.000	2219	3.686E-04	Specialist	Fonticella
ASV314	2.704	2140	1.279E-04	Generalist	Bryocella
ASV315	4.174	2219	5.266E-05	Generalist	Abditibacterium
ASV316	1.161	1087	2.783E-04	Specialist	NA
ASV317	2.000	1992	2.106E-04	Intermediate	Roseomonas
ASV318	1.986	1087	1.279E-04	Intermediate	Galbitalea
ASV319	1.000	437	2.783E-04	Specialist	Rhizorhapis

ASV320	1.984	1992	1.805E-04	Intermediate	Novosphingobium
ASV321	2.640	1087	1.429E-04	Generalist	Novosphingobium
ASV322	4.483	2219	9.779E-05	Generalist	NA
ASV323	1.682	1992	2.482E-04	Intermediate	Hymenobacter
ASV324	1.000	1087	4.363E-04	Specialist	NA
ASV325	1.000	1087	2.858E-04	Specialist	NA
ASV326	1.000	1087	4.288E-04	Specialist	Acinetobacter
ASV327	4.927	2140	5.266E-05	Generalist	NA
ASV328	1.000	1087	2.783E-04	Specialist	Sphingomonas
ASV329	1.000	1087	2.783E-04	Specialist	Chryseobacterium
ASV330	1.000	1087	2.783E-04	Specialist	Rubellimicrobium
ASV331	1.000	1087	2.407E-04	Specialist	Caenimonas
ASV332	2.870	1992	1.204E-04	Generalist	Novosphingobium
ASV333	2.299	1606	8.274E-05	Generalist	Roseomonas
ASV334	3.415	1087	1.279E-04	Generalist	Sphingomonas
ASV335	2.996	1606	9.779E-05	Generalist	NA
ASV336	2.822	605	1.429E-04	Generalist	Hymenobacter
ASV337	1.968	437	1.655E-04	Intermediate	Duganella
ASV338	1.742	1992	1.128E-04	Intermediate	Xylophilus
ASV339	2.455	2140	1.128E-04	Generalist	Kineococcus
ASV340	1.000	1087	2.708E-04	Specialist	Thermomonas
ASV341	1.239	2140	9.779E-05	Specialist	Pseudonocardia
ASV342	2.034	2219	1.805E-04	Intermediate	Sphingomonas
ASV343	1.994	1606	9.027E-05	Intermediate	Marmoricola
ASV344	3.013	2219	1.805E-04	Generalist	1174-901-12
ASV345	1.324	1087	2.708E-04	Specialist	Streptococcus
ASV346	1.000	2219	2.633E-04	Specialist	Brevundimonas
ASV347	3.967	1087	7.522E-05	Generalist	Nocardioides
ASV348	1.000	1087	2.633E-04	Specialist	NA
ASV349	1.410	1087	2.106E-04	Specialist	Aeromicrobium
ASV350	1.000	1606	2.858E-04	Specialist	Segetibacter
ASV351	1.146	1992	2.106E-04	Specialist	NA
ASV352	2.913	1606	1.279E-04	Generalist	Sphingomonas

ASV353	1.978	1087	1.580E-04	Intermediate	NA
ASV354	1.508	1992	2.482E-04	Intermediate	1174-901-12
ASV355	1.956	2219	1.730E-04	Intermediate	Abditibacterium
ASV356	1.000	1087	3.987E-04	Specialist	Oryzihumus
ASV357	1.486	437	2.031E-04	Specialist	Dyadobacter
ASV358	1.000	1087	2.633E-04	Specialist	Iamia
ASV359	1.000	1087	2.633E-04	Specialist	Demequina
ASV360	1.239	2219	2.482E-04	Specialist	Hymenobacter
ASV361	1.000	2140	2.181E-04	Specialist	Methylobacterium-Methylorubrum
ASV362	1.000	1087	2.558E-04	Specialist	NA
ASV363	1.443	1606	2.257E-04	Specialist	Hymenobacter
ASV364	1.000	2219	3.084E-04	Specialist	Georgenia
ASV365	1.000	605	1.053E-04	Specialist	Nocardioides
ASV366	1.000	1087	2.482E-04	Specialist	Xylophilus
ASV367	1.000	1087	2.482E-04	Specialist	Psychrobacter
ASV368	1.000	1087	2.482E-04	Specialist	Mycobacterium
ASV369	2.246	1087	1.204E-04	Intermediate	Flavobacterium
ASV371	2.625	1087	1.580E-04	Generalist	Allorhizobium-Neorhizobium-Pararhizobium- Rhizobium
ASV372	1.955	1606	1.429E-04	Intermediate	P3OB-42
ASV373	2.830	605	1.128E-04	Generalist	NA
ASV374	1.385	1606	2.257E-04	Specialist	Brevundimonas
ASV375	2.059	1087	1.805E-04	Intermediate	Pseudonocardia
ASV376	1.819	2140	1.429E-04	Intermediate	Acinetobacter
ASV377	2.351	2219	1.204E-04	Generalist	Hymenobacter
ASV378	1.153	437	2.934E-04	Specialist	Conyzicola
ASV379	1.280	437	1.881E-04	Specialist	Streptococcus
ASV380	1.000	1087	3.686E-04	Specialist	NA
ASV381	1.000	1087	2.407E-04	Specialist	Sphingomonas
ASV382	1.000	1087	2.407E-04	Specialist	NA
ASV383	2.905	1087	1.053E-04	Generalist	Klebsiella
ASV384	1.000	1992	2.558E-04	Specialist	Polaromonas
ASV385	2.541	437	7.522E-05	Generalist	Actinomycetospora

ASV386	2.138	2219	1.655E-04	Intermediate	Chryseobacterium
ASV387	1.000	2219	3.235E-04	Specialist	1174-901-12
ASV388	1.000	1992	2.858E-04	Specialist	1174-901-12
ASV389	2.445	1992	1.429E-04	Generalist	Corynebacterium
ASV390	2.170	437	1.805E-04	Intermediate	Kytococcus
ASV391	1.000	2219	2.934E-04	Specialist	Moheibacter
ASV392	1.000	2219	2.332E-04	Specialist	Sphingomonas
ASV393	2.626	1606	9.779E-05	Generalist	Amaricoccus
ASV394	2.941	1606	9.027E-05	Generalist	MN 122.2a
ASV395	2.524	1606	1.279E-04	Generalist	Nocardioides
ASV396	2.219	2140	9.779E-05	Intermediate	Huanghella
ASV397	2.716	2219	1.204E-04	Generalist	Massilia
ASV398	1.000	2219	2.858E-04	Specialist	Prevotella_7
ASV399	1.000	1087	3.460E-04	Specialist	Marmoricola
ASV400	1.000	437	2.106E-04	Specialist	NA
ASV401	1.000	1087	2.257E-04	Specialist	Oryzihumus
ASV402	1.000	1087	2.257E-04	Specialist	Novosphingobium
ASV403	1.000	1087	2.257E-04	Specialist	Actinoallomurus
ASV404	1.581	1087	1.053E-04	Intermediate	Hymenobacter
ASV405	1.000	2140	1.053E-04	Specialist	NA
ASV406	1.600	1992	2.031E-04	Intermediate	Corynebacterium
ASV407	4.588	2140	8.274E-05	Generalist	NA
ASV408	1.000	1087	2.181E-04	Specialist	Pedococcus-Phycococcus
ASV409	1.000	1087	1.730E-04	Specialist	Nocardioides
ASV410	1.942	2219	1.279E-04	Intermediate	Altererythrobacter
ASV411	1.618	1992	1.956E-04	Intermediate	NA
ASV412	1.000	1606	1.504E-04	Specialist	Corynebacterium
ASV413	1.000	1606	2.332E-04	Specialist	Rhizobacter
ASV414	1.000	1992	2.558E-04	Specialist	Amnibacterium
ASV415	1.000	1087	2.332E-04	Specialist	NA
ASV416	2.340	605	1.504E-04	Generalist	Nocardioides
ASV417	2.786	2219	1.053E-04	Generalist	Acinetobacter
ASV418	1.890	605	8.274E-05	Intermediate	Azohydromonas

ASV419	1.000	1087	3.310E-04	Specialist	Blautia
ASV420	1.000	1087	2.106E-04	Specialist	NA
ASV421	1.000	1087	2.106E-04	Specialist	Subtercola
ASV422	1.000	1087	2.106E-04	Specialist	NA
ASV423	1.000	1087	2.106E-04	Specialist	Halica
ASV424	2.576	605	8.274E-05	Generalist	NA
ASV425	1.000	2140	2.708E-04	Specialist	NA
ASV426	1.000	2140	2.257E-04	Specialist	NA
ASV427	1.454	2219	1.881E-04	Specialist	Kocuria
ASV428	1.000	2219	2.558E-04	Specialist	Clostridium sensu stricto 10
ASV429	1.000	2219	2.558E-04	Specialist	Geobacillus
ASV430	1.000	2140	2.106E-04	Specialist	NA
ASV431	1.000	437	1.956E-04	Specialist	Sphingomonas
ASV432	1.000	1087	2.106E-04	Specialist	Corynebacterium
ASV433	1.000	1087	2.106E-04	Specialist	NA
ASV434	1.000	1087	2.106E-04	Specialist	Hymenobacter
ASV435	2.362	2140	1.204E-04	Generalist	Sphingomonas
ASV436	1.748	2140	8.274E-05	Intermediate	NA
ASV437	1.000	1087	2.558E-04	Specialist	Sphingomonas
ASV438	1.923	1087	1.580E-04	Intermediate	Caulobacter
ASV439	1.780	1087	1.881E-04	Intermediate	Corynebacterium
ASV440	1.220	2219	2.031E-04	Specialist	Gaiella
ASV441	1.000	1087	3.084E-04	Specialist	Granulicella
ASV442	1.000	1087	3.084E-04	Specialist	Pseudomonas
ASV443	1.508	2219	9.027E-05	Intermediate	MN 122.2a
ASV444	1.492	437	1.429E-04	Specialist	Acidiphilium
ASV445	1.000	1087	2.031E-04	Specialist	Chryseobacterium
ASV446	2.504	1606	1.053E-04	Generalist	Hymenobacter
ASV447	2.796	437	7.522E-05	Generalist	Robbsia
ASV448	3.240	1992	8.274E-05	Generalist	Neisseria
ASV449	2.445	1087	6.770E-05	Generalist	Spirosoma
ASV450	1.000	1606	2.106E-04	Specialist	Rubellimicrobium
ASV451	1.845	1606	1.504E-04	Intermediate	Spirosoma

ASV452	1.293	2140	9.027E-05	Specialist	Cryobacterium
ASV453	1.000	1992	1.881E-04	Specialist	Methylobacterium-Methylorubrum
ASV454	1.000	2140	1.730E-04	Specialist	Ensifer
ASV455	1.000	2219	1.956E-04	Specialist	Sphingomonas
ASV456	2.594	1606	1.053E-04	Generalist	1174-901-12
ASV457	1.415	1087	9.027E-05	Specialist	Kineosporia
ASV458	1.000	1087	2.181E-04	Specialist	Paracoccus
ASV459	1.874	2219	1.279E-04	Intermediate	NA
ASV460	1.000	2140	2.332E-04	Specialist	Methylobacterium-Methylorubrum
ASV461	1.220	1992	2.031E-04	Specialist	Mucilaginibacter
ASV462	1.000	1992	2.332E-04	Specialist	NA
ASV463	1.600	1992	1.128E-04	Intermediate	Endobacter
ASV464	1.624	2219	1.128E-04	Intermediate	Sphingomonas
ASV465	1.000	2219	1.881E-04	Specialist	Rubellimicrobium
ASV466	2.904	1992	8.274E-05	Generalist	Polaromonas
ASV467	1.000	1087	1.881E-04	Specialist	Rubellimicrobium
ASV468	1.000	1087	1.881E-04	Specialist	Myroides
ASV469	1.715	1606	1.429E-04	Intermediate	Hymenobacter
ASV470	2.580	1606	6.018E-05	Generalist	Blastococcus
ASV471	2.300	2219	1.204E-04	Generalist	NA
ASV472	1.000	1606	1.956E-04	Specialist	Psychroglaciecola
ASV473	1.990	1606	1.128E-04	Intermediate	Modestobacter
ASV474	2.455	1606	9.027E-05	Generalist	Mucilaginibacter
ASV475	2.753	1606	8.274E-05	Generalist	Corynebacterium
ASV476	1.972	2140	1.053E-04	Intermediate	Subdoligranulum
ASV477	1.923	2219	7.522E-05	Intermediate	Pseudonocardia
ASV478	1.000	2219	2.257E-04	Specialist	Chelatococcus
ASV479	3.286	1606	7.522E-05	Generalist	Nocardioides
ASV480	2.195	1087	9.779E-05	Intermediate	Abditibacterium
ASV481	1.508	437	8.274E-05	Intermediate	Alloprevotella
ASV482	1.000	1087	1.805E-04	Specialist	Adhaeribacter
ASV483	1.000	1992	1.580E-04	Specialist	Sphingomonas
ASV484	1.986	1992	9.779E-05	Intermediate	NA

ASV485	1.000	2140	1.655E-04	Specialist	NA
ASV486	1.855	2140	9.027E-05	Intermediate	NA
ASV487	1.000	1087	1.730E-04	Specialist	Corynebacterium
ASV488	1.000	1087	1.730E-04	Specialist	Sphingomonas
ASV489	1.000	1087	1.730E-04	Specialist	Amaricoccus
ASV490	1.293	1087	1.504E-04	Specialist	Acinetobacter
ASV491	2.840	437	8.274E-05	Generalist	Rothia
ASV492	1.338	605	1.204E-04	Specialist	NA
ASV493	1.000	1087	1.805E-04	Specialist	Endobacter
ASV494	1.000	1992	2.031E-04	Specialist	Chryseobacterium
ASV495	1.000	1992	1.956E-04	Specialist	P3OB-42
ASV496	1.000	605	2.332E-04	Specialist	Hymenobacter
ASV497	1.000	605	2.332E-04	Specialist	Variovorax
ASV498	1.000	1087	2.633E-04	Specialist	NA
ASV499	1.658	437	6.770E-05	Intermediate	Brevundimonas
ASV500	2.793	2219	9.027E-05	Generalist	Acidiphilium
ASV501	1.000	1606	1.730E-04	Specialist	Sphingomonas
ASV502	1.000	1606	1.730E-04	Specialist	NA
ASV503	1.690	605	1.504E-04	Intermediate	Piscinibacter
ASV504	1.000	2140	2.106E-04	Specialist	Amantichitinum
ASV505	1.988	2219	1.053E-04	Intermediate	Hymenobacter
ASV506	1.280	437	1.580E-04	Specialist	Clostridium sensu stricto 13
ASV507	1.000	2219	2.031E-04	Specialist	Levilactobacillus
ASV508	1.000	2219	2.031E-04	Specialist	Tepidimonas
ASV509	1.000	605	2.257E-04	Specialist	Sphingomonas
ASV510	1.000	605	2.257E-04	Specialist	Amnibacterium
ASV511	1.000	1087	1.580E-04	Specialist	Streptomyces
ASV512	1.000	1087	1.580E-04	Specialist	Solirubrobacter
ASV513	1.742	437	9.027E-05	Intermediate	Hymenobacter
ASV514	1.855	605	6.018E-05	Intermediate	Bacillus
ASV515	1.000	1087	1.655E-04	Specialist	Prauserella
ASV516	1.800	2140	5.266E-05	Intermediate	Abditibacterium
ASV517	1.403	1606	1.429E-04	Specialist	Rubellimicrobium

ASV518	1.862	1606	1.053E-04	Intermediate	Kineosporia
ASV519	1.827	437	1.279E-04	Intermediate	Dietzia
ASV520	2.989	2219	6.018E-05	Generalist	Methylobacterium-Methylorubrum
ASV521	1.734	2219	1.204E-04	Intermediate	Paenibacillus
ASV522	1.000	2219	1.730E-04	Specialist	NA
ASV523	1.000	2219	1.730E-04	Specialist	Methylobacterium-Methylorubrum
ASV524	1.000	2219	1.730E-04	Specialist	Hansschlegelia
ASV525	1.665	1087	1.580E-04	Intermediate	Phenylobacterium
ASV526	1.000	2219	1.580E-04	Specialist	Brevundimonas
ASV527	1.208	1606	1.429E-04	Specialist	Acidipropionibacterium
ASV528	1.766	1992	6.018E-05	Intermediate	Sphingomonas
ASV529	1.000	1087	1.504E-04	Specialist	Pseudomonas
ASV530	1.742	2140	1.354E-04	Intermediate	Fronidhabitans
ASV531	1.960	1087	9.027E-05	Intermediate	Clostridium sensu stricto 1
ASV532	1.000	1606	1.655E-04	Specialist	Sphingomonas
ASV533	1.000	2140	1.504E-04	Specialist	P3OB-42
ASV534	1.000	2140	1.881E-04	Specialist	PMMR1
ASV535	1.000	1992	1.730E-04	Specialist	NA
ASV536	1.000	2219	9.779E-05	Specialist	Falsirhodobacter
ASV537	1.000	2140	1.279E-04	Specialist	Pedobacter
ASV538	1.980	2140	8.274E-05	Intermediate	Skermanella
ASV539	1.000	1087	2.332E-04	Specialist	NA
ASV540	1.000	1087	1.504E-04	Specialist	Hymenobacter
ASV541	1.000	1087	1.504E-04	Specialist	NA
ASV542	1.954	437	1.128E-04	Intermediate	Corynebacterium
ASV543	1.000	1087	1.504E-04	Specialist	Alteribacillus
ASV544	1.000	605	1.429E-04	Specialist	Noviherbaspirillum
ASV545	1.835	1606	9.779E-05	Intermediate	Rubellimicrobium
ASV546	1.835	1606	9.779E-05	Intermediate	Aerosphaera
ASV547	1.324	2219	1.354E-04	Specialist	Rubellimicrobium
ASV548	1.000	1606	1.580E-04	Specialist	Spirosoma
ASV549	1.000	1606	1.580E-04	Specialist	Devosia
ASV550	1.923	1992	1.128E-04	Intermediate	Devosia

ASV551	2.689	1992	7.522E-05	Generalist	Blautia
ASV552	1.967	1992	9.779E-05	Intermediate	Hymenobacter
ASV553	1.000	1992	1.730E-04	Specialist	NA
ASV554	1.541	2219	1.279E-04	Intermediate	Bifidobacterium
ASV555	1.000	2219	9.027E-05	Specialist	Bacteroides
ASV556	1.000	2219	1.580E-04	Specialist	Granulicella
ASV557	1.000	1087	1.655E-04	Specialist	Rothia
ASV558	1.000	2219	1.429E-04	Specialist	Devosia
ASV559	1.000	1087	2.181E-04	Specialist	Nocardioides
ASV560	1.000	1087	1.429E-04	Specialist	Acinetobacter
ASV561	1.000	1087	1.429E-04	Specialist	NA
ASV562	1.000	1087	1.429E-04	Specialist	Stenotrophomonas
ASV563	2.656	2140	6.018E-05	Generalist	Actinomyces
ASV564	2.418	1087	6.770E-05	Generalist	NA
ASV566	1.000	1606	1.504E-04	Specialist	Flavisolibacter
ASV567	1.342	2219	1.279E-04	Specialist	Williamsia
ASV568	2.384	1087	9.027E-05	Generalist	Pseudonocardia
ASV569	1.000	1087	1.580E-04	Specialist	Sphingomonas
ASV570	1.870	1087	9.027E-05	Intermediate	Hymenobacter
ASV571	1.761	2140	5.266E-05	Intermediate	Nocardioides
ASV572	1.569	1087	1.204E-04	Intermediate	Jatrophihabitans
ASV573	1.000	1087	9.779E-05	Specialist	Hymenobacter
ASV574	1.000	2140	1.429E-04	Specialist	Hymenobacter
ASV575	1.000	2140	1.504E-04	Specialist	NA
ASV576	1.000	2140	1.504E-04	Specialist	Quadrisphaera
ASV577	1.976	1992	7.522E-05	Intermediate	Acidiphilium
ASV578	1.000	1992	1.655E-04	Specialist	Endobacter
ASV579	1.000	1992	1.204E-04	Specialist	Bryocella
ASV580	1.724	2140	1.053E-04	Intermediate	Acinetobacter
ASV581	1.000	2219	1.730E-04	Specialist	NA
ASV582	1.000	2219	1.504E-04	Specialist	Rubellimicrobium
ASV583	1.000	2219	1.504E-04	Specialist	Pseudomonas
ASV584	1.000	605	1.881E-04	Specialist	NA

ASV585	1.000	1087	1.354E-04	Specialist	Kocuria
ASV586	1.835	1992	6.018E-05	Intermediate	Acidiphilium
ASV587	1.000	437	1.504E-04	Specialist	Abiotrophia
ASV588	1.000	1606	1.204E-04	Specialist	Flavobacterium
ASV589	1.000	1606	1.429E-04	Specialist	Gaiella
ASV590	1.000	605	9.779E-05	Specialist	Psychroglaciecola
ASV591	1.000	1992	1.279E-04	Specialist	NA
ASV593	1.000	1992	1.580E-04	Specialist	Spirosoma
ASV594	1.000	1992	1.580E-04	Specialist	Abditibacterium
ASV595	1.342	437	8.274E-05	Specialist	Anaerococcus
ASV596	1.000	2219	1.655E-04	Specialist	Timonella
ASV597	1.000	2219	1.429E-04	Specialist	Sphingomonas
ASV598	1.000	2219	1.429E-04	Specialist	Qipengyuania
ASV599	1.000	2219	1.429E-04	Specialist	Abditibacterium
ASV600	1.976	2140	7.522E-05	Intermediate	Hymenobacter
ASV601	1.000	2219	1.429E-04	Specialist	Sphingomonas
ASV602	1.000	2219	1.279E-04	Specialist	Defluviicoccus
ASV603	1.000	605	9.027E-05	Specialist	Hymenobacter
ASV604	1.642	2140	8.274E-05	Intermediate	Nakamurella
ASV605	1.000	1087	1.279E-04	Specialist	Sphingomonas
ASV606	1.000	1087	1.279E-04	Specialist	Solirubrobacter
ASV607	1.976	1087	7.522E-05	Intermediate	NA
ASV608	1.000	1606	1.128E-04	Specialist	MND1
ASV609	1.670	1992	9.779E-05	Intermediate	Pseudomonas
ASV610	1.000	1606	1.354E-04	Specialist	Craurococcus-Caldovatus
ASV611	1.690	605	1.128E-04	Intermediate	Haliangium
ASV612	1.000	2140	1.580E-04	Specialist	Bryobacter
ASV613	1.633	2219	1.053E-04	Intermediate	Mogibacterium
ASV614	1.000	2140	7.522E-05	Specialist	Spirosoma
ASV615	1.000	1606	1.279E-04	Specialist	NA
ASV616	1.000	1992	1.504E-04	Specialist	Acidiphilium
ASV617	1.000	2219	1.354E-04	Specialist	Nocardioides
ASV618	1.000	2140	1.053E-04	Specialist	NA

ASV619	1.000	2219	1.354E-04	Specialist	NA
ASV620	1.600	2140	9.027E-05	Intermediate	Aureimonas
ASV621	1.000	1087	1.204E-04	Specialist	NA
ASV622	1.800	1606	5.266E-05	Intermediate	Neisseria
ASV623	1.800	1992	9.027E-05	Intermediate	NA
ASV624	2.651	1606	6.018E-05	Generalist	Nocardioides
ASV625	1.000	1606	1.279E-04	Specialist	Hymenobacter
ASV626	1.835	1087	5.266E-05	Intermediate	NA
ASV627	1.000	1087	1.279E-04	Specialist	Kineosporia
ASV628	1.923	437	9.027E-05	Intermediate	Methylobacterium-Methylorubrum
ASV629	1.000	2140	1.504E-04	Specialist	NA
ASV630	1.000	1606	1.504E-04	Specialist	NA
ASV631	1.000	2219	1.279E-04	Specialist	Roseomonas
ASV632	1.000	605	1.580E-04	Specialist	Arthrobacter
ASV633	1.000	1087	1.128E-04	Specialist	Lysobacter
ASV634	1.000	1087	1.128E-04	Specialist	Acidiphilium
ASV635	1.000	1087	1.128E-04	Specialist	Shewanella
ASV637	1.800	2140	7.522E-05	Intermediate	Novosphingobium
ASV639	1.000	1087	1.128E-04	Specialist	Kribbella
ASV640	1.000	1606	9.779E-05	Specialist	Quadrisphaera
ASV641	1.923	2140	6.770E-05	Intermediate	Methylobacterium-Methylorubrum
ASV642	1.600	1606	9.027E-05	Intermediate	Streptococcus
ASV643	1.000	1992	1.730E-04	Specialist	Corynebacterium
ASV644	1.000	1087	1.204E-04	Specialist	Pajaroellobacter
ASV645	1.000	1087	1.204E-04	Specialist	Huanghella
ASV646	2.945	1087	5.266E-05	Generalist	Rubrivirga
ASV647	1.000	2140	1.429E-04	Specialist	Massilia
ASV648	1.841	1087	8.274E-05	Intermediate	Paenarthrobacter
ASV649	1.301	2140	5.266E-05	Specialist	Fibrella
ASV650	1.923	1992	6.770E-05	Intermediate	NA
ASV651	1.000	1992	1.354E-04	Specialist	1174-901-12
ASV652	1.000	1992	1.354E-04	Specialist	Spirosoma
ASV653	1.000	2140	1.053E-04	Specialist	Hymenobacter

ASV654	1.000	2219	1.354E-04	Specialist	NA
ASV655	1.000	2219	1.354E-04	Specialist	Ethanoligenens
ASV656	1.000	2219	1.354E-04	Specialist	Tepidiphilus
ASV657	1.000	2219	1.204E-04	Specialist	NA
ASV658	1.000	2219	1.204E-04	Specialist	Staphylococcus
ASV659	1.000	2219	1.204E-04	Specialist	Capnocytophaga
ASV660	1.000	605	1.429E-04	Specialist	Leucobacter
ASV661	1.000	2140	9.779E-05	Specialist	Sphingomonas
ASV662	1.000	2140	9.779E-05	Specialist	NA
ASV663	1.000	1087	1.053E-04	Specialist	Iamia
ASV664	1.000	1992	1.128E-04	Specialist	Sphingomonas
ASV665	1.753	437	8.274E-05	Intermediate	Aggregatibacter
ASV666	1.000	1606	9.779E-05	Specialist	Nocardioides
ASV667	1.849	1606	6.770E-05	Intermediate	Microvirga
ASV668	1.841	605	8.274E-05	Intermediate	Acidiphilium
ASV669	1.000	2219	6.770E-05	Specialist	NA
ASV670	1.000	1606	1.128E-04	Specialist	NA
ASV671	1.000	2219	1.429E-04	Specialist	Endobacter
ASV672	1.000	1087	1.128E-04	Specialist	P3OB-42
ASV673	1.000	1087	1.128E-04	Specialist	NA
ASV674	1.000	1992	6.018E-05	Specialist	Nocardioides
ASV675	1.000	1606	1.053E-04	Specialist	NA
ASV676	1.000	1992	1.279E-04	Specialist	Conexibacter
ASV677	1.000	2219	1.204E-04	Specialist	Chryseobacterium
ASV678	1.000	2219	1.204E-04	Specialist	Limosilactobacillus
ASV679	1.000	2140	9.027E-05	Specialist	Endobacter
ASV680	1.000	605	1.279E-04	Specialist	NA
ASV681	1.000	2219	1.053E-04	Specialist	Hymenobacter
ASV682	1.000	2219	1.053E-04	Specialist	Mycobacterium
ASV683	1.000	1606	9.027E-05	Specialist	Caedibacter
ASV684	1.562	605	9.779E-05	Intermediate	Leucobacter
ASV685	1.000	605	9.779E-05	Specialist	NA
ASV686	1.000	437	1.279E-04	Specialist	Hymenobacter

ASV687	1.000	1087	1.053E-04	Specialist	Anaerococcus
ASV688	1.969	605	6.770E-05	Intermediate	NA
ASV690	1.991	2219	6.018E-05	Intermediate	NA
ASV691	1.000	1606	1.053E-04	Specialist	Domibacillus
ASV692	1.000	1606	1.053E-04	Specialist	NA
ASV693	1.000	1087	1.128E-04	Specialist	Corynebacterium
ASV694	1.923	437	6.770E-05	Intermediate	Hymenobacter
ASV695	1.899	1087	6.018E-05	Intermediate	Prevotella_7
ASV696	1.923	1992	6.770E-05	Intermediate	Hymenobacter
ASV697	1.882	605	7.522E-05	Intermediate	Porphyromonas
ASV698	1.000	1087	1.279E-04	Specialist	Aurantisolimonas
ASV699	2.000	1087	6.018E-05	Intermediate	NA
ASV700	1.993	605	6.018E-05	Intermediate	NA
ASV701	1.800	437	9.027E-05	Intermediate	Abditibacterium
ASV702	1.000	2140	1.204E-04	Specialist	Blastococcus
ASV703	1.000	1992	1.204E-04	Specialist	Methylopila
ASV704	1.000	1992	1.204E-04	Specialist	Chryseobacterium
ASV705	1.000	437	1.128E-04	Specialist	NA
ASV706	1.000	437	1.279E-04	Specialist	Aurantimonas
ASV707	1.000	2219	1.128E-04	Specialist	Sphingomonas
ASV708	1.000	605	1.354E-04	Specialist	Marmoricola
ASV709	1.000	2140	1.053E-04	Specialist	Brachybacterium
ASV710	1.000	2140	9.779E-05	Specialist	P3OB-42
ASV711	1.000	2140	8.274E-05	Specialist	Microvirga
ASV712	1.000	2140	8.274E-05	Specialist	NA
ASV713	1.000	2219	1.128E-04	Specialist	Hymenobacter
ASV714	1.000	2140	8.274E-05	Specialist	Mucilaginibacter
ASV715	1.000	2140	8.274E-05	Specialist	Sphingomonas
ASV716	1.000	1087	1.504E-04	Specialist	Nocardioides
ASV717	1.550	1087	7.522E-05	Intermediate	Dyadobacter
ASV718	1.000	1087	9.027E-05	Specialist	Candidatus Alysiosphaera
ASV719	2.528	437	6.018E-05	Generalist	NA
ASV720	1.000	2219	1.128E-04	Specialist	Bacillus

ASV721	1.000	2219	1.128E-04	Specialist	Nocardioides
ASV722	1.000	1606	8.274E-05	Specialist	Sphingobium
ASV723	1.800	605	7.522E-05	Intermediate	Lactobacillus
ASV724	1.988	1992	5.266E-05	Intermediate	Halomonas
ASV725	1.000	1606	9.779E-05	Specialist	Psychroglaciacola
ASV726	1.000	1606	9.779E-05	Specialist	Rhizorhapis
ASV727	1.000	605	9.779E-05	Specialist	Craurococcus-Caldovatus
ASV728	1.000	1087	1.053E-04	Specialist	Altererythrobacter
ASV729	1.000	1087	7.522E-05	Specialist	Roseomonas
ASV730	1.000	1992	1.429E-04	Specialist	Catenuloplanes
ASV731	1.000	2140	1.204E-04	Specialist	P3OB-42
ASV732	1.000	437	6.770E-05	Specialist	Hymenobacter
ASV733	1.849	2140	6.770E-05	Intermediate	Pajaroellobacter
ASV734	1.753	605	8.274E-05	Intermediate	Ellin6055
ASV735	1.000	2140	1.128E-04	Specialist	NA
ASV736	1.000	2140	1.128E-04	Specialist	Butyricoccus
ASV737	1.969	605	6.770E-05	Intermediate	Abditibacterium
ASV738	1.508	1992	8.274E-05	Intermediate	Blastococcus
ASV739	1.000	2140	9.027E-05	Specialist	Spirillospora
ASV740	1.000	2140	9.027E-05	Specialist	Aureimonas
ASV741	1.562	1992	9.779E-05	Intermediate	NA
ASV742	1.000	2219	1.053E-04	Specialist	Ruminococcus
ASV743	1.000	2140	9.779E-05	Specialist	Hymenobacter
ASV744	1.000	2140	8.274E-05	Specialist	Cnuella
ASV745	1.000	2140	4.513E-05	Specialist	Herbiconiux
ASV746	1.000	2219	9.779E-05	Specialist	Marisediminicola
ASV747	1.000	605	1.204E-04	Specialist	Leucobacter
ASV748	1.000	2140	8.274E-05	Specialist	NA
ASV749	1.000	2140	8.274E-05	Specialist	NA
ASV750	1.000	1087	1.429E-04	Specialist	Pseudoclavibacter
ASV751	1.000	1087	8.274E-05	Specialist	Ornithinimicrobium
ASV752	1.800	1087	6.018E-05	Intermediate	Agathobacter
ASV753	1.000	437	8.274E-05	Specialist	Sphingomonas

ASV754	1.988	437	5.266E-05	Intermediate	NA
ASV755	1.000	605	8.274E-05	Specialist	Cedecea
ASV756	1.000	1992	9.027E-05	Specialist	NA
ASV758	1.000	1087	7.522E-05	Specialist	1174-901-12
ASV759	1.984	2140	4.513E-05	Intermediate	Paucibacter
ASV760	1.000	1606	7.522E-05	Specialist	Sphingomonas
ASV761	1.000	1606	7.522E-05	Specialist	Aureimonas
ASV762	1.000	1606	7.522E-05	Specialist	Adhaeribacter
ASV763	1.000	605	8.274E-05	Specialist	Paracoccus
ASV764	1.000	605	9.779E-05	Specialist	NA
ASV765	1.000	1606	9.027E-05	Specialist	NA
ASV766	1.000	1606	9.027E-05	Specialist	Dyella
ASV767	1.000	1606	9.027E-05	Specialist	NA
ASV768	1.000	1606	9.027E-05	Specialist	Sphingomonas
ASV769	1.899	1606	6.018E-05	Intermediate	NA
ASV771	1.000	1087	9.779E-05	Specialist	NA
ASV772	1.000	2219	1.204E-04	Specialist	Larkinella
ASV773	1.642	1992	8.274E-05	Intermediate	Granulicella
ASV774	1.000	2140	7.522E-05	Specialist	Haemophilus
ASV775	1.000	1087	9.027E-05	Specialist	Acidiphilium
ASV776	1.000	1087	9.027E-05	Specialist	1174-901-12
ASV777	1.000	1087	9.027E-05	Specialist	NA
ASV778	1.000	1087	1.053E-04	Specialist	Granulicella
ASV779	1.324	605	9.027E-05	Specialist	Ferruginibacter
ASV780	1.000	1992	9.779E-05	Specialist	NA
ASV781	1.000	1992	9.779E-05	Specialist	Pseudolabrys
ASV782	1.000	2140	1.053E-04	Specialist	Bacteroides
ASV783	1.000	2140	1.053E-04	Specialist	Mycobacterium
ASV784	1.000	2140	1.053E-04	Specialist	Rhizobacter
ASV785	1.000	1992	9.779E-05	Specialist	Acidiphilium
ASV786	1.000	2140	8.274E-05	Specialist	NA
ASV787	1.000	2140	8.274E-05	Specialist	Defluviicoccus
ASV788	1.000	2140	8.274E-05	Specialist	Spirosoma

ASV789	1.000	2219	9.779E-05	Specialist	Brevibacterium
ASV790	1.000	2219	9.779E-05	Specialist	P3OB-42
ASV791	1.000	2219	1.053E-04	Specialist	NA
ASV792	1.000	605	1.128E-04	Specialist	Abditibacterium
ASV793	1.000	605	1.128E-04	Specialist	Hymenobacter
ASV794	1.000	605	1.128E-04	Specialist	NA
ASV795	1.000	2140	9.027E-05	Specialist	Corynebacterium
ASV796	1.000	2140	7.522E-05	Specialist	NA
ASV797	1.000	2140	7.522E-05	Specialist	NA
ASV798	1.000	605	1.053E-04	Specialist	NA
ASV799	1.000	2219	9.027E-05	Specialist	Quadrisphaera
ASV800	1.000	2219	8.274E-05	Specialist	Spirosoma
ASV801	1.000	2219	8.274E-05	Specialist	NA
ASV802	1.000	437	7.522E-05	Specialist	Aurantisolimonas
ASV803	1.000	437	7.522E-05	Specialist	NA
ASV804	1.000	605	7.522E-05	Specialist	Methylobacterium-Methylorubrum
ASV805	1.000	1992	8.274E-05	Specialist	Bdellovibrio
ASV806	2.000	1992	4.513E-05	Intermediate	Abditibacterium
ASV808	2.778	1087	3.009E-05	Generalist	Lactococcus
ASV809	1.000	1606	7.522E-05	Specialist	Nocardioides
ASV810	1.000	1606	7.522E-05	Specialist	NA
ASV811	1.000	605	9.027E-05	Specialist	Nordella
ASV812	1.000	605	9.027E-05	Specialist	NA
ASV813	1.000	2219	6.770E-05	Specialist	P3OB-42
ASV814	1.000	1606	8.274E-05	Specialist	Solirubrobacter
ASV815	1.000	1606	8.274E-05	Specialist	Actinomycetospora
ASV816	1.000	1606	8.274E-05	Specialist	Psychroglaciecola
ASV817	1.000	605	6.770E-05	Specialist	Gemmatimonas
ASV818	1.000	1087	9.027E-05	Specialist	Solirubrobacter
ASV819	1.000	2219	1.053E-04	Specialist	NA
ASV820	1.000	1992	1.204E-04	Specialist	Conexibacter
ASV821	1.000	1087	8.274E-05	Specialist	Dermacoccus
ASV822	1.000	1087	8.274E-05	Specialist	NA

ASV823	1.000	1087	9.779E-05	Specialist	Ellin6055
ASV824	1.550	1087	7.522E-05	Intermediate	Abditibacterium
ASV825	1.000	2140	1.053E-04	Specialist	Prauserella
ASV826	1.899	2140	6.018E-05	Intermediate	Streptococcus
ASV827	1.000	1992	8.274E-05	Specialist	Sphingomonas
ASV828	2.000	1992	4.513E-05	Intermediate	Sphingobacterium
ASV829	1.000	2140	8.274E-05	Specialist	Sphingaurantiacus
ASV830	1.000	2140	8.274E-05	Specialist	Rhabdobacter
ASV831	1.000	2140	8.274E-05	Specialist	Actinoplanes
ASV832	1.000	2140	8.274E-05	Specialist	Hymenobacter
ASV833	1.000	2140	9.779E-05	Specialist	Marmoricola
ASV834	1.000	1992	9.779E-05	Specialist	1174-901-12
ASV835	1.000	1992	9.779E-05	Specialist	NA
ASV836	1.000	437	9.027E-05	Specialist	Marisediminicola
ASV837	1.000	437	1.053E-04	Specialist	PMMR1
ASV838	1.000	2219	9.027E-05	Specialist	Nocardioides
ASV839	1.000	2219	9.779E-05	Specialist	Caldibacillus
ASV840	1.000	2219	9.779E-05	Specialist	Proteiniphilum
ASV841	1.000	2219	9.027E-05	Specialist	Aliidongia
ASV842	1.000	2219	9.027E-05	Specialist	Hymenobacter
ASV843	1.000	605	1.053E-04	Specialist	Cellulomonas
ASV844	1.000	2140	6.770E-05	Specialist	NA
ASV845	1.000	2140	6.770E-05	Specialist	NA
ASV846	1.000	605	9.779E-05	Specialist	Sphingobium
ASV847	1.000	2219	8.274E-05	Specialist	Clostridium sensu stricto 1
ASV848	1.000	2219	7.522E-05	Specialist	Hymenobacter
ASV849	1.000	1087	6.770E-05	Specialist	NA
ASV850	1.000	1992	7.522E-05	Specialist	NA
ASV851	2.000	1992	2.257E-05	Intermediate	Caulobacter
ASV852	1.000	437	6.770E-05	Specialist	Sphingomonas
ASV853	1.724	1606	5.266E-05	Intermediate	Ferruginibacter
ASV854	2.632	437	3.761E-05	Generalist	Gemella
ASV855	1.000	2219	9.027E-05	Specialist	Hymenobacter

ASV856	1.000	1606	6.770E-05	Specialist	Rhizobacter
ASV857	1.000	1606	6.770E-05	Specialist	Methylobacterium-Methylorubrum
ASV858	1.000	1606	6.770E-05	Specialist	Acinetobacter
ASV859	1.000	1606	3.761E-05	Specialist	Sediminibacterium
ASV860	1.000	1606	3.009E-05	Specialist	Pseudomonas
ASV861	1.000	1606	7.522E-05	Specialist	Sphingomonas
ASV862	1.000	1606	7.522E-05	Specialist	NA
ASV863	1.000	1606	7.522E-05	Specialist	Nitrospira
ASV864	1.000	1992	1.128E-04	Specialist	NA
ASV865	1.000	1087	7.522E-05	Specialist	Amaricoccus
ASV866	1.000	1087	7.522E-05	Specialist	Melittangium
ASV867	1.000	1087	7.522E-05	Specialist	Sphingomonas
ASV868	1.000	605	9.027E-05	Specialist	Pseudonocardia
ASV870	1.000	1087	9.027E-05	Specialist	Sphingomonas
ASV871	1.000	1087	9.027E-05	Specialist	Clavibacter
ASV872	1.000	1087	9.027E-05	Specialist	Hymenobacter
ASV873	1.000	2140	9.027E-05	Specialist	NA
ASV874	2.000	2140	3.761E-05	Intermediate	Dyadobacter
ASV875	1.000	2140	7.522E-05	Specialist	NA
ASV876	1.000	2140	7.522E-05	Specialist	Sphingomonas
ASV877	1.000	2140	7.522E-05	Specialist	Craurococcus-Caldovatus
ASV878	1.000	2140	7.522E-05	Specialist	NA
ASV879	1.000	2140	7.522E-05	Specialist	NA
ASV880	1.000	1992	8.274E-05	Specialist	Hymenobacter
ASV881	1.000	1992	6.770E-05	Specialist	Solirubrobacter
ASV882	1.000	2140	9.027E-05	Specialist	[Eubacterium] siraeum group
ASV883	1.000	2140	9.027E-05	Specialist	Rhizorhapis
ASV884	1.000	2140	9.027E-05	Specialist	NA
ASV885	1.000	1992	9.027E-05	Specialist	Nocardioides
ASV886	1.000	1992	9.027E-05	Specialist	Sphingomonas
ASV887	1.000	1992	9.027E-05	Specialist	NA
ASV888	1.923	1992	4.513E-05	Intermediate	Brevibacillus
ASV889	1.000	1992	8.274E-05	Specialist	NA

ASV890	1.923	2219	4.513E-05	Intermediate	Melittangium
ASV891	1.000	1606	8.274E-05	Specialist	P3OB-42
ASV892	1.000	1606	8.274E-05	Specialist	Nocardioides
ASV894	1.000	437	9.779E-05	Specialist	Spirosoma
ASV895	1.000	2219	9.027E-05	Specialist	Schlegelella
ASV896	1.000	2219	8.274E-05	Specialist	Rubellimicrobium
ASV898	1.000	2219	8.274E-05	Specialist	Coprococcus
ASV899	1.000	2140	6.770E-05	Specialist	NA
ASV900	1.000	2140	6.018E-05	Specialist	Roseomonas
ASV901	1.000	2140	6.018E-05	Specialist	Muricoccus
ASV902	1.000	2140	6.018E-05	Specialist	Sphingomonas
ASV903	1.000	2219	7.522E-05	Specialist	Sphingomonas
ASV904	1.000	2219	8.274E-05	Specialist	Amnibacterium
ASV905	1.000	2219	8.274E-05	Specialist	Caedibacter
ASV906	1.000	2219	7.522E-05	Specialist	Stenotrophomonas
ASV907	1.000	2219	7.522E-05	Specialist	Fibrella
ASV908	1.000	437	8.274E-05	Specialist	1174-901-12
ASV909	1.000	1087	1.128E-04	Specialist	NA
ASV910	1.000	437	4.513E-05	Specialist	Arcticibacter
ASV911	1.000	1087	6.770E-05	Specialist	Pseudomonas
ASV912	1.000	1087	5.266E-05	Specialist	Staphylococcus
ASV913	1.000	437	8.274E-05	Specialist	NA
ASV914	1.000	1606	6.018E-05	Specialist	NA
ASV915	1.000	1606	6.018E-05	Specialist	NA
ASV916	1.000	1606	6.018E-05	Specialist	Methylobacterium-Methylorubrum
ASV917	1.000	1606	6.018E-05	Specialist	Rubellimicrobium
ASV918	1.000	1606	6.018E-05	Specialist	NA
ASV919	1.976	1606	3.761E-05	Intermediate	Rothia
ASV920	1.000	605	7.522E-05	Specialist	Microvirga
ASV921	1.000	1606	6.770E-05	Specialist	Sphingomonas
ASV922	1.000	1606	6.770E-05	Specialist	OM27 clade
ASV923	1.000	1606	6.770E-05	Specialist	Acidothermus
ASV924	1.000	1606	6.770E-05	Specialist	Thermoactinomyces

ASV925	1.000	1606	6.770E-05	Specialist	NA
ASV926	1.000	605	6.770E-05	Specialist	Sphingomonas
ASV927	1.000	1087	7.522E-05	Specialist	Defluviicoccus
ASV928	1.000	2219	9.027E-05	Specialist	Actinomycetospora
ASV929	1.000	1992	1.053E-04	Specialist	NA
ASV930	1.000	1087	6.770E-05	Specialist	1174-901-12
ASV931	1.000	1087	8.274E-05	Specialist	Spirosoma
ASV932	1.000	1087	8.274E-05	Specialist	Hymenobacter
ASV933	1.000	1087	8.274E-05	Specialist	NA
ASV934	2.000	1992	3.761E-05	Intermediate	Collinsella
ASV935	1.000	2140	6.770E-05	Specialist	NA
ASV936	1.000	2140	6.770E-05	Specialist	Hymenobacter
ASV937	1.000	2140	6.770E-05	Specialist	Iamia
ASV938	1.000	2140	6.770E-05	Specialist	Pajaroellobacter
ASV939	1.000	1992	7.522E-05	Specialist	Hyphomicrobium
ASV940	1.000	1992	6.018E-05	Specialist	Citricoccus
ASV941	1.000	2140	8.274E-05	Specialist	Sphingomonas
ASV942	1.000	1606	8.274E-05	Specialist	NA
ASV943	1.000	1992	8.274E-05	Specialist	Micromonospora
ASV944	1.000	437	7.522E-05	Specialist	Prevotella_9
ASV945	1.000	437	5.266E-05	Specialist	NA
ASV946	1.000	2140	6.018E-05	Specialist	Sphingomonas
ASV947	1.000	2140	6.018E-05	Specialist	Methylobacterium-Methylorubrum
ASV948	1.000	1606	7.522E-05	Specialist	Terriglobus
ASV949	1.000	437	9.027E-05	Specialist	Neomicrococcus
ASV950	1.000	2219	8.274E-05	Specialist	Actinomycetospora
ASV951	1.000	2219	8.274E-05	Specialist	Prevotella_7
ASV952	1.000	2219	7.522E-05	Specialist	Acidibacter
ASV953	1.000	437	8.274E-05	Specialist	NA
ASV954	1.000	605	9.027E-05	Specialist	Ferruginibacter
ASV955	1.000	605	9.027E-05	Specialist	Sphingaurantiacus
ASV956	1.000	605	9.027E-05	Specialist	Bryobacter
ASV957	1.000	2140	7.522E-05	Specialist	NA

ASV958	1.000	2140	6.018E-05	Specialist	Novosphingobium
ASV960	1.000	1087	7.522E-05	Specialist	Ellin6055
ASV961	1.000	1087	7.522E-05	Specialist	NA
ASV962	1.000	605	8.274E-05	Specialist	Oligoflexus
ASV963	1.000	605	8.274E-05	Specialist	Nocardioides
ASV964	1.000	605	8.274E-05	Specialist	Solirubrobacter
ASV965	1.000	605	8.274E-05	Specialist	Sphingomonas
ASV966	1.000	2219	6.770E-05	Specialist	Abditibacterium
ASV967	1.000	2219	6.770E-05	Specialist	NA
ASV968	1.000	2219	6.770E-05	Specialist	Streptomyces
ASV969	1.000	605	8.274E-05	Specialist	Vagococcus
ASV970	1.000	605	8.274E-05	Specialist	NA
ASV971	1.000	437	7.522E-05	Specialist	Qipengyuania
ASV972	1.000	2140	6.018E-05	Specialist	Nocardioides
ASV973	1.000	1087	6.018E-05	Specialist	Clostridium sensu stricto 1
ASV974	2.000	1087	3.009E-05	Intermediate	Peptoniphilus
ASV976	1.000	1992	6.018E-05	Specialist	NA
ASV977	1.000	1992	6.018E-05	Specialist	NA
ASV978	1.000	437	5.266E-05	Specialist	Rhodoferax
ASV979	1.000	437	5.266E-05	Specialist	Cellulomonas
ASV980	1.000	437	5.266E-05	Specialist	Hymenobacter
ASV981	1.000	605	6.018E-05	Specialist	Pajaroellobacter
ASV982	1.976	1087	3.761E-05	Intermediate	NA
ASV983	1.000	1992	6.018E-05	Specialist	Acinetobacter
ASV984	1.000	1992	6.018E-05	Specialist	Amnibacterium
ASV985	1.528	2140	5.266E-05	Intermediate	Spirosoma
ASV986	1.000	437	6.770E-05	Specialist	Capnocytophaga
ASV987	1.000	437	4.513E-05	Specialist	Gardnerella
ASV988	1.000	1087	6.018E-05	Specialist	Allorhizobium-Neorhizobium-Pararhizobium- Rhizobium
ASV989	1.000	2219	7.522E-05	Specialist	NA
ASV990	1.000	1606	5.266E-05	Specialist	Granulicatella
ASV991	1.000	1606	5.266E-05	Specialist	Devosia

ASV992	1.000	1606	5.266E-05	Specialist	Brevundimonas
ASV993	1.000	605	6.770E-05	Specialist	NA
ASV994	1.000	605	6.770E-05	Specialist	Abditibacterium
ASV995	1.000	1606	6.018E-05	Specialist	Gaiella
ASV996	1.800	2219	3.009E-05	Intermediate	NA
ASV997	1.000	1606	6.018E-05	Specialist	NA
ASV998	1.000	1606	6.018E-05	Specialist	Rhodovarius
ASV999	1.000	605	6.018E-05	Specialist	Gaiella
ASV1000	1.000	2140	5.266E-05	Specialist	Amaricoccus
ASV1001	1.000	1087	6.018E-05	Specialist	Sphingomonas
ASV1002	1.000	1087	6.018E-05	Specialist	Nakamurella
ASV1003	1.000	1087	6.018E-05	Specialist	NA
ASV1004	1.000	1087	6.018E-05	Specialist	Huanghella
ASV1005	1.000	1087	6.018E-05	Specialist	Sphingomonas
ASV1006	1.000	1087	6.018E-05	Specialist	NA
ASV1007	1.000	1087	6.018E-05	Specialist	Limnobacter
ASV1008	1.000	2219	6.770E-05	Specialist	Ligilactobacillus
ASV1009	1.000	2140	7.522E-05	Specialist	NA
ASV1010	1.000	2140	7.522E-05	Specialist	NA
ASV1011	1.000	1992	6.770E-05	Specialist	Pseudomonas
ASV1012	1.000	2140	6.770E-05	Specialist	NA
ASV1013	1.000	2140	6.770E-05	Specialist	Blautia
ASV1014	1.000	2140	6.770E-05	Specialist	Sphingomonas
ASV1015	1.000	1992	6.770E-05	Specialist	Hymenobacter
ASV1016	1.000	1992	6.770E-05	Specialist	P3OB-42
ASV1017	1.000	1992	5.266E-05	Specialist	Streptosporangium
ASV1018	1.000	1606	7.522E-05	Specialist	Spirosoma
ASV1019	1.000	1606	7.522E-05	Specialist	NA
ASV1020	1.000	1992	7.522E-05	Specialist	Pseudonocardia
ASV1021	1.000	1992	7.522E-05	Specialist	Pedobacter
ASV1022	1.000	1606	5.266E-05	Specialist	Cellulosimicrobium
ASV1023	1.000	2140	5.266E-05	Specialist	NA
ASV1024	1.000	1606	6.770E-05	Specialist	Hymenobacter

ASV1025	1.000	1606	6.770E-05	Specialist	Solirubrobacter
ASV1026	1.000	1606	6.770E-05	Specialist	Monoglobus
ASV1027	1.000	437	7.522E-05	Specialist	Marmoricola
ASV1028	1.000	437	7.522E-05	Specialist	NA
ASV1029	1.000	2219	6.770E-05	Specialist	Flavisolibacter
ASV1030	1.000	2219	6.770E-05	Specialist	Carnobacterium
ASV1031	1.000	2219	6.770E-05	Specialist	Ruminococcus
ASV1032	1.000	2219	6.770E-05	Specialist	Aureimonas
ASV1033	1.724	605	5.266E-05	Intermediate	Corynebacterium
ASV1034	1.000	605	8.274E-05	Specialist	NA
ASV1035	1.000	605	8.274E-05	Specialist	NA
ASV1036	1.000	605	8.274E-05	Specialist	Abditibacterium
ASV1037	1.000	605	8.274E-05	Specialist	NA
ASV1038	1.000	2140	5.266E-05	Specialist	Edaphobaculum
ASV1039	1.000	2140	5.266E-05	Specialist	NA
ASV1040	1.000	2140	5.266E-05	Specialist	NA
ASV1041	1.000	2140	5.266E-05	Specialist	Paenibacillus
ASV1042	1.000	1087	6.770E-05	Specialist	Methylorosula
ASV1043	1.000	1087	6.770E-05	Specialist	Parviterribacter
ASV1044	1.000	1087	6.770E-05	Specialist	Acidibacter
ASV1045	1.000	1087	6.770E-05	Specialist	Polymorphobacter
ASV1046	1.000	605	7.522E-05	Specialist	NA
ASV1048	1.000	2219	6.770E-05	Specialist	Sphingourantiacus
ASV1049	1.882	2219	3.761E-05	Intermediate	Frederiksenia
ASV1050	1.000	1606	5.266E-05	Specialist	Nocardioides
ASV1051	1.000	1606	5.266E-05	Specialist	Abditibacterium
ASV1052	1.000	605	7.522E-05	Specialist	Bacillus
ASV1053	1.000	1992	4.513E-05	Specialist	NA
ASV1054	1.000	1992	4.513E-05	Specialist	Pseudomonas
ASV1055	1.000	2140	5.266E-05	Specialist	NA
ASV1056	1.000	1087	9.027E-05	Specialist	Acidibacter
ASV1057	1.000	437	5.266E-05	Specialist	Acidiphilium
ASV1058	1.000	437	5.266E-05	Specialist	NA

ASV1059	1.000	605	5.266E-05	Specialist	Amaricoccus
ASV1060	1.000	605	5.266E-05	Specialist	P3OB-42
ASV1061	1.000	605	5.266E-05	Specialist	Sphingomonas
ASV1062	1.882	1087	3.761E-05	Intermediate	Agathobacter
ASV1063	1.000	1087	5.266E-05	Specialist	NA
ASV1064	1.000	437	6.018E-05	Specialist	Prevotella
ASV1065	1.000	437	6.018E-05	Specialist	Corynebacterium
ASV1066	1.000	437	6.018E-05	Specialist	Corynebacterium
ASV1067	1.000	2219	6.770E-05	Specialist	NA
ASV1068	2.000	2219	3.009E-05	Intermediate	Dolosigranulum
ASV1069	1.000	1606	4.513E-05	Specialist	Jatrophihabitans
ASV1070	1.000	1606	4.513E-05	Specialist	NA
ASV1071	1.000	1606	4.513E-05	Specialist	Chitinophaga
ASV1072	1.000	605	6.018E-05	Specialist	Flavobacterium
ASV1073	1.000	605	6.018E-05	Specialist	NA
ASV1074	1.000	1606	5.266E-05	Specialist	Gemmatimonas
ASV1075	1.000	1606	5.266E-05	Specialist	Ohtaekwangia
ASV1076	1.000	1606	6.018E-05	Specialist	Spirosoma
ASV1077	1.976	2219	3.761E-05	Intermediate	NA
ASV1078	1.000	1087	6.018E-05	Specialist	Allorhizobium-Neorhizobium-Pararhizobium- Rhizobium
ASV1079	1.000	1087	6.018E-05	Specialist	Kineosporia
ASV1080	1.000	1087	6.018E-05	Specialist	NA
ASV1081	1.000	1087	6.018E-05	Specialist	NA
ASV1082	1.000	1087	6.018E-05	Specialist	Acidiphilium
ASV1083	1.000	1087	6.018E-05	Specialist	NA
ASV1085	1.000	605	6.770E-05	Specialist	Qipengyuania
ASV1086	1.000	605	6.770E-05	Specialist	Romboutsia
ASV1087	1.000	1087	6.770E-05	Specialist	NA
ASV1088	1.000	2140	6.770E-05	Specialist	NA
ASV1089	1.000	2140	6.770E-05	Specialist	Gemmatimonas
ASV1090	1.000	1992	6.018E-05	Specialist	Fusobacterium
ASV1091	1.000	2140	6.018E-05	Specialist	Sphingobium

ASV1092	1.000	2140	6.018E-05	Specialist	Saccharibacillus
ASV1093	1.000	2140	6.018E-05	Specialist	NA
ASV1094	1.000	1992	4.513E-05	Specialist	Hymenobacter
ASV1095	1.000	1992	4.513E-05	Specialist	Phenyllobacterium
ASV1096	1.000	2140	6.770E-05	Specialist	NA
ASV1097	1.000	1606	6.770E-05	Specialist	Jatrophihabitans
ASV1098	1.000	1606	6.770E-05	Specialist	Nocardioides
ASV1099	1.000	1992	6.018E-05	Specialist	NA
ASV1100	1.000	1992	6.018E-05	Specialist	Hymenobacter
ASV1101	1.000	1992	6.018E-05	Specialist	Bdellovibrio
ASV1102	1.000	1606	4.513E-05	Specialist	NA
ASV1103	1.000	1606	4.513E-05	Specialist	NA
ASV1104	1.000	1992	6.018E-05	Specialist	alphaI cluster
ASV1105	1.000	1992	6.018E-05	Specialist	NA
ASV1106	1.000	437	6.018E-05	Specialist	Rheinheimera
ASV1107	1.000	2140	5.266E-05	Specialist	Hymenobacter
ASV1108	1.000	1606	6.018E-05	Specialist	Pseudoxanthomonas
ASV1109	1.000	1606	6.018E-05	Specialist	Chryseobacterium
ASV1110	1.000	437	6.770E-05	Specialist	Dyadobacter
ASV1111	1.000	437	6.770E-05	Specialist	Paracoccus
ASV1112	1.000	2219	6.018E-05	Specialist	Flavobacterium
ASV1113	1.000	2219	6.018E-05	Specialist	Flavobacterium
ASV1114	1.000	2219	6.018E-05	Specialist	Rubroacter
ASV1115	1.000	437	6.018E-05	Specialist	Fusicatenibacter
ASV1116	1.000	605	6.770E-05	Specialist	Buchnera
ASV1117	1.000	605	6.770E-05	Specialist	Ellin6055
ASV1118	1.000	605	6.770E-05	Specialist	Arenimonas
ASV1119	1.000	605	6.770E-05	Specialist	Solirubroacter
ASV1120	1.000	2140	6.018E-05	Specialist	Prevotella
ASV1121	1.000	2140	5.266E-05	Specialist	Roseburia
ASV1122	1.000	2140	4.513E-05	Specialist	Endobacter
ASV1123	1.000	2140	4.513E-05	Specialist	Haliangium
ASV1124	1.000	2140	4.513E-05	Specialist	Qipengyuania

ASV1126	1.000	1087	6.018E-05	Specialist	Actinomycetospora
ASV1127	1.000	1087	6.018E-05	Specialist	Hymenobacter
ASV1128	1.000	605	6.770E-05	Specialist	NA
ASV1129	1.000	605	6.770E-05	Specialist	Bryobacter
ASV1130	1.000	605	6.770E-05	Specialist	Sphingomonas
ASV1131	1.000	605	6.770E-05	Specialist	Rubellimicrobium
ASV1132	1.000	605	6.770E-05	Specialist	Sphingomonas
ASV1133	1.000	605	6.770E-05	Specialist	Hymenobacter
ASV1134	1.000	2219	5.266E-05	Specialist	Ferruginibacter
ASV1135	1.000	1606	4.513E-05	Specialist	NA
ASV1136	1.000	1992	4.513E-05	Specialist	Pseudomonas
ASV1137	1.000	437	6.018E-05	Specialist	Arenimonas
ASV1138	1.000	2140	4.513E-05	Specialist	NA
ASV1139	1.000	1087	4.513E-05	Specialist	NA
ASV1140	1.000	437	4.513E-05	Specialist	Aurantimonas
ASV1141	1.000	437	4.513E-05	Specialist	Acidiphilium
ASV1142	1.000	437	4.513E-05	Specialist	Paenisporosarcina
ASV1143	1.800	437	3.009E-05	Intermediate	Sphingomonas
ASV1144	2.000	437	2.257E-05	Intermediate	Anaerococcus
ASV1145	1.000	1087	5.266E-05	Specialist	Nocardioides
ASV1146	1.000	1992	5.266E-05	Specialist	Bdellovibrio
ASV1147	1.000	437	5.266E-05	Specialist	Porphyromonas
ASV1148	1.000	437	5.266E-05	Specialist	[Eubacterium] brachy group
ASV1149	1.000	437	6.018E-05	Specialist	NA
ASV1150	1.000	437	6.018E-05	Specialist	Hymenobacter
ASV1151	2.000	437	2.257E-05	Intermediate	Nannocystis
ASV1152	1.000	2219	6.018E-05	Specialist	Flavobacterium
ASV1153	1.000	1606	4.513E-05	Specialist	Nocardioides
ASV1154	1.000	1606	4.513E-05	Specialist	NA
ASV1155	1.000	605	6.018E-05	Specialist	Skermanella
ASV1156	1.000	605	5.266E-05	Specialist	Spirosoma
ASV1157	1.000	605	5.266E-05	Specialist	Sphingomonas
ASV1158	1.000	1606	4.513E-05	Specialist	NA

ASV1159	1.000	1606	4.513E-05	Specialist	Stomatobaculum
ASV1160	1.000	1606	4.513E-05	Specialist	Nakamurella
ASV1161	1.000	2219	6.018E-05	Specialist	NA
ASV1162	1.000	1606	5.266E-05	Specialist	Romboutsia
ASV1163	1.000	1606	5.266E-05	Specialist	NA
ASV1164	1.000	1606	5.266E-05	Specialist	Aurantisolimonas
ASV1165	1.000	605	5.266E-05	Specialist	Chryseobacterium
ASV1166	1.000	2219	6.018E-05	Specialist	Rubellimicrobium
ASV1167	1.000	1087	5.266E-05	Specialist	NA
ASV1168	1.000	1087	5.266E-05	Specialist	Roseomonas
ASV1169	1.000	1087	5.266E-05	Specialist	NA
ASV1170	1.000	605	5.266E-05	Specialist	Lactobacillus
ASV1171	1.000	605	5.266E-05	Specialist	Luteibacter
ASV1172	1.000	1087	6.018E-05	Specialist	Hymenobacter
ASV1173	1.000	1087	6.018E-05	Specialist	Kineosporia
ASV1174	1.000	1087	6.018E-05	Specialist	Ramlibacter
ASV1175	1.000	2140	6.018E-05	Specialist	NA
ASV1176	1.000	2140	6.018E-05	Specialist	NA
ASV1177	1.000	1992	5.266E-05	Specialist	Peptoniphilus
ASV1178	1.000	437	5.266E-05	Specialist	Acidiphilium
ASV1179	1.000	437	5.266E-05	Specialist	Chryseobacterium
ASV1180	1.000	2140	3.761E-05	Specialist	Spirosoma
ASV1181	1.000	1992	5.266E-05	Specialist	NA
ASV1182	1.000	1992	3.761E-05	Specialist	Hymenobacter
ASV1183	1.000	1992	3.761E-05	Specialist	Pedosphaera
ASV1184	1.000	1606	4.513E-05	Specialist	Nocardioides
ASV1186	1.000	1606	4.513E-05	Specialist	NA
ASV1187	1.000	2140	6.018E-05	Specialist	Nocardioides
ASV1188	1.000	2140	6.018E-05	Specialist	Sphingomonas
ASV1189	1.000	2140	6.018E-05	Specialist	Parabacteroides
ASV1190	1.000	1606	6.018E-05	Specialist	Solirubrobacter
ASV1191	1.000	1992	5.266E-05	Specialist	Marmoricola
ASV1192	1.000	1992	5.266E-05	Specialist	Sphingomonas

ASV1193	1.000	1606	4.513E-05	Specialist	Nocardioides
ASV1194	1.000	1992	5.266E-05	Specialist	P3OB-42
ASV1195	1.000	1992	5.266E-05	Specialist	Terriglobus
ASV1196	1.000	2140	4.513E-05	Specialist	Hyphomicrobium
ASV1197	1.000	1606	5.266E-05	Specialist	Nocardioides
ASV1198	1.000	437	6.018E-05	Specialist	NA
ASV1199	1.000	2219	6.018E-05	Specialist	Lactobacillus
ASV1201	1.000	605	6.018E-05	Specialist	NA
ASV1202	1.000	605	6.018E-05	Specialist	NA
ASV1203	1.000	605	6.018E-05	Specialist	Marmoricola
ASV1204	1.000	605	6.018E-05	Specialist	Gulbenkiania
ASV1205	1.000	2140	3.761E-05	Specialist	Edaphobaculum
ASV1206	1.000	2140	3.761E-05	Specialist	NA
ASV1207	1.000	2140	3.761E-05	Specialist	NA
ASV1208	1.000	2140	3.761E-05	Specialist	Alloprevotella
ASV1209	1.000	1087	5.266E-05	Specialist	Mesorhizobium
ASV1210	1.000	1087	5.266E-05	Specialist	Sphingomonas
ASV1211	1.000	1087	5.266E-05	Specialist	NA
ASV1212	1.000	1087	5.266E-05	Specialist	NA
ASV1213	1.000	1087	5.266E-05	Specialist	Actinomyces
ASV1214	1.000	605	6.018E-05	Specialist	Rathayibacter
ASV1215	1.000	2219	5.266E-05	Specialist	Pedobacter
ASV1216	1.000	2219	5.266E-05	Specialist	NA
ASV1217	1.000	1606	3.761E-05	Specialist	Sphingomonas
ASV1218	1.000	605	6.018E-05	Specialist	Paenibacillus
ASV1219	1.000	605	6.018E-05	Specialist	Aureimonas
ASV1220	1.000	605	6.018E-05	Specialist	Leuconostoc
ASV1221	1.000	605	6.018E-05	Specialist	NA
ASV1222	1.000	2140	3.761E-05	Specialist	Lachnoanaerobaculum
ASV1223	1.000	2140	3.761E-05	Specialist	NA
ASV1224	1.000	2140	3.761E-05	Specialist	Amaricoccus
ASV1225	1.000	2140	3.761E-05	Specialist	Hymenobacter
ASV1226	1.000	1087	3.761E-05	Specialist	Glutamicibacter

ASV1227	1.000	1992	3.761E-05	Specialist	Flavobacterium
ASV1228	1.000	437	3.761E-05	Specialist	1174-901-12
ASV1229	1.000	605	3.761E-05	Specialist	NA
ASV1230	1.000	605	3.761E-05	Specialist	NA
ASV1231	1.000	605	3.761E-05	Specialist	Rubellimicrobium
ASV1232	1.000	605	3.761E-05	Specialist	Streptococcus
ASV1233	1.000	1087	4.513E-05	Specialist	Pseudomonas
ASV1234	1.000	1087	4.513E-05	Specialist	Pseudoclavibacter
ASV1235	1.000	1087	3.761E-05	Specialist	Iamia
ASV1236	1.000	1087	3.761E-05	Specialist	NA
ASV1238	1.000	1992	4.513E-05	Specialist	NA
ASV1239	1.000	1087	3.009E-05	Specialist	NA
ASV1240	1.000	437	4.513E-05	Specialist	Prevotella
ASV1241	1.000	437	4.513E-05	Specialist	Alloprevotella
ASV1242	1.000	437	5.266E-05	Specialist	Endobacter
ASV1243	1.000	437	5.266E-05	Specialist	Nocardioides
ASV1244	1.000	1087	3.761E-05	Specialist	Devosia
ASV1245	1.000	2219	5.266E-05	Specialist	Anaerococcus
ASV1246	1.000	2219	5.266E-05	Specialist	Methylobacterium-Methylorubrum
ASV1247	1.000	2219	5.266E-05	Specialist	Kineococcus
ASV1248	1.000	1606	3.761E-05	Specialist	Xanthomonas
ASV1249	1.000	1606	3.761E-05	Specialist	Frigoribacterium
ASV1250	1.000	1606	3.761E-05	Specialist	Solirubrobacter
ASV1251	1.000	1606	3.761E-05	Specialist	Herpetosiphon
ASV1252	1.000	1606	3.761E-05	Specialist	Nocardioides
ASV1253	1.000	605	3.761E-05	Specialist	Quadrisphaera
ASV1254	1.000	605	3.761E-05	Specialist	Steroidobacter
ASV1255	1.000	605	3.761E-05	Specialist	Novosphingobium
ASV1256	1.000	605	3.761E-05	Specialist	NA
ASV1257	1.000	605	5.266E-05	Specialist	Nocardioides
ASV1258	1.000	605	4.513E-05	Specialist	Nocardioides
ASV1259	1.000	605	4.513E-05	Specialist	NA
ASV1260	1.000	605	4.513E-05	Specialist	NA

ASV1261	1.000	605	4.513E-05	Specialist	NA
ASV1262	1.000	605	4.513E-05	Specialist	NA
ASV1263	1.000	1606	3.761E-05	Specialist	Marmoricola
ASV1264	1.000	1606	3.761E-05	Specialist	Rhodopseudomonas
ASV1265	1.000	2219	5.266E-05	Specialist	NA
ASV1267	1.000	1606	3.761E-05	Specialist	Lachnospiraceae NK4A136 group
ASV1268	1.000	605	4.513E-05	Specialist	NA
ASV1269	1.000	1087	4.513E-05	Specialist	Pseudonocardia
ASV1270	1.000	1087	4.513E-05	Specialist	Flavobacterium
ASV1271	1.000	2140	3.761E-05	Specialist	Oryzihumus
ASV1272	1.000	2140	3.761E-05	Specialist	Conexibacter
ASV1273	1.000	2140	3.761E-05	Specialist	NA
ASV1274	1.000	1992	6.018E-05	Specialist	Phaselicystis
ASV1275	1.000	1992	6.018E-05	Specialist	Bdellovibrio
ASV1276	1.000	1087	4.513E-05	Specialist	NA
ASV1277	1.000	1087	4.513E-05	Specialist	Granulicella
ASV1278	1.000	605	4.513E-05	Specialist	Nocardioides
ASV1279	1.000	605	4.513E-05	Specialist	NA
ASV1280	1.000	605	4.513E-05	Specialist	Spirosoma
ASV1281	1.000	605	4.513E-05	Specialist	Haliangium
ASV1282	1.000	2219	4.513E-05	Specialist	Nocardioides
ASV1283	1.000	2140	5.266E-05	Specialist	Sphingomonas
ASV1284	1.000	1992	4.513E-05	Specialist	Corynebacterium
ASV1285	1.000	1992	4.513E-05	Specialist	NA
ASV1286	1.000	437	4.513E-05	Specialist	NA
ASV1287	1.000	437	4.513E-05	Specialist	NA
ASV1288	1.000	2140	4.513E-05	Specialist	Sphingomonas
ASV1289	1.000	1992	4.513E-05	Specialist	Nocardioides
ASV1290	1.000	1992	4.513E-05	Specialist	Sphingomonas
ASV1291	1.000	1992	3.761E-05	Specialist	Hymenobacter
ASV1292	1.000	1992	3.761E-05	Specialist	NA
ASV1293	1.000	1992	3.761E-05	Specialist	NA
ASV1294	1.000	1992	3.761E-05	Specialist	NA

ASV1295	1.000	1992	3.761E-05	Specialist	Roseomonas
ASV1296	1.000	1992	3.761E-05	Specialist	Bdellovibrio
ASV1298	1.000	1606	3.761E-05	Specialist	Abditibacterium
ASV1299	1.000	1606	3.761E-05	Specialist	NA
ASV1300	1.000	2140	5.266E-05	Specialist	Hymenobacter
ASV1301	1.000	1606	5.266E-05	Specialist	Piscinibacter
ASV1302	1.000	1992	4.513E-05	Specialist	NA
ASV1303	1.000	1992	4.513E-05	Specialist	NA
ASV1304	1.000	1606	3.761E-05	Specialist	Solirubrobacter
ASV1305	1.000	1992	4.513E-05	Specialist	Granulicella
ASV1306	1.000	1992	4.513E-05	Specialist	NA
ASV1307	1.000	437	4.513E-05	Specialist	Alcanivorax
ASV1308	1.000	2140	3.761E-05	Specialist	MN 122.2a
ASV1309	1.000	2140	3.761E-05	Specialist	Jeotgalicoccus
ASV1310	1.000	2140	3.761E-05	Specialist	Spirosoma
ASV1311	1.000	1606	4.513E-05	Specialist	Nocardioides
ASV1312	1.000	1606	4.513E-05	Specialist	NA
ASV1313	1.000	1606	4.513E-05	Specialist	Bdellovibrio
ASV1314	1.000	1606	4.513E-05	Specialist	Haemophilus
ASV1315	1.000	437	5.266E-05	Specialist	Hymenobacter
ASV1316	1.000	1992	6.018E-05	Specialist	NA
ASV1317	1.000	437	5.266E-05	Specialist	Methylobacterium-Methylorubrum
ASV1318	1.000	437	5.266E-05	Specialist	Spirosoma
ASV1319	1.000	437	5.266E-05	Specialist	Salinimicrobium
ASV1320	1.000	2219	4.513E-05	Specialist	Bacteroides
ASV1321	1.000	2219	4.513E-05	Specialist	NA
ASV1322	1.000	2219	4.513E-05	Specialist	NA
ASV1323	1.000	2219	4.513E-05	Specialist	Rubellimicrobium
ASV1324	1.000	605	5.266E-05	Specialist	Sphingomonas
ASV1325	1.000	605	5.266E-05	Specialist	Pedobacter
ASV1326	1.000	605	5.266E-05	Specialist	Pedomicrobium
ASV1327	1.000	2140	4.513E-05	Specialist	Flavobacterium
ASV1328	1.000	2140	3.761E-05	Specialist	Hyphomicrobium

ASV1329	1.000	2140	3.761E-05	Specialist	Pedobacter
ASV1330	1.000	1087	3.761E-05	Specialist	Sphingomonas
ASV1333	1.000	1087	4.513E-05	Specialist	Nakamurella
ASV1334	1.000	1087	4.513E-05	Specialist	Devosia
ASV1335	1.000	605	5.266E-05	Specialist	Gaiella
ASV1336	1.000	1606	3.761E-05	Specialist	Marmoricola
ASV1337	1.000	605	5.266E-05	Specialist	Sphingomonas
ASV1338	1.000	605	5.266E-05	Specialist	NA
ASV1339	1.000	1992	3.009E-05	Specialist	Endobacter
ASV1340	1.000	2140	3.761E-05	Specialist	Psychroglaciecola
ASV1342	1.000	1087	3.009E-05	Specialist	Chthonobacter
ASV1343	1.000	1992	3.009E-05	Specialist	Fibrella
ASV1344	1.000	437	3.009E-05	Specialist	Sphingomonas
ASV1345	1.000	605	3.009E-05	Specialist	Longimicrobium
ASV1346	1.000	605	3.009E-05	Specialist	Rubellimicrobium
ASV1347	1.000	605	3.009E-05	Specialist	Sphingomonas
ASV1348	1.000	605	3.009E-05	Specialist	NA
ASV1349	1.000	1087	3.761E-05	Specialist	Dorea
ASV1350	1.923	1087	2.257E-05	Intermediate	Bacteroides
ASV1351	1.000	1992	3.761E-05	Specialist	1174-901-12
ASV1352	1.000	1992	3.761E-05	Specialist	Roseomonas
ASV1353	1.000	1087	3.009E-05	Specialist	Thiobacillus
ASV1354	1.000	1087	3.009E-05	Specialist	NA
ASV1355	1.000	1087	3.009E-05	Specialist	Brevibacterium
ASV1356	1.000	437	3.761E-05	Specialist	Lautropia
ASV1357	1.000	437	3.761E-05	Specialist	Sphingomonas
ASV1358	1.000	2219	3.761E-05	Specialist	NA
ASV1359	1.000	1606	3.009E-05	Specialist	Nocardioides
ASV1360	1.000	1606	3.009E-05	Specialist	Sphingomonas
ASV1361	1.000	1606	3.009E-05	Specialist	Roseomonas
ASV1362	1.000	605	3.009E-05	Specialist	NA
ASV1363	1.000	605	3.761E-05	Specialist	NA
ASV1364	1.000	605	3.761E-05	Specialist	Cellulomonas

ASV1365	1.000	605	3.761E-05	Specialist	Actinoallomurus
ASV1366	1.000	605	3.761E-05	Specialist	Iamia
ASV1367	1.000	1606	3.009E-05	Specialist	NA
ASV1368	1.000	1606	3.009E-05	Specialist	Corynebacterium
ASV1369	1.000	1606	3.009E-05	Specialist	Psychroglaciecola
ASV1370	1.000	2219	4.513E-05	Specialist	NA
ASV1371	1.000	605	3.761E-05	Specialist	Marmoricola
ASV1372	1.000	605	3.761E-05	Specialist	Hymenobacter
ASV1373	1.000	605	3.761E-05	Specialist	Psychroglaciecola
ASV1374	1.000	605	3.761E-05	Specialist	Rubellimicrobium
ASV1375	1.000	605	3.761E-05	Specialist	Segetibacter
ASV1376	1.000	605	3.761E-05	Specialist	Iamia
ASV1377	1.000	2219	4.513E-05	Specialist	Novosphingobium
ASV1379	1.000	2219	4.513E-05	Specialist	Acinetobacter
ASV1381	1.000	1087	3.761E-05	Specialist	NA
ASV1382	1.000	1087	3.761E-05	Specialist	Pajaroellobacter
ASV1383	1.000	605	3.761E-05	Specialist	Bryocella
ASV1384	1.000	605	3.761E-05	Specialist	Bdellovibrio
ASV1385	1.000	2219	3.761E-05	Specialist	UCG-002
ASV1386	1.000	2219	3.761E-05	Specialist	Sphingomonas
ASV1387	1.000	1087	4.513E-05	Specialist	Mucilaginibacter
ASV1388	1.000	2140	4.513E-05	Specialist	NA
ASV1389	1.000	2140	4.513E-05	Specialist	Novosphingobium
ASV1390	1.000	2140	4.513E-05	Specialist	Candidatus Trichorickettsia
ASV1391	1.000	2140	4.513E-05	Specialist	Knoellia
ASV1392	1.000	2140	4.513E-05	Specialist	Hydrogenophaga
ASV1393	1.000	2140	4.513E-05	Specialist	Lacibacter
ASV1394	1.000	2140	4.513E-05	Specialist	NA
ASV1395	1.000	2140	4.513E-05	Specialist	NA
ASV1396	1.000	1992	3.761E-05	Specialist	Azospirillum
ASV1397	1.000	1992	3.761E-05	Specialist	NA
ASV1398	1.000	1992	3.761E-05	Specialist	Pajaroellobacter
ASV1399	1.000	1992	3.009E-05	Specialist	Hymenobacter

ASV1401	1.000	1606	3.761E-05	Specialist	Jatrophihabitans
ASV1402	1.000	1606	3.761E-05	Specialist	UCG-002
ASV1403	1.000	1606	3.761E-05	Specialist	Ellin6067
ASV1405	1.000	437	4.513E-05	Specialist	Altererythrobacter
ASV1406	1.000	2140	3.761E-05	Specialist	NA
ASV1407	1.000	2140	3.761E-05	Specialist	Hyphomicrobium
ASV1408	1.000	1606	3.761E-05	Specialist	Tardiphaga
ASV1409	1.000	1992	3.761E-05	Specialist	Williamsia
ASV1410	1.000	1992	3.761E-05	Specialist	NA
ASV1411	1.000	1992	3.761E-05	Specialist	NA
ASV1412	1.000	1992	3.761E-05	Specialist	Solirubrobacter
ASV1413	1.000	1992	3.761E-05	Specialist	1174-901-12
ASV1414	1.000	1992	3.761E-05	Specialist	Paracoccus
ASV1415	1.000	437	3.761E-05	Specialist	Anaerococcus
ASV1416	1.000	2140	3.009E-05	Specialist	Actibacter
ASV1417	1.000	2140	3.761E-05	Specialist	Bryocella
ASV1418	1.000	1606	3.761E-05	Specialist	NA
ASV1419	1.000	1606	3.761E-05	Specialist	Hymenobacter
ASV1420	1.000	1606	3.761E-05	Specialist	NA
ASV1421	1.000	1606	3.761E-05	Specialist	Marmoricola
ASV1422	1.000	1992	5.266E-05	Specialist	Prevotella
ASV1423	1.000	1992	5.266E-05	Specialist	Spirosoma
ASV1424	1.000	1992	5.266E-05	Specialist	NA
ASV1425	1.000	1992	5.266E-05	Specialist	P3OB-42
ASV1426	1.000	437	4.513E-05	Specialist	Spirosoma
ASV1427	1.000	437	4.513E-05	Specialist	Pseudomonas
ASV1428	1.000	2219	3.761E-05	Specialist	Starkeya
ASV1429	1.000	2219	3.761E-05	Specialist	NA
ASV1430	1.000	2219	3.761E-05	Specialist	Paenibacillus
ASV1431	1.000	2219	3.761E-05	Specialist	NA
ASV1432	1.000	2219	3.761E-05	Specialist	Wolinella
ASV1433	1.000	437	3.761E-05	Specialist	Asticcacaulis
ASV1434	1.000	437	3.761E-05	Specialist	Pseudomonas

ASV1435	1.000	437	3.761E-05	Specialist	NA
ASV1436	1.000	437	3.761E-05	Specialist	Ellin6055
ASV1437	1.000	1606	3.009E-05	Specialist	NA
ASV1438	1.000	605	4.513E-05	Specialist	Hymenobacter
ASV1439	1.000	605	4.513E-05	Specialist	NA
ASV1440	1.000	605	4.513E-05	Specialist	Flavobacterium
ASV1441	1.000	605	4.513E-05	Specialist	NA
ASV1442	1.000	605	4.513E-05	Specialist	YC-ZSS-LKJ147
ASV1443	1.000	2140	3.009E-05	Specialist	Aeromicrobium
ASV1444	1.000	2140	3.009E-05	Specialist	NA
ASV1445	1.000	2140	3.009E-05	Specialist	Chryseobacterium
ASV1446	1.000	2140	3.009E-05	Specialist	PMMR1
ASV1449	1.000	1087	3.761E-05	Specialist	NA
ASV1450	1.000	1087	3.761E-05	Specialist	Streptomyces
ASV1451	1.000	1087	3.761E-05	Specialist	NA
ASV1452	1.000	1087	3.761E-05	Specialist	Ferruginibacter
ASV1453	1.000	1087	3.761E-05	Specialist	CL500-29 marine group
ASV1454	1.000	605	3.761E-05	Specialist	Spirosoma
ASV1455	1.000	605	3.761E-05	Specialist	NA
ASV1456	1.000	605	3.761E-05	Specialist	Segetibacter
ASV1457	1.000	605	3.761E-05	Specialist	Acidiphilium
ASV1458	1.000	2219	3.761E-05	Specialist	Motilibacter
ASV1459	1.000	1606	3.009E-05	Specialist	Rubroacter
ASV1460	1.000	605	4.513E-05	Specialist	Oryzihumus
ASV1461	1.000	605	4.513E-05	Specialist	Nakamurella
ASV1462	1.000	605	4.513E-05	Specialist	NA
ASV1463	1.000	605	4.513E-05	Specialist	Microvirga
ASV1464	1.000	605	4.513E-05	Specialist	Hymenobacter
ASV1465	1.000	605	4.513E-05	Specialist	Kineosporia
ASV1466	1.000	1992	3.009E-05	Specialist	Hymenobacter
ASV1467	1.000	2140	3.009E-05	Specialist	NA
ASV1468	1.000	2140	3.009E-05	Specialist	NA
ASV1469	1.000	2140	3.009E-05	Specialist	Hymenobacter

ASV1470	1.000	1087	5.266E-05	Specialist	Serratia
ASV1471	1.000	1087	2.257E-05	Specialist	Jatrophihabitans
ASV1472	1.000	1992	2.257E-05	Specialist	Prevotella_7
ASV1473	1.000	1992	2.257E-05	Specialist	NA
ASV1474	1.000	437	2.257E-05	Specialist	Nocardioides
ASV1475	1.000	437	2.257E-05	Specialist	Flavobacterium
ASV1476	1.000	437	2.257E-05	Specialist	Micrococcus
ASV1477	1.000	437	2.257E-05	Specialist	Pedobacter
ASV1478	1.000	437	2.257E-05	Specialist	1174-901-12
ASV1479	1.000	605	2.257E-05	Specialist	Alteribacillus
ASV1480	1.000	1087	3.009E-05	Specialist	YC-ZSS-LKJ147
ASV1481	1.000	1087	3.009E-05	Specialist	Ilumatobacter
ASV1482	1.000	1087	3.009E-05	Specialist	NA
ASV1483	1.000	1087	3.009E-05	Specialist	Ornithinibacter
ASV1484	1.000	1087	3.009E-05	Specialist	Staphylococcus
ASV1485	1.000	1992	3.009E-05	Specialist	NA
ASV1486	1.000	1992	3.009E-05	Specialist	Polymorphobacter
ASV1487	1.000	437	3.009E-05	Specialist	Blastococcus
ASV1488	1.000	437	3.009E-05	Specialist	Alloprevotella
ASV1489	1.000	437	3.009E-05	Specialist	NA
ASV1490	1.000	437	3.009E-05	Specialist	NA
ASV1491	1.000	437	3.009E-05	Specialist	Bergeyella
ASV1492	1.000	437	3.761E-05	Specialist	Piscinibacter
ASV1493	1.000	437	3.761E-05	Specialist	Flavisolibacter
ASV1494	1.000	437	3.761E-05	Specialist	Sphingomonas
ASV1495	1.000	2219	3.009E-05	Specialist	Modestobacter
ASV1496	1.000	1606	2.257E-05	Specialist	Rhodococcus
ASV1497	1.000	1606	2.257E-05	Specialist	Streptacidiphilus
ASV1498	1.000	605	2.257E-05	Specialist	Nocardioides
ASV1499	1.000	605	2.257E-05	Specialist	Phytohabitans
ASV1500	1.000	605	3.761E-05	Specialist	Abditibacterium
ASV1501	1.000	1606	3.009E-05	Specialist	Nocardioides
ASV1502	1.000	1606	3.009E-05	Specialist	Lactobacillus

ASV1503	1.000	2219	3.761E-05	Specialist	Granulicatella
ASV1504	1.000	2219	3.761E-05	Specialist	NA
ASV1505	1.000	2219	3.761E-05	Specialist	NA
ASV1506	1.000	1606	3.009E-05	Specialist	Craurococcus-Caldovatus
ASV1507	1.000	605	3.009E-05	Specialist	Spirosoma
ASV1508	1.000	605	3.009E-05	Specialist	Croceicoccus
ASV1509	1.000	605	3.009E-05	Specialist	NA
ASV1510	1.000	605	3.009E-05	Specialist	Rubellimicrobium
ASV1511	1.000	1087	3.009E-05	Specialist	Glutamicibacter
ASV1512	1.000	2140	2.257E-05	Specialist	Aeromicrobium
ASV1513	1.000	2140	2.257E-05	Specialist	Hymenobacter
ASV1514	1.000	1087	3.009E-05	Specialist	Spirosoma
ASV1515	1.000	1087	3.009E-05	Specialist	Klenkia
ASV1516	1.000	605	3.009E-05	Specialist	Hymenobacter
ASV1517	1.000	2219	3.009E-05	Specialist	NA
ASV1518	1.000	1087	3.009E-05	Specialist	NA
ASV1519	1.000	1087	3.009E-05	Specialist	Jatrophihabitans
ASV1520	1.000	1087	3.009E-05	Specialist	Jeotgalicoccus
ASV1521	1.000	2140	3.761E-05	Specialist	YC-ZSS-LKJ147
ASV1522	1.000	2140	3.761E-05	Specialist	Devosia
ASV1523	1.000	2140	3.761E-05	Specialist	Rhodovarius
ASV1524	1.000	2140	3.761E-05	Specialist	NA
ASV1525	1.000	2140	3.761E-05	Specialist	Mycobacterium
ASV1526	1.000	1992	3.009E-05	Specialist	NA
ASV1527	1.000	1992	3.009E-05	Specialist	Subdoligranulum
ASV1528	1.000	1992	3.009E-05	Specialist	Weissella
ASV1529	1.000	1992	3.009E-05	Specialist	Endobacter
ASV1530	1.000	437	3.009E-05	Specialist	Phaselicystis
ASV1531	1.000	2140	3.009E-05	Specialist	Rubellimicrobium
ASV1532	1.000	2140	3.009E-05	Specialist	NA
ASV1533	1.000	2140	3.009E-05	Specialist	Legionella
ASV1534	1.000	1992	3.009E-05	Specialist	Sphingomonas
ASV1535	1.000	1992	2.257E-05	Specialist	Edaphobaculum

ASV1536	1.000	1992	2.257E-05	Specialist	NA
ASV1537	1.000	1992	2.257E-05	Specialist	Nocardioides
ASV1538	1.000	2140	3.009E-05	Specialist	Rothia
ASV1539	1.000	2140	3.009E-05	Specialist	Ferruginibacter
ASV1540	1.000	1992	3.009E-05	Specialist	Byssovorax
ASV1541	1.000	1992	3.009E-05	Specialist	Neisseria
ASV1542	1.000	437	3.009E-05	Specialist	NA
ASV1543	1.000	437	3.009E-05	Specialist	NA
ASV1544	1.000	437	3.009E-05	Specialist	NA
ASV1545	1.000	2140	3.009E-05	Specialist	Geodermatophilus
ASV1546	1.000	1606	3.009E-05	Specialist	NA
ASV1547	1.000	437	3.761E-05	Specialist	NA
ASV1548	1.000	437	3.761E-05	Specialist	Marmoricola
ASV1549	1.000	437	3.761E-05	Specialist	NA
ASV1550	1.000	437	3.761E-05	Specialist	Hymenobacter
ASV1551	1.000	2219	3.009E-05	Specialist	Paenibacillus
ASV1552	1.000	2219	3.009E-05	Specialist	NA
ASV1553	1.000	2219	3.009E-05	Specialist	NA
ASV1554	1.000	2219	3.009E-05	Specialist	NA
ASV1555	1.000	2219	3.009E-05	Specialist	NA
ASV1556	1.000	2219	3.009E-05	Specialist	Flavobacterium
ASV1557	1.000	2219	3.009E-05	Specialist	Clostridium sensu stricto 1
ASV1559	1.000	437	3.009E-05	Specialist	NA
ASV1560	1.000	437	3.009E-05	Specialist	Psychroglacieceola
ASV1561	1.000	437	3.009E-05	Specialist	Hymenobacter
ASV1562	1.000	437	3.009E-05	Specialist	Hymenobacter
ASV1563	1.000	437	3.009E-05	Specialist	Paracoccus
ASV1564	1.000	1606	2.257E-05	Specialist	Spirochaeta 2
ASV1565	1.000	605	3.761E-05	Specialist	Pseudomonas
ASV1566	1.000	605	3.761E-05	Specialist	Conexibacter
ASV1567	1.000	605	3.761E-05	Specialist	Solirubrobacter
ASV1568	1.000	2140	3.009E-05	Specialist	Caulobacter
ASV1569	1.000	2140	3.009E-05	Specialist	Puia

ASV1570	1.000	2140	2.257E-05	Specialist	Streptococcus
ASV1571	1.000	2140	2.257E-05	Specialist	Exiguobacterium
ASV1572	1.000	2140	2.257E-05	Specialist	Telluria
ASV1573	1.000	1087	3.009E-05	Specialist	NA
ASV1574	1.000	1087	3.009E-05	Specialist	Sphingomonas
ASV1575	1.000	1087	3.009E-05	Specialist	Incertae Sedis
ASV1577	1.000	1087	3.009E-05	Specialist	Novosphingobium
ASV1578	1.000	1087	3.009E-05	Specialist	NA
ASV1579	1.000	1087	3.009E-05	Specialist	Gemmatimonas
ASV1580	1.000	1087	3.009E-05	Specialist	Paracoccus
ASV1581	1.000	1087	3.009E-05	Specialist	NA
ASV1582	1.000	1087	3.009E-05	Specialist	Arenimonas
ASV1583	1.000	1087	3.009E-05	Specialist	Gaiella
ASV1584	1.000	605	3.009E-05	Specialist	Prosthecomicrobium
ASV1585	1.000	605	3.009E-05	Specialist	Fibrella
ASV1586	1.000	2219	3.009E-05	Specialist	Sphingomonas
ASV1587	1.000	2219	3.009E-05	Specialist	Lachnospiraceae FCS020 group
ASV1588	1.000	2219	3.009E-05	Specialist	Corynebacterium
ASV1589	1.000	2219	2.257E-05	Specialist	Dyadobacter
ASV1590	1.000	1606	2.257E-05	Specialist	Hymenobacter
ASV1591	1.000	605	3.761E-05	Specialist	Alcaligenes
ASV1592	1.000	605	3.761E-05	Specialist	Psychroglaciecola
ASV1594	1.000	1992	2.257E-05	Specialist	Nocardioides
ASV1595	1.000	1992	2.257E-05	Specialist	Stenotrophomonas
ASV1596	1.000	1992	2.257E-05	Specialist	Dyadobacter
ASV1597	1.000	437	3.009E-05	Specialist	NA
ASV1598	1.000	437	3.009E-05	Specialist	Aurantisolimonas
ASV1599	1.000	2140	2.257E-05	Specialist	NA
ASV1600	1.000	2140	2.257E-05	Specialist	NA
ASV1601	1.000	1087	3.761E-05	Specialist	Flavisolibacter
ASV1603	1.000	1992	2.257E-05	Specialist	Nocardioides
ASV1604	1.000	437	1.504E-05	Specialist	Actinoplanes
ASV1605	1.000	605	2.257E-05	Specialist	Iamia

ASV1606	1.000	605	2.257E-05	Specialist	Sphingomonas
ASV1608	1.000	605	2.257E-05	Specialist	NA
ASV1609	1.000	605	2.257E-05	Specialist	Ancylobacter
ASV1610	1.000	605	2.257E-05	Specialist	Legionella
ASV1611	1.000	1087	2.257E-05	Specialist	Sphingomonas
ASV1612	1.000	1087	2.257E-05	Specialist	Cutibacterium
ASV1613	1.000	1087	2.257E-05	Specialist	IMCC26207
ASV1614	1.000	1992	2.257E-05	Specialist	Phytohabitans
ASV1615	1.000	1992	2.257E-05	Specialist	NA
ASV1616	1.000	1992	2.257E-05	Specialist	NA
ASV1617	1.000	1992	2.257E-05	Specialist	Nocardioides
ASV1618	1.000	437	2.257E-05	Specialist	Shuttleworthia
ASV1619	1.000	437	2.257E-05	Specialist	Prevotella
ASV1620	1.000	437	2.257E-05	Specialist	Abditibacterium
ASV1621	1.000	437	2.257E-05	Specialist	Leucobacter
ASV1622	1.000	437	2.257E-05	Specialist	Rhodovarius
ASV1623	1.000	1606	1.504E-05	Specialist	Sphingomonas
ASV1624	1.000	1606	1.504E-05	Specialist	NA
ASV1625	1.000	1606	1.504E-05	Specialist	Bosea
ASV1626	1.000	605	2.257E-05	Specialist	Microvirga
ASV1627	1.000	605	2.257E-05	Specialist	NA
ASV1628	1.000	605	2.257E-05	Specialist	NA
ASV1629	1.000	605	2.257E-05	Specialist	Pseudokineococcus
ASV1630	1.000	605	2.257E-05	Specialist	Flavobacterium
ASV1631	1.000	605	2.257E-05	Specialist	Limibaculum
ASV1632	1.000	605	2.257E-05	Specialist	NA
ASV1634	1.000	1606	2.257E-05	Specialist	Massilia
ASV1635	1.000	2219	2.257E-05	Specialist	Sphingomonas
ASV1636	1.000	2219	2.257E-05	Specialist	NA
ASV1637	1.000	1606	2.257E-05	Specialist	Anaerococcus
ASV1638	1.000	1606	2.257E-05	Specialist	Wolbachia
ASV1639	1.000	1606	2.257E-05	Specialist	NA
ASV1640	1.000	1606	2.257E-05	Specialist	Actinomyces

ASV1641	1.000	1606	2.257E-05	Specialist	NA
ASV1643	1.000	2219	3.009E-05	Specialist	Sphingomonas
ASV1644	1.000	2140	1.504E-05	Specialist	Methylobacterium-Methylorubrum
ASV1645	1.000	1087	2.257E-05	Specialist	Motilibacter
ASV1646	1.000	1087	2.257E-05	Specialist	NA
ASV1647	1.000	605	2.257E-05	Specialist	Acidiphilium
ASV1648	1.000	2219	2.257E-05	Specialist	[Eubacterium] ruminantium group
ASV1649	1.000	2219	2.257E-05	Specialist	Kocuria
ASV1650	1.000	2219	2.257E-05	Specialist	Pseudomonas
ASV1651	1.000	2219	2.257E-05	Specialist	Blautia
ASV1652	1.000	1087	2.257E-05	Specialist	Microvirga
ASV1653	1.000	2140	2.257E-05	Specialist	NA
ASV1654	1.000	2140	2.257E-05	Specialist	Caedibacter
ASV1655	1.000	1992	2.257E-05	Specialist	Myxococcus
ASV1656	1.000	1992	2.257E-05	Specialist	Capnocytophaga
ASV1657	1.000	1992	2.257E-05	Specialist	Paenibacillus
ASV1658	1.000	437	2.257E-05	Specialist	Flavobacterium
ASV1659	1.000	437	2.257E-05	Specialist	Thermoactinomyces
ASV1660	1.000	2140	2.257E-05	Specialist	Dactylosporangium
ASV1661	1.000	2140	2.257E-05	Specialist	Psychroglaciacola
ASV1662	1.000	2140	2.257E-05	Specialist	NA
ASV1663	1.000	1992	2.257E-05	Specialist	Actinoplanes
ASV1664	1.000	1992	2.257E-05	Specialist	Brachybacterium
ASV1665	1.000	1992	2.257E-05	Specialist	Devosia
ASV1666	1.000	1992	2.257E-05	Specialist	NA
ASV1667	1.000	1606	2.257E-05	Specialist	Turicella
ASV1668	1.000	1606	2.257E-05	Specialist	NA
ASV1669	1.000	1606	2.257E-05	Specialist	Leptotrichia
ASV1670	1.000	1606	2.257E-05	Specialist	Nocardioides
ASV1671	1.000	2140	2.257E-05	Specialist	Hymenobacter
ASV1672	1.000	1606	2.257E-05	Specialist	PMMR1
ASV1673	1.000	1606	2.257E-05	Specialist	Legionella
ASV1674	1.000	1992	2.257E-05	Specialist	Terrimonas

ASV1675	1.000	1606	1.504E-05	Specialist	Acidiphilium
ASV1676	1.000	1606	1.504E-05	Specialist	Nocardioides
ASV1677	1.000	1992	2.257E-05	Specialist	Sphingomonas
ASV1678	1.000	1992	2.257E-05	Specialist	NA
ASV1679	1.000	1992	2.257E-05	Specialist	NA
ASV1680	1.000	1992	2.257E-05	Specialist	NA
ASV1681	1.000	437	2.257E-05	Specialist	1174-901-12
ASV1682	1.000	437	2.257E-05	Specialist	NA
ASV1683	1.000	437	2.257E-05	Specialist	Streptomyces
ASV1684	1.000	2140	1.504E-05	Specialist	NA
ASV1685	1.000	2140	2.257E-05	Specialist	NA
ASV1686	1.000	1606	2.257E-05	Specialist	Pedomicrobium
ASV1687	1.000	1606	2.257E-05	Specialist	NA
ASV1688	1.000	1606	2.257E-05	Specialist	Nakamurella
ASV1689	1.000	1606	2.257E-05	Specialist	NA
ASV1690	1.000	1992	3.009E-05	Specialist	Corynebacterium
ASV1691	1.000	437	2.257E-05	Specialist	Roseisolibacter
ASV1692	1.000	437	2.257E-05	Specialist	Altererythrobacter
ASV1693	1.000	437	2.257E-05	Specialist	Dyadobacter
ASV1694	1.000	437	2.257E-05	Specialist	Nocardioides
ASV1695	1.000	2219	2.257E-05	Specialist	Roseburia
ASV1696	1.000	2219	2.257E-05	Specialist	Roseomonas
ASV1697	1.000	2219	2.257E-05	Specialist	Thiofaba
ASV1698	1.000	2219	2.257E-05	Specialist	NA
ASV1699	1.000	437	2.257E-05	Specialist	Campylobacter
ASV1700	1.000	437	2.257E-05	Specialist	Devosia
ASV1701	1.000	1606	1.504E-05	Specialist	NA
ASV1702	1.000	1606	1.504E-05	Specialist	NA
ASV1703	1.000	1606	1.504E-05	Specialist	Staphylococcus
ASV1704	1.000	1606	1.504E-05	Specialist	NA
ASV1705	1.000	605	3.009E-05	Specialist	NA
ASV1706	1.000	2140	2.257E-05	Specialist	Friedmanniella
ASV1707	1.000	2140	2.257E-05	Specialist	NA

ASV1708	1.000	2140	2.257E-05	Specialist	Clostridium sensu stricto 1
ASV1709	1.000	2140	2.257E-05	Specialist	P3OB-42
ASV1710	1.000	2140	1.504E-05	Specialist	Ilumatobacter
ASV1716	1.000	1087	2.257E-05	Specialist	Sphingomonas
ASV1717	1.000	605	2.257E-05	Specialist	NA
ASV1718	1.000	605	2.257E-05	Specialist	Hymenobacter
ASV1719	1.000	605	2.257E-05	Specialist	Pseudonocardia
ASV1720	1.000	605	2.257E-05	Specialist	Cytophaga
ASV1721	1.000	1992	1.504E-05	Specialist	NA
ASV1723	1.000	2140	1.504E-05	Specialist	Dermabacter
ASV1724	1.000	2140	1.504E-05	Specialist	YC-ZSS-LKJ90
ASV1725	1.000	2140	1.504E-05	Specialist	Flavobacterium
ASV1726	1.000	1087	1.504E-05	Specialist	NA
ASV1727	1.000	605	1.504E-05	Specialist	Pseudomonas
ASV1728	1.000	605	1.504E-05	Specialist	Ferruginibacter
ASV1729	1.000	605	1.504E-05	Specialist	Candidatus Alysiosphaera
ASV1730	1.000	1087	7.522E-06	Specialist	Bifidobacterium
ASV1731	1.000	437	1.504E-05	Specialist	Prevotella_7
ASV1732	1.000	1606	1.504E-05	Specialist	Haloechothrix
ASV1733	1.000	605	1.504E-05	Specialist	NA
ASV1734	1.000	605	1.504E-05	Specialist	CL500-29 marine group
ASV1735	1.000	605	1.504E-05	Specialist	Rubellimicrobium
ASV1736	1.000	2219	1.504E-05	Specialist	NA
ASV1737	1.000	1606	1.504E-05	Specialist	NA
ASV1738	1.000	1606	1.504E-05	Specialist	Patulibacter
ASV1739	1.000	605	1.504E-05	Specialist	Anaerococcus
ASV1740	1.000	2219	1.504E-05	Specialist	NA
ASV1741	1.000	2219	1.504E-05	Specialist	NA
ASV1742	1.000	1087	1.504E-05	Specialist	NA
ASV1743	1.000	605	1.504E-05	Specialist	Cellvibrio
ASV1744	1.000	2140	1.504E-05	Specialist	NA
ASV1745	1.000	2140	1.504E-05	Specialist	Segetibacter
ASV1746	1.000	437	1.504E-05	Specialist	NA

ASV1747	1.000	2140	1.504E-05	Specialist	Abditibacterium
ASV1748	1.000	2140	1.504E-05	Specialist	NA
ASV1749	1.000	1992	1.504E-05	Specialist	NA
ASV1750	1.000	1992	1.504E-05	Specialist	Methylobacterium-Methylorubrum
ASV1751	1.000	437	2.257E-05	Specialist	Euzebya
ASV1752	1.000	1606	1.504E-05	Specialist	NA
ASV1754	1.000	1992	1.504E-05	Specialist	Enhydrobacter
ASV1755	1.000	1606	1.504E-05	Specialist	Streptomyces
ASV1756	1.000	1606	1.504E-05	Specialist	NA
ASV1759	1.000	1992	1.504E-05	Specialist	Caedibacter
ASV1760	1.000	1606	1.504E-05	Specialist	Sellimonas
ASV1764	1.000	437	1.504E-05	Specialist	Hyphomicrobium
ASV1766	1.000	2219	1.504E-05	Specialist	Ruminiclostridium
ASV1767	1.000	2219	1.504E-05	Specialist	Desulfovibrio
ASV1768	1.000	2219	1.504E-05	Specialist	Aliidongia
ASV1769	1.000	437	1.504E-05	Specialist	Micromonospora
ASV1770	1.000	1606	1.504E-05	Specialist	NA
ASV1771	1.000	1606	1.504E-05	Specialist	NA
ASV1772	1.000	1606	1.504E-05	Specialist	Lachnoclostridium
ASV1773	1.000	2140	1.504E-05	Specialist	Melittangium
ASV1775	1.000	2140	1.504E-05	Specialist	NA
ASV1776	1.000	2140	1.504E-05	Specialist	Phenylobacterium
ASV1778	1.000	1087	1.504E-05	Specialist	NA
ASV1781	1.000	1087	1.504E-05	Specialist	Sandaracinus
ASV1782	1.000	605	1.504E-05	Specialist	CL500-29 marine group
ASV1783	1.000	2219	1.504E-05	Specialist	NA
ASV1785	1.000	2219	1.504E-05	Specialist	Friedmanniella
ASV1786	1.000	605	1.504E-05	Specialist	NA
ASV1787	1.000	1992	7.522E-06	Specialist	Conexibacter
ASV1788	1.000	1992	7.522E-06	Specialist	Methylobacterium-Methylorubrum
ASV1789	1.000	1992	7.522E-06	Specialist	NA
ASV1790	1.000	2140	1.504E-05	Specialist	NA

<sup>a</sup> ASVs were retained only if they exhibited non-zero abundance in at least two distinct GDD values. ASVs were classified as thermal specialists (niche width  $\leq 1.5$ ), generalists ( $\geq 2.25$ ), or intermediates (between thresholds). The table includes each ASV's niche width, peak GDD (the GDD at which its relative abundance was highest), relative abundance at that peak, niche classification, and assigned bacterial genus.